IOWA STATE UNIVERSITY
Digital Repository

2015

Phase field approach for multiphase phase transformations, twinning, and variant-variant transformations in martensite

Arunabha Mohan Roy
Iowa State University

Follow this and additional works at: https://lib.dr.iastate.edu/etd

Part of the Materials Science and Engineering Commons, Mathematics Commons, Mechanics of Materials Commons, and the Physics Commons

www.manaraa.com

Phase field approach for multiphase phase transformations, twinning, and variant-variant transformations in martensite

by

Arunabha Mohan Roy

A dissertation submitted to the graduate faculty
in partial fulfillment of the requirement for the degree of

DOCTOR OF PHILOSOPHY

Major: Engineering Mechanics

Program of Study Committee:
Valery I. Levitas, Major Professor
Thomas Rudolphi
Wei Hong
Baskar Ganapathysubramanian
Liming Xiong

Iowa State University
Ames, Iowa
2015

Dedication

I would like to dedicate this dissertation to my **Baba** and **Ma** (Dad and Mom) for their love, support, patience, and sacrifice.

TABLE OF CONTENTS

.

CHAPTER 3. MULTIPHASE FIELD THEROY FOR TEMPERATURE- AND STRESS INDUCED PHASE TRANSFORMATION……………………………..........74

CHAPTER 4. MULTIPHASE PHASE FIELD THEROY FOR TEMPERATURE-INDUCED PHASE TRANSFORMATION …………………………………………..88

CHAPTER 5. DETAILED PHASE FIELD THEORY FOR MULTIPHASE THEORY FOR TEMPERATURE- AND STRESS-INDUCED PHASE TRANSFORMATIONS: GENERAL MODEL, STABILITY CONDITIONS AND SIMULATIONS…………...120

ACKNOWLEDGMENTS

I express my sincere heartfelt gratitude to my thesis supervisor Dr. **V. I. Levitas**. I felt blessed to have got an opportunity to do my PhD thesis under him. I take this opportunity to thank him for his guidance, support and encouragement throughout the duration of my thesis. Long discussions and his critical suggestions have helped me to overcome many difficulties faced during the progress and gained a lot of insight in many arears. He also my constant source of inspiration to complete my thesis to the point of satisfaction. I also helpful to my entire POS committee members, Dr. Thomas Rudolphi, Dr. Baskar Ganapathysubramanian, Dr. Liming Xiong, Dr. Wei Hong and Dr. Ashraf Bastawros for their suggestion and support.

I thank my all PhD lab mates and dear friends, especially Dr. Mahdi Javanbakht, Dr. Kamran Samani, Dr. Hamed Attarani, Dr. Kasra Momeni, Dr. Biao Feng, Yong-Seok Hong and all my other friends who helped and contribute to my research.

Last, but not the least, words are not enough to explain my feeling towards my parents and relatives. They have always been the constant source of inspiration for me. I am thankful to them for their love, sacrifice and support. I am extending the thankfulness to the people who have directly or indirectly help me in completion of my thesis. I acknowledge the blessing of my elders in my family. It's the outcome of their best wishes only which enable me to reach to this joyous end.

Arunabha Mohan Roy

20th June, 2015

ABSTRACT

New advanced phase field model of transformations between martensitic variants and multiple twinning within martensitic variants is developed for large strains and lattice rotations. It resolves numerous existing problems. The model, which involves just one order parameter for the description of each variant-variant transformation and multiple twinnings within each martensitic variant, provides a well-controlled description of variant-variant transformations and multiple twinning, including expressions for interface tension which are consistent with the sharp interface limit. The finite element approach is developed and applied to the solution of a number of examples of twinning and combined austenite-martensite and martensite-martensite phase transformations (PTs) and nanostructure evolution.

In multiphase phase field theory, a critical outstanding problem on developing of phase field approach for temperature- and stress-induced phase transformations between arbitrary n phases is solved. Thermodynamic Ginzburg-Landau potential for temperature and stress-induced phase transformations (PTs) between n- phases is developed. It describes each of the PTs with a single order parameter without explicit constraint equation, which allows one to use analytical solution to calibrate each interface energy, width, and mobility; reproduces the desired PT criteria via instability conditions; introduces interface stresses, and allows controlling presence of the third phase at the interface between two other phases. A finite-element approach is developed and utilized to solve problem on microstructure formation for multivariant martensitic PTs. Results are in quantitative agreement with experiment. The developed approach is applicable to various PTs between multiple, solid, and liquid phases and grain evolution and can be extended for diffusive, electric, and magnetic PTs.

CHAPTER 1. MULTIPLE TWINNING AND VARIANT-VARIANT TRANSFORMATIONS IN MARTENSITE: PHASE-FIELD APPROACH

Modified from a paper published in Physical Review B

Valery I. Levitas[1], Arunabha M. Roy[2] and Dean L. Preston[3]

[1]*Iowa State University, Departments of Mechanical Engineering, Aerospace Engineering, and Material Science and Engineering, Ames, Iowa 50011, U.S.A.*

[2]*Iowa State University, Department of Aerospace Engineering, Ames, Iowa 50011, U.S.A.*

[3]*Computational Physics Division, Los Alamos National Laboratory, Los Alamos, New Mexico 87545, USA*

Abstract

A phase field theory of transformations between martensitic variants and multiple twinning within martensitic variants is developed for large strains and lattice rotations. It resolves numerous existing problems. The model, which involves just one order parameter for the description of each variant-variant transformation and multiple twinnings within each martensitic variant, allows one to prescribe the twin interface energy and width, and to introduce interface stresses consistent with the sharp interface limit. A finite element approach is developed and applied to the solution of a number of examples of twinning and combined austenite-martensite and martensite-martensite phase transformations (PTs) and nanostructure evolution. A similar approach can be developed for reconstructive, electric, and magnetic PTs.

1.1 Introduction

Twinning is a mechanism for plastic deformation in crystalline materials whereby a region of the crystal lattice is homogeneously sheared into a new orientation [1]. It is most pronounced at low temperatures, high strain rates, and in small grains. Martensitic PTs are usually accompanied by twinning which reduces the energy associated with internal elastic stresses. Martensitic

PTs involve several martensitic variants M_i, $i = 1, 2, ..., n$, where n equals the ratio of the order of the point group of the austenite A to that of the martensite. Since the M_i are usually in a twin relation to each other, variant-variant transformations and twinning in martensite are closely related. The sharp-interface approach to martensitic PTs and twinning [2, 3] was a significant advance, but it is based on the optimization of crystallographic parameters of the prescribed microstructure under stress-free conditions or applied homogeneous stresses. The phase field approach is widely used for modeling microstructure evolution during multivariant martensitic PTs and twinning [4–8]. Phase field models that incorporate the main features of stress-strain curves, the correct instability conditions, a large strain formulation, and surface tension were developed in [7, 9–12]; those models utilize order parameters based on the transformation strain. Since it was shown in [9] that it is not possible to realize all of these model features using total-strain order parameters, we will only consider order parameters based on transformation strain. In this paper, we present a novel phase field model for variant-variant transformations and multiple twinning within the martensite, which resolves numerous problems outlined below. It also includes $\mathsf{A} \leftrightarrow \mathsf{M}_i$ PTs. For each twinning system $\{\mathsf{T}_1, \mathsf{T}_2, ...,\mathsf{T}_n\}$, where the T_i are crystallographically equivalent, the transformation-deformation gradient $\boldsymbol{F}_{ti} = \boldsymbol{I} + \gamma(\eta_i)\, \boldsymbol{m}_i^0 \otimes \boldsymbol{n}_i^0$ transforms the parent (reference) lattice L into a twinned lattice T_i by a simple shear γ in direction $\boldsymbol{m}_i^0$ in the plane with normal $\boldsymbol{n}_i^0$ in the reference state; here η_i, the ith order parameter, varies between 0 for L and 1 for T_i, $\otimes$ designates a dyadic product of vectors, and $\boldsymbol{I}$ is the unit tensor. It is usually assumed that twinning can be described by a phase field model of PT for which the thermal part of the free energy does not change and the transformation strain corresponds to the twinning shear [7–9]. However, this is not completely consistent because of an essential difference between twinning and PTs: twinning does not change the crystal structure, i.e. the unit cell of the twin is the same as that of the parent crystal to within a rigid-body rotation. This fact introduces a symmetry requirement not present in the PT theory: the thermodynamic potential and the transformation-deformation gradient must be completely symmetric with respect to the interchange $\mathsf{L} \leftrightarrow \mathsf{T}_i$; thus, any twin T_i can be considered as a parent reference lattice L. Our $2-3-4$ Landau potential for martensitic PT [9, 10] possesses this symmetry but our $2-4-6$ potential [9, 10] does not. However, the main theoretical complication is multiple twinning, that is, secondary and further twinnings

of the primary twin T_i, which commonly occurs. Again, since the crystal lattice of any twin T_i is indistinguishable to within rigid-body rotations from the parent lattice L, the thermodynamic potential and transformation-deformation gradient must be completely symmetric with respect to the interchanges $\mathsf{L} \leftrightarrow \mathsf{T}_i$ and $\mathsf{T}_j \leftrightarrow \mathsf{T}_i$ for all i and j. This condition was not satisfied in any previous model of PTs and twinning but is satisfied in the present model for twinning in martensite. Crystal lattice of the austenite A will be considered as the parent (reference) lattice, independent of whether we consider PT $\mathsf{A} \leftrightarrow \mathsf{M}_i$ or only $\mathsf{M}_i \leftrightarrow \mathsf{M}_j$ transformations. Below, we will not consider designation L anymore and designations M_i and T_i are equivalent. Even for small strains, neither transformations between martensitic variants nor twinning in any known theory is described as consistently as $\mathsf{A} \leftrightarrow \mathsf{T}_i$ transformations. Indeed, the $\mathsf{A} \leftrightarrow \mathsf{T}_i$ transformation can be described by a single order parameter η_i, the temperature-dependence of the stress-strain curve and the A-T_i interface energy and width are completely determined by a small number of material parameters, and we obtained analytic solutions for the variation of η_i through both static and propagating interfaces [10, 12, 13]. In contrast, at a T_i-T_j interface in any known theory, the order parameters η_i and η_j vary independently, and the transformation path in the $\eta_i - \eta_j$ plane and the interface energy and width have an unrealistic dependence on temperature, stresses, and a larger number of material parameters; these dependencies can only be determined by numerical methods [11]. Thus, one cannot prescribe a desired T_i-T_j interface energy and width. Consequently, the consistency of the expression introduced in [11, 12] for the interface (surface) tension $\boldsymbol{\sigma}_{st}$ in the sharp-interface limit can be proved for $\mathsf{A}-\mathsf{T}_i$ interfaces but not for T_i-T_j interfaces; in fact, simulations show that $\boldsymbol{\sigma}_{st}$ does not describe the sharp T_i-T_j interface limit. This shortcoming is rectified in the model presented here. Also, in large strain theory [7, 8], in which each martensitic variant or twin is characterized by the transformation deformation gradient $\boldsymbol{F}_{ti}$, the transformations $\mathsf{T}_i \leftrightarrow \mathsf{T}_j$ between $\boldsymbol{F}_{ti}$ and $\boldsymbol{F}_{tj}$ do not represent simple shears without additional rotations. There are an infinite number of combinations of rotations and twinning parameters for which two martensitic variants are twin related, e.g., zigzag twins [3]. Thus, it is impossible to parameterize all simple shears between two martensitic variants with a single order parameter. In this paper, we present a new phase field model of martensitic variant-variant ($\mathsf{T}_i \leftrightarrow \mathsf{T}_j$) transformations and twinning within the variants which resolves all of the above problems. Each martensitic

variant is characterized by the rotation-free deformation of the crystal lattice $\boldsymbol{U}_{ti}$. We define a new minimal set of n order parameters for n martensitic variants. The key point is that each $\mathsf{T}_i \leftrightarrow \mathsf{T}_j$ transformation and all twinnings within them are described with a single order parameter. This significantly simplifies the description of $\mathsf{T}_i\text{-}\mathsf{T}_j$ transformations and multiple twinnings, and moreover, one can prescribe the $\mathsf{T}_i\text{-}\mathsf{T}_j$ interface energy and width and introduce interface stresses consistent with the sharp interface approach, which is completely analogous to the description of $\mathsf{A} \leftrightarrow \mathsf{T}_i$ PT. For the fully geometrically nonlinear theory (large strains and material rotation), the twinning parameters and lattice rotations are not parameterized with the order parameters but obtained from the solution of the coupled phase field and mechanics boundary-value problem. Model problems on twinning in martensite and combined $\mathsf{A} \leftrightarrow \mathsf{T}_i$ and $\mathsf{T}_j \leftrightarrow \mathsf{T}_i$ transformations and nanostructure evolution in a nanosize sample are solved by means of the finite element method (FEM) COMSOL code [14]. We designate contractions of tensors $\boldsymbol{A} = \{A_{ij}\}$ and $\boldsymbol{B} = \{B_{ji}\}$ over one and two indices as $\boldsymbol{A}\cdot\boldsymbol{B} = \{A_{ij}B_{jk}\}$ and $\boldsymbol{A}\!:\!\boldsymbol{B} = A_{ij}B_{ji}$, respectively. The subscripts s, e and t mean symmetrization, and elastic and transformational strains, the superscript T designates transposition, and $\boldsymbol{\nabla}$ is the gradient operator in the *deformed* states.

1.2 General model

The motion of the elastic material undergoing twinning will be described by a vector-valued function $\boldsymbol{r} = \boldsymbol{r}(\boldsymbol{r}_0, t)$, where $\boldsymbol{r}_0$ and $\boldsymbol{r}$ are the positions of points in the reference Ω_0 and the deformed Ω configurations, respectively, and t is the time. The austenite A lattice will be considered as the reference configuration, independent of whether we consider PT $\mathsf{A} \leftrightarrow \mathsf{T}_i$ or only $\mathsf{T}_i \leftrightarrow \mathsf{T}_j$ transformations. The transformation deformation gradient $\boldsymbol{U}_{ti} = \boldsymbol{I} + \boldsymbol{\varepsilon}_{ti}$ transforms the crystal lattice of A into the lattice of the ith martensitic variant T_i, $i = 1, 2, ..., n$, both in the unloaded state. The multiplicative decomposition of the deformation gradient, $\boldsymbol{F} = \boldsymbol{F}_e \cdot \boldsymbol{U}_t$, into elastic $\boldsymbol{F}_e$ and transformational $\boldsymbol{U}_t$ parts will be used. Since $\boldsymbol{U}_t = \boldsymbol{U}_t^T$, lattice rotation is included in $\boldsymbol{F}_e$. We assume the martensitic variants are in twin relation with each other, hence they satisfy the twinning equation $\boldsymbol{Q}_i \cdot \boldsymbol{U}_{ti} - \boldsymbol{Q}_j \cdot \boldsymbol{U}_{tj} = \gamma_{ij}\,\boldsymbol{m}_{ij}^0\boldsymbol{n}_{ij}^0$ for some twinning system parameters γ_{ij}, $\boldsymbol{m}_{ij}^0$, $\boldsymbol{n}_{ij}^0$ and rigid-body rotations $\boldsymbol{Q}_m$. There are numerous solutions to the

twinning equation for the same $\boldsymbol{U}_{ti}$ and $\boldsymbol{U}_{tj}$ and different $\boldsymbol{Q}_m$. E.g., for zigzag twins [3], if each of the pairs of variants $\{\boldsymbol{R}\cdot\boldsymbol{U}_{ti};\boldsymbol{U}_{tj}\}$ and $\{\boldsymbol{Q}\cdot\boldsymbol{U}_{tj};\boldsymbol{R}\cdot\boldsymbol{U}_{ti}\}$ satisfies the twinning equations for some specific rotations $\boldsymbol{R}$ and $\boldsymbol{Q}$, then the pair of variants $\{\boldsymbol{Q}^p\cdot\boldsymbol{R}\cdot\boldsymbol{U}_{ti};\boldsymbol{Q}^p\cdot\boldsymbol{U}_{tj}\}$ satisfies the twinning equations as well for any integer number p of sequential rotations $\boldsymbol{Q}$. Thus, it is impractical (and unnecessary) to parameterize all *simple shears* between all pairs of martensitic variants with a separate order parameter. Instead, we describe martensitic variant T_i with the rotation-free transformation deformation gradient $\boldsymbol{U}_{ti}$, and all possible twinnings and variant-variant transformations between two variants will be described with a single order parameter. The twinning system parameters are not functions of the order parameters but are determined via the solution of the coupled large-strain phase field and mechanics boundary-value problem.

In our n-dimensional order parameter space, the austenite A is located at the origin and the ith martensitic variant T_i is located at the intersection of the positive i^{th} axis with the unit sphere. The radial coordinate, designated $\boldsymbol{\Upsilon}$, describes $\mathsf{A}\leftrightarrow\mathsf{T}_i$ transformations, while the angular order parameters $0 \leq \vartheta_i \leq 1$, where $\pi\vartheta_i/2$ is the angle between the radius vector $\boldsymbol{\Upsilon}$ and the positive i^{th} axis, describe twinning $\mathsf{T}_k\leftrightarrow\mathsf{T}_i$ (variant-variant) transformations. This geometric interpretation leads to the constraint $\sum_{k=1}^{n}\cos^2\left(\frac{\pi}{2}\vartheta_k\right)=1$, which significantly complicates the development of the thermodynamic potential. However, for each variant-variant or twinning transformation $\mathsf{T}_i\leftrightarrow\mathsf{T}_j$ (at $\Upsilon=1$, $\vartheta_k=1$ for $k\neq i,j$) this constraint reduces to the linear constraint $\vartheta_j+\vartheta_i=1$. In the general case we also employ a linear constraint: $\sum_{i=1}^{n}\vartheta_i=n-1$. This slightly changes the geometric interpretation when more than two order parameters ϑ_i deviate from 1 but it allows us to develop a potential that predicts both A-T_i and T_i-T_j interface widths and energies. Then $\vartheta_n=n-1-\sum_{i=1}^{n-1}\vartheta_i$ replaces all occurrences of the parameter ϑ_n in all equations below. The Helmholtz free energy per unit undeformed volume is given by the following expression:

$$\psi = \psi^e(\boldsymbol{B},\Upsilon,\vartheta_i,\theta) + \frac{\rho_0}{\rho}\breve{\psi}^\theta + \psi^\theta + \frac{\rho_0}{\rho}\psi^\nabla; \tag{1}$$

$$\breve{\psi}^\theta = (A_0\left(\theta-\theta_c\right)+3\Delta s_0(\theta-\theta_e))\Upsilon^2(1-\Upsilon)^2 + \bar{A}\sum_{i,j=1;i\neq j}^{n}(1-\vartheta_i)^2(1-\vartheta_j)^2 q(\Upsilon)$$

$$+D\sum_{i,j,k=1;i\neq j\neq k}^{n}(1-\vartheta_i)(1-\vartheta_j)(1-\vartheta_k)q(\Upsilon); \quad \psi^\nabla = \frac{\beta}{2}|\boldsymbol{\nabla}\Upsilon|^2 + q(\Upsilon)\frac{\beta_\vartheta}{4}\sum_{i=1}^{n}|\boldsymbol{\nabla}\vartheta_i|^2; \tag{2}$$

$$\psi^\theta = -\Delta s_0(\theta-\theta_e)q(\Upsilon); \quad q(\Upsilon)=\Upsilon^2(3-2\Upsilon); \tag{3}$$

$$\boldsymbol{U}_t = \boldsymbol{I} + \sum_{k=1}^{n} \boldsymbol{\varepsilon}_{tk} \left(1 - 3\vartheta_k^2 + 2\vartheta_k^3\right) \varphi(\Upsilon); \quad \varphi(\Upsilon) = a\Upsilon^2 + (4 - 2a)\,\Upsilon^3 + (a - 3)\Upsilon^4. \quad (4)$$

Here $\boldsymbol{B} = (\boldsymbol{V} \cdot \boldsymbol{V} - \boldsymbol{I})/2$ is the finite strain measure, $\boldsymbol{V}$ is the left stretch tensor, θ is the temperature, θ_e is the equilibrium temperature, A becomes unstable at temperature θ_c, ρ and ρ_0 are the mass densities in the deformed and undeformed states, β and β_ϑ are gradient energy coefficients, A_0 and $\bar{A}$ characterize the barriers for A-T_i and T_i-T_j transformations, respectively, the parameter a controls the transformation strain for A-T_i PT, and ψ^e is the elastic energy. The term with D in Eq.(2) describes the interaction of three twins at their triple junctions; it was not present in previous theories and it disappears for two variants. Thermodynamics and Landau-Ginzburg kinetics (see, e.g. [11]) lead to

$$\boldsymbol{\sigma} = \frac{\rho}{\rho_0} \boldsymbol{V} \cdot \frac{\partial \psi}{\partial \boldsymbol{B}} \cdot \boldsymbol{V} - \frac{\rho}{\rho_0} \left(\boldsymbol{\nabla}\Upsilon \otimes \frac{\partial \psi}{\partial \boldsymbol{\nabla}\Upsilon}\right)_s - \sum_{i=1}^{n-1} \frac{\rho}{\rho_0} \left(\boldsymbol{\nabla}\vartheta_i \otimes \frac{\partial \psi}{\partial \boldsymbol{\nabla}\vartheta_i}\right)_s; \quad (5)$$

$$\frac{1}{L_\Upsilon}\frac{\partial \Upsilon}{\partial t} = -\frac{\rho}{\rho_0}\frac{\partial \psi}{\partial \Upsilon}|\boldsymbol{B} + \boldsymbol{\nabla} \cdot \left(\frac{\rho}{\rho_0}\frac{\partial \psi}{\partial \boldsymbol{\nabla}\Upsilon}\right); \quad \frac{1}{L_\vartheta}\frac{\partial \vartheta_i}{\partial t} = -\frac{\rho}{\rho_0}\frac{\partial \psi}{\partial \vartheta_i}|\boldsymbol{B} + \boldsymbol{\nabla} \cdot \left(\frac{\rho}{\rho_0}\frac{\partial \psi}{\partial \boldsymbol{\nabla}\vartheta_i}\right), \quad (6)$$

where L_Υ and L_ϑ are kinetic coefficients, $\boldsymbol{\sigma}$ is the true Cauchy stress tensor, and $\partial\psi/\partial\Upsilon$ and $\partial\psi/\partial\vartheta_i$ are evaluated at constant finite strain $\boldsymbol{B}$. Eqs.(1)-(4) satisfy all conditions for the thermodynamic potential formulated in [9]. In particular, A and the variants T_i are homogeneous solutions of the Ginzburg-Landau equations (6) for arbitrary stresses and temperature; the transformation strain for any transformation is independent of stresses and temperature; the transformation criteria that follow from the thermodynamic instability conditions have the same (correct) form as in [9]. The potential (1)-(4) is much simpler than those previously used for martensitic PTs [7, 9–11] and does not require the introduction of sophisticated cross terms, which has several important consequences. In particular, the potential does not possess spurious minima (unphysical phases). All of our modeling goals are satisfied using a simple fourth degree polynomial in Υ and ϑ_i. The variant-variant or twinning transformations $\mathsf{T}_i \leftrightarrow \mathsf{T}_j$ are described by a single order parameter ϑ_i (at $\Upsilon = 1$, $\vartheta_k = 1$ for $k \neq i, j$, and $\vartheta_j = 1 - \vartheta_i$) and are completely analogous to $\mathsf{A} \leftrightarrow \mathsf{T}_i$ PTs. The ratio ρ_0/ρ and the gradient with respect to the deformed configuration are used in Eqs.(1)-(4) to introduce interface tension, as in [11, 12]. Since the $\mathsf{T}_j \leftrightarrow \mathsf{T}_i$ transformations are here described in the same way as $\mathsf{A} \leftrightarrow \mathsf{T}_i$ PT, it is now trivial to demonstrate (see Section III) the consistency of the expression for the interface tension (obtained from Eq. (5) after subtracting the elastically-supported stress) with the sharp

interface limit, whereas this could be proved only for $\mathsf{A}-\mathsf{T}_i$ interfaces in [12]. The thermodynamic potential and $\boldsymbol{U}_t$ are symmetric with respect to the interchanges $\mathsf{T}_j \leftrightarrow \mathsf{T}_i$; they need not be symmetric with respect to the interchange $\mathsf{A} \leftrightarrow \mathsf{T}_i$ because $\mathsf{A} \leftrightarrow \mathsf{T}_i$ is not a twinning.

1.3 Equivalence of equations for $\mathsf{L}\text{-}\mathsf{T}_k$ and $\mathsf{T}_i\text{-}\mathsf{T}_j$ transformations

Let us simplify Eqs.(2)-(6) for the austenite-martensite phase transformation by putting $\vartheta_2 = 0$, $\vartheta_i = 1$ for $i \neq 2$. We also put $a = 3$, which leads to $\varphi(\Upsilon) = q(\Upsilon)$. This is necessary to make the transformation strain between the austenite and martensite symmetric with respect to the interchanges $\mathsf{A} \leftrightarrow \mathsf{T}_i$, in the same sense as it is symmetric for variant-variant transformation. Then

$$\breve{\psi}^\theta = (A_0 (\theta - \theta_c) + 3\Delta s_0(\theta - \theta_e))\Upsilon^2(1 - \Upsilon)^2; \tag{7}$$

$$\psi^\nabla = \frac{\beta}{2}|\boldsymbol{\nabla}\Upsilon|^2; \tag{8}$$

$$\boldsymbol{U}_t = \boldsymbol{I} + \boldsymbol{\varepsilon}_{t2}q(\Upsilon); \tag{9}$$

$$\boldsymbol{\sigma} = \frac{\rho}{\rho_0}\boldsymbol{V} \cdot \frac{\partial\psi}{\partial\boldsymbol{B}} \cdot \boldsymbol{V} - \frac{\rho}{\rho_0}\left(\boldsymbol{\nabla}\Upsilon \otimes \frac{\partial\psi}{\partial\boldsymbol{\nabla}\Upsilon}\right)_s; \tag{10}$$

$$\frac{1}{L_\Upsilon}\frac{\partial\Upsilon}{\partial t} = -\frac{\rho}{\rho_0}\frac{\partial\psi}{\partial\Upsilon}|_{\boldsymbol{B}} + \boldsymbol{\nabla} \cdot \left(\frac{\rho}{\rho_0}\frac{\partial\psi}{\partial\boldsymbol{\nabla}\Upsilon}\right). \tag{11}$$

Next, let us simplify Eqs.(2)-(6) for the $\mathsf{T}_1 \leftrightarrow \mathsf{T}_2$ transformation but putting $\Upsilon = 1$, $\vartheta = \vartheta_1$, $\vartheta_2 = 1 - \vartheta$, and $\vartheta_i = 1$ for $2 < i \leq n$. Then

$$\breve{\psi}^\theta = \bar{A}\vartheta^2(1 - \vartheta)^2; \tag{12}$$

$$\psi^\nabla = \frac{\beta_\vartheta}{2}|\boldsymbol{\nabla}\vartheta|^2; \tag{13}$$

$$\boldsymbol{U}_t = \boldsymbol{I} + \boldsymbol{\varepsilon}_{t1} + (\boldsymbol{\varepsilon}_{t2} - \boldsymbol{\varepsilon}_{t1})q(\vartheta); \tag{14}$$

$$\boldsymbol{\sigma} = \frac{\rho}{\rho_0}\boldsymbol{V} \cdot \frac{\partial\psi}{\partial\boldsymbol{B}} \cdot \boldsymbol{V} - \frac{\rho}{\rho_0}\left(\boldsymbol{\nabla}\vartheta \otimes \frac{\partial\psi}{\partial\boldsymbol{\nabla}\vartheta}\right)_s; \tag{15}$$

$$\frac{1}{L_\vartheta}\frac{\partial\vartheta}{\partial t} = -\frac{\rho}{\rho_0}\frac{\partial\psi}{\partial\vartheta}|_{\boldsymbol{B}} + \boldsymbol{\nabla} \cdot \left(\frac{\rho}{\rho_0}\frac{\partial\psi}{\partial\boldsymbol{\nabla}\vartheta}\right). \tag{16}$$

It is clear that Eqs.(7)-(11) are equivalent to Eqs.(12)-(16) after substituting $\Upsilon \leftrightarrow \vartheta$ with the

following correspondence of parameters:

$$(A_0 \left(\theta - \theta_c\right) + 3\Delta s_0(\theta - \theta_e)) \leftrightarrow \bar{A}; \qquad \beta \leftrightarrow \beta_\vartheta; \qquad \boldsymbol{\varepsilon}_{t1} \leftrightarrow 0; \qquad L_\Upsilon \leftrightarrow L_\vartheta. \qquad (17)$$

For the austenite-martensite interface, the combination of Eq.(1) and Eqs.(7)-(11) resulted in the desired expression for the interface (surface) tension $\boldsymbol{\sigma}_{st}$ [11, 12]. Since Eqs.(12)-(16) for twinning are equivalent to Eqs.(7)-(11) for the austenite-martensite transformation, the expression for the interface tension $\boldsymbol{\sigma}_{st}$ for the T_i-T_j interface has the same desired expression. This proves the advantage of the chosen order parameters and phase field formulation in comparison with previous studies. Note that for the particular case considered in simulations, $A_0 = -3\Delta s_0$, the term $(A_0 \left(\theta - \theta_c\right) + 3\Delta s_0(\theta - \theta_e)) = A_0(\theta_e - \theta_c)$ is temperature independent.

1.4 Analytical solutions

An analytical solution for a nonequilibrium plane austenite-martensite interface moving in an infinite medium in x-direction under stress-free conditions ($\psi^e = 0$) is [10, 12]:

$$\begin{aligned}
\Upsilon &= 1/\left[1 + e^{-p(x - v_\Upsilon t)/\delta_\Upsilon}\right]; \quad \delta_\Upsilon = p\sqrt{\beta/\left[2\left(A_0 \left(\theta - \theta_c\right) + 3\Delta s_0(\theta - \theta_e)\right)\right]}; \\
v_\Upsilon &= -6L_\Upsilon\delta_\Upsilon\Delta s_0(\theta - \theta_e)/p; \quad E_\Upsilon = \sqrt{2\beta\left(A_0 \left(\theta - \theta_c\right) + 3\Delta s_0(\theta - \theta_e)\right)}/6, \qquad (18)
\end{aligned}$$

where $p = 2.667$ [10], v_Υ, δ_Υ, and E_Υ are is the interface velocity, width, and energy, respectively. Using the above equivalence, similar equations can be obtained for a stationary variant-variant interface (since stresses are absent):

$$\vartheta = 1/\left[1 + e^{-p(x - v_\vartheta t)/\delta_\vartheta}\right]; \quad \delta_\vartheta = p\sqrt{\beta_\vartheta/\left(2\bar{A}\right)}; \quad E_\vartheta = \sqrt{2\beta_\vartheta\bar{A}}/6. \qquad (19)$$

These equations allow us to calibrate material parameters β, A_0, $\bar{A}$, and L when the temperature dependence of the interface energy, width, and velocity is known. Explicit expression for a variant-variant interface energy allows us to correctly define interface stresses at a variant-variant interface.

1.5 Complete system of equations for two martensitic variants

Below we enumerate the total system of equations for two martensitic variants used in our simulations. Elastic strains are considered to be small, which simplifies significantly equations. Transformation strains and rotations are finite.

Kinematic decomposition:

$$\boldsymbol{F} = \boldsymbol{F}_e \cdot \boldsymbol{U}_t; \quad \boldsymbol{F}_e = \boldsymbol{V}_e \cdot \boldsymbol{R}_e; \quad \boldsymbol{V}_e = \boldsymbol{I} + \boldsymbol{\varepsilon}_e; \quad \boldsymbol{\varepsilon}_e \ll \boldsymbol{I}, \tag{20}$$

where $\boldsymbol{V}_e$ is the elastic left stretch tensor, $\boldsymbol{R}_e$ is the lattice rotation, $\boldsymbol{\varepsilon}_e$ is the small elastic strains.

Transformation deformation gradient ($\vartheta = \vartheta_1$, $\vartheta_2 = 1 - \vartheta$, and $a = 3$):

$$\boldsymbol{U}_t = \boldsymbol{I} + \left[\boldsymbol{\varepsilon}_{t1} \left(1 - 3\vartheta^2 + 2\vartheta^3 \right) + \boldsymbol{\varepsilon}_{t2} \left(3\vartheta^2 - 2\vartheta^3 \right) \right] q(\Upsilon). \tag{21}$$

The Helmholtz free energy per unit undeformed volume:

$$\psi = \psi^e + \frac{\rho_0}{\rho} \breve{\psi}^\theta + \psi^\theta + \frac{\rho_0}{\rho} \psi^\nabla; \tag{22}$$

$$\psi^e = \frac{1}{2} K \varepsilon_{0e}^2 + \mu \boldsymbol{e}_e : \boldsymbol{e}_e; \tag{23}$$

$$\breve{\psi}^\theta = A_0 \left(\theta_e - \theta_c \right) \Upsilon^2 (1 - \Upsilon)^2 + \bar{A}(1 - \vartheta)^2 \vartheta^2 q(\Upsilon); \tag{24}$$

$$\psi^\nabla = \frac{\beta}{2} |\boldsymbol{\nabla}\Upsilon|^2 + q(\Upsilon) \frac{\beta_\vartheta}{2} |\boldsymbol{\nabla}\vartheta|^2; \tag{25}$$

$$\psi^\theta = -\Delta s_0 (\theta - \theta_e) q(\Upsilon); \quad q(\Upsilon) = \Upsilon^2 (3 - 2\Upsilon), \tag{26}$$

where ε_{0e} and $\boldsymbol{e}_e$ are the volumetric and deviatoric parts of the elastic strain tensor.

Decomposition of the Cauchy stress $\boldsymbol{\sigma}$ into elastic $\boldsymbol{\sigma_e}$ and surface tension $\boldsymbol{\sigma_{st}}$ tensors:

$$\boldsymbol{\sigma} = \boldsymbol{\sigma_e} + \boldsymbol{\sigma_{st}}; \qquad \boldsymbol{\sigma_e} = K \varepsilon_{0e} \boldsymbol{I} + 2\mu \boldsymbol{e}_e;$$

$$\boldsymbol{\sigma}_{st} = (\psi^\nabla + \breve{\psi}_\theta) \boldsymbol{I} - \beta_\Upsilon \boldsymbol{\nabla}\Upsilon \otimes \boldsymbol{\nabla}\Upsilon - q(\Upsilon) \beta_\vartheta \boldsymbol{\nabla}\vartheta \otimes \boldsymbol{\nabla}\vartheta. \tag{27}$$

Ginzburg-Landau equations:

$$\frac{1}{L_\Upsilon} \frac{\partial \Upsilon}{\partial t} = \boldsymbol{\sigma}_e : \left(\boldsymbol{R}_e \cdot \frac{\partial \boldsymbol{U}_t}{\partial \Upsilon} \cdot \boldsymbol{U}_t^{-1} \cdot \boldsymbol{R}_e^t \right)_s - \frac{\rho}{\rho_o} \frac{\partial \psi^\theta}{\partial \Upsilon} - \frac{\partial \breve{\psi}^\theta}{\partial \Upsilon} - \frac{\partial \psi^\nabla}{\partial \Upsilon} + \boldsymbol{\nabla} \cdot \left(\frac{\partial \psi^\nabla}{\partial \boldsymbol{\nabla}\Upsilon} \right)$$

$$= \boldsymbol{\sigma}_e : \left(\boldsymbol{R}_e \cdot \frac{\partial \boldsymbol{U}_t}{\partial \Upsilon} \cdot \boldsymbol{U}_t^{-1} \cdot \boldsymbol{R}_e^t \right)_s + \frac{6\Delta s_0 (\theta - \theta_e)}{1 + \varepsilon_o} \Upsilon(1 - \Upsilon) - 6\bar{A}\Upsilon(1 - \Upsilon)\vartheta^2(1 - \vartheta)^2 -$$

$$2A_0 \left(\theta_e - \theta_c \right) \Upsilon(1 - 3\Upsilon + 2\Upsilon^2) - 3\beta_\vartheta \Upsilon(1 - \Upsilon) |\boldsymbol{\nabla}\vartheta|^2 + \beta_\Upsilon \boldsymbol{\nabla}^2 \Upsilon; \tag{28}$$

$$\frac{1}{L_\vartheta}\frac{\partial\vartheta}{\partial t} = \boldsymbol{\sigma}_e:\left(\boldsymbol{R}_e\cdot\frac{\partial\boldsymbol{U}_t}{\partial\vartheta}\cdot\boldsymbol{U}_t^{-1}\cdot\boldsymbol{R}_e^t\right)_s - \frac{\partial\breve\psi^\theta}{\partial\vartheta} + \boldsymbol{\nabla}\cdot\left(\frac{\partial\psi^\nabla}{\partial\boldsymbol{\nabla}\vartheta}\right)$$

$$= \boldsymbol{\sigma}_e:\left(\boldsymbol{R}_e\cdot\frac{\partial\boldsymbol{U}_t}{\partial\vartheta}\cdot\boldsymbol{U}_t^{-1}\cdot\boldsymbol{R}_e^t\right)_s - 2\bar{A}\vartheta q(\Upsilon)(1-3\vartheta+2\vartheta^2)+\beta_\vartheta q(\Upsilon)\boldsymbol{\nabla}^2\vartheta. \qquad (29)$$

Equilibrium equation:

$$\boldsymbol{\nabla}\cdot\boldsymbol{\sigma} = 0. \qquad (30)$$

In our example simulations we use the material parameters for the cubic to tetragonal PT in NiAl found in [9, 10, 13]: $a = 3$, $A_0 = -3\Delta s_0 = 4.4 MPaK^{-1}$, $\bar{A} = 5320$ MPa, $\theta_c = -183$ K, $\theta_e = 215$ K, $L_\Upsilon = L_\vartheta = 2596.5\, m^2/Ns$, $\beta = \beta_\vartheta = 5.18 \times 10^{-10}\, N$; $\theta = 100$K, unless other stated. These parameters correspond to a twin interface energy $E_{TT} = 0.958 J/m^2$ and width $\Delta_{TT} = 0.832$ nm. Isotropic linear elasticity is used for simplicity; bulk modulus $K = 112.8\, GPa$ and shear modulus $\mu = 65.1\, GPa$. In the plane stress 2D problems, only T_1 and T_2 are considered; the corresponding transformation strains in the cubic axes are $\boldsymbol{\varepsilon}_{t1} = (0.215, -0.078, -0.078)$ and $\boldsymbol{\varepsilon}_{t2} = (-0.078, 0.215, -0.078)$. The FEM approach was developed and incorporated in the COMSOL code. All lengths, stresses, and times are given in units of nm, GPa, and ps. All external stresses are normal to the deformed surface.

1.6 Benchmark problem: bending and splitting of martensite tips in NiAl alloy

Our goal here is to reproduce several nontrivial microstructures observed in experiments for NiAl alloys [15, 16]. Since numerous alternative solutions exist, one has to carefully choose initial conditions. We did this in several steps. Initial random distribution of order parameter Υ in the range $[0; 0.4]$ was prescribed in a square sample of 50×50 with the austenite lattice rotated by $\alpha = 45^o$. Initial value of $\vartheta = 0.5$. For one horizontal and one vertical surfaces, the roller support was used, i.e., normal displacements and shear stresses are zero. Homogeneous normal displacements at two other surfaces were prescribed and kept constant during simulations, resulted in biaxial normal strain of 0.01. Shear stresses were kept zero at external surfaces. Two dimensional problem under plane stress condition and temperature $\theta = 50K$

was studied. The evolution of $2\Upsilon(\vartheta-0.5)$ is presented in Fig. 1, demonstrating transformation of the austenite into martensite and coalescence of martensitic units. Despite the symmetry in geometry and boundary conditions, accidental asymmetry in the initial conditions led to formation of alternating horizontal martensitic twin structure with austenitic regions near vertical sides, in order to satisfy boundary conditions. Invariant plane conditions for the austenite-martensite interfaces are consequence of a simplified plane-stress two-dimensional formulation.

The stationary solution from Fig. 1 was taken as an initial condition for the next problem
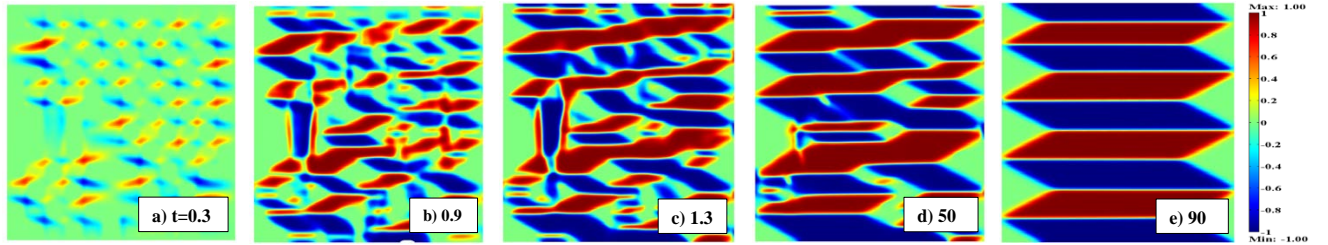
Fig. 1: Evolution of $2\Upsilon(\vartheta - 0.5)$ in a square sample of size 50×50 with an initial stochastic distribution of order parameter Υ under biaxial normal strain of 0.01.
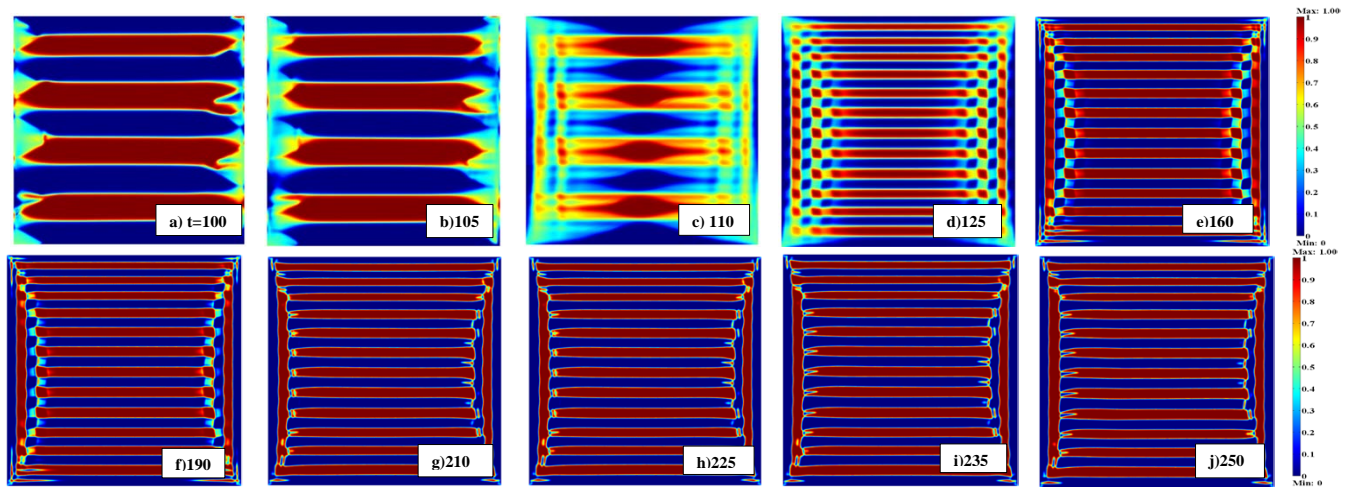
Fig. 2: Evolution of ϑ in a square sample of size 50×50 under biaxial normal strain of 0.01 with an initial condition shown in Fig. 1(e), reduced temperature $\theta = 0K$ and parameter $\beta_\vartheta = 5.18 \times 10^{-11}\,N$ and changed transformation strain.

with the following modifications: temperature was reduced to $\theta = 0K$; parameter β_ϑ was reduced to $\beta_\vartheta = 5.18 \times 10^{-11}\,N$, which led to twin interface energy $E_{MM} = 0.303 J/m^2$ and width $\Delta_{MM} = 0.263 nm$; components of transformation strains have been changed to the values $\boldsymbol{U}_{t1} = (k_1, k_2, k_2)$ and $\boldsymbol{U}_{t2} = (k_2, k_1, k_2)$ with $k_1 = 1.15$ and $k_2 = 0.93$ corresponding to NiAl alloy in [15]. Then Υ was made equal to 1 everywhere and kept during the entire simulation. Due to reduction in the interface energy, number of twins increased by splitting of the initial twins (Fig. 2). Without austenite, rigid vertical boundaries led to high elastic energy. That is why restructuring produced vertical twins near each of vertical sides in proportion, reducing energy of elastic stresses due to prescribed horizontal strain. When microstructure transformed to fully formed twins separated by diffuse interfaces, narrowing and bending of the tips of horizontal T_2 plates is observed (Fig. 2 and 3), similar to experiments [15]. Note, that since invariant plane interface between T_1 and T_2 requires mutual rotation of these variants by the angle $\omega = 12.1^o$ ($\cos\omega = 2k_1 k_2/(k_1^2 + k_2^2) = 0.9778$) [15], angle between horizontal and vertical variants T_2 is $1.5\omega = 18.15^o$, which is in good agreement with our simulations. Thus, due to lattice rotations, interface between horizontal and vertical variants T_2 cannot be invariant plane interface, and reduction in the internal stresses at this boundary leads to reduction of the boundary area by narrowing and bending of the tips of one horizontal plates. Measured angles between tangent to the bent tip and horizontal line in the experiment [15] and in calculations (Fig. 3) are in good quantitative agreement.
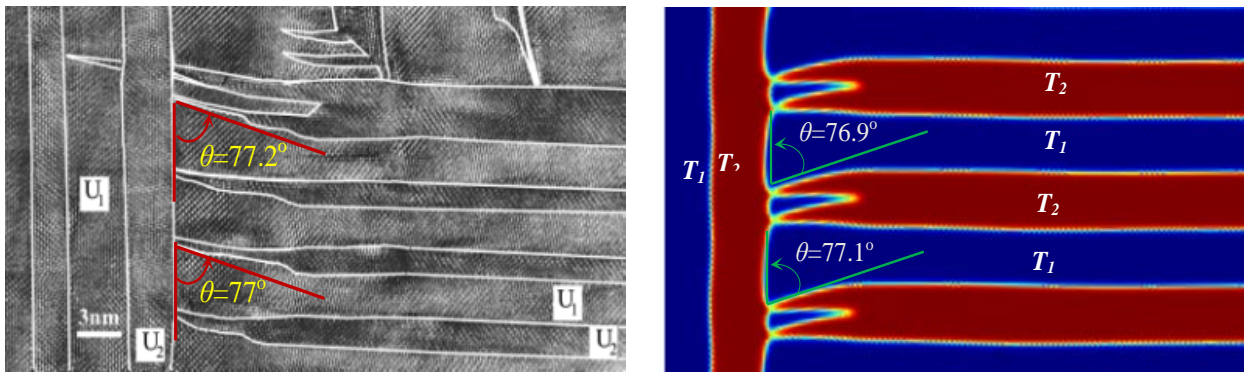

Fig. 3: Comparison of transmission electron microscopy image of a nanaostructure for NiAl alloy from [15] and zoomed part of simulation results from Fig. 2(j). Simulations reproduce well tip splitting and bending angel.
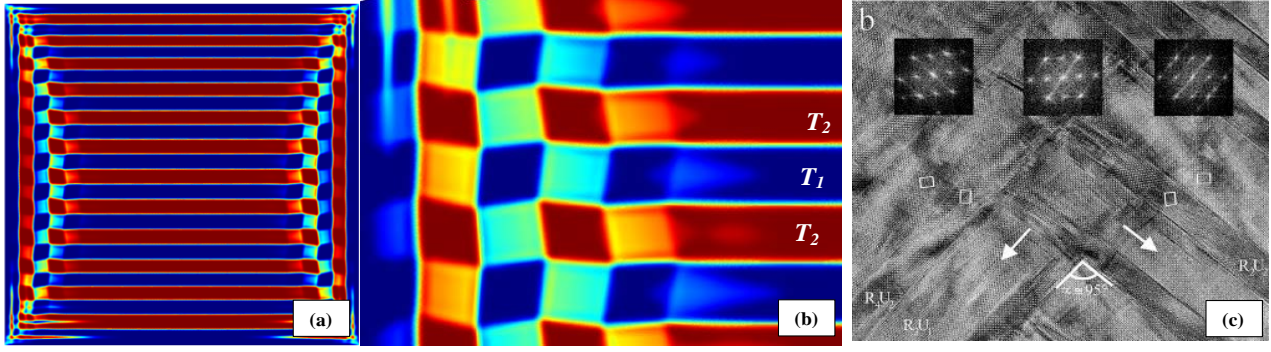
Fig. 4: (a) Stationary solution for $2\Upsilon(\vartheta - 0.5)$ in a sample and (b) its zoomed part near left side of a sample; (c) transmission electron microscopy of a nanaostructure for NiAl from [15]. Crossing twins are observed in experiment and simulation.

Note that microstructure evolution occurs through intermediate values of ϑ in some regions (see $t = 125$ and 160 in Fig. 2), i.e., when transformation strain of one twin penetrates in to region of another one, producing crossed twins. Such crossed twins have been observed in some experiments [16] and have been arrested (Fig. 4). In our simulations in Fig. 2, they represent intermediate stage of evolution. However, if we reduce $\bar{A}$ to 0.532 GPa, the such crossed twins represent stationary solutions (Fig. 4). Also, on the right side of the solution in Fig. 2, an alternative way for stress relaxation is visible, when twins T_2 are surrounded by twins T_1, which is also observed in experiments [15].

Thus, starting with a microstructure in Fig. 1, which is quite far from the final one, our solution reproduced three types of nontrivial experimentally observed microstructures involving finite rotations, including tip splitting and bending, twins crossing, and good quantitative agreement for the bending angle. Note that tip splitting and bending were also reproduced in [5] utilizing strain-based phase field formulation and initial conditions closer to the final solution than here.

1.7 Phase transformation and twinning under applied load

1.7.A Nanoindentation: applied uniform pressure

Nanoindentation-induced twinning $T_2 \rightarrow T_1$ was studied in a T_2 sample with a pre-existing T_1 embryo of radius 2 under the indenter (Fig. 5). The sample was obtained from a square A sample of size 50×50 by transforming it homogeneously to T_2. The cubic axes and transformation strain were rotated by $\alpha = 31^o$ with respect to the coordinate axes. Initial conditions were: $\Upsilon = 1$ everywhere; $\vartheta = 0.9$ inside the embryo and $\vartheta = 0.999$ in the rest of the sample. A uniform pressure between the indenter of width 4 and the sample was increased linearly from 2 to 3 GPa over $110ps$. The bottom sample surface was constrained by a roller support and point F was fixed; all other surfaces are stress-free. With increasing load, a twin T_1 appears under the indenter and grows in a wedge shape with a sharp tip (Fig. 5a, b). Since the bottom of the sample was constrained by the roller support, the twin T_1 could not propagate through the entire sample. In the same problem but with a stress-free section of length 20 at the bottom (Fig. 5c-d), the twin propagated completely through the sample and widened with increasing load. The load was then reduced to zero: the width of the twin then decreased to zero without a change in length (Fig. 5e-f). These results are in qualitative agreement with experiments [1] and previous simulations [8]. Since dislocation plasticity and interface friction [6, 13] are neglected, there is no residual twin.

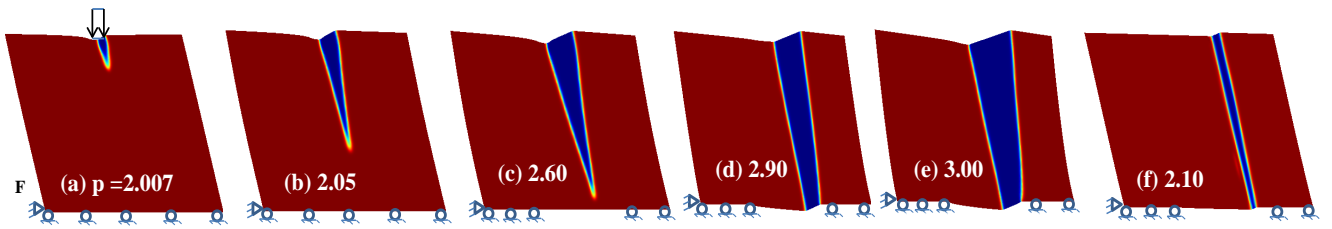Fig. 5: Twinning T_2 (red) $\rightarrow T_1$ (blue) under indentation with the rigid support (a)-(b), support with the hole (c)-(e), and during unloading (f).

1.7.B Nanoindentation: applied uniform displacement

Nanoindentation of a square 50×50 A sample with $\alpha = 15^0$ was modeled by prescribing uniform vertical displacements growing from 2 to 2.5 over a section of width 4; friction was

neglected (Fig. 6). Adjacent lateral surfaces of the sample were constrained by the roller supports. In an initial embryo of radius 2 we set $\Upsilon = 0.1$; $\Upsilon = 0.01$ outside of the embryo. The order parameter $\vartheta = 0.5$ everywhere. The transformed twinned martensite first grew only in the vertical direction; note the presence of a small non-transformed region under the indenter (Fig. 6 (a)-(f)). When the stress concentration due to the indenter became smaller than the internal stresses due to transformation strain and the bottom constraint, a morphological transition occurred: the growth of T_2 changed direction away from T_1 toward a corner of the sample, and ultimately reached the corner. The T_2-T_1 interface is curvilinear and consequently cannot be described by crystallographic theories presented in e.g., $[2, 3]$.
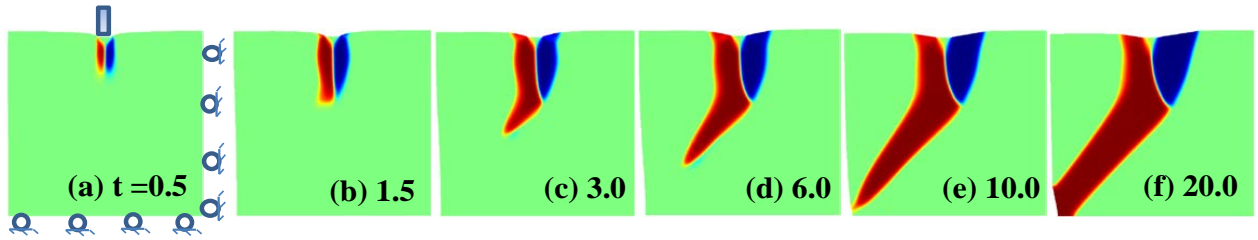
Fig. 6: Evolution of $2\Upsilon(\vartheta - 0.5)$ for indentation of A (green) sample; T_2: red and T_1: blue.

1.7.C Biaxial stresses

A square A sample of size 100×100 with $\alpha = 15^o$ and an embryo of 2 nm radius in the center of the sample was subjected to uniform vertical and horizontal stresses $\sigma_y = 3$ and $\sigma_x = 0.1$, respectively (Fig. 7). Because of the reflection symmetry, only one-quarter of the sample was directly simulated; roller supports were applied along the symmetry axes. The parameter values $\bar{A} = 61.6 MPa$ and $\beta_{TT} = 19.4 \times 10^{-12} N$ were used, corresponding to $E_{TT} = 0.01 J/m^2$ and $\Delta_{TT} = 1nm$. The initial conditions in the embryo were $\Upsilon = 0.1$, and $\Upsilon = 0.001$ outside the embryo; $\vartheta = 0.5$ everywhere. Within $1ps$, A was transformed to a mixture of T_i twins, which further evolve to produce a nontrivial stationary morphology. Note that varying the ratio L_ϑ/L_Υ from 1 to 1000 with $L_\Upsilon = 2596.5 m^2/Ns$ did not change the stationary solution and only slightly affected the evolution.
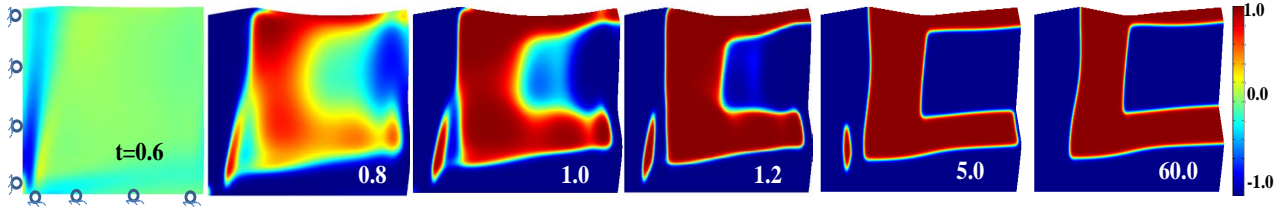
Figure 7: Evolution of $2\Upsilon(\vartheta - 0.5)$ in a quarter of 100×100 sample with an initial embryo at the center under homogeneous compressive stress of $\sigma_y = 3$ and $\sigma_x = 0.1$.

1.7.D Double indentation

Two indenters of width $4\ nm$ were placed on adjacent sides of a square 50×50 A sample with $\alpha = 45^0$ (Fig. 8). At $t = 0$, there were uniform pressures $p_1 = p_2 = 3$ across the indenters. The remaining lateral surfaces of the sample were constrained by roller supports. In two initial embryos of radius 2 under the indenters, $\Upsilon = 0.1$; outside the embryos $\Upsilon = 0.01$. Again, $\vartheta = 0.5$ everywhere. The complex evolution of the twinned nanostructure is shown in Fig. 8a-i. Starting with state (h), p_2 was slowly reduced to zero while keeping $p_1 = 3$. The quasi-stationary solutions in Fig. 8j-l show an initial reversal of the nanostructure (see Figs. 8j and g) followed by the predominance of T_1.
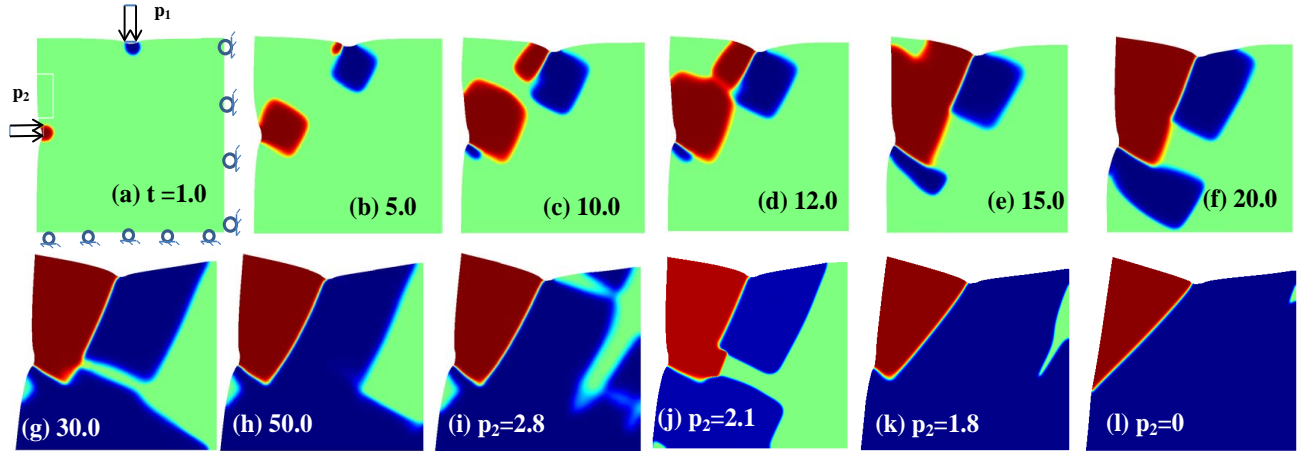
Fig. 8: Evolution of $2\Upsilon(\vartheta - 0.5)$ in time (a-i) for double indentation of an A sample at $p_1 = p_2 = 3$, followed by reduction of p_2 to zero at $p_1 = 3$ (j-l) from state (h).

1.8 Concluding remarks

To summarize, a phase field model of transformations between martensitic variants and multiple twinning in martensitic variants was developed. It accounts for large strains and lattice rotations, and incorporates a new minimal set of order parameters. Each martensitic variant is characterized by the rotation-free deformation of the crystal lattice $\boldsymbol{U}_{ti}$. The twinning parameters and lattice rotations are not parameterized with the order parameters but obtained from the solution of the coupled phase field and mechanics boundary-value problem. Each variant-variant transformation and all of the infinite number of possible twinnings within them are described with a single order parameter. Despite this economy of order parameters, arbitrarily complex twin-within-a-twin martensitic microstructures can in principle be described by the model. The energies and widths of the $\mathsf{A}-\mathsf{T}_i$ and $\mathsf{T}_j-\mathsf{T}_i$ interfaces can be controlled (prescribed), and the corresponding interface stresses are consistent with the sharp interface limit. A similar approach in terms of order parameters (Υ, ϑ_i) could be developed for reconstructive, electric and magnetic PTs and for other phenomena described by multiple order parameters. Problems on twinning in martensite and combined $\mathsf{A}\leftrightarrow\mathsf{M}_i$ and $\mathsf{M}_j\leftrightarrow\mathsf{M}_i$ transformations and nanostructure evolution in a nanosize sample are solved utilizing FEM. In particular, for thermally-induced transformation, we reproduced three types of nontrivial experimentally observed microstructures involving finite rotations, including tip splitting and bending, and twins crossing; good quantitative agreement for the bending angle is obtained.

Acknowledgements

References

[1] J. W. Christian and S. Mahajan, Prog. Mater. Sci. **39**, 1157 (1995); V. S. Boiko, R. I. Garber and A. M. Kosevich, *Reversible Crystal Plasticity* (New York: AIP, 1994).

[2] A.G. Khachaturyan, G.A. Shatalov, Sov. Phys. JETP **29**, 557561 (1969); A.L. Roitburd, Sov. Phys. Uspehi **17**, 3255 (1974); J.M. Ball and R.D. James, Arch. Rat. Mech. Anal. **100**, 1352 (1987); M.A. Grinfeld, *Thermodynamic Methods in the Theory of Heterogeneous Systems* (Sussex, Longman, 1991).

[3] K. Bhattacharya, *Microstructure of Martensite. Why it Forms and How It Gives Rise to the Shape-Memory Effect* (Oxford, Oxford University Press, 2003).

[4] T. W. Heoa *et al.*, Phil. Mag. Lett. **91**, 110 (2011); L.Q. Chen, Annu. Rev. Mater. Res. **32**, 113 (2002); A. Artemev, Y. Jin and A.G. Khachaturyan, Acta Mat. **49**, 1165 (2001); M. Porta et al. Phys. Rev. B **79**, 214117 (2009); O. U. Salman, B. K. Muite, A. Finel, arXiv:1101.4748v1 [cond-mat.mtrl-sci] (2011); O. U. Salman, A. Finel, R. Delville, and D. Schryvers, J. Appl. Phys. **111**, 103517 (2012).

[5] A. Finel, Y. Le Bouar, A. Gaubert and U. Salman, C. R. Physique **11**, 245 (2010).

[6] V.I. Levitas and D-W. Lee, Phys. Rev. Lett. **99**, 245701 (2007).

[7] Levitas V.I., Preston D.L. Physics Letters A, **343**, 32 (2005); V.I. Levitas, V. A. Levin, K. M. Zingerman, and E. I. Freiman, Phys. Rev. Lett. **103**, 025702 (2009); V.I. Levitas, Int. J. Plasticity **49**, 85 (2013); V. A. Levin, V. I. Levitas, K.M. Zingerman, E.I. Freiman, Int. J. Solids and Structures **50**, 2914 (2013).

[8] J.D. Clayton, J. Knap, Physica D. **240**, 841 (2011); Model. Simul. Mater. Sci. Eng. **19**, 085005 (2011).

[9] V.I. Levitas and D.L. Preston, Phys. Rev. B **66**, 134206 (2002); 134207 (2002);

[10] V. I. Levitas, D. Preston, and D.-W. Lee, Phys. Rev. B, **68**, 134201 (2003).

[11] V.I. Levitas and M. Javanbakht, Phys. Rev. Lett. **105**, 165701 (2010); V.I. Levitas and M. Javanbakht, Int. J. Mat. Res. **102**, 652 (2011).

[12] V.I. Levitas, Phys. Rev. B **87**, 054112 (2013); V.I. Levitas, Acta Mater. **61**, 4305 (2013).

[13] V.I. Levitas, D.-W. Lee and D.L. Preston, Int. J. Plast. **26**, 395 (2010).

[14] COMSOL, Inc., website: www.comsol.com.

[15] Ph. Boullay, D. Schryvers, R.V. Kohn and J.M. Ball, J. de Physique IV **11**, 23 (2001); Ph. Boullay, D. Schryvers and R.V. Kohn, Phys. Rev. B **64**, 144105 (2001).

[16] Ph. Boullaya, D. Schryvers, J.M. Ball, Acta Materialia **51**, 1421 (2002).

CHAPTER 2. DETAILED PHASE-FIELD THEORY OF MULTIPLE TWINNING AND VARIANT-VARIANT TRANSFORMATIONS IN MARTENSITE: ANALYTICAL SOLUTION AND MICROSTRUCTURE EVOLUTION

Abstract

A phase field theory of transformations between martensitic variants and multiple twinning within martensitic variants is developed for large strains and lattice rotations. It resolves numerous existing problems. The model, which involves just one order parameter for the description of each variant-variant transformation and multiple twinnings within each martensitic variant, provides a well-controlled (desired) description of variant-variant transformations and multiple twinning, including expressions for interface tension which are consistent with the sharp interface limit. The finite element approach is developed and applied to the solution of a number of examples of twinning and combined austenite-martensite and martensite-martensite phase transformations (PTs) and nanostructure evolution. A similar approach can be developed for electric and magnetic PTs.

2.1 Introduction

Twinning is a mechanism for plastic deformation in crystalline materials whereby a region of the crystal lattice is homogeneously sheared into a new orientation [1, 2]. It is most pronounced at low temperatures, high strain rates, and in small grains. Martensitic PTs are usually accompanied by twinning which reduces the energy associated with internal elastic stresses. Martensitic PTs involve several martensitic variants M_i, $i = 1, 2, ..., n$, where n equals the ratio of the order of the point group of the austenite A to that of the martensite. Since the M_i are usually in a twin relation to each other, variant-variant transformations and twinning in martensite are closely related. The phase field approach is widely used for modeling microstructure evolution during multivariant martensitic PTs and twinning [3–10]. Phase field models that incorporate the main features of stress-strain curves, large strain transformations,

and include surface tension were developed in [8, 11–14, 20]. In this section, we present a phase field model of variant-variant transformations and multiple twinning within the martensite.

2.2 Theory of twinning in martensite

For each twinning system $\{\mathsf{M}_1, \mathsf{M}_2, ...\mathsf{M}_n\}$, where the M_i are crystallographically equivalent, the transformation-deformation gradient $\boldsymbol{F}_{ti} = \boldsymbol{I} + \gamma(\eta_i)\,\boldsymbol{m}_i^0\boldsymbol{n}_i^0$ transforms the parent lattice L into a twinned lattice M_i by a simple shear γ in direction $\boldsymbol{m}_i^0$ in the plane with normal $\boldsymbol{n}_i^0$ in the reference state; here η_i, the ith order parameter, which varies between 0 for L and 1 for M_i, and $\boldsymbol{I}$ is the unit tensor. It is usually assumed that twinning can be described by a phase field model of PT for which the thermal part of the free energy does not change and the transformation strain corresponds to the twinning shear [8–10, 12, 16]. However, this is not completely consistent. The main difference is that, in contrast to PTs, twinning does not change the crystal structure: the unit cell of the twin is the same as that of the parent crystal to within a rigid-body rotation. This fact introduces a symmetry requirement not present in the PT theory: the thermodynamic potential and the transformation-deformation gradient must be completely symmetric with respect to the interchange $\mathsf{L}\leftrightarrow\mathsf{M}_i$. Our $2-3-4$ Landau potential for martensitic PT [11, 12] possesses this symmetry but our $2-4-6$ potential [13] does not. However, the main theoretical complication is multiple twinning, that is, secondary and further twinnings of the primary twin M_i, which commonly occurs. Again, since the crystal lattice of any twin M_i is indistinguishable to within rigid-body rotations from the parent lattice L, the thermodynamic potential and transformation-deformation gradient must be completely symmetric with respect to the interchanges $\mathsf{L}\leftrightarrow\mathsf{M}_i$ and $\mathsf{M}_j\leftrightarrow\mathsf{M}_i$ for all i and j. This condition is satisfied in the present model, but is not in any previous model of PTs and twinning.

Even for small strains, neither transformations between martensitic variants nor twinning in any known theory is described as consistent as $\mathsf{L}\leftrightarrow\mathsf{M}_i$ transformations. Indeed, the $\mathsf{L}\leftrightarrow\mathsf{M}_i$ transformation can be described by a single order parameter η_i, and the temperature-dependence of the stress-strain curve, and the L-M_i interface energy and width are completely determined by a small number of material parameters, and are well-controlled through analytical solutions for static and propagating interfaces [11–13]. In contrast, at a M_i-M_j interface in any known theory, the order parameters η_i and η_j vary independently, and the transformation path in the $\eta_i - \eta_j$ plane and the interface energy and width have an unrealistic dependence

on temperature, stresses, and a larger number of material parameters; these dependences can only be determined by numerical methods [21]. Thus, one cannot prescribe a desired M_i-M_j interface energy and width. Consequently, the consistency of the expression introduced in [20] for the interface (surface) tension $\boldsymbol{\sigma}_{st}$ with the sharp-interface limit can be proved for $L-M_i$ interfaces but not for M_i-M_j interfaces; in fact, simulations show that $\boldsymbol{\sigma}_{st}$ does not describe the sharp M_i-M_j interface limit. This shortcoming is rectified in the model presented here. Also, in large strain theory [8–10], the transformations $M_i \leftrightarrow M_j$ do not represent simple shears. There are an infinite number of combinations of rotations and twinning parameters for which two martensitic variants are twin related, e.g., zigzag twins [27], a situation that is to some extent similar to that for reconstructive PTs [19, 26]. Thus, it is impossible to parameterize all simple shears between two martensitic variants with a single order parameter.

2.3 New phase field theory of twinning in martensite

In this section, we present a new phase field model of martensitic variant-variant ($M_i \leftrightarrow M_j$) transformations and twinning within the variants which resolves all of the above problems. We define a minimal set of order parameters, each of them describes rotation-free deformation of crystal lattice: just n order parameters are required for n martensitic variants. The key point is that each $M_i \leftrightarrow M_j$ transformation and all twinnings within them are described with a single order parameter. This significantly simplifies the description of $M_j \leftrightarrow M_i$ transformations and multiple twinnings, including an expression for the interface tension, which is completely analogous to the description of $L \leftrightarrow M_i$ PT. One can prescribe a desired M_i-M_j interface energy and width. For the fully geometrically nonlinear theory (large strains and material rotation), the twinning parameters and lattice rotations are obtained from the solution of the coupled phase field and mechanics boundary-value problem. Model problems on twinning and combined $L \leftrightarrow M_i$ and $M_j \leftrightarrow M_i$ transformations and nanostructure evolution in a nanosize sample are solved by means of the finite element method (FEM) COMSOL code.

We designate contractions of tensors $\boldsymbol{A} = \{A_{ij}\}$ and $\boldsymbol{B} = \{B_{ji}\}$ over one and two indices as $\boldsymbol{A} \cdot \boldsymbol{B} = \{A_{ij} B_{jk}\}$ and $\boldsymbol{A} : \boldsymbol{B} = A_{ij} B_{ji}$, respectively. The subscripts s, e, and t mean symmetrization and elastic and transformational strains; $\boldsymbol{I}$ is the unit tensor; $\overset{\circ}{\nabla}$ and ∇ are the gradient operators in the undeformed and deformed states; and $\otimes$ designates a dyadic product.

2.3.A Advantages of current theory

In this theory, new advanced phase field model of transformations between martensitic variants and multiple twinning within martensitic variants is developed. It resolves numerous existing problems:

1. Large strain and rotation formulation is developed, which is not based on simple shears along all numerous possible twinning systems. Instead, it is based on just n rotation-free deformation tensors for each of n martensitic variants (e.g., n=3 for cubic-tetragonal transformation); all twinning parameters and lattice rotations are obtained from the solution of the coupled phase field and mechanics boundary-value problem. In such a way, the number of order parameters is reduced from infinity (in general case) to the number of martensitic variants.

2. With new order parameters, each twinning and variant-variant transformation is described by a single order parameter, similar to the austenite-martensite transformation. This allowed us to prescribe the desired values for the energies and widths of the variant-variant interfaces through known analytical solutions.

3. The interface stresses for twinning (variant-variant) interfaces are introduced, which are consistent with the sharp interface limit.

The finite element approach is developed and applied to the solution of a number of nontrivial examples of twinning and combined austenite-martensite and martensite-martensite phase transformations and nanostructure evolution. A similar approach in terms of our order parameters could be developed for electric and magnetic PTs and for other phenomena described by multiple order parameters.

2.4 General equation for n martensitic variants

The motion of the elastic material undergoing twinning will be described by a vector-valued function $\boldsymbol{r} = \boldsymbol{r}(\boldsymbol{r}_0, t)$, where $\boldsymbol{r}_0$ and $\boldsymbol{r}$ are the positions of points in the reference Ω_0 and

the deformed Ω configurations, respectively, and t is the time. The austenite A lattice will be considered as the reference configuration, independent of whether we consider PT A$\leftrightarrow$M$_i$ or M$_i\leftrightarrow$M$_j$ transformations only. The transformation deformation gradient $\boldsymbol{U}_{ti} = \boldsymbol{I} + \boldsymbol{\varepsilon}_{ti}$ transforms the crystal lattice of A into the lattice of the ith martensitic variant M$_i$, $i = 1, 2, ..., n$, both in the unloaded state. The multiplicative decomposition of the deformation gradient, $\boldsymbol{F} = \boldsymbol{F}_e \cdot \boldsymbol{U}_t$, into elastic $\boldsymbol{F}_e$ and transformational $\boldsymbol{U}_t$ parts will be used [18]. Since $\boldsymbol{U}_t = \boldsymbol{U}_t^T$, lattice rotation is included in $\boldsymbol{F}_e$. We assume the martensitic variants are in twin relation with each other, hence they satisfy the twinning equation $\boldsymbol{Q}_i \cdot \boldsymbol{U}_{ti} - \boldsymbol{Q}_j \cdot \boldsymbol{U}_{tj} = \gamma_{ij}\, \boldsymbol{m}_{ij}^0 \boldsymbol{n}_{ij}^0$ for some twinning system parameters γ_{ij}, $\boldsymbol{m}_{ij}^0$, $\boldsymbol{n}_{ij}^0$ and rigid-body rotations $\boldsymbol{Q}_m$. Since there are numerous solutions to the twinning equation for the same i and j (which is to some extent similar to that for reconstructive PTs [19, 26]), e.g., zigzag twins [27], it is impractical (and unnecessary) to parameterize simple shear between each of them with a separate order parameter. Instead, we describe all possible twinnings and variant-variant transformations with only n order parameters. The solution of the coupled large-strain phase field and mechanics boundary-value problem gives the twinning system parameters.

In our n-dimensional order parameter space, the austenite A is located at the origin and the ith martensitic variant M$_i$ is located at the intersection of the positive i^{th} axis with the unit sphere. The radial coordinate, designated $\boldsymbol{r}$, describes A$\leftrightarrow$M$_i$ transformations, while the angular order parameters $0 \leq \vartheta_i \leq 1$, where $\pi\, \vartheta_i/2$ is the angle between the radius vector $\boldsymbol{r}$ and the positive i^{th} axis, describe twinning M$_k\leftrightarrow$M$_i$ (variant-variant) transformations. Such geometric interpretation leads to the constraint $\sum_{k=1}^n \cos^2\left(\frac{\pi}{2}\vartheta_k\right) = 1$, which significantly complicates the development of the thermodynamic potential. However, for each variant-variant or twinning transformations M$_i\leftrightarrow$M$_j$ (at $r = 1$, $\vartheta_k = 1$ for $k \neq i, j$) this constraint reduces to the linear one $\vartheta_j + \vartheta_i = 1$. That is why we accept a linear constraint $\sum_{i=1}^n \vartheta_i = n - 1$ for the general case, which slightly changes geometric interpretation when more than two order parameters ϑ_i deviate from 1 but allow us to develop a desired potential. Then $\vartheta_n = n - 1 - \sum_{i=1}^{n-1} \vartheta_i$ replaces all occurrences of the parameter ϑ_n in all equations below. The Helmholtz free energy per unit undeformed volume is given by the following expression:

$$\psi = \psi^e(\boldsymbol{B}, r, \vartheta_i, \theta) + \frac{\rho_0}{\rho}\breve{\psi}^\theta + \psi^\theta + \frac{\rho_0}{\rho}\psi^\nabla; \tag{1}$$

$$\breve{\psi}^{\theta} = A_0(\theta_e - \theta_c)r^2(1-r)^2 + \bar{A}\sum_{i,j=1;i\neq j}^{n}(1-\vartheta_i)^2(1-\vartheta_j)^2 q(r); \tag{2}$$

$$\psi^{\nabla} = \frac{\beta}{2}|\boldsymbol{\nabla}r|^2 + q(r)\frac{\beta_\vartheta}{4}\sum_{i=1}^{n}|\boldsymbol{\nabla}\vartheta_i|^2; \tag{3}$$

$$\psi^{\theta} = A_0/3(\theta - \theta_e)q(r); \quad q(r) = r^2(3-2r); \tag{4}$$

$$\boldsymbol{U}_t = \boldsymbol{I} + \sum_{k=1}^{n}\boldsymbol{\varepsilon}_{tk}\left(1 - 3\vartheta_k^2 + 2\vartheta_k^3\right)\varphi(r); \quad \varphi(r) = ar^2 + (4-2a)r^3 + (a-3)r^4. \tag{5}$$

Here $\boldsymbol{B} = (\boldsymbol{V}\cdot\boldsymbol{V} - \boldsymbol{I})/2$ is the finite strain measure, $\boldsymbol{V}$ is the left stretch tensor, θ is the temperature, θ_e is the equilibrium temperature, A becomes unstable at temperature θ_c, ρ and ρ_0 are the mass densities in the deformed and undeformed states, β and β_ϑ are gradient energy coefficients, A_0, $\bar{A}$, and a are material parameters, and ψ^e is the elastic energy (the same as in [20]). Thermodynamics and Landau-Ginzburg kinetics (see, e.g. [20]) leads to

$$\boldsymbol{\sigma} = \frac{\rho}{\rho_0}\boldsymbol{V}\cdot\frac{\partial\psi}{\partial\boldsymbol{B}}\cdot\boldsymbol{V} - \frac{\rho}{\rho_0}\left(\boldsymbol{\nabla}r\otimes\frac{\partial\psi}{\partial\boldsymbol{\nabla}r}\right)_s - \sum_{i=1}^{n-1}\frac{\rho}{\rho_0}\left(\boldsymbol{\nabla}\vartheta_i\otimes\frac{\partial\psi}{\partial\boldsymbol{\nabla}\vartheta_i}\right)_s; \tag{6}$$

$$\frac{1}{\lambda_r}\frac{\partial r}{\partial t} = -\frac{\rho}{\rho_0}\frac{\partial\psi}{\partial r}|_{\boldsymbol{B}} + \boldsymbol{\nabla}\cdot\left(\frac{\rho}{\rho_0}\frac{\partial\psi}{\partial\boldsymbol{\nabla}r}\right); \quad \frac{1}{\lambda_\vartheta}\frac{\partial\vartheta_i}{\partial t} = -\frac{\rho}{\rho_0}\frac{\partial\psi}{\partial\vartheta_i}|_{\boldsymbol{B}} + \boldsymbol{\nabla}\cdot\left(\frac{\rho}{\rho_0}\frac{\partial\psi}{\partial\boldsymbol{\nabla}\vartheta_i}\right), \tag{7}$$

where λ_r and λ_ϑ are kinetic coefficients, $\boldsymbol{\sigma}$ is the true Cauchy stress tensor, and $\partial\psi/\partial r$ and $\partial\psi/\partial\vartheta_i$ are evaluated at constant finite strain $\boldsymbol{B}$. Eqs.(1)-(14) satisfy all conditions for the thermodynamic potential formulated in [11–13]. In particular, A and the variants M_i are homogeneous solutions of the Ginzburg-Landau equations (19) for arbitrary stresses and temperature; the transformation strain for any transformation is independent of stresses and temperature; the transformation criteria that follow from the thermodynamic instability conditions have the same (correct) form as in [11–13]. The potential (1)-(14) is much simpler than those previously used for martensitic PTs [8, 11–13, 20] and does not require the introduction of sophisticated cross terms, which has several important consequences. In particular, the potential does not possess spurious minima (unphysical phases). The variant-variant or twinning transformations $\mathsf{M}_i\leftrightarrow\mathsf{M}_j$ are described by a single order parameter ϑ_i (at $r=1$, $\vartheta_k = 1$ for $k \neq i, j$, and $\vartheta_j = 1 - \vartheta_i$) and are controllable in the same way as $\mathsf{A}\leftrightarrow\mathsf{M}_i$ PTs. The ratio ρ_0/ρ and the gradient with respect to the deformed configuration are used in Eqs.(1)-(14) to introduce interface tension, as in [20]. Since the $\mathsf{M}_j\leftrightarrow\mathsf{M}_i$ transformations are here described in the same way as $\mathsf{A}\leftrightarrow\mathsf{M}_i$ PT, it is now trivial to demonstrate the consistency of the expression for the in-

terface tension (obtained from Eq. (15) after subtracting the elastically-supported stress) with the sharp interface limit, whereas this could be proved only for $\mathsf{A}-\mathsf{M}_i$ interfaces in [20]. The thermodynamic potential and $\boldsymbol{U}_t$ are symmetric with respect to the interchanges $\mathsf{M}_j \leftrightarrow \mathsf{M}_i$; they need not be symmetric with respect to the interchange $\mathsf{A} \leftrightarrow \mathsf{M}_i$ because $\mathsf{A} \leftrightarrow \mathsf{M}_i$ is not a twinning.

2.5 Problem description and formulation for 2 martensitic variants

Helmholtz free energy and its contributions for 2 martensitic variants

$$\psi = \psi^e(\varepsilon_0, r, \vartheta_1, \theta) + \frac{\rho_0}{\rho}\breve{\psi}^\theta + \psi^\theta + \frac{\rho_0}{\rho}\psi^\nabla; \tag{8}$$

1. Elastic energy for equal elastic properties of phases

$$\psi^e = \frac{1}{2}K\varepsilon_{0e}^2 + \mu\boldsymbol{e}_e : \boldsymbol{e}_e; \tag{9}$$

2. The thermal part of Helmholtz free energy responsible for the driving force for phase transformation

$$\psi^\theta = A_0/3(\theta - \theta_e)q(r); \quad q(r) = r^2(3 - 2r); \tag{10}$$

3. Thermal Part of the Helmholtz free energy responsible for the barrier between phases

$$\breve{\psi}^\theta = A_0(\theta_e - \theta_c)r^2(1 - r)^2 + \bar{A}\vartheta_1^2(1 - \vartheta_1)^2 q(r); \tag{11}$$

4. Gradient Energy

$$\psi^\nabla = \frac{\beta_{AM}}{2}|\boldsymbol{\nabla}r|^2 + q(r)\frac{\beta_{MM}}{2}\left(|\boldsymbol{\nabla}\vartheta_1|^2 + |\boldsymbol{\nabla}\vartheta_2|^2\right); \tag{12}$$

Transformation deformation gradient

$$\boldsymbol{U}_t = \boldsymbol{I} + \boldsymbol{\varepsilon}_{t1}\left(1 - 3\vartheta_1^2 + 2\vartheta_1^3\right)\varphi(r) + \boldsymbol{\varepsilon}_{t2}\left(1 - 3\vartheta_2^2 + 2\vartheta_2^3\right)\varphi(r);$$

$$\varphi(r) = ar^2 + (4 - 2a)r^3 + (a - 3)r^4 \tag{13}$$

In terms on independent order parameter

$$\boldsymbol{U}_t = \boldsymbol{I} + \boldsymbol{\varepsilon}_{t1}\left(1 - 3\vartheta_1^2 + 2\vartheta_1^3\right)\varphi(r) + \boldsymbol{\varepsilon}_{t2}\left(3\vartheta_1^2 - 2\vartheta_1^3\right)\varphi(r) \tag{14}$$

Expression for the Cauchy Stress

$$\boldsymbol{\sigma} = \frac{\rho}{\rho_0}\boldsymbol{V}\cdot\frac{\partial\psi}{\partial\boldsymbol{B}}\cdot\boldsymbol{V} - \frac{\rho}{\rho_0}\left(\boldsymbol{\nabla}r\otimes\frac{\partial\psi}{\partial\boldsymbol{\nabla}r}\right)_s - \sum_{i=1}^{2}\frac{\rho}{\rho_0}\left(\boldsymbol{\nabla}\vartheta_i\otimes\frac{\partial\psi}{\partial\boldsymbol{\nabla}\vartheta_i}\right)_s; \tag{15}$$

$$\boldsymbol{\sigma} = \boldsymbol{\sigma_e} + \boldsymbol{\sigma_{st}} \tag{16}$$

Hook's law for elastic stresses

$$\boldsymbol{\sigma_e} = \frac{\partial\,\psi^e}{\partial\,\boldsymbol{\varepsilon}} = K\varepsilon_{0e}I + 2\mu\boldsymbol{e}_e \tag{17}$$

Interface tension tensor for 2 martensitic variants

$$\boldsymbol{\sigma}_{st} = (\psi^\nabla + \breve{\psi}_\theta)\boldsymbol{I} - \beta_{AM}(\boldsymbol{\nabla}r\otimes\boldsymbol{\nabla}r) - q(r)\,\beta_{MM}(\boldsymbol{\nabla}\vartheta_1\otimes\boldsymbol{\nabla}\vartheta_1) \tag{18}$$

Ginzburg-Landau Equations

$$\frac{1}{\lambda_{AM}}\frac{\partial r}{\partial t} = -\frac{\rho}{\rho_0}\frac{\partial\psi}{\partial r}|_{\boldsymbol{B}} + \boldsymbol{\nabla}\cdot\left(\frac{\rho}{\rho_0}\frac{\partial\psi}{\partial\boldsymbol{\nabla}r}\right); \quad \frac{1}{\lambda_{MM}}\frac{\partial\vartheta_1}{\partial t} = -\frac{\rho}{\rho_0}\frac{\partial\psi}{\partial\vartheta_1}|_{\boldsymbol{B}} + \boldsymbol{\nabla}\cdot\left(\frac{\rho}{\rho_0}\frac{\partial\psi}{\partial\boldsymbol{\nabla}\vartheta_1}\right) \tag{19}$$

For two martensitic variants, G-L equation for Austenite to Martensitic variant transformation

$$\frac{1}{\lambda_{AM}}\frac{\partial r}{\partial t} = \frac{\rho}{\rho_o}\boldsymbol{\sigma}_e\boldsymbol{:}\frac{\partial\boldsymbol{\varepsilon}_t}{\partial r} - \frac{\rho}{\rho_o}\frac{\partial\psi^\theta}{\partial r} - \frac{\partial\breve{\psi}^\theta}{\partial r} - \frac{\partial\psi^\nabla}{\partial r} + \boldsymbol{\nabla}\left(\frac{\rho}{\rho_o}\frac{\partial\psi}{\partial\boldsymbol{\nabla}r}\right) \tag{20}$$

In expanded form

$$\frac{1}{\lambda_{AM}}\frac{\partial r}{\partial t} = \frac{1}{1+\varepsilon_o}[\,(\boldsymbol{\sigma}-\boldsymbol{\sigma}_{st})\boldsymbol{:}\boldsymbol{\varepsilon}_{t1}(1-3\vartheta_1^2+2\vartheta_1^3) - (\boldsymbol{\sigma}-\boldsymbol{\sigma}_{st})\boldsymbol{:}\boldsymbol{\varepsilon}_{t2}(3\vartheta_1^2-2\vartheta_1^3)][2ar+3(4-2a)r^2$$

$$+4(a-3)r^3] - \frac{6\Delta G^\theta}{1+\varepsilon_o}r(1-r) - 6\bar{A}r(1-r)\vartheta_1^2(1-\vartheta_1)^2 -$$

$$2Ar(1-3r+2r^2) - 3\beta_{MM}r(1-r)(|\boldsymbol{\nabla}\vartheta_1|)^2 + \beta_{AM}\boldsymbol{\nabla}^2\vartheta_1 \tag{21}$$

For two martensitic variants, G-L equations for Martensite to Martensite transformation

$$\frac{1}{\lambda_{MM}}\frac{\partial \vartheta_1}{\partial t} = \frac{\rho}{\rho_o}\boldsymbol{\sigma}_e\colon\frac{\partial \boldsymbol{\varepsilon}_t}{\partial \vartheta_1} - \frac{\rho}{\rho_o}\frac{\partial \psi^\theta}{\partial \vartheta_1} - \frac{\partial \breve{\psi}^\theta}{\partial \vartheta_1} - \frac{\partial \psi^\nabla}{\partial \vartheta_1} + \boldsymbol{\nabla}\left(\frac{\rho}{\rho_o}\frac{\partial \psi}{\partial \boldsymbol{\nabla}\vartheta_1}\right) \tag{22}$$

In expanded form

$$\frac{1}{\lambda_{MM}}\frac{\partial \vartheta_1}{\partial t} = \frac{1}{1+\varepsilon_o}\big[\,(\boldsymbol{\sigma}-\boldsymbol{\sigma}_{st})\colon\boldsymbol{\varepsilon}_{t1}(6\vartheta_1^2-6\vartheta_1) - (\boldsymbol{\sigma}-\boldsymbol{\sigma}_{st})\colon\boldsymbol{\varepsilon}_{t2}(6\vartheta_1-6\vartheta_1^2)\big][ar^2+(4-2a)r^3$$
$$+(a-3)r^4] - 2\bar{A}\vartheta_1 r^2(3-2r)(1-3\vartheta_1+2\vartheta_1^2) + r^2(3-2r)\boldsymbol{\nabla}^2\vartheta_1\beta_{MM} \tag{23}$$

Equilibrium equation

$$\boldsymbol{\nabla}\cdot\boldsymbol{\sigma}=0 \tag{24}$$

Boundary conditions for the order parameters

$$\boldsymbol{n}\cdot\boldsymbol{\nabla}\eta_i=0 \tag{25}$$

2.6 Equivalence of equations for austenite martensite and martensite-martensite transformations

Let us simplify Eqs.(2)-(7) for the austenite-martensite phase transformation by putting $\vartheta_2=0$, $\vartheta_i=1$ for $i\neq 2$. We also put $a=3$, which leads to $\varphi(r)=q(r)$. This is necessary to make the transformation strain between the austenite and martensite symmetric with respect to the interchanges $\mathsf{L}\leftrightarrow\mathsf{A}_i$, in the same sense as it is symmetric for variant-variant transformation. Then

$$\breve{\psi}^\theta = A_0(\theta_e-\theta_c)r^2(1-r)^2; \tag{26}$$

$$\psi^\nabla = \frac{\beta}{2}|\boldsymbol{\nabla}r|^2; \tag{27}$$

$$\boldsymbol{U}_t = \boldsymbol{I}+\boldsymbol{\varepsilon}_{t2}q(r); \tag{28}$$

$$\boldsymbol{\sigma} = \frac{\rho}{\rho_0}\boldsymbol{V}\cdot\frac{\partial \psi}{\partial \boldsymbol{B}}\cdot\boldsymbol{V} - \frac{\rho}{\rho_0}\left(\boldsymbol{\nabla}r\otimes\frac{\partial \psi}{\partial \boldsymbol{\nabla}r}\right)_s; \tag{29}$$

$$\frac{1}{\lambda_r}\frac{\partial r}{\partial t} = -\frac{\rho}{\rho_0}\frac{\partial \psi}{\partial r}\big|_{\boldsymbol{B}} + \boldsymbol{\nabla}\cdot\left(\frac{\rho}{\rho_0}\frac{\partial \psi}{\partial \boldsymbol{\nabla}r}\right). \tag{30}$$

Next, let us simplify Eqs.(2)-(7) for the $M_1 \leftrightarrow M_2$ transformation but putting $r = 1$, $\vartheta = \vartheta_1$, $\vartheta_2 = 1 - \vartheta$, and $\vartheta_i = 1$ for $2 < i \leq n$. Then

$$\breve{\psi}^\theta = \bar{A}\vartheta^2(1-\vartheta)^2; \tag{31}$$

$$\nabla = \frac{\beta_\vartheta}{2}|\boldsymbol{\nabla}\vartheta|^2; \tag{32}$$

$$\boldsymbol{U}_t = \boldsymbol{I} + \boldsymbol{\varepsilon}_{t1} + (\boldsymbol{\varepsilon}_{t2} - \boldsymbol{\varepsilon}_{t1})q(\vartheta); \tag{33}$$

$$\boldsymbol{\sigma} = \frac{\rho}{\rho_0}\boldsymbol{V} \cdot \frac{\partial\psi}{\partial\boldsymbol{B}} \cdot \boldsymbol{V} - \frac{\rho}{\rho_0}\left(\boldsymbol{\nabla}\vartheta \otimes \frac{\partial\psi}{\partial\boldsymbol{\nabla}\vartheta}\right)_s; \tag{34}$$

$$\frac{1}{\lambda_\vartheta}\frac{\partial\vartheta}{\partial t} = -\frac{\rho}{\rho_0}\frac{\partial\psi}{\partial\vartheta}|_{\boldsymbol{B}} + \boldsymbol{\nabla} \cdot \left(\frac{\rho}{\rho_0}\frac{\partial\psi}{\partial\boldsymbol{\nabla}\vartheta}\right). \tag{35}$$

It is clear that Eqs.(26)-(30) are equivalent to Eqs.(31)-(35) after substituting $r \leftrightarrow \vartheta$ with the following correspondence of constants:

$$A_0(\theta_e - \theta_c) \leftrightarrow \bar{A}; \qquad \beta \leftrightarrow \beta_\vartheta; \qquad \boldsymbol{\varepsilon}_{t1} \leftrightarrow 0; \qquad \lambda_r \leftrightarrow \lambda_\vartheta. \tag{36}$$

For the austenite-martensite interface, the combination of Eq.(1) and Eqs.(26)-(30) resulted in the desired expression for the interface (surface) tension $\boldsymbol{\sigma}_{st}$ [20, 21]. Since Eqs.(31)-(35) for twinning are equivalent to Eqs.(26)-(30) for the austenite-martensite transformation, the expression for the interface tension $\boldsymbol{\sigma}_{st}$ for the M_i-M_j interface has the same desired expression. This proves the advantage of the chosen order parameters and phase field formulation in comparison with previous studies.

2.7 Gibbs Energy for 2 Martensitic Variants and Small Strains

In the 2-dimensional plane of order parameters, both martensitic variants are located on the unit circle, and $\vartheta := \vartheta_1 = 1 - \vartheta_2$. Thus, Gibbs potentials can be developed using the radial order parameters r and single angular order parameter ϑ. New Gibbs potentials in r and ϑ_1 can be derived from $2 - 3 - 4$ and potentials $G(r)$ for a single martensitic variant by allowing for ϑ_1 dependence in the transformation strain and including a term that introduces ϑ_1-dependent barriers between all variants.

Gibbs Potential for n martensitic variants is

$$G = -\frac{1}{2}\boldsymbol{\sigma} : \boldsymbol{\lambda} : \boldsymbol{\sigma} - \boldsymbol{\sigma} : \sum_{k=1}^{n} \boldsymbol{\varepsilon}_{tk}\left(1 - 3\,\vartheta_k^2 + 2\,\vartheta_k^3\right)\,\varphi(r) + f(\theta, r) + \bar{A}\sum_{i,j=1;i\neq j}^{n}(1 - \vartheta_i)^2(1 - \vartheta_j)^2 q(r)\,, \tag{37}$$

where

$$\varphi\left(r\right) = a\,r^2 + (4 - 2\,a)\,r^3 + (a - 3)\,r^4\,, \qquad 0 < a < 6\,,$$

$$f\left(\theta, r\right) = A\,r^2 + \left(4\,\Delta\,G^\theta - 2\,A\right)r^3 + \left(A - 3\,\Delta\,G^\theta\right)r^4\,, \tag{38}$$

and

$$q\left(r\right) = 3\,r^2 - 2\,r^3\,. \tag{39}$$

Then for 2 martensitic variants it simplifies to

$$G = -\frac{1}{2}\boldsymbol{\sigma} : \boldsymbol{\lambda} : \boldsymbol{\sigma} - \boldsymbol{\sigma} : \boldsymbol{\varepsilon}_{t1}\left(1 - 3\,\vartheta_1^2 + 2\,\vartheta_1^3\right)\,\varphi(r) - \boldsymbol{\sigma} : \boldsymbol{\varepsilon}_{t2}\left(1 - 3\,\vartheta_2^2 + 2\,\vartheta_2^3\right)\,\varphi(r) + f(\theta, r)$$
$$+ \bar{A}(1 - \vartheta_1)^2(1 - \vartheta_2)^2 q(r)\,. \tag{40}$$

Substituting $\vartheta_2 = 1 - \vartheta_1$ to Eqs. (40) leads to

$$G = -\frac{1}{2}\boldsymbol{\sigma} : \boldsymbol{\lambda} : \boldsymbol{\sigma} - \boldsymbol{\sigma} : \boldsymbol{\varepsilon}_{t1}\left(1 - 3\,\vartheta_1^2 + 2\,\vartheta_1^3\right)\,\varphi(r) - \boldsymbol{\sigma} : \boldsymbol{\varepsilon}_{t2}\left(3\,\vartheta_1^2 - 2\,\vartheta_1^3\right)\,\varphi(r) + f(\theta, r)$$
$$+ \bar{A}\vartheta_1^2(1 - \vartheta_1^2)q(r)\,. \tag{41}$$

Differentiating G in Eq.(41) with respect to order parameter r, one obtains

$$\frac{\partial G}{\partial r} = -\boldsymbol{\sigma} : \boldsymbol{\varepsilon}_{t1}\left(1 - 3\,\vartheta_1^2 + 2\,\vartheta_1^3\right)\,\varphi'(r) - \boldsymbol{\sigma} : \boldsymbol{\varepsilon}_{t2}\left(3\,\vartheta_1^2 - 2\,\vartheta_1^3\right)\,\varphi'(r) + f^r(\theta, r)$$
$$+ \bar{A}\vartheta_1^2(1 - \vartheta_1^2)q'(r)\,. \tag{42}$$

where

$$\varphi'\left(r\right) = 2a\,r + 3\left(4 - 2\,a\right)r^2 + 4(a - 3)\,r^3\,, \tag{43}$$

$$f^r\left(\theta, r\right) = 2\,A\,r + 3\left(4\,\Delta\,G^\theta - 2\,A\right)r^2 + 4\left(A - 3\,\Delta\,G^\theta\right)r^3\,, \tag{44}$$

and

$$q'\left(r\right) = 6\,r - 6\,r^2\,. \tag{45}$$

Similar, differentiating G in Eq.(41) with respect to order parameter ϑ_1, we obtain

$$\frac{\partial G}{\partial \vartheta_1} = -\boldsymbol{\sigma} : \boldsymbol{\varepsilon}_{t1} \left(6\,\vartheta_1^2 - 6\,\vartheta_1\right)\, \varphi(r) - \boldsymbol{\sigma} : \boldsymbol{\varepsilon}_{t2} \left(6\,\vartheta_1 - 6\,\vartheta_1^2\right)\, \varphi(r) + f(\theta, r)$$

$$+ \bar{A}(2\vartheta_1 - 6\vartheta_1^2 + 4\vartheta_1^3)q(r) \tag{46}$$

It is easy to check that the austenite $r = 0$ and martensitic variants M_1 $(r = 1, \vartheta_1 = 0)$ and M_2 $(r = 1, \vartheta_1 = 1)$ satisfy thermodynamic equilibrium conditions

$$\frac{\partial G}{\partial r} = \frac{\partial G}{\partial \vartheta_1} = 0 \tag{47}$$

for all stresses $\boldsymbol{\sigma}$ and temperature θ. For two variants, our new model reduces to the model in [13].

2.8 Formulation for 3 Martensitic variants

For 3 martensitic variants, the constraints equation reduces to

$$\sum_{k=1}^{3} \vartheta_k = 2 \,; \quad \vartheta_1 + \vartheta_2 + \vartheta_3 = 2 \tag{48}$$

Gibbs Potential for 3 Martensitic variants is

$$G = -\frac{1}{2}\boldsymbol{\sigma} : \boldsymbol{\lambda} : \boldsymbol{\sigma} - \boldsymbol{\sigma} : \sum_{k=1}^{3} \boldsymbol{\varepsilon}_{tk} \left(1 - 3\,\vartheta_k^2 + 2\,\vartheta_k^3\right)\, \varphi(r) + f(\theta, r) + \tag{49}$$

$$\bar{A} \left[(1 - \vartheta_1)^2\, (1 - \vartheta_2)^2 + (1 - \vartheta_2)^2\, (1 - \vartheta_3)^2 + (1 - \vartheta_1)^2\, (1 - \vartheta_3)^2 \right] q(r) \,.$$

Here it is noted that we have 4 order parameters to describe the 3 Martensitic Variants. Out of 4 order parameters, we have 3 independent order parameters and one dependent order parameter (ϑ_3), which is related to other order parameters through Eqs. (48). Replacing $\vartheta_3 = (2 - \vartheta_1 - \vartheta_2)$ in Eq. (50), we get

$$G = -\frac{1}{2}\boldsymbol{\sigma} : \boldsymbol{\lambda} : \boldsymbol{\sigma} - \boldsymbol{\sigma} : \boldsymbol{\varepsilon}_{t1} \left(1 - 3\,\vartheta_1^2 + 2\,\vartheta_1^3\right)\, \varphi(r) - \boldsymbol{\sigma} : \boldsymbol{\varepsilon}_{t2} \left(1 - 3\,\vartheta_2^2 + 2\,\vartheta_2^3\right)\, \varphi(r) \tag{50}$$

$$- \boldsymbol{\sigma} : \boldsymbol{\varepsilon}_{t3} \left[1 - 3\left(2 - \vartheta_1 - \vartheta_2\right)^2 + 2\left(2 - \vartheta_1 - \vartheta_2\right)^3\right]\, \varphi(r) + f(\theta, r)$$

$$+ \bar{A} \left[(1 - \vartheta_1)^2\, (1 - \vartheta_2)^2 + (1 - \vartheta_2)^2\, (\vartheta_1 + \vartheta_2 - 1)^2 + (1 - \vartheta_1)^2\, (\vartheta_1 + \vartheta_2 - 1)^2 \right] q(r) \,.$$

$$\varphi(r) = a\,r^2 + (4 - 2\,a)\,r^3 + (a - 3)\,r^4 \,, \qquad 0 < a < 6 \,,$$

$$f(\theta, r) = A\,r^2 + \left(4\,\Delta\,G^\theta - 2\,A\right)r^3 + \left(A - 3\,\Delta\,G^\theta\right)r^4 \,, \tag{51}$$

and

$$q(r) = 3r^2 - 2r^3. \tag{52}$$

Differentiating Eqs.(51) with respect to order parameter r, we obtain

$$\frac{\partial G}{\partial r} = -\boldsymbol{\sigma} : \sum_{k=1}^{n} \boldsymbol{\varepsilon}_{tk} \left(1 - 3\vartheta_k^2 + 2\vartheta_k^3\right) \varphi'(r) + f^r(\theta, r) + \bar{A} \left[(1 - \vartheta_1)^2 (1 - \vartheta_2)^2 \right. \tag{53}$$
$$\left. + (1 - \vartheta_2)^2 (\vartheta_1 + \vartheta_2 - 1)^2 + (1 - \vartheta_1)^2 (\vartheta_1 + \vartheta_2 - 1)^2 \right] q'(r).$$

where

$$\varphi'(r) = 2ar + 3(4 - 2a)r^2 + 4(a - 3)r^3,$$
$$f^r(\theta, r) = 2Ar + 3\left(4\Delta G^\theta - 2A\right)r^2 + 4\left(A - 3\Delta G^\theta\right)r^3, \tag{54}$$

and

$$q'(r) = 6r - 6r^2. \tag{55}$$

Differentiating Eqs.(51) with respect to ϑ_1, one derives

$$\frac{\partial G}{\partial \vartheta_1} = -\boldsymbol{\sigma} : \boldsymbol{\varepsilon}_{t1} \left(6\vartheta_1^2 - 6\vartheta_1\right) \varphi(r) + \boldsymbol{\sigma} : \boldsymbol{\varepsilon}_{t3} [12 - 6\vartheta_1 - 6\vartheta_2 - 6(2 - \vartheta_1 - \vartheta_2)^2] \varphi(r)$$
$$- \bar{A} [2(1 - \vartheta_2)^2(\vartheta_1 + \vartheta_2 - 1) - 2(1 - \vartheta_1)(\vartheta_1 + \vartheta_2 - 1)^2$$
$$+ 2(1 - \vartheta_1)^2(\vartheta_1 + \vartheta_2 - 1) - 2(1 - \vartheta_1)(1 - \vartheta_2)^2] q(r). \tag{56}$$

Similar, differentiating Eqs.(51) with respect to ϑ_2

$$\frac{\partial G}{\partial \vartheta_2} = -\boldsymbol{\sigma} : \boldsymbol{\varepsilon}_{t2} \left(6\vartheta_2^2 - 6\vartheta_2\right) \varphi(r) + \boldsymbol{\sigma} : \boldsymbol{\varepsilon}_{t3} [12 - 6\vartheta_1 - 6\vartheta_2 - 6(2 - \vartheta_1 - \vartheta_2)^2] \varphi(r)$$
$$- \bar{A} [2(1 - \vartheta_2)^2(\vartheta_1 + \vartheta_2 - 1) - 2(1 - \vartheta_2)(\vartheta_1 + \vartheta_2 - 1)^2$$
$$+ 2(1 - \vartheta_1)^2(\vartheta_1 + \vartheta_2 - 1) - 2(1 - \vartheta_1)(1 - \vartheta_2)^2] q(r). \tag{57}$$

It is easy to check that the austenite ($r = 0$ and arbitrary ϑ) and martensitic variants M_1 ($r = 1$, $\vartheta_1 = 0$, $\vartheta_2 = 1$, $\vartheta_3 = 1$), M_2 ($r = 1$, $\vartheta_2 = 0$, $\vartheta_1 = 1$, and $\vartheta_3 = 1$), and M_3 ($r = 1$, $\vartheta_0 = 0$, $\vartheta_1 = 1$, and $\vartheta_2 = 1$) satisfy *thermodynamic equilibrium conditions*

$$\frac{\partial G}{\partial r} = \frac{\partial G}{\partial \vartheta_1} = \frac{\partial G}{\partial \vartheta_2} = 0 \tag{58}$$

for all stresses $\boldsymbol{\sigma}$ and temperature θ.

2.9 Thermodynamics Stability in terms of Gibbs Potential

Differentiating Eqs.(54) with respect to r, one obtains

$$
\begin{aligned}
\frac{\partial^2 G}{\partial r^2} ={}& -\boldsymbol{\sigma} : \boldsymbol{\varepsilon}_{t1} \left(1 - 3\,\vartheta_1^2 + 2\,\vartheta_2^3\right) \; \varphi''(r) - \boldsymbol{\sigma} : \boldsymbol{\varepsilon}_{t2} \left(1 - 3\,\vartheta_2^2 + 2\,\vartheta_2^3\right) \; \varphi''(r) \\
& -\boldsymbol{\sigma} : \boldsymbol{\varepsilon}_{t3}[1 - 3\left(2 - \vartheta_1 - \vartheta_2\right)^2 + 2\left(2 - \vartheta_1 - \vartheta_2\right)^3]\,\varphi''(r) + f^{rr}(\theta, r) \\
& + \bar{A}\,[\,(1 - \vartheta_1)^2\,(1 - \vartheta_2)^2 + (1 - \vartheta_2)^2\,(\vartheta_1 + \vartheta_2 - 1)^2 \\
& \qquad\qquad + (1 - \vartheta_1)^2\,(\vartheta_1 + \vartheta_2 - 1)^2]q''(r)\,.
\end{aligned}
\tag{59}
$$

where

$$
\varphi''(r) = 2a + 6\left(4 - 2\,a\right)r + 12(a - 3)\,r^2\,,
$$

$$
f^{rr}(\theta, r) = 2A + 6\left(4\Delta\,G^\theta - 2A\right)r + 12\left(A - 3\Delta\,G^\theta\right)r^2\,,
\tag{60}
$$

and

$$
q''(r) = 6 - 12\,r\,.
\tag{61}
$$

Differentiating Eqs.(56) with respect to ϑ_1, we receive

$$
\begin{aligned}
\frac{\partial^2 G}{\partial \vartheta_1^2} ={}& -\boldsymbol{\sigma} : \boldsymbol{\varepsilon}_{t1} \left(12\vartheta_1 - 6\right)\;\varphi(r) - \boldsymbol{\sigma} : \boldsymbol{\varepsilon}_{t3} \left(18 - 12\vartheta_1 - 12\vartheta_2\right)\;\varphi(r) + f(\theta, r) \\
& + \bar{A}\,[2(1 - \vartheta_1)^2 + 4(1 - \vartheta_2)^2 - 8(1 - \vartheta_1)(\vartheta_1 + \vartheta_2 - 1) \\
& \qquad\qquad + 2(\vartheta_1 + \vartheta_2 - 1)^2]q(r)\,.
\end{aligned}
\tag{62}
$$

Differentiating Eqs.(57) with respect to ϑ_2

$$
\begin{aligned}
\frac{\partial^2 G}{\partial \vartheta_2^2} ={}& -\boldsymbol{\sigma} : \boldsymbol{\varepsilon}_{t2} \left(12\vartheta_2 - 6\right)\;\varphi(r) - \boldsymbol{\sigma} : \boldsymbol{\varepsilon}_{t3} \left(18 - 12\vartheta_2 - 12\vartheta_1\right)\;\varphi(r) + f(\theta, r) \\
& + \bar{A}\,[2(1 - \vartheta_2)^2 + 4(1 - \vartheta_1)^2 - 8(1 - \vartheta_2)(\vartheta_1 + \vartheta_2 - 1) \\
& \qquad\qquad + 2(\vartheta_1 + \vartheta_2 - 1)^2]q(r)\,.
\end{aligned}
\tag{63}
$$

Similar, we obtain all mixed derivatives:

$$
\frac{\partial^2 G}{\partial r\,\partial \vartheta_1} = -\boldsymbol{\sigma} : \boldsymbol{\varepsilon}_{t1} \left(6\vartheta_1^2 - 6\vartheta_1\right)\;\varphi'(r) - \boldsymbol{\sigma} : \boldsymbol{\varepsilon}_{t3}[(12 - 6\vartheta_1 - 6\vartheta_2) - 6(2 - \vartheta_1 - \vartheta_2)^2]\;\varphi'(r)
\tag{64}
$$

$$+ \bar{A}\left[2(\vartheta_1 - 1)(1 - \vartheta_2)^2 + 2(1 - \vartheta_1)^2(\vartheta_1 + \vartheta_2 - 1) + 2(1 - \vartheta_2)^2(\vartheta_1 + \vartheta_2 - 1) - \right.$$
$$\left. 2(1 - \vartheta_1)(\vartheta_1 + \vartheta_2 - 1)^2\right]q'(r) .$$

$$\frac{\partial^2 G}{\partial r\, \partial\, \vartheta_2} = -\boldsymbol{\sigma} : \boldsymbol{\varepsilon}_{t2}\left(6\vartheta_2^2 - 6\vartheta_2\right)\, \varphi'(r) - \boldsymbol{\sigma} : \boldsymbol{\varepsilon}_{t3}[(12 - 6\vartheta_1 - 6\vartheta_2) - 6(2 - \vartheta_1 - \vartheta_2)^2]\, \varphi'(r) \quad (65)$$
$$+ \bar{A}\left[2(\vartheta_1 - 1)(1 - \vartheta_2)^2 + 2(1 - \vartheta_2)^2(\vartheta_1 + \vartheta_2 - 1) + 2(1 - \vartheta_2)^2(\vartheta_1 + \vartheta_2 - 1)\right.$$
$$\left. -2(1 - \vartheta_1)(\vartheta_1 + \vartheta_2 - 1)^2\right]q'(r) .$$

$$\frac{\partial^2 G}{\partial \vartheta_1\, \partial\, \vartheta_2} = -\boldsymbol{\sigma} : \boldsymbol{\varepsilon}_{t3}\left(18 - \vartheta_1 - \vartheta_2\right)\, \varphi(r) + \bar{A}\left[2(1 - \vartheta_1)^2 + 4(1 - \vartheta_1)(1 - \vartheta_2) + 2(1 - \vartheta_2)^2 \quad (66)\right.$$
$$\left. -4(1 - \vartheta_1)(\vartheta_1 + \vartheta_2 - 1) - 4(1 - \vartheta_2)(\vartheta_1 + \vartheta_2 - 1)\right]q(r) .$$

2.10 Thermodynamics Stability conditions for 3 Variants

Main Conditions that Simplifying the instability criteria

Let consider $r = \vartheta_0$ and the phase $\hat{\vartheta}_j$ will lose its stability if, for any perturbation $\dot{\vartheta}_k$, the following conditions are satisfied in terms of Gibbs energy

$$\sum_{m=0;i,j,k}^{n-1} \frac{\partial^2\, G(\boldsymbol{\sigma},\, \hat{\vartheta}_j)}{\partial\, \vartheta_i\, \partial\, \vartheta_k}\, \dot{\vartheta}_i\, \dot{\vartheta}_k \leq 0 \tag{67}$$

Thus, the instability occurs when $n \times n$ matrix $\frac{\partial^2\, G(\boldsymbol{\sigma},\hat{\vartheta}_j)}{\partial\, \vartheta_i\, \partial\, \vartheta_k}$ first ceases to be negative definite. Sylvester's criterion states that a symmetric matrix $\mathbf{B}$ is negative-definite if and only if all the following matrics have a negative determinant: the upper left 1- by-1 corner of $\mathbf{B}$, the upper left 2-by-2 corner of $\mathbf{B}$, the upper left 3-by-3 corner of B i.e.,all of the leading principal minors must be negative. Thus for three martensitic variants, the matrix $\mathbf{B}$ is

$$\mathbf{B} = \begin{pmatrix} b_{11} & b_{12} & b_{13} \\ b_{21} & b_{22} & b_{23} \\ b_{31} & b_{32} & b_{33} \end{pmatrix} \tag{68}$$

and the one of the following conditions should be fulfilled for instability of the phase $\hat{\vartheta}_j$

$$b_{ik} := \frac{\partial^2\, G(\boldsymbol{\sigma},\, \hat{\vartheta}_j)}{\partial\, \vartheta_i\, \partial\, \vartheta_k}; \;\; b_{11} \leq 0 \tag{69}$$

$$b_{11}b_{22} - b_{12}^2 \leq 0 \qquad ;$$

$$b_{11}(b_{22}b_{33} - b_{23}^2) - b_{12}(b_{21}b_{33} - b_{31}b_{23}) + b_{33}(b_{12}b_{32} - b_{22}b_{31}) \leq 0.$$

General stability condition for Austenite

Consider $r = 0$ into Eqs.(54), we get the condition for loss of stability of Austenite

$$b_{11} = \frac{\partial^2 G(r=0)}{\partial r^2} = -2a\,\boldsymbol{\sigma}:\boldsymbol{\varepsilon}_{t1}\left(1 - 3\vartheta_1^2 - 2\vartheta_1^3\right) - 2a\,\boldsymbol{\sigma}:\boldsymbol{\varepsilon}_{t2}\left(1 - 3\vartheta_2^2 - 2\vartheta_2^3\right) \qquad (70)$$

$$-2a\,\boldsymbol{\sigma}:\boldsymbol{\varepsilon}_{t3}[1 - 3(2 - \vartheta_1 - \vartheta_2)^2 + 2(2 - \vartheta_1 - \vartheta_2)^3]$$

$$+6\bar{A}\left[(1 - \vartheta_1)^2(1 - \vartheta_2)^2 + (1 - \vartheta_1)^2(\vartheta_1 + \vartheta_2 - 1)^2 + (1 - \vartheta_2)^2(\vartheta_1 + \vartheta_2 - 1)^2\right] \leq 0 .$$

and

$$b_{12} = b_{21} = \frac{\partial^2 G(r=0)}{\partial r\,\partial \vartheta_1} = 0; \quad b_{13} = b_{31} = \frac{\partial^2 G(r=0)}{\partial r\,\partial \vartheta_2} = 0; \qquad (71)$$

$$b_{22} = \frac{\partial^2 G(r=0)}{\partial \vartheta_1^2} = 0; \quad b_{33} = \frac{\partial^2 G(r=0)}{\partial \vartheta_2^2} = 0;$$

To find the the roots of $b11$ for corresponding minima which infer the loss of stability of Austenite to others Martensitic variants, we put $\frac{\partial b11}{\partial \vartheta_1} = 0$ and $\frac{\partial b11}{\partial \vartheta_2} = 0$

Hence,

$$\frac{\partial b11}{\partial \vartheta_1} = -2a\,\boldsymbol{\sigma}:\boldsymbol{\varepsilon}_{t1}(6\vartheta_1^2 - 6\vartheta) - 2a\,\boldsymbol{\sigma}:\boldsymbol{\varepsilon}_{t3}[6(2 - \vartheta_1 - \vartheta_2) - 6(2 - \vartheta_1 - \vartheta_2)^2] \qquad (72)$$

$$+6\bar{A}[2(1 - \vartheta_1)^2(\vartheta_1 + \vartheta_2 - 1) + 2(1 - \vartheta_2)^2(\vartheta_1 + \vartheta_2 - 1)$$

$$-2(1 - \vartheta_1)(\vartheta_1 + \vartheta_2 - 1)^2 - 2(1 - \vartheta_1)(1 - \vartheta_2)^2] = 0$$

and

$$\frac{\partial b11}{\partial \vartheta_2} = -2a\,\boldsymbol{\sigma}:\boldsymbol{\varepsilon}_{t2}(6\vartheta_1^2 - 6\vartheta) - 2a\,\boldsymbol{\sigma}:\boldsymbol{\varepsilon}_{t3}[6(2 - \vartheta_1 - \vartheta_2) - 6(2 - \vartheta_1 - \vartheta_2)^2] \qquad (73)$$

$$+6\bar{A}[2(1 - \vartheta_1)^2(\vartheta_1 + \vartheta_2 - 1) + 2(1 - \vartheta_2)^2(\vartheta_1 + \vartheta_2 - 1)$$

$$-2(1 - \vartheta_1)(\vartheta_1 + \vartheta_2 - 1)^2 - 2(1 - \vartheta_1)(1 - \vartheta_2)^2] = 0$$

For further simplification lets subtract Eqs.(73) and Eqs.(74) and we get

$$-12[a\,\boldsymbol{\sigma}:(\boldsymbol{\varepsilon}_{t1}(\vartheta_1 - 1)\vartheta_1 - \boldsymbol{\varepsilon}_{t2}(\vartheta_2 - 1)\vartheta_2) + \bar{A}[\vartheta_1^2 - \vartheta_1^3 + \vartheta_2^2(\vartheta_2 - 1)] = 0 \qquad (74)$$

Its obvious that we have 3 set of solution of ϑ_1, ϑ_2 , which are

$$(\vartheta_1, \vartheta_2) = (0, 1); (\vartheta_1, \vartheta_2) = (1, 0); (\vartheta_1, \vartheta_2) = (1, 1); \tag{75}$$

So put these solutions into Eqs.(74) we get possible conditions for loss of stability of Austenite as follow

$$A \rightarrow M_1 : \quad \boldsymbol{\sigma} : \boldsymbol{\varepsilon}_{t1} \geq \frac{A}{a} \quad : (\vartheta_1, \vartheta_2) = (0, 1) \tag{76}$$

$$A \rightarrow M_2 : \quad \boldsymbol{\sigma} : \boldsymbol{\varepsilon}_{t2} \geq \frac{A}{a} \quad : (\vartheta_1, \vartheta_2) = (1, 0) \tag{77}$$

and

$$A \rightarrow M_3 : \quad \boldsymbol{\sigma} : \boldsymbol{\varepsilon}_{t3} \geq \frac{A}{a} \quad : (\vartheta_1, \vartheta_2) = (1, 1) \tag{78}$$

Drawback of this approach is that we can have extra solutions of $(\vartheta_1, \vartheta_2)$ which are difficult to get analytically.

Case I: when $\boldsymbol{\sigma} = 0$

Let assume $\boldsymbol{\sigma} = 0$ then we can rewrite Eqs.(73) and Eqs.(74) as

$$\frac{\partial b_{11}}{\partial \vartheta_1} = 6\bar{A}[2(1 - \vartheta_1)^2(\vartheta_1 + \vartheta_2 - 1) \quad + 2(1 - \vartheta_2)^2(\vartheta_1 + \vartheta_2 - 1) \tag{79}$$
$$-2(1 - \vartheta_1)(\vartheta_1 + \vartheta_2 - 1)^2 - 2(1 - \vartheta_1)(1 - \vartheta_2)^2] = 0$$

and

$$\frac{\partial b_{11}}{\partial \vartheta_2} = 12\bar{A}[2(1 - \vartheta_1)^2(\vartheta_1 + \vartheta_2 - 1) \quad + 2(1 - \vartheta_2)^2(\vartheta_1 + \vartheta_2 - 1) \tag{80}$$
$$-2(1 - \vartheta_1)(\vartheta_1 + \vartheta_2 - 1)^2 - 2(1 - \vartheta_1)(1 - \vartheta_2)^2] = 0$$

Solving Eqs.(73) and Eqs.(74) we get following roots

$$(\vartheta_1, \vartheta_2) = (0, 1); (\vartheta_1, \vartheta_2) = (1, 0); (\vartheta_1, \vartheta_2) = (1, 1); (\vartheta_1, \vartheta_2) = (2/3, 2/3); \tag{81}$$

First 3 values of $(\vartheta_1, \vartheta_2)$ gives the same condition in the equations Eqs.(76), Eqs.(77), Eqs.(78)

Lets prove that $(\vartheta_1, \vartheta_2) = (2/3, 2/3)$ corresponds to maxima of the function b_{11} and does not contribute the instability of Austenite (A).

Consider all the second and cross derivative of b_{11} with respect to ϑ_1 and ϑ_2 from the Eqs.(80) and Eqs.(81),

$$\frac{\partial^2 b_{11}}{\partial \vartheta_1^2} = 12\bar{A}[8 + 6(\vartheta_1 - 2)\vartheta_1 - 10\vartheta_2 + 6\vartheta_1\vartheta_2 + 3\vartheta_2^2] \tag{82}$$

$$\frac{\partial^2 b_{11}}{\partial \vartheta_2^2} = 12\bar{A}[8 + 6(\vartheta_2 - 2)\vartheta_2 - 10\vartheta_1 + 6\vartheta_1\vartheta_2 + 3\vartheta_1^2] \tag{83}$$

$$\frac{\partial^2 b_{11}}{\partial \vartheta_1 \partial \vartheta_2} = 12\bar{A}(\vartheta_1 + \vartheta_2 - 2)(3\vartheta_1 + 3\vartheta_2 - 4) \tag{84}$$

Lets consider Hessian matrix of all the partial derivatives of the function b_{11}.

$$\mathbf{H} = \begin{pmatrix} h_{11} & h_{12} \\ h_{21} & h_{22} \end{pmatrix} = \begin{pmatrix} \frac{\partial^2 b_{11}}{\partial \vartheta_1^2} & \frac{\partial^2 b_{11}}{\partial \vartheta_1 \partial \vartheta_2} \\ \frac{\partial^2 b_{11}}{\partial \vartheta_1 \partial \vartheta_2} & \frac{\partial^2 b_{11}}{\partial \vartheta_2^2} \end{pmatrix} \tag{85}$$

Lets consider root $(\vartheta_1, \vartheta_2) = (0, 1)$ and put into Eqs.(85) we get

$$\mathbf{H} = \begin{pmatrix} 12\bar{A} & 12\bar{A} \\ 12\bar{A} & 24\bar{A} \end{pmatrix} \tag{86}$$

Here, $h_{11} = 12\bar{A} \geq 0$ and $h_{11}h_{22} - h_{12}h_{21} = 144\bar{A}^2 \geq 0$ .Hence function b_{11} does have local minima here.

Lets consider root $(\vartheta_1, \vartheta_2) = (1, 0)$ and put into Eqs.(85) we get

$$\mathbf{H} = \begin{pmatrix} 24\bar{A} & 12\bar{A} \\ 12\bar{A} & 12\bar{A} \end{pmatrix} \tag{87}$$

Here, also $h_{11} = 24\bar{A} \geq 0$ and $h_{11}h_{22} - h_{12}h_{21} = 144\bar{A}^2 \geq 0$ .Hence function b_{11} does have local minima here.

Lets consider root $(\vartheta_1, \vartheta_2) = (1, 1)$ and put into Eqs.(85) we get

$$\mathbf{H} = \begin{pmatrix} 12\bar{A} & 0 \\ 0 & 24\bar{A} \end{pmatrix} \tag{88}$$

Here, $h_{11} = 12\bar{A} \geq 0$ and $h_{11}h_{22} - h_{12}h_{21} = 144\bar{A}^2 \geq 0$ .Hence function b_{11} does have local minima here.

Lets consider root $(\vartheta_1, \vartheta_2) = (2/3, 2/3)$ and put into Eqs.(85) we get

$$\mathbf{H} = \begin{pmatrix} 0 & -24\bar{A} \\ -24\bar{A} & 0 \end{pmatrix} \tag{89}$$

Here, $h_{11} = 0$ and $h_{11}h_{22} - h_{12}h_{21} = 576\bar{A}^2 \geq 0$ .Hence function b_{11} does have local Maxima here. So it does not contribute anything to the instability conditions.

$$\text{Case II: when } \boldsymbol{\sigma} : \boldsymbol{\varepsilon}_{ti} = \frac{A}{a}$$

Lets assume $\boldsymbol{\sigma} : \boldsymbol{\varepsilon}_{ti} = \frac{A}{a}$, then we can rewrite Eqs.(73)

$$\frac{\partial b_{11}}{\partial \vartheta_1} = 12(2\vartheta_1 + \vartheta_2 - 2)[\bar{A}(2 - 2\vartheta_1 + \vartheta_1^2) + A(\vartheta_2 - 1) + \bar{A}(\vartheta_2^2 + \vartheta_1\vartheta_2 - 3\vartheta_2)] = 0 \tag{90}$$

and

$$\frac{\partial b_{11}}{\partial \vartheta_2} = 12(2\vartheta_2 + \vartheta_1 - 2)[\bar{A}(2 - 2\vartheta_2 + \vartheta_2^2) + A(\vartheta_1 - 1) + \bar{A}(\vartheta_1^2 + \vartheta_1\vartheta_2 - 3\vartheta_1)] = 0 \tag{91}$$

Solving Eqs.(90) and Eqs.(91) we get following roots

$$(\vartheta_1, \vartheta_2) = (0, 1); (\vartheta_1, \vartheta_2) = (1, 0); (\vartheta_1, \vartheta_2) = (1, 1); (\vartheta_1, \vartheta_2) = (2/3, 2/3); \tag{92}$$

$$\tag{93}$$

$$(\vartheta_1, \vartheta_2) = (\frac{2\bar{A} - A}{3\bar{A}}, \frac{2\bar{A} + 2A}{3\bar{A}}); \quad (\vartheta_1, \vartheta_2) = (\frac{2\bar{A} - A}{3\bar{A}}, \frac{2\bar{A} - A}{3\bar{A}});$$

$$\tag{94}$$

$$(\vartheta_1, \vartheta_2) = (\frac{2\bar{A} + 2A}{3\bar{A}}, \frac{2\bar{A} - A}{3\bar{A}});$$

First 3 values of $(\vartheta_1, \vartheta_2)$ gives the same condition in the equations Eqs.(76), Eqs.(77), Eqs.(78)

Consider all the second and cross derivative of b_{11} with respect to ϑ_1 and ϑ_2 from the Eqs.(90) and Eqs.(91),

$$\frac{\partial^2 b_{11}}{\partial \vartheta_1^2} = 12[2A(\vartheta_2 - 1) + \bar{A}(\vartheta_1^2 + 6\vartheta_1\vartheta_2 - 10\vartheta_2 + 3\vartheta_2^2 - 4)] \tag{95}$$

$$\frac{\partial^2 b_{11}}{\partial \vartheta_2^2} = 12[2A(\vartheta_1 - 1) + \bar{A}(\vartheta_2^2 + 6\vartheta_1\vartheta_2 - 10\vartheta_1 + 3\vartheta_1^2 - 4)] \tag{96}$$

$$\frac{\partial^2 b_{11}}{\partial \vartheta_1 \partial \vartheta_2} = 12[A(2\vartheta_1 + 2\vartheta_2 - 3) + \bar{A}(\vartheta_1 + \vartheta_2 - 2)(3\vartheta_1 + 3\vartheta_2 - 4)] \tag{97}$$

Lets consider Hessian matrix of all the partial derivatives of the function b_{11}.

$$\mathbf{H} = \begin{pmatrix} h_{11} & h_{12} \\ h_{21} & h_{22} \end{pmatrix} = \begin{pmatrix} \frac{\partial^2 b_{11}}{\partial \vartheta_1^2} & \frac{\partial^2 b_{11}}{\partial \vartheta_1 \partial \vartheta_2} \\ \frac{\partial^2 b_{11}}{\partial \vartheta_1 \partial \vartheta_2} & \frac{\partial^2 b_{11}}{\partial \vartheta_2^2} \end{pmatrix} \tag{98}$$

Lets consider root $(\vartheta_1, \vartheta_2) = (0, 1)$ and put into Eqs.(98) we get

$$\mathbf{H} = \begin{pmatrix} 12\bar{A} & 12\bar{A} - 12A \\ 12\bar{A} - 12A & 24\bar{A} - A \end{pmatrix} \tag{99}$$

Here, $h_{11} = 12\bar{A}$ and $h = h_{11}h_{22} - h_{12}h_{21} = -144(A - \bar{A})(A + \bar{A})$.

Here if $h_{11}, h \geq 0$, then function b_{11} does have local Minima here. From this condition we have $\bar{A} \geq 0, \bar{A} \geq A$, which is true. Hence it has local mini ma for corresponding roots.

However from the condition of local maxima, i.e $h_{11}, h \leq 0$, we get $\bar{A} \leq 0, \bar{A} \leq A$, which is not physical.So this root does not have local maxima here in any case.

Lets consider root $(\vartheta_1, \vartheta_2) = (1, 0)$ and put into Eqs.(98) we get

$$\mathbf{H} = \begin{pmatrix} 24\bar{A} - 24A & 12\bar{A} - 12A \\ 12\bar{A} - 12A & 12\bar{A} \end{pmatrix} \tag{100}$$

Here, $h_{11} = 24\bar{A} - 24A$ and $h = h_{11}h_{22} - h_{12}h_{21} = -144(A - \bar{A})(A + \bar{A})$.

Here if $h_{11}, h \geq 0$, then function b_{11} does have local Minima here. From this condition we have $\bar{A} \geq A$, which is true. Hence it has local minima for corresponding roots.

However from the condition of local maxima, i.e $h_{11}, h \leq 0$, we get $\bar{A} \leq A$, .So this root can have local maxima here for case.

Lets consider root $(\vartheta_1, \vartheta_2) = (1, 1)$ and put into Eqs.(98) we get

$$\mathbf{H} = \begin{pmatrix} 12\bar{A} & 12A \\ 12A & 12\bar{A} \end{pmatrix} \tag{101}$$

Here, $h_{11} = 12\bar{A}$ and $h = h_{11}h_{22} - h_{12}h_{21} = -144(A - \bar{A})(A + \bar{A})$.

Here if $h_{11}, h \geq 0$, then function b_{11} does have local Minima here. From this condition we have $\bar{A} \geq 0, \bar{A} \geq A$, which is true. Hence it has local mini ma for corresponding roots.

However from the condition of local maxima, i.e $h_{11}, h \leq 0$, we get $\bar{A} \leq 0, \bar{A} \leq A$, which is not physical.So this root does not have local maxima here in any case.

Lets consider root $(\vartheta_1, \vartheta_2) = (1, 1)$ and put into Eqs.(86) we get

$$\mathbf{H} = \begin{pmatrix} 12\bar{A} & 12A \\ 12A & 12\bar{A} \end{pmatrix} \tag{102}$$

Here, $h_{11} = 12\bar{A}$ and $h = h_{11}h_{22} - h_{12}h_{21} = -144(A - \bar{A})(A + \bar{A})$.

Here if $h_{11}, h \geq 0$, then function b_{11} does have local Minima here. From this condition we have $\bar{A} \geq 0, \bar{A} \geq A$, which is true. Hence it has local mini ma for corresponding roots.

However from the condition of local maxima, i.e $h_{11}, h \leq 0$, we get $\bar{A} \leq 0, \bar{A} \leq A$, which is not physical.So this root does not have local maxima here in any case.

Lets consider root $(\vartheta_1, \vartheta_2) = (2/3, 2/3)$ and put into Eqs.(86) we get

$$\mathbf{H} = \begin{pmatrix} -8A & -4A \\ -4A & -8A \end{pmatrix} \tag{103}$$

Here, $h_{11} = -8A$ and $h = h_{11}h_{22} - h_{12}h_{21} = 48A^2$.

Here if $h_{11}, h \geq 0$, then function b_{11} does have local Minima here. From this condition we have $A \leq 0$,, which is unphysical. Hence it does not have local minima for corresponding root for any case.

However from the condition of local maxima, i.e $h_{11}, h \leq 0$, we get $A \geq 0$.

For all 3 other remaining roots we have following $h_{11} = 12\frac{A^2}{A}$ and $h = h_{11}h_{22} - h_{12}h_{21} = 144A^2(\frac{A^2}{A} - 1)$.

2.11 Simplified instability criteria

For general thermodynamic expression for loss of stability of any phase corresponding ϑ for 3 variants as follows

$$\frac{\partial^2 G}{\partial r^2}\dot{r}^2 + 2\frac{\partial^2 G}{\partial r \partial \vartheta_1}\dot{r}\dot{\vartheta}_1 + 2\frac{\partial^2 G}{\partial r \partial \vartheta_2}\dot{r}\dot{\vartheta}_2 + \frac{\partial^2 G}{\partial \vartheta_1^2}\dot{\vartheta}_1^2 + \frac{\partial^2 G}{\partial \vartheta_2^2}\dot{\vartheta}_2^2 + 2\frac{\partial^2 G}{\partial \vartheta_1 \partial \vartheta_2}\dot{\vartheta}_1\dot{\vartheta}_2 \leq 0 \tag{104}$$

Stability condition for $A \leftrightarrow M_1$

Let , $\vartheta_2 = 1$ and any general values of $r, \vartheta_1, \vartheta_3$, and $\dot{\vartheta}_2 = 0$ Considering all the cross derivatives in the Eqs.(104)

$$\frac{\partial^2 G}{\partial r^2}\dot{r}^2 + 2\frac{\partial^2 G}{\partial r \partial \vartheta_1}\dot{r}\dot{\vartheta}_1 + \frac{\partial^2 G}{\partial \vartheta_1^2}\dot{\vartheta}_1^2 \leq 0 \tag{105}$$

For the loss of stability of A, consider $r = 0$ and we get following expression from

$$\frac{\partial^2 G(r = 0)}{\partial r^2} = 2A - 2a\,\boldsymbol{\sigma} : \boldsymbol{\varepsilon}_{t1} \tag{106}$$

$$\frac{\partial^2 G\left(r=0\right)}{\partial\, r\,\partial\vartheta_1} = 0 \tag{107}$$

$$\frac{\partial^2 G\left(r=0\right)}{\partial\,\vartheta_1^2} = 0 \tag{108}$$

Replacing Eqs.(105), Eqs.(106) and Eqs.(107) into Eqs.(**??**) we get for the loss of Austenite $A, (A \to M_1)$

$$A \to M_1: \quad \boldsymbol{\sigma}:\boldsymbol{\varepsilon}_{t1} \geq \frac{A}{a} \tag{109}$$

Similarly,

For the loss of stability of M_1, we consider $r = 1$ and we get following expression from

$$\frac{\partial^2 G\left(r=1\right)}{\partial\, r^2} = 2A - 12\Delta G - (2a-12)\boldsymbol{\sigma}:\boldsymbol{\varepsilon}_{t1} \tag{110}$$

$$\frac{\partial^2 G\left(r=1\right)}{\partial\, r\,\partial\vartheta_1} = 0; \tag{111}$$

$$\frac{\partial^2 G\left(r=1\right)}{\partial\,\vartheta_1^2} = -2\bar{A} + 6\,\boldsymbol{\sigma}:\boldsymbol{\varepsilon}_{t1} - 6\,\boldsymbol{\sigma}:\boldsymbol{\varepsilon}_{t3} \tag{112}$$

Replacing Eqs.(110), Eqs.(111) and Eqs.(112) into Eqs.(107) we get for the loss of Martensite M_1

$$[2A - 12\Delta G - (2a-12)\boldsymbol{\sigma}:\boldsymbol{\varepsilon}_{t1}]\dot{r}^2 + [-2\bar{A} + 6\,\boldsymbol{\sigma}:\boldsymbol{\varepsilon}_{t1} - 6\,\boldsymbol{\sigma}:\boldsymbol{\varepsilon}_{t3}]\dot{\vartheta}_1^2 \leq 0 \tag{113}$$

case I:

Condition for loss of stability of $(M_1 \to A)$

$$[2A - 12\Delta G - (2a-12)\boldsymbol{\sigma}:\boldsymbol{\varepsilon}_{t1}] \leq 0 \tag{114}$$

Hence,

$$(M_1 \to A) \; : \quad \boldsymbol{\sigma} : \boldsymbol{\varepsilon}_{t1} \geq \frac{6\Delta G - A}{6 - a} \tag{115}$$

case II:

Condition for loss of stability of $(M_1 \to M_3)$

$$[-2\bar{A} + 6\,\boldsymbol{\sigma} : \boldsymbol{\varepsilon}_{t1} - 6\,\boldsymbol{\sigma} : \boldsymbol{\varepsilon}_{t3}] \leq 0 \tag{116}$$

Hence

$$(M_1 \to M_3) \; : \quad \boldsymbol{\sigma} : (\boldsymbol{\varepsilon}_{t3} - \boldsymbol{\varepsilon}_{t1}) \geq \frac{\bar{A}}{a} \tag{117}$$

Stability condition for $A \leftrightarrow M_2$

Let , $\vartheta_1 = 1$ and any general values of $r, \vartheta_2, \vartheta_3$, and $\dot{\vartheta}_1 = 0$ Considering all the cross derivatives in the Eqs.(104)we get

$$\frac{\partial^2 G}{\partial r^2}\dot{r}^2 + 2\frac{\partial^2 G}{\partial r \, \partial \vartheta_2}\dot{r}\dot{\vartheta}_2 + \frac{\partial^2 G}{\partial \vartheta_2^2}\dot{\vartheta}_2^2 \leq 0 \tag{118}$$

For the loss of stability of A, consider $r = 0$ and we get following expression from

$$\frac{\partial^2 G\,(r=0)}{\partial r^2} = 2A - 2\,a\,\boldsymbol{\sigma} : \boldsymbol{\varepsilon}_{t2} \tag{119}$$

$$\frac{\partial^2 G\,(r=0)}{\partial r \, \partial \vartheta_2} = 0 \tag{120}$$

$$\frac{\partial^2 G\,(r=0)}{\partial \vartheta_2^2} = 0 \tag{121}$$

Replacing Eqs.(119), Eqs.(120) and Eqs.(121) into Eqs.(118) we get for the loss of Austenite $A, (A \to M_2)$

$$A \to M_2 : \quad \boldsymbol{\sigma} : \boldsymbol{\varepsilon}_{t2} \geq \frac{A}{a} \tag{122}$$

Similarly,

For the loss of stability of M_2, we consider $r = 1$ and we get following expression from

$$\frac{\partial^2 G\,(r = 1)}{\partial\, r^2} = 2A - 12\Delta G - (2a - 12)\boldsymbol{\sigma} : \boldsymbol{\varepsilon}_{t2} \tag{123}$$

$$\frac{\partial^2 G\,(r = 1)}{\partial\, r\, \partial\vartheta_2} = 0; \tag{124}$$

$$\frac{\partial^2 G\,(r = 1)}{\partial\, \vartheta_2^2} = -2\bar{A} + 6\,\boldsymbol{\sigma} : \boldsymbol{\varepsilon}_{t2} - 6\,\boldsymbol{\sigma} : \boldsymbol{\varepsilon}_{t3} \tag{125}$$

Replacing Eqs.(123), Eqs.(124) and Eqs.(125) into Eqs.(118) we get for the loss of Martensite M_2

$$[2A - 12\Delta G - (2a - 12)\boldsymbol{\sigma} : \boldsymbol{\varepsilon}_{t2}]\dot{r}^2 + [-2\bar{A} + 6\,\boldsymbol{\sigma} : \boldsymbol{\varepsilon}_{t2} - 6\,\boldsymbol{\sigma} : \boldsymbol{\varepsilon}_{t3}]\dot{\vartheta}_2^2 \le 0 \tag{126}$$

case I:

Condition for loss of stability of $(M_2 \to A)$

$$[2A - 12\Delta G - (2a - 12)\boldsymbol{\sigma} : \boldsymbol{\varepsilon}_{t2}] \le 0 \tag{127}$$

Hence,

$$(M_2 \to A) \quad : \quad \boldsymbol{\sigma} : \boldsymbol{\varepsilon}_{t2} \ge \frac{6\Delta G - A}{6 - a} \tag{128}$$

case II:

Condition for loss of stability of $(M_2 \to M_3)$

$$[-2\bar{A} + 6\,\boldsymbol{\sigma} : \boldsymbol{\varepsilon}_{t2} - 6\,\boldsymbol{\sigma} : \boldsymbol{\varepsilon}_{t3}] \le 0 \tag{129}$$

Hence

$$(M_2 \to M_3) \; : \quad \boldsymbol{\sigma} : (\boldsymbol{\varepsilon}_{t3} - \boldsymbol{\varepsilon}_{t2}) \geq \frac{\bar{A}}{a} \tag{130}$$

Stability condition for $A \leftrightarrow M_3$

Let , $\vartheta_1 = 1$ and any general values of $r, \vartheta_2, \vartheta_3$, and $\dot{\vartheta}_1 = 0$ Considering all the cross derivatives in the Eqs.(104)we get

$$\frac{\partial^2 G}{\partial r^2} \dot{r}^2 + 2 \frac{\partial^2 G}{\partial r \, \partial \vartheta_2} \dot{r} \dot{\vartheta}_2 + \frac{\partial^2 G}{\partial \vartheta_2^2} \dot{\vartheta}_2^2 \leq 0 \tag{131}$$

For the loss of stability of A, consider $r = 0$ and we get following expression from

$$\frac{\partial^2 G \left(r = 0, \vartheta_2 = 1 \right)}{\partial r^2} = 2A - 2 \, a \, \boldsymbol{\sigma} : \boldsymbol{\varepsilon}_{t3} \tag{132}$$

$$\frac{\partial^2 G \left(r = 0, \vartheta_2 = 1 \right)}{\partial r \, \partial \vartheta_2} = 0 \tag{133}$$

$$\frac{\partial^2 G \left(r = 0, \vartheta_2 = 1 \right)}{\partial \vartheta_2^2} = 0 \tag{134}$$

Replacing Eqs.(132), Eqs.(133) and Eqs.(134) into Eqs.(131) we get for the loss of Austenite $A, (A \to M_3)$

$$A \to M_3 : \quad \boldsymbol{\sigma} : \boldsymbol{\varepsilon}_{t3} \geq \frac{A}{a} \tag{135}$$

Similarly,

For the loss of stability of M_3, we consider $r = 1$ and we get following expression from

$$\frac{\partial^2 G \left(r = 1, \vartheta_2 = 1 \right)}{\partial r^2} = 2A - 12\Delta G - (2a - 12)\boldsymbol{\sigma} : \boldsymbol{\varepsilon}_{t3} \tag{136}$$

$$\frac{\partial^2 G \left(r = 1, \vartheta_2 = 1 \right)}{\partial r \, \partial \vartheta_2} = 0; \tag{137}$$

$$\frac{\partial^2 G\left(r=1, \vartheta_2=1\right)}{\partial \vartheta_2^2} = -2\bar{A} + 6\,\boldsymbol{\sigma}:\boldsymbol{\varepsilon}_{t2} - 6\,\boldsymbol{\sigma}:\boldsymbol{\varepsilon}_{t3} \tag{138}$$

Replacing Eqs.(136), Eqs.(137) and Eqs.(138) into Eqs.(131) we get for the loss of Martensite M_3

$$[2A - 12\Delta G - (2a-12)\boldsymbol{\sigma}:\boldsymbol{\varepsilon}_{t3}]\dot{r}^2 + [-2\bar{A} + 6\,\boldsymbol{\sigma}:\boldsymbol{\varepsilon}_{t3} - 6\,\boldsymbol{\sigma}:\boldsymbol{\varepsilon}_{t2}]\dot{\vartheta}_2^2 \leq 0 \tag{139}$$

case I:

Condition for loss of stability of $(M_3 \to A)$

$$[2A - 12\Delta G - (2a-12)\boldsymbol{\sigma}:\boldsymbol{\varepsilon}_{t3}] \leq 0 \tag{140}$$

Hence,

$$(M_3 \to A) \ : \quad \boldsymbol{\sigma}:\boldsymbol{\varepsilon}_{t3} \geq \frac{6\Delta G - A}{6 - a} \tag{141}$$

case II:

Condition for loss of stability of $(M_3 \to M_2)$

$$[-2\bar{A} + 6\,\boldsymbol{\sigma}:\boldsymbol{\varepsilon}_{t3} - 6\,\boldsymbol{\sigma}:\boldsymbol{\varepsilon}_{t2}] \leq 0 \tag{142}$$

Hence

$$(M_3 \to M_2) \ : \quad \boldsymbol{\sigma}:(\boldsymbol{\varepsilon}_{t2} - \boldsymbol{\varepsilon}_{t3}) \geq \frac{\bar{A}}{a} \tag{143}$$

2.12 Examples for martensitic microstructure evolution and twinning

In our example simulations we use the material parameters for the cubic to tetragonal PT in NiAl found in [12, 13, 29]: $a = 3$, $\bar{A} = 5320$ MPa, $\theta_c = -183$ K, $\theta_e = 215$ K, $\lambda_r = \lambda_\vartheta = 2596.5 \, m^2/Ns$, $\beta = \beta_\vartheta = 5.18 \times 10^{-10} \, N$; $\theta = 100$K, unless other stated. These parameters correspond to a twin interface energy $E_{MM} = 0.958 J/m^2$ and width $\Delta_{MM} = 0.832$ nm. Isotropic linear elasticity is used for simplicity; Young's modulus $E = 177.034 GPa$ and Poisson's ratio $\nu = 0.238$. The equilibrium equation $\boldsymbol{\nabla} \cdot \boldsymbol{\sigma} = 0$ is utilized. In the plane stress 2D problems, only M_1 and M_2 were considered; the corresponding transformation strains in the cubic axes are $\boldsymbol{\varepsilon}_{t1} = (0.215, -0.078, -0.078)$ and $\boldsymbol{\varepsilon}_{t2} = (-0.078, 0.215, -0.078)$. The FEM approach was developed and incorporated in the COMSOL code. All lengths, stresses, and times are given in units of nm, and GPa, and ps. All external stresses are normal to the deformed surface.

Example 1

Benchmark problem: bending and splitting of martensite tips in NiAl alloy

Initial random distribution of order parameter Υ in the range $[0; 0.4]$ was prescribed in a square sample of 50×50 with the austenite lattice rotated by $\alpha = 45^o$. Initial value of $\vartheta = 0.5$. For one horizontal and one vertical surfaces, the roller support was used. Homogeneous normal displacements at two other surfaces were prescribed and kept constant during simulations, resulted in biaxial normal strain of 0.01. Shear stresses were kept zero at external surfaces. Two dimensional problem under plane stress condition and temperature $\theta = 50K$ was studied with the material parameters described in the main text. The evolution of $2\Upsilon(\vartheta - 0.5)$ is presented in Fig. S1, demonstrating transformation of the austenite into martensite and coalescence of martensitic units. Despite the symmetry in geometry and boundary conditions, accidental asymmetry in the initial conditions led to formation of alternating horizontal martensitic twin structure with austenitic regions near vertical sides, in order to satisfy boundary conditions. Invariant plane conditions for the austenite-martensite interfaces are consequence of a simplified plane-stress two-dimensional formulation.

The stationary solution from Fig. S1 was taken as an initial condition for the next problem with the following modifications: temperature was reduced to $\theta = 0K$; parameter β_ϑ was
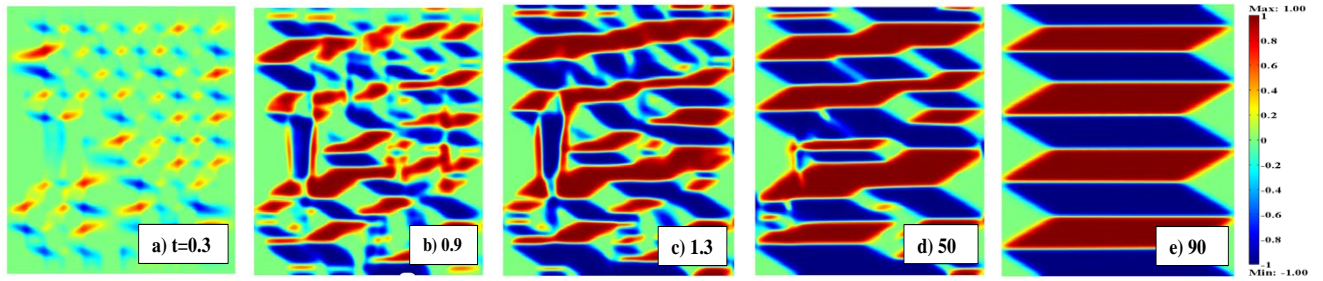
Fig. S 1: Evolution of $2\Upsilon(\vartheta - 0.5)$ in a square sample of size 50×50 with an initial stochastic distribution of order parameter Υ under biaxial normal strain of 0.01.

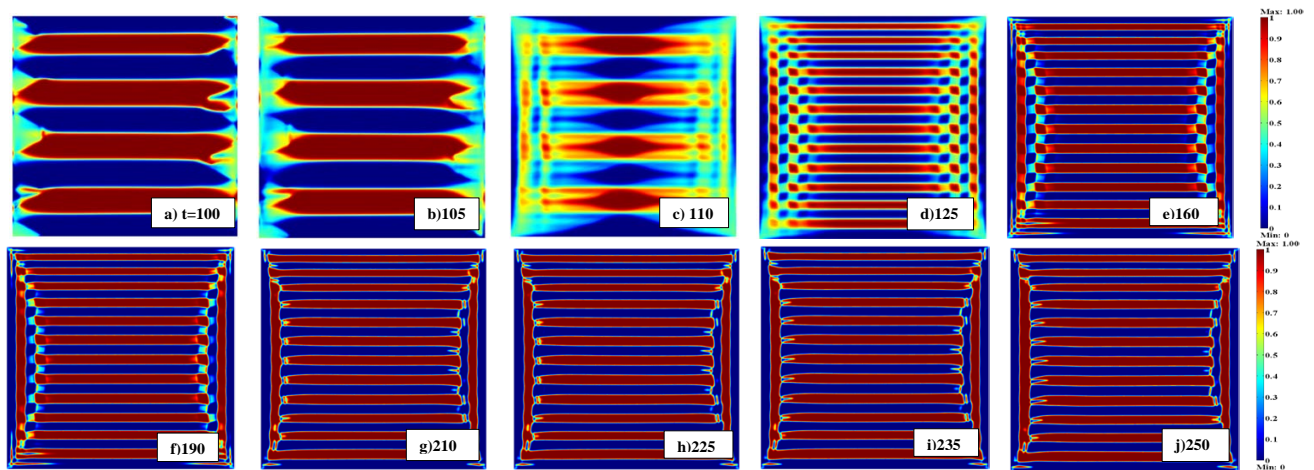Fig. S 2: Evolution of ϑ in a square sample of size 50×50 under biaxial normal strain of 0.01 with an initial condition shown in Fig. S1(e), reduced temperature $\theta = 0K$ and parameter $\beta_\vartheta = 5.18 \times 10^{-11}\,N$ and changed transformation strain.

reduced to $\beta_\vartheta = 5.18 \times 10^{-11}\,N$, which led to twin interface energy $E_{MM} = 0.303 J/m^2$ and width $\Delta_{MM} = 0.263nm$; components of transformation strains have been changed to the values $\boldsymbol{U}_{t1} = (k_1, k_2, k_2)$ and $\boldsymbol{U}_{t2} = (k_2, k_1, k_2)$ with $k_1 = 1.15$ and $k_2 = 0.93$ corresponding to NiAl alloy in [23]. Then Υ was made equal to 1 everywhere and kept during the entire simulation. Due to reduction in the interface energy, number of twins increased by splitting of the initial twins (Fig. S2). Without austenite, rigid vertical boundaries led to high elastic energy. That is why restructuring produced vertical twins near each of vertical sides in proportion, reducing energy of elastic stresses due to prescribed horizontal strain. When microstructure transformed to fully formed twins separated by diffuse interfaces, narrowing and bending of the tips of horizontal T_2 plates is observed (Figs. S2 and S3), similar to experiments [23, 24]. Note, that since invariant plane interface between T_1 and T_2 requires mutual rotation of these variants by the angle $\omega = 12.1^o$ ($\cos\omega = 2k_1 k_2/(k_1^2 + k_2^2) = 0.9778$) [23], angle between horizontal and vertical variants T_2 is $1.5\omega = 18.15^o$, which is in good agreement with our simulations. Thus, due to lattice rotations, interface between horizontal and vertical variants T_2 cannot be invariant plane interface, and reduction in the internal stresses at this boundary leads to reduction of the boundary area by narrowing and bending of the tips of one horizontal plates. Measured angles between tangent to the bent tip and horizontal line in the experiment [23] and in calculations (Fig. S3) are in good quantitative agreement.
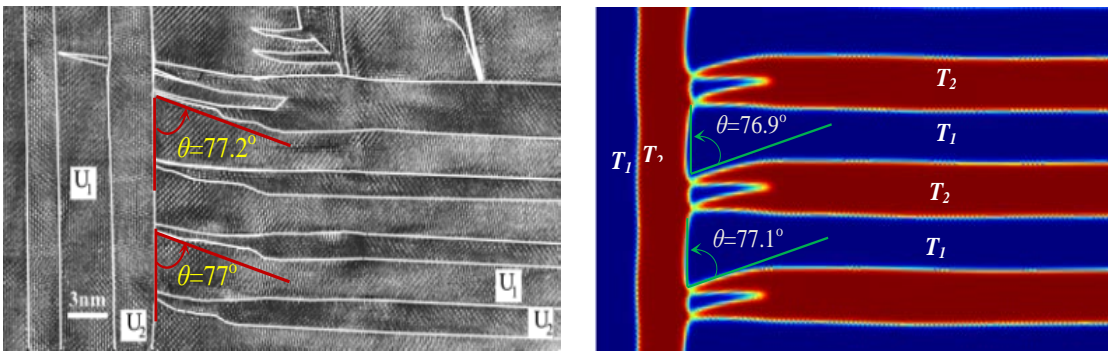

Fig. S 3: Comparison of transmission electron microscopy image of a nanaostructure for NiAl alloy from [23, 24] and zoomed part of simulation results from Fig. S 2(j). Simulations reproduce well tip splitting and bending angel.

Note that microstructure evolution occurs through intermediate values of ϑ in some regions (see $t = 125$ and 160 in Fig. 2), i.e., when transformation strain of one twin penetrates in to region of another one, producing crossed twins. Such crossed twins have been observed in some experiments [25] and have been arrested (Fig. S4). In our simulations in Fig. S2, they represent intermediate stage of evolution. However, if we reduce $\bar{A}$ to 0.532 GPa, the such crossed twins represent stationary solutions (Figs. S4). Also, on the right side of the solution in Fig. S2, an alternative way for stress relaxation is visible, when twins T_2 are surrounded by twins T_1, which is also observed in experiments [24].
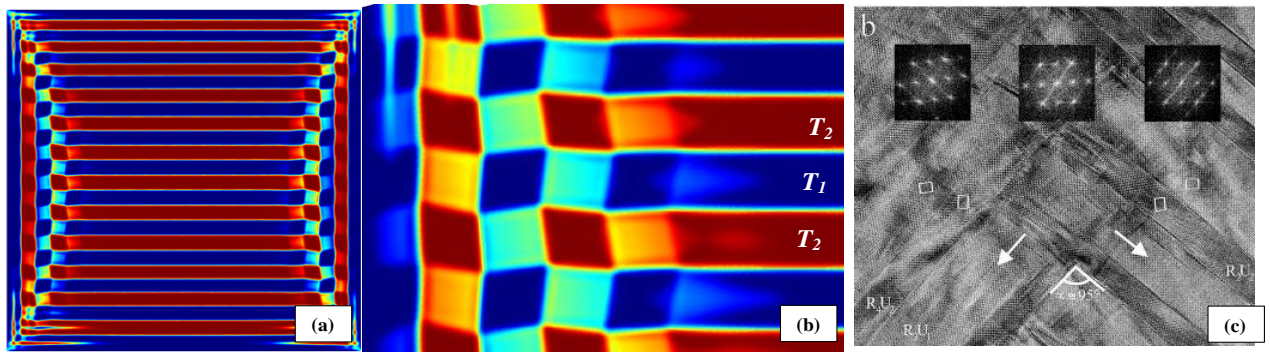

Fig. S 4: (a) Stationary solution for $2\Upsilon(\vartheta - 0.5)$ in a sample and (b) its zoomed part near left side of a sample; (c) transmission electron microscopy of a nanaostructure for NiAl from [23]. Crossing twins are observed in experiment and simulation.

Thus, starting with a microstructure in Fig. S1, which is quite far from the final one, our solution reproduced three types of nontrivial experimentally observed microstructures involving finite rotations, including good quantitative agreement for bending angle.

Example 2

1 Indentation Problem
(Under dynamic Pressure)

Nanoindentation-induced twinning $\mathsf{M}_2 \rightarrow \mathsf{M}_1$ was studied in a M_2 sample with a pre-existing M_1 embryo of radius 2 under the indentor (Fig. 1-3). The sample was obtained from a square A sample of size 50×50 by transforming it homogeneously to M_2. The cubic axes and transformation strain were rotated by $\alpha = 31^o$ with respect to the coordinate axes. Initial

conditions were: $r = 1$ everywhere; $\vartheta = 0.9$ inside the embryo and $\vartheta = 0.999$ in the rest of the sample. A uniform pressure between the indentor of width 4 and the sample was increased linearly from 2 to 3 GPa over $110ps$. The bottom sample surface was constrained by a roller support (zero normal displacements and zero shear stresses) and point F was fixed; all other surfaces are stress-free. With increasing load, a twin M_1 appears under the indenter and grows in a wedge shape with a sharp tip (Fig. 1a, b). Since the bottom of the sample was constrained by the roller support, the twin M_1 could not propagate through the entire sample. In the same problem but with a stress-free section of length 20 at the bottom (Fig.1c-d), the twin propagated completely through the sample and widened with increasing load. The load was then reduced to zero: the width of the twin then decreased to zero without a change in length (Fig.1e-f). These results are in qualitative agreement with experiments [1, 2] and previous simulations [10]. Since dislocation plasticity and interface friction [5, 29] are neglected, there is no residual twin.
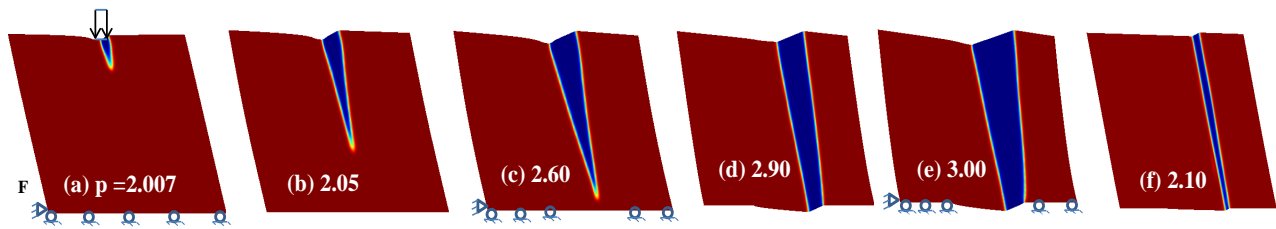

Figure 5: Twinning M_2 (red) $\rightarrow \mathsf{M}_1$ (blue) under indentation with the rigid support (a)-(b), support with the hole (c)-(e), and during unloading (f).
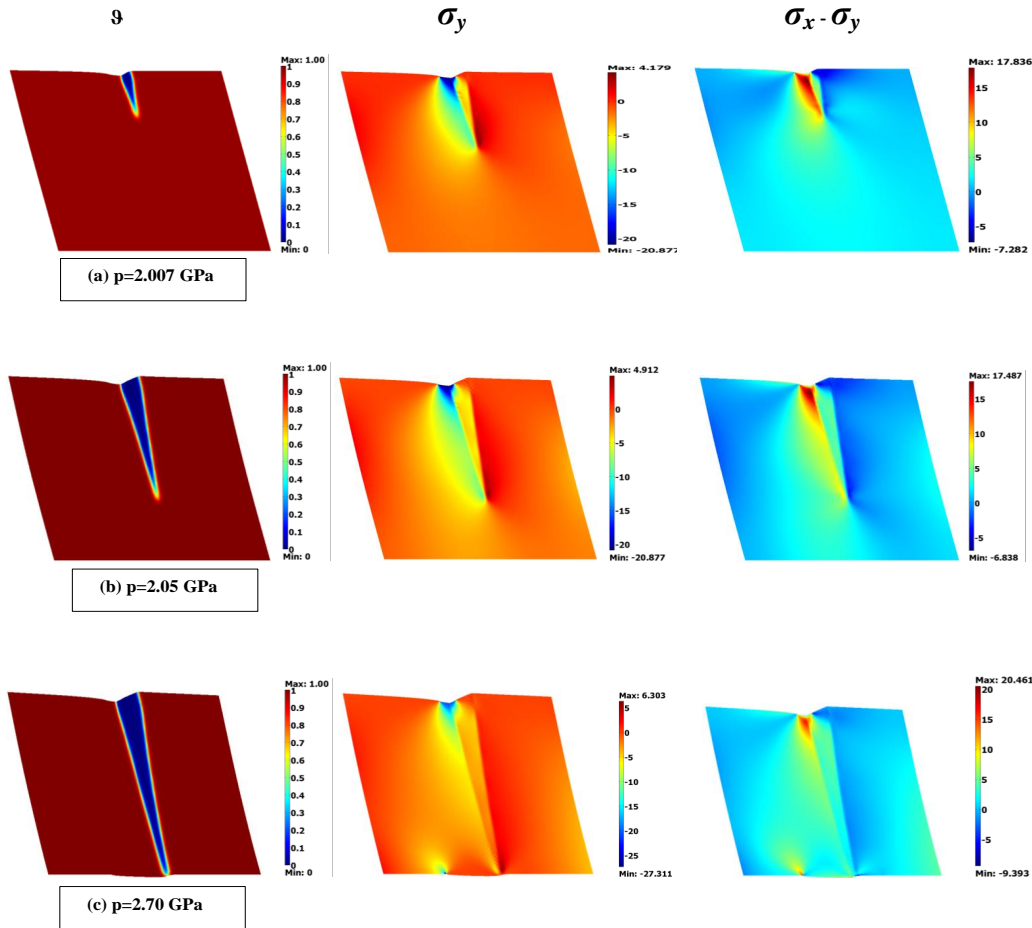
Figure 6: Evolution of twin microsture under dynamic pressure in an intial M_2 sample.Left Column: ϑ; second and third columns: σ_y and $\sigma_x - \sigma_y$; right column:σ_{xy}. Twinning M_2 (red) $\rightarrow M_1$ (blue) under indentation with the rigid support (a)-(b), support with the hole (c).
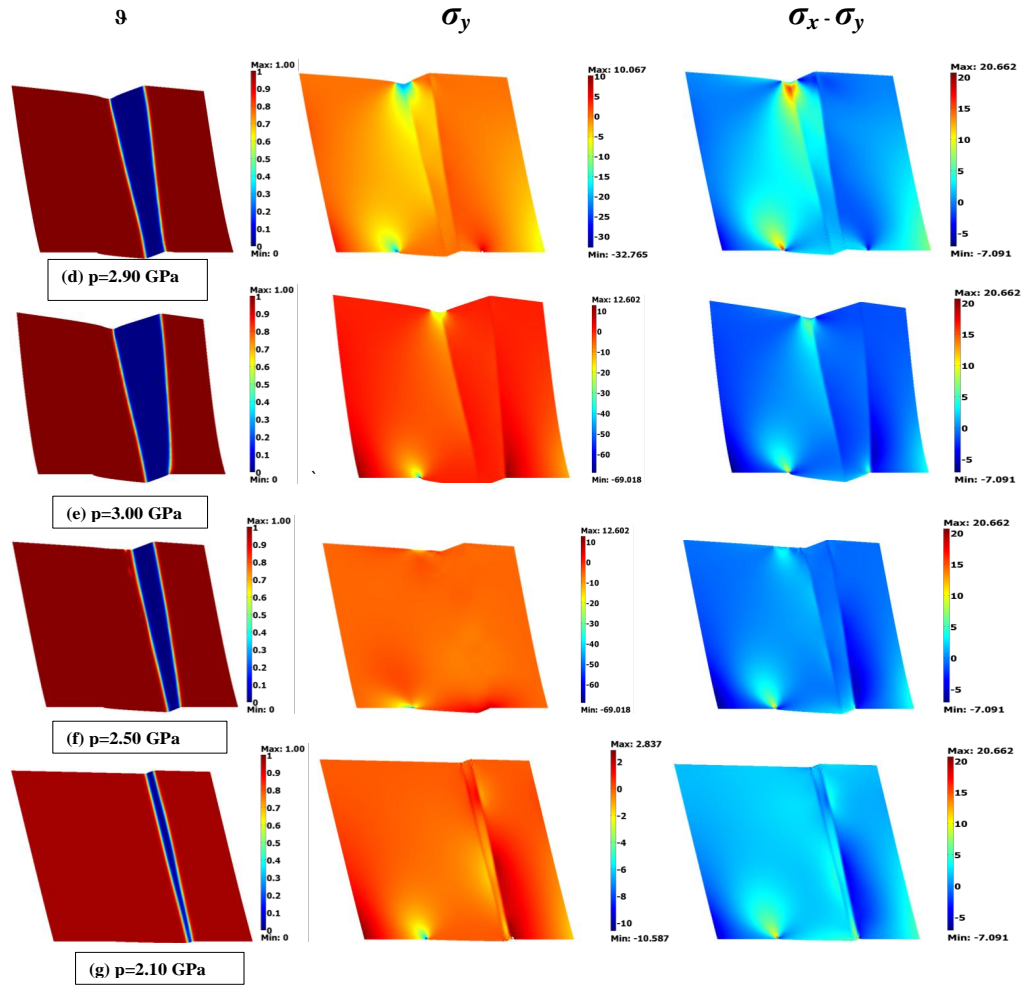
Figure 7: (continue) Evolution of twin microsture under dynamic pressure in an intial M_2 sample.Left Column: ϑ; second and third columns: σ_y and $\sigma_x - \sigma_y$; right column:σ_{xy}. Twinning M_2 (red) $\rightarrow M_1$ (blue) under indentation when support with the hole (d)-(e) and during unloading (f)-(g).

Example 3

1 Indentation Problem
(Under dynamic displacement)

Nanoindentation of a square 50×50 A sample with $\alpha = 15^0$ was modeled by prescribing uniform vertical displacements growing from 2 to 2.5 over a section of width 4; friction was neglected (Fig. 4-6). Adjacent lateral surfaces of the sample were constrained by the roller supports. In an initial embryo of radius 2 we set $r = 0.1$; $r = 0.01$ outside of the embryo. The order parameter $\vartheta = 0.5$ everywhere. The transformed twinned martensite first grew only in the vertical direction; note the presence of a small non-transformed region under the indenter (Fig. 4 (a)-(f)). When the stress concentration due to the indenter became smaller than the internal stresses due to transformation strain and the bottom constraint, a morphological transition occurred: the growth of M_2 changed direction away from M_1 toward a corner of the sample, and ultimately reached the corner. The M_2-M_1 interface is curvilinear and consequently cannot be described by pure crystallographic theory presented in e.g., [27].

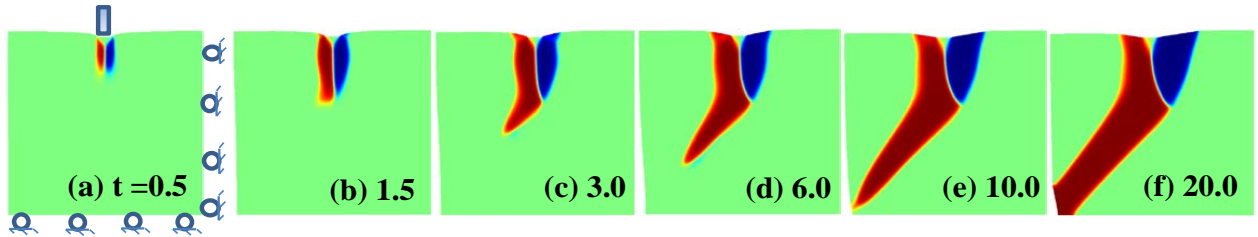Figure 8: Evolution of $2r(\vartheta - 0.5)$ for indentation of A (green) sample; M_2: red and M_1: blue.
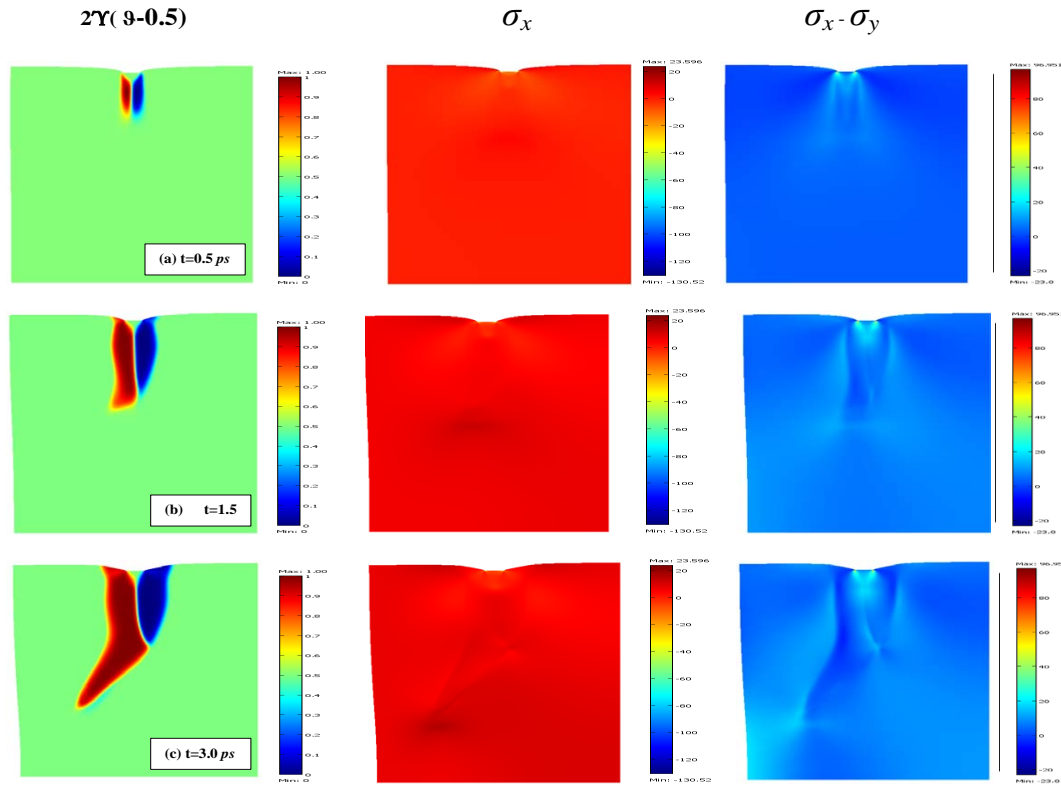
Figure 9: Evolution of twin martensitic microsture under dynamic displacement in an intial A sample. Left Column: $2r(\vartheta - 0.5)$; second and third columns: σ_x and $\sigma_x - \sigma_y$; right column: σ_{xy}. Here M_2 (red), M_1 (blue) and A(green) under double indentation from $t = 0.5ps$ (a) to $t = 3.0ps$ (c).
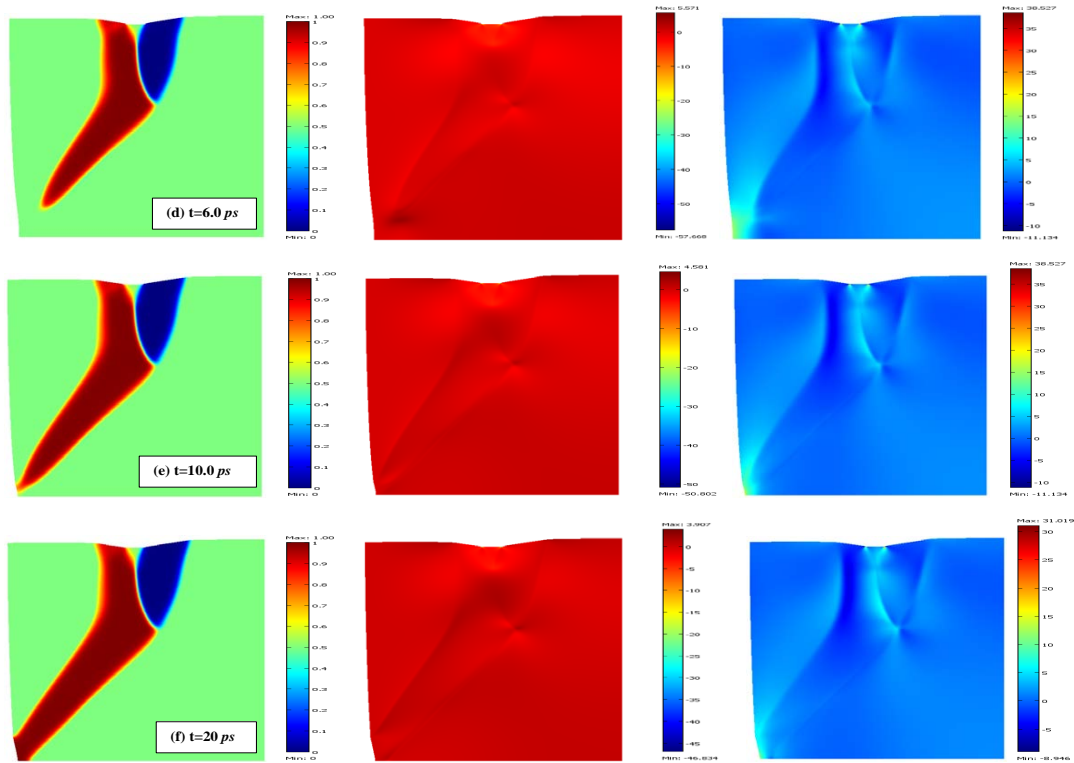
Figure 10: (continue) Evolution of twin martensitic microsture under dynamic displacement in an intial A sample.Left Column: $2r(\vartheta - 0.5)$; second and third columns: σ_x and $\sigma_x - \sigma_y$; right column:σ_{xy}. Here M_2 (red),M_1 (blue)and A(green) under double indentation from $t = 6.0ps$ (d) to $t = 20ps$ (f).

Example 4

2 Indentation Problem

Two indentors of width $4\ nm$ were placed on adjacent sides of a square 50×50 A sample with $\alpha = 45^0$ (Fig. 7-10). At $t = 0$, there were uniform pressures $p_1 = p_2 = 3$ across the indentors. The remaining lateral surfaces of the sample were constrained by roller supports. In two initial embryos of radius 2 under the indentors, $r = 0.1$; outside the embryos $r = 0.01$. Again, $\vartheta = 0.5$ everywhere. The complex evolution of the twinned nanostructure is shown in Fig. 7a-i. Starting with state (h), p_2 was slowly reduced to zero while keeping $p_1 = 3$. The quasi-stationary solutions in Fig. 7j-l show an initial reversal of the nanostructure (see Figs. 7j and g) followed by the predominance of M_1.
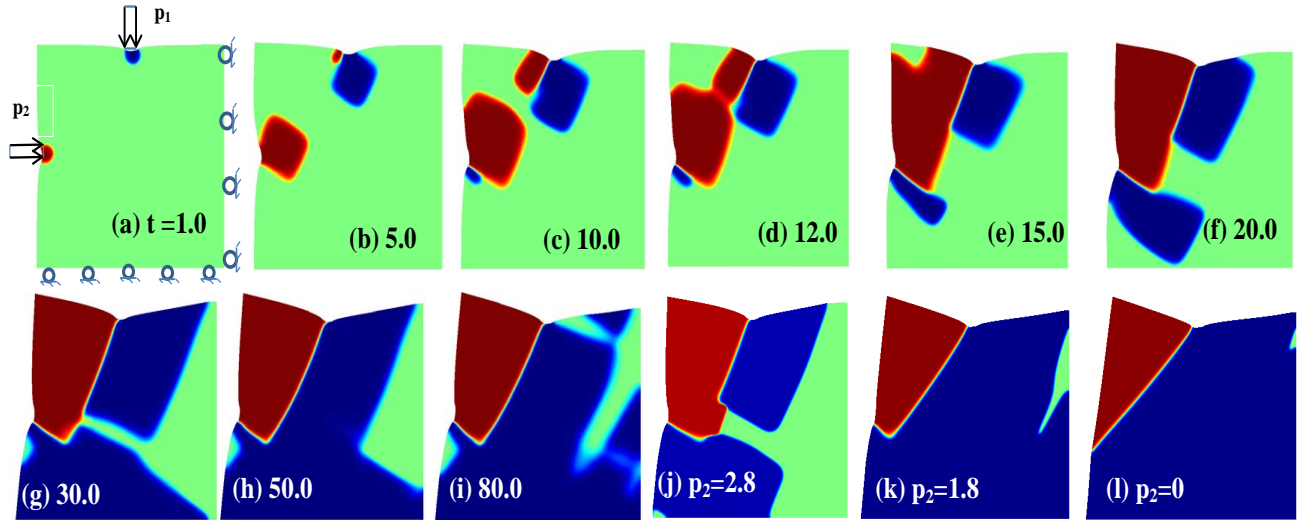

Figure 11: Evolution of $2r(\vartheta - 0.5)$ in time (a-i) for double indentation of an A sample at $p_1 = p_2 = 3$, followed by reduction of p_2 to zero at $p_1 = 3$ (j-l) from state (h).
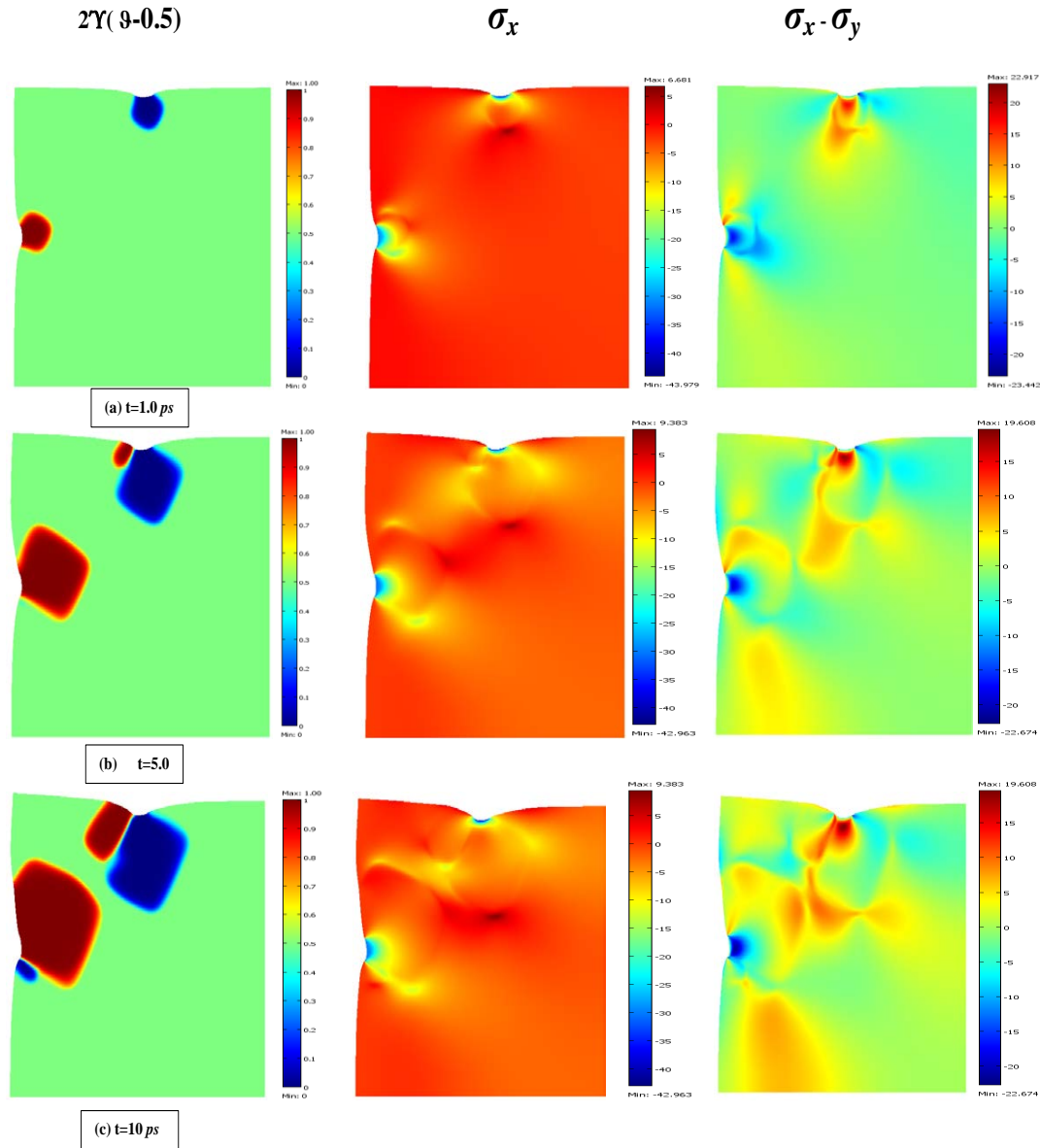
Figure 12: Evolution of Evolution of $2r(\vartheta - 0.5)$ under double indentors in an intial A sample.Left Column: $2r(\vartheta - 0.5)$; second and third columns: σ_x and $\sigma_x - \sigma_y$; right column:σ_{xy}. Here M_2 (red),M_1 (blue)and A(green) in time (a-c) for double indentation of an A sample at $p_1 = p_2 = 3\text{GPa}$

Figure 13: (continue) Evolution of Evolution of $2r(\vartheta-0.5)$ under double indentors in an intial A sample.Left Column: $2r(\vartheta-0.5)$; second and third columns: σ_x and $\sigma_x-\sigma_y$; right column:σ_{xy}. Here M_2 (red),M_1 (blue)and A(green) in time (d-f) for double indentation of an A sample at $p_1=p_2=3\mathrm{GPa}$

(g) p=2.8 *GPa*

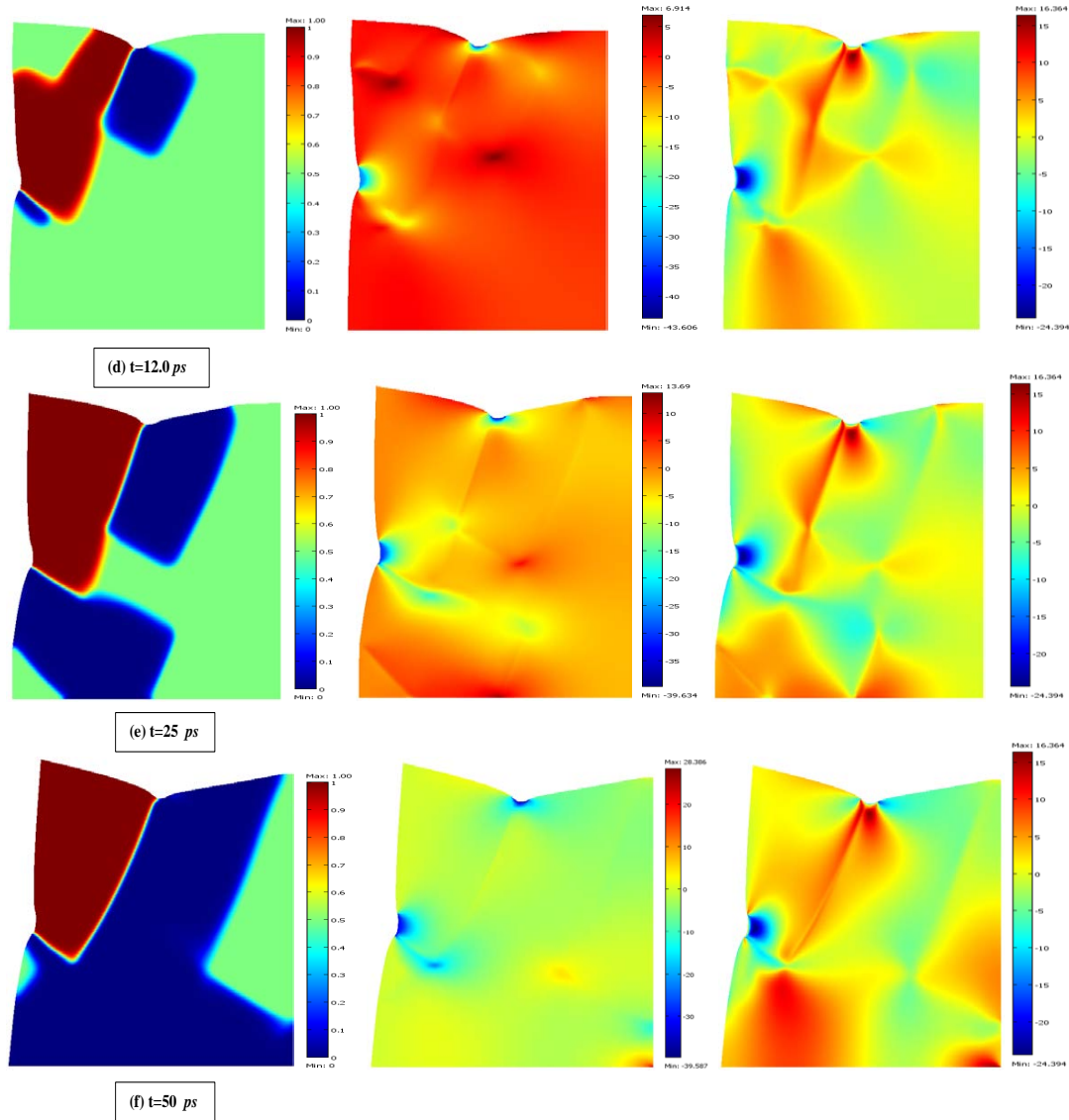(h) p=1.8 *GPa*

(i) p=0 *GPa*

Figure 14: (continue) Evolution of Evolution of $2r(\vartheta-0.5)$ under double indentors in an intial A sample.Left Column: $2r(\vartheta-0.5)$; second and third columns: σ_x and $\sigma_x - \sigma_y$; right column:σ_{xy}. Here M_2 (red),M_1 (blue)and A(green) in time (d-f) for double indentation of an A sample at reduction of p_2 to zero at $p_1 = 3$ (g-i) from state (f).

Example 5

Homogeneous Loading Problem with initial Austenite

A square A sample of size 100×100 with $\alpha = 15^o$ and an embryo of 2 nm radius in the center of the sample (Fig. 11-13) was subjected to uniform vertical and horizontal stresses $\sigma_y = 3$ and $\sigma_x = 0.1$, respectively. Because of the reflection symmetry, only one-quarter of the sample was directly simulated; roller supports were applied along the symmetry axes. The parameter values $\bar{A} = 61.6 MPa$ and $\beta_{MM} = 19.4 \times 10^{-12} N$ were used, corresponding to $E_{MM} = 0.01 J/m^2$ and $\Delta_{MM} = 1nm$. The initial conditions in the embryo were $r = 0.1$, and $r = 0.001$ outside the embryo; $\vartheta = 0.5$ everywhere. Within $1ps$, A was transformed to a mixture of M_i twins, which further evolve to produce a nontrivial stationary morphology. Note that varying the ratio $\lambda_\vartheta / \lambda_r$ from 1 to 1000 with $\lambda_r = 2596.5 m^2/Ns$ did not change the stationary solution and only slightly affected the evolution.
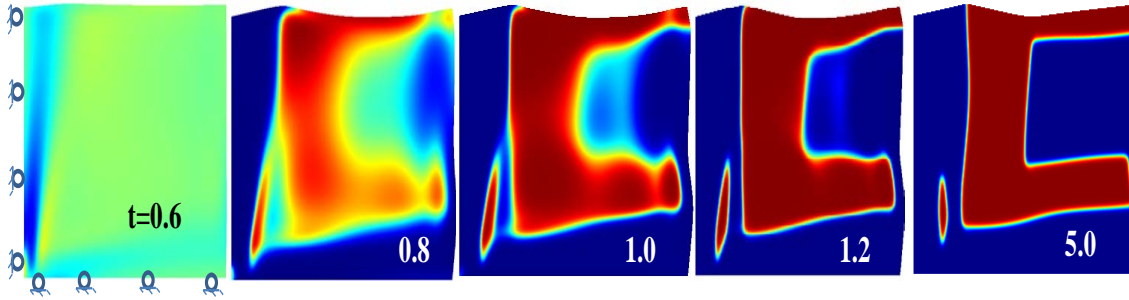
Figure 15: Evolution of $2r(\vartheta - 0.5)$ in a quarter of 100×100 sample with an initial embryo at the center under homogeneous compressive stress of $\sigma_y = 3$ and $\sigma_x = 0.1$.
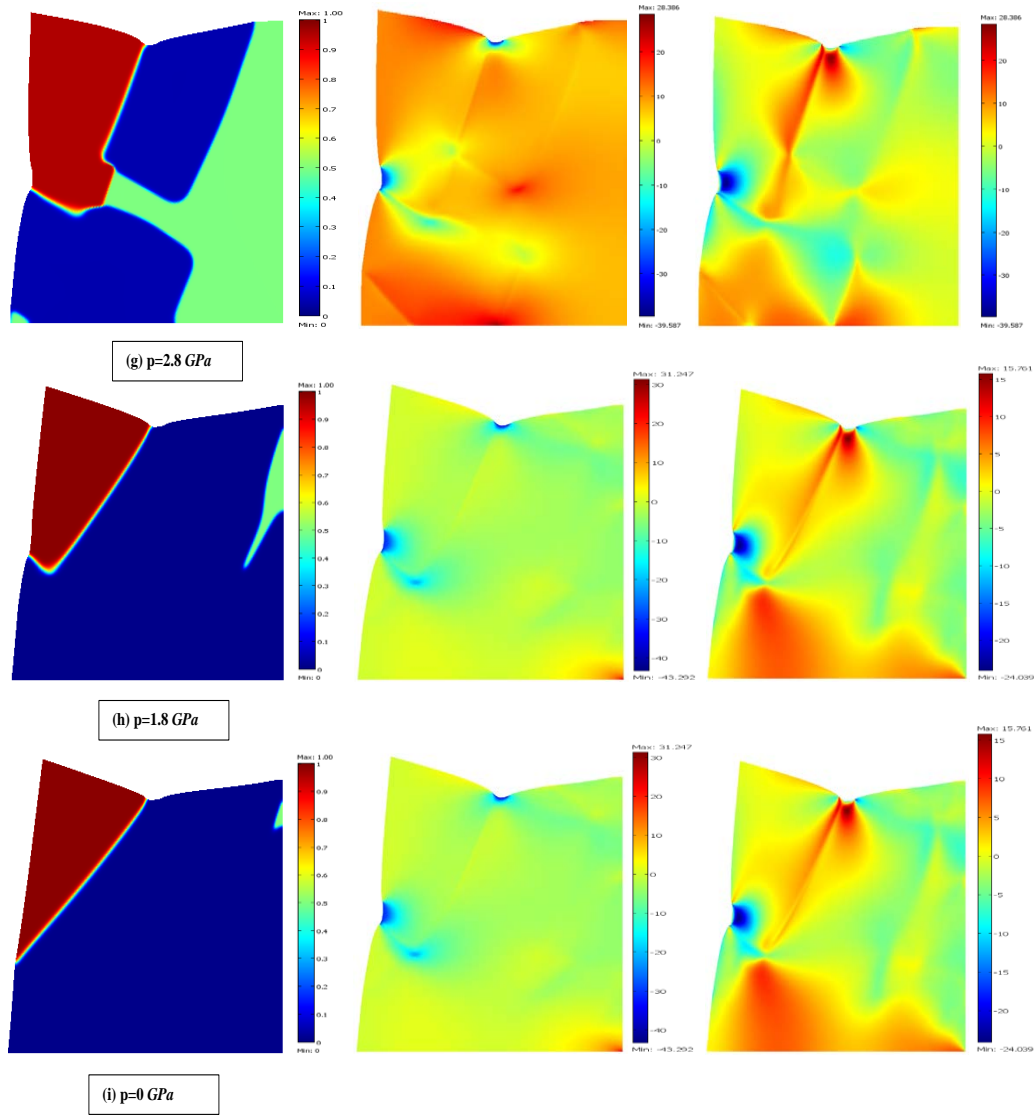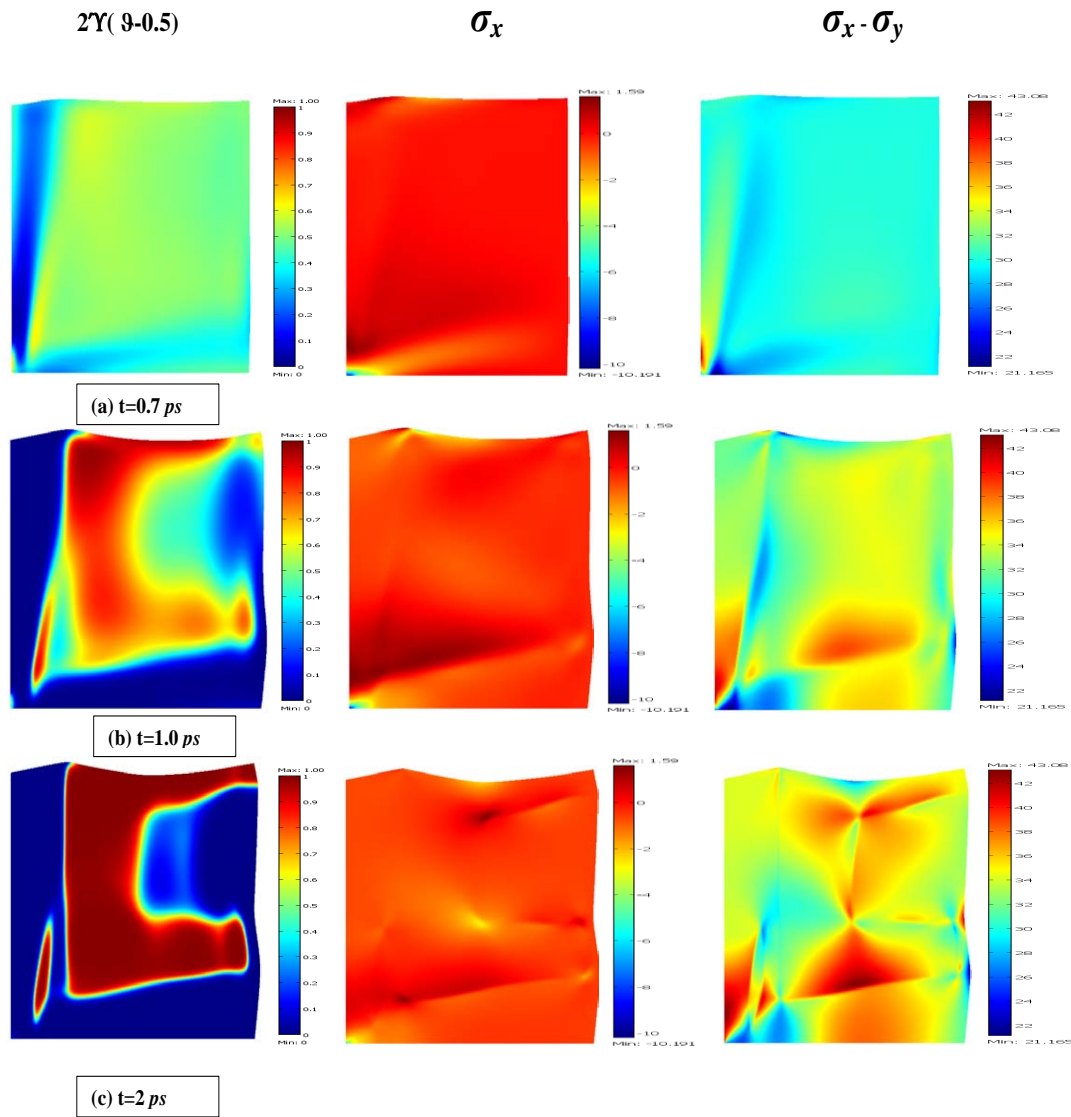
Figure 16: (continue)Evolution of Evolution of $2r(\vartheta-0.5)$ under homogenous compressive load in an intial A sample.Left Column: $2r(\vartheta-0.5)$; second and third columns: σ_x and $\sigma_x-\sigma_y$; right column:σ_{xy}. Here M_2 (red),M_1 (blue)and A(green) in time from t=0.7ps (a) to t=2ps (c).

(d) t=8.0 *ps*

(e) t=20 *ps*

(f) t=60 *ps*

Figure 17: (continue) Evolution of Evolution of $2r(\vartheta - 0.5)$ under homogenous compressive load in an intial A sample. Left Column: $2r(\vartheta - 0.5)$; second and third columns: σ_x and $\sigma_x - \sigma_y$; right column:σ_{xy}. Here M_2 (red),M_1 (blue)and A(green) in time from t=8 ps (d) to t=60 ps (f).
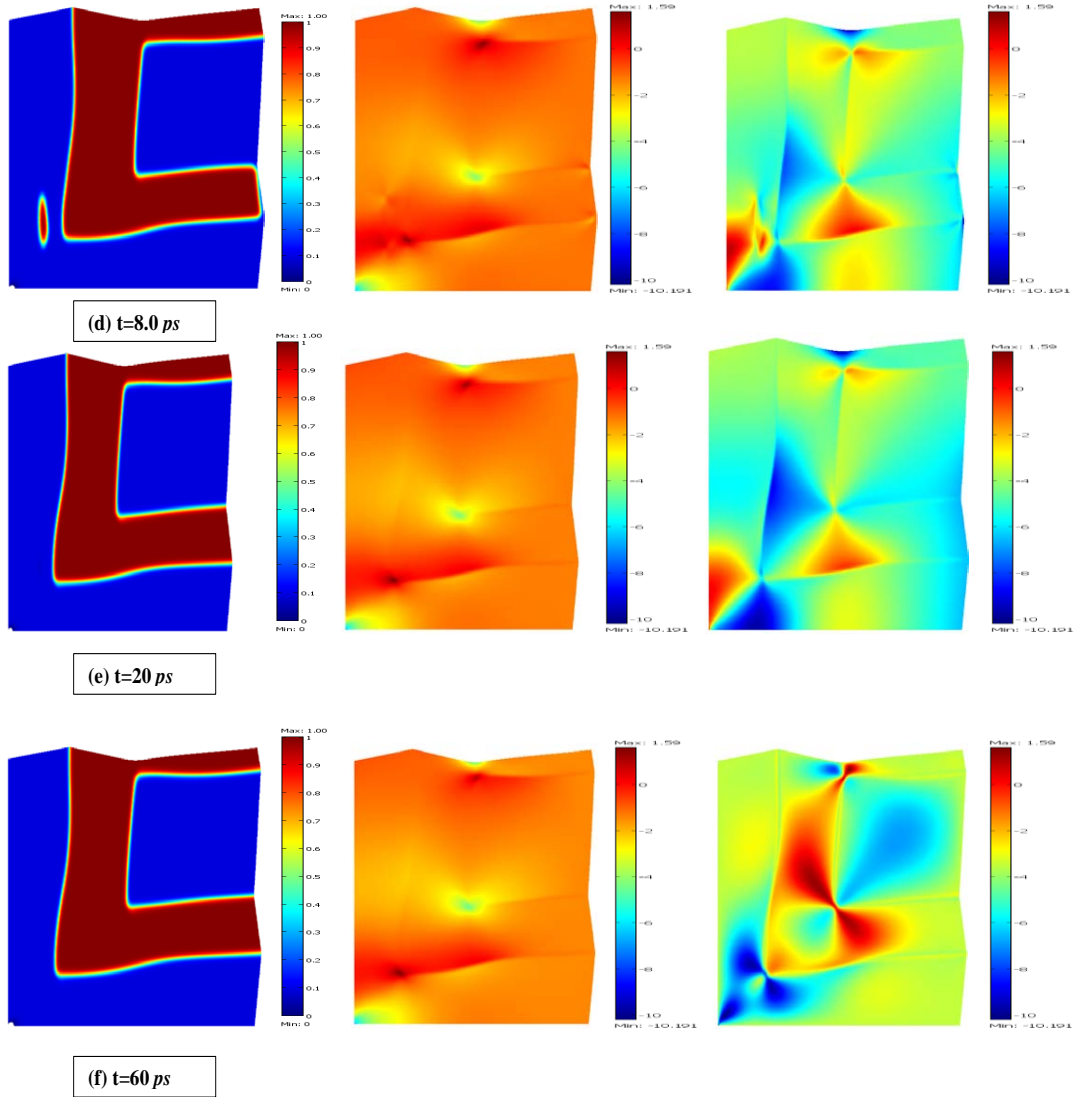
Example 6

Homogeneous Loading Problem with initial Martensite

A square M1 sample of size 100×100 with $\alpha = 31^o$ and an embryo of 2 nm radius in the center of the sample (Fig. 14-15) was subjected to uniform vertical stresses $\sigma_y = 100 N/m^2$. Because of the reflection symmetry, only one-quarter of the sample was directly simulated; roller supports were applied along the symmetry axes. The initial sample was M1, so order parameter, ϑ was 0.1 inside the embryo and ϑ was 0.01 outside the sample, with parameter $r = 1$ everywhere.The results are shown in Fig. 14-15:the first column shows the evolution of $2r(\vartheta - 0.5)$, the second and third columns show the stresses σ_x and $\sigma_x - \sigma_y($ since the thermodynamic driving force is proportional to $\sigma_x - \sigma_y$, and the last column depicts the shear stress (σ_{xy}) distribution with time. Here the part of M1 transformed to M2 to get sophisticated twinning plane at the end. The evolution starts with nucleation in the zone of stress concentration (a-b) and part of M1 get converted to M2. A complex multi connected nanostructure passes through the coalescence stage(c-d) and finally produce nice twinning plane (e-f). The stationary solution is not a homogeneous solution due to boundary constraints and with the evolution of time martensitic variants cycle between two type(e and f) of micro structures.

Figure 18: Evolution of martensitic variants due to external loading of an A sample in time (a-c) . Left Column: $2r(\vartheta - 0.5)$; second and third columns: σ_x and $\sigma_x - \sigma_y$; right column:σ_{xy}. Here M_2 (red),M_1 (blue)and A(green) in time (a-c).
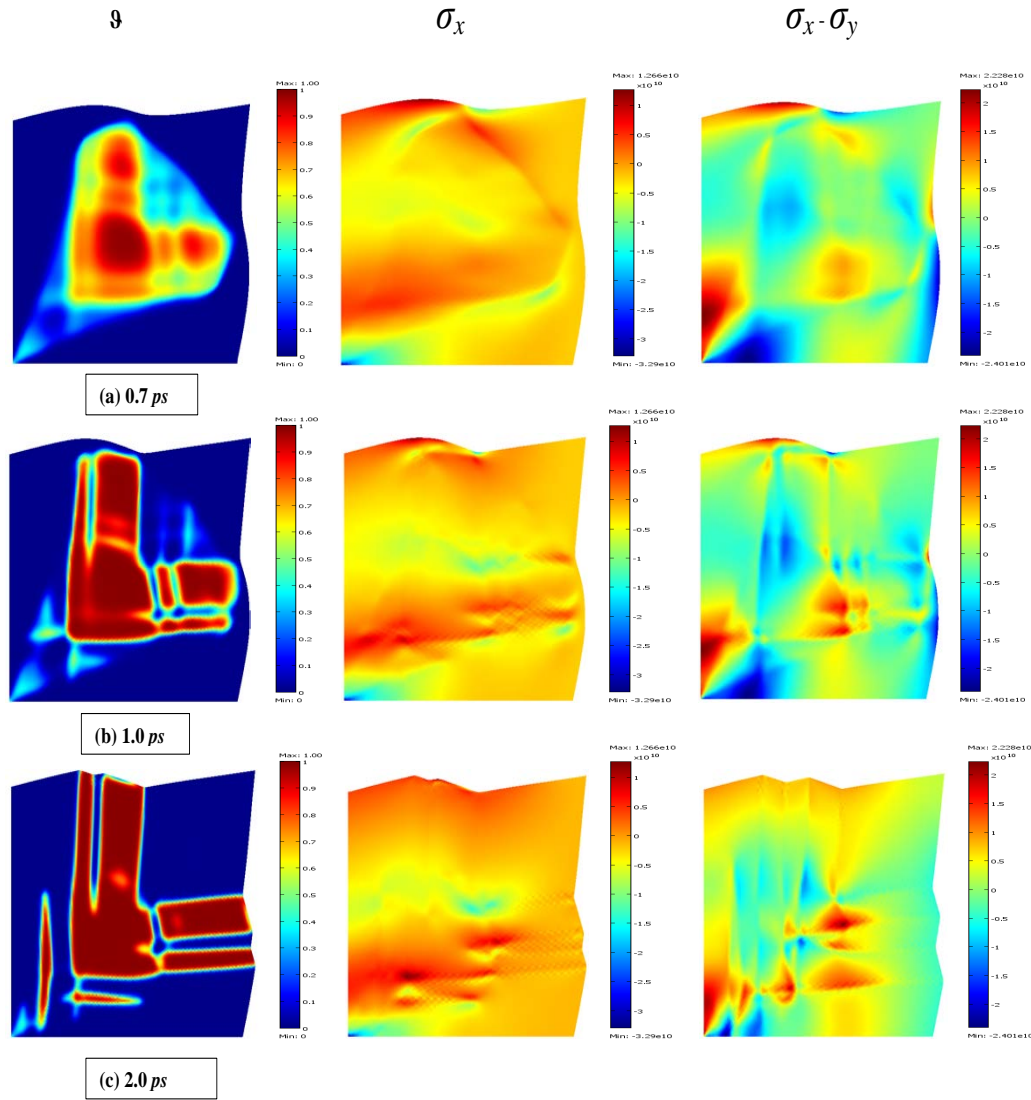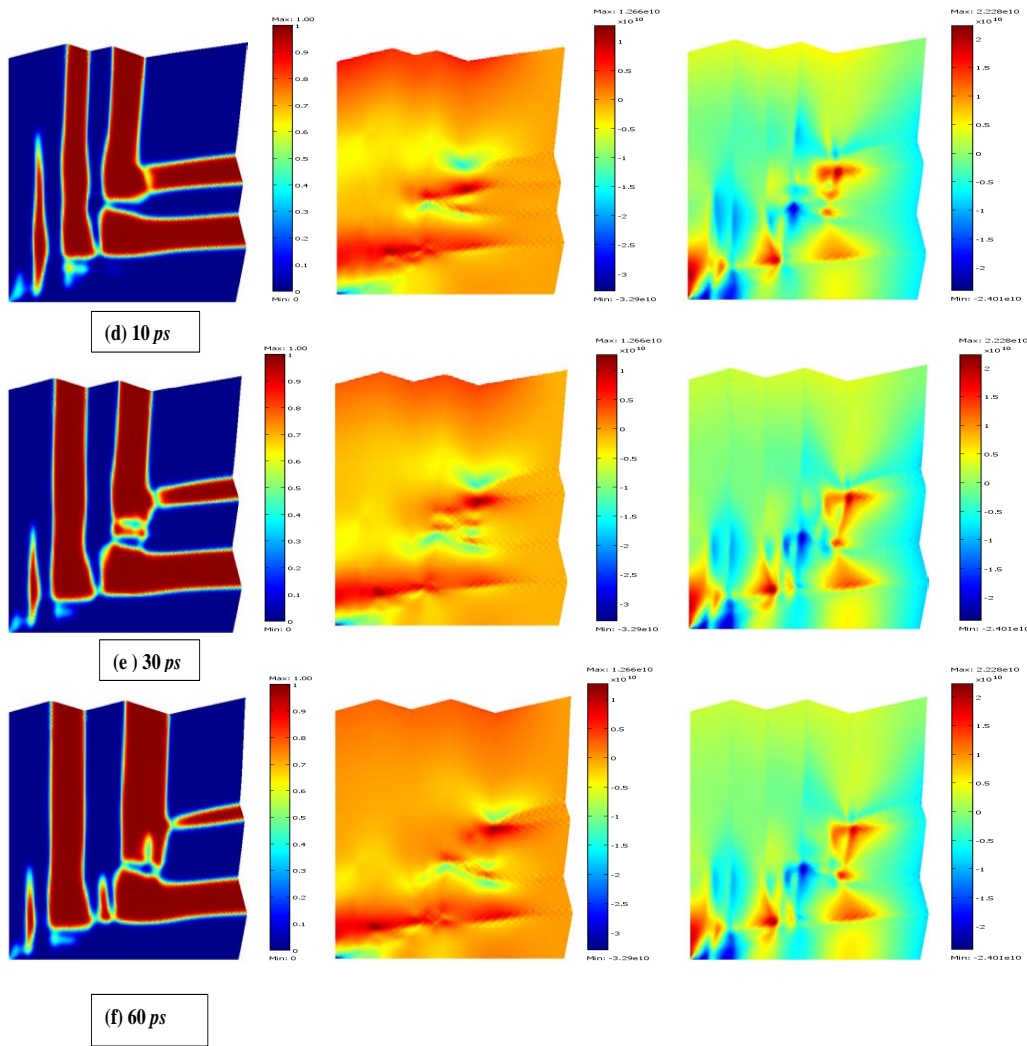
Figure 19: Evolution of martensitic variants due to external loading of an A sample in time (d-f). Left Column: $2r(\vartheta - 0.5)$; second and third columns: σ_x and $\sigma_x - \sigma_y$; right column:σ_{xy}. Here M_2 (red),M_1 (blue)and A(green) in time (d-f).

Example 7

Stochastic Problem

Initial random distribution of order parameter r was studied in square 50×50 sample with $\alpha = 15^o$ under homogeneous initial starin (Fig.16-17). Here initial distribution of order parameter r , varies between 0.0 to 0.4 randomly throughout the sample and ϑ was 0.5 throughout. We consider homogeneous initial strain of magnitude 0.1 to all four free surfaces.The sample is under plane stress condtion and temperature is $\theta = 50K$ which is below critical martensitic start temperature to faciliate twinning. The results are shown in Fig. 16-17:the first column shows the evolution of $2r(\vartheta - 0.5)$, the second and third columns show the stresses σ_x and $\sigma_x - \sigma_y$(since the thermodynamic driving force is proportional to $\sigma_x - \sigma_y$, and the last column depicts the shear stress (σ_{xy}) distribution with time.The initial perturbation exicted the system and intial martensite variants emarged initially (a) and they get connected to each other (b).They rapidly grows in horizontal direction (c-d) and formed nice martensitic plane prodominant in horizontal direction. At the end we get stationary very sophisticated microsture in which martensitic variants from nice twinning plan (f).

Figure 20: Evolution of twinning microsture in time (a-c) for randomly distributed order parameter r of an A sample. Left Column: $2r(\vartheta - 0.5)$; second and third columns: σ_x and $\sigma_x - \sigma_y$; right column:σ_{xy}. Here M_2 (red),M_1 (blue)and A(green) in time (a-c).

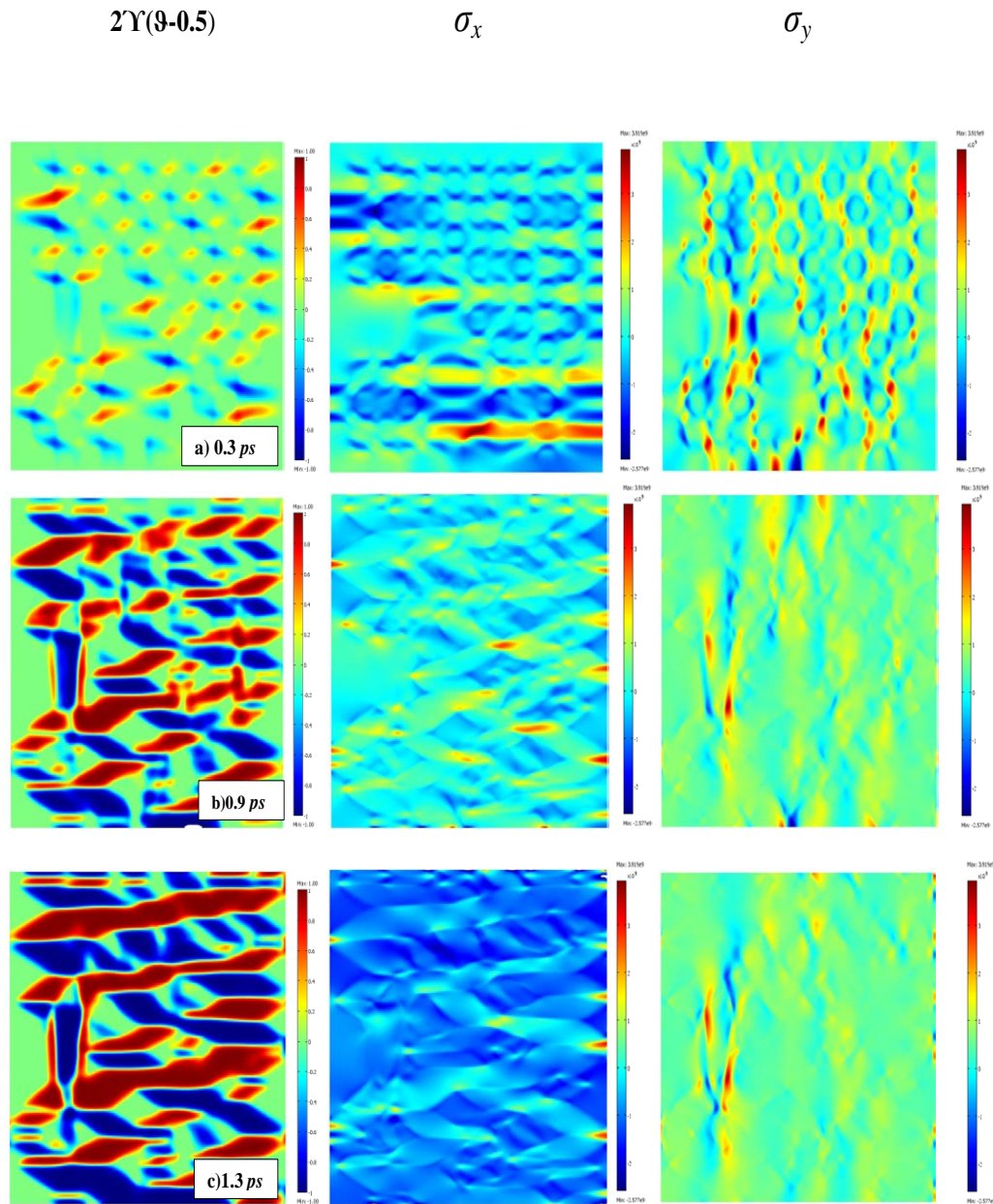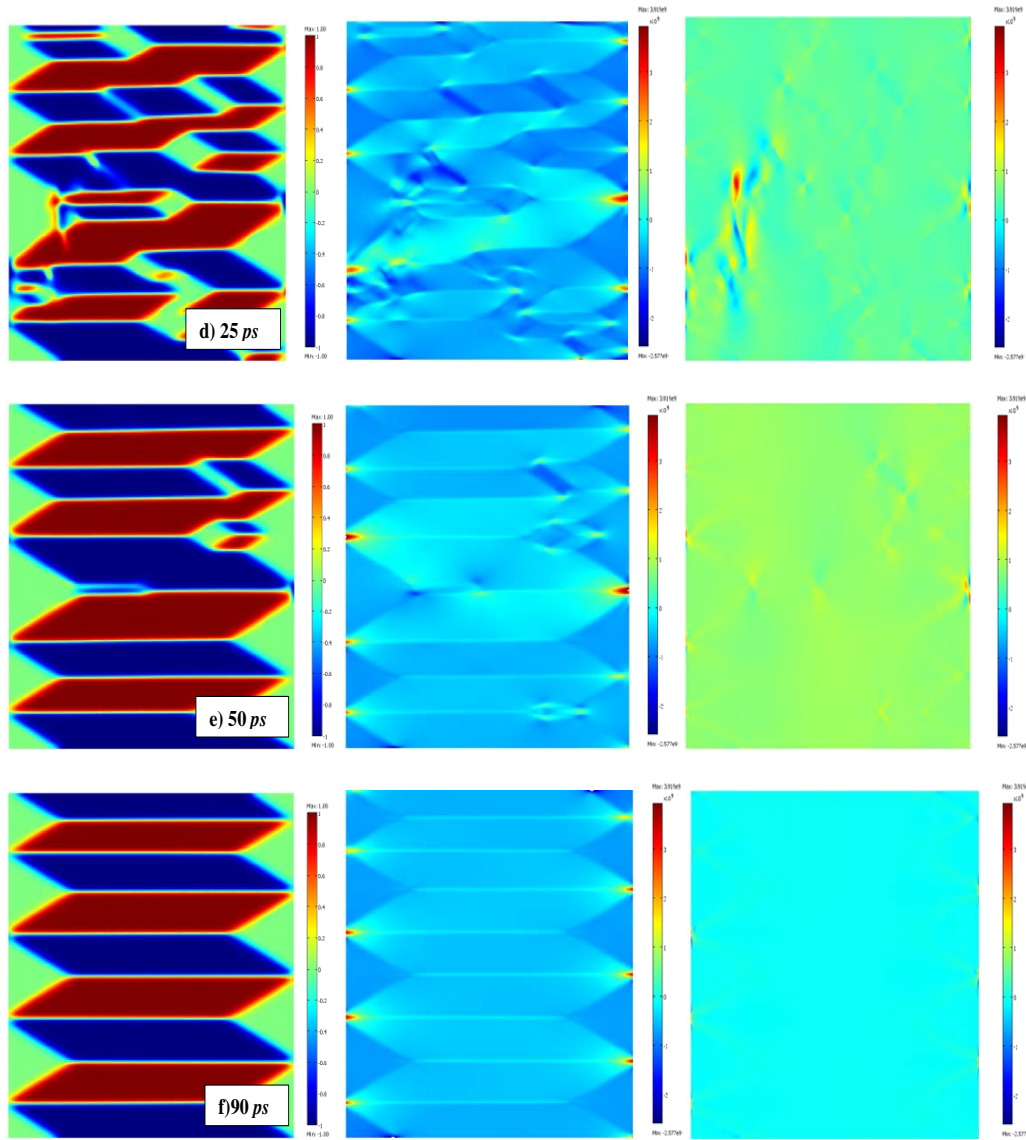Figure 21: (Continue)Evolution of twinning microsture in time (d-f) for randomly distributed order parameter r of an A sample. Left Column: $2r(\vartheta - 0.5)$; second and third columns: σ_x and $\sigma_x - \sigma_y$; right column:σ_{xy}. Here M_2 (red),M_1 (blue)and A(green) in time (d-f).

Example 8

Homogeneous Loading Problem

In our last problem, we consider a square sample of size $60 \times 60 nm^2$ with a preexisting embryo of 2 nm radius in the middle of the sample subjected to homogenous loding of $\sigma_x = \sigma_y = 20$ GPa with $\alpha = 31^0$.Temperature $\theta = 100K$ were used. Because of the reflection symmetry, only one-quarter of the sample was directly simulated; roller supports were applied along the symmetry axes. Inside the embryo, order parameter r considered as 0.1 and outside it was 0.01. Order parameter ϑ was 0.5 throughout the sample.The results are shown in Fig. 18-19:the first column shows the evolution of $2r(\vartheta - 0.5)$, the second and third columns show the stresses σ_x and $\sigma_x - \sigma_y$(since the thermodynamic driving force is proportional to $\sigma_x - \sigma_y$, and the last column depicts the local driving force,$\frac{\partial G}{\partial \vartheta}$, for the evolution of ϑ with time.The evolution of $2r(\vartheta - 0.5)$ started with the spiting with of the embryo into two martensitic variants separated by Austenite (a-b). A complex multiconnected nanostructure passed through the coalescence stage(c-e) and finally ended in a single variant homogeneous state (f) as a stationary solution at the end. Here different ratio of λ_{MM} to λ_{AM} (200 to 1000) were used to compare the rate of evolution of order parameter and different magnitude of biaxial load (3Gpa to 30GPa) in two lateral surfaces to check the difference in evolution pattern in martensitic variants in the sample. It is noted that evolution pattern in the micro structure are quite same for different magnitude of pressure. Also different ratio of $\frac{\lambda_{MM}}{\lambda_{AM}}$ indifferent to evolution of microstructure pattern.

2.13 Future Scope

To summarize, a phase field model of transformations between martensitic variants and multiple twinning in martensitic variants was developed. It accounts for large strains and lattice rotations, and incorporates only a minimal set of order parameters, one for each martensitic variant. Each variant-variant transformation and all of the infinite number of possible twinnings within them are described with a single order parameter. Despite this economy of order parameters, arbitrarily complex twin-within-a-twin martensitic microstructures can in principle be described by the model. The energies and widths of the $A-M_i$ and M_j-M_i interfaces can be controlled (prescribed), and the corresponding interface stresses are consistent with

Figure 22: Evolution of martensitic variants due to homogenous loading in time (a-d) of an initial A sample. Left Column: $2r(\vartheta - 0.5)$; second and third columns: σ_x and $\sigma_x - \sigma_y$; right column:σ_{xy}. Here M_2 (red),M_1 (blue)and A(green) in time (a-c).
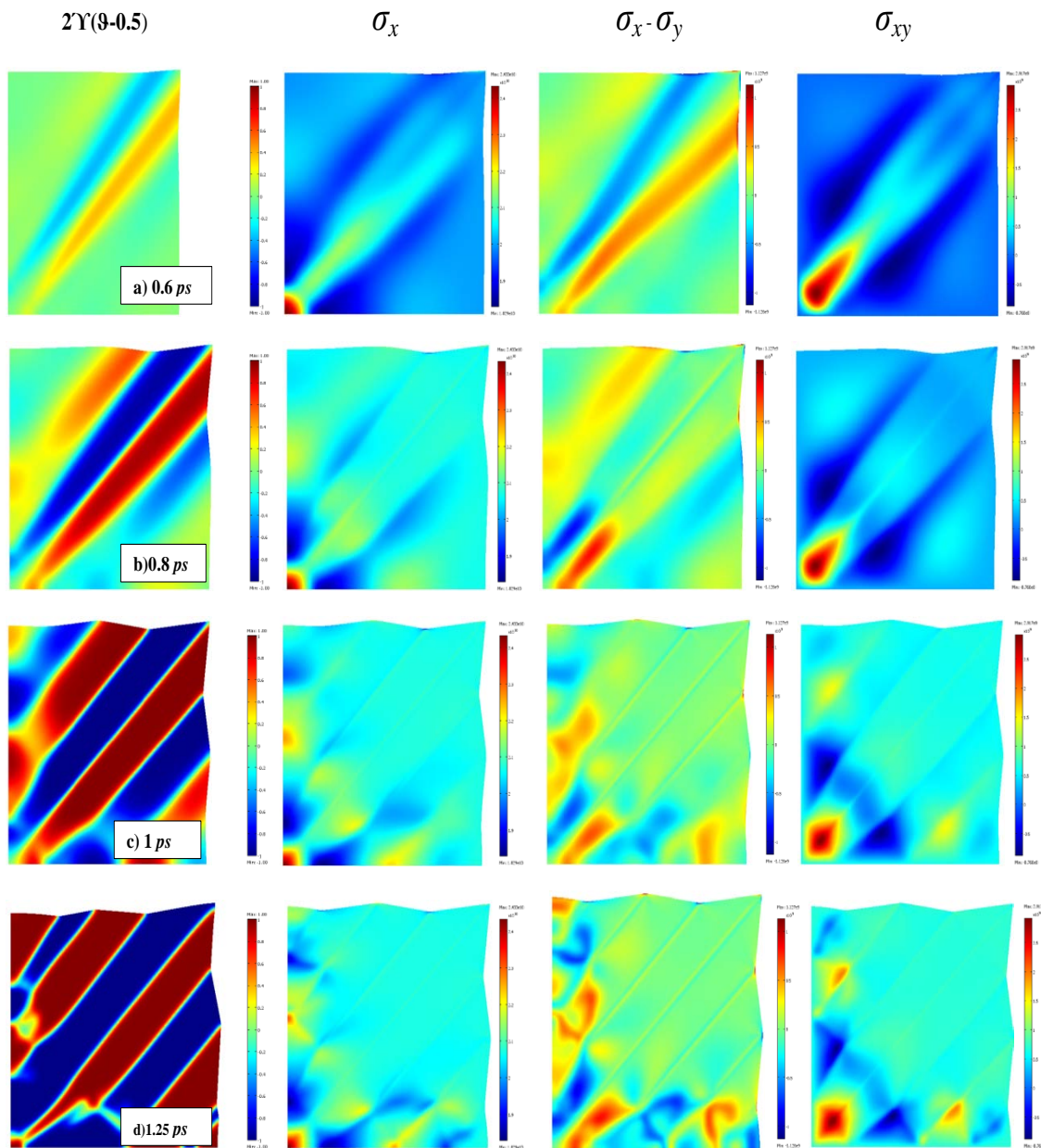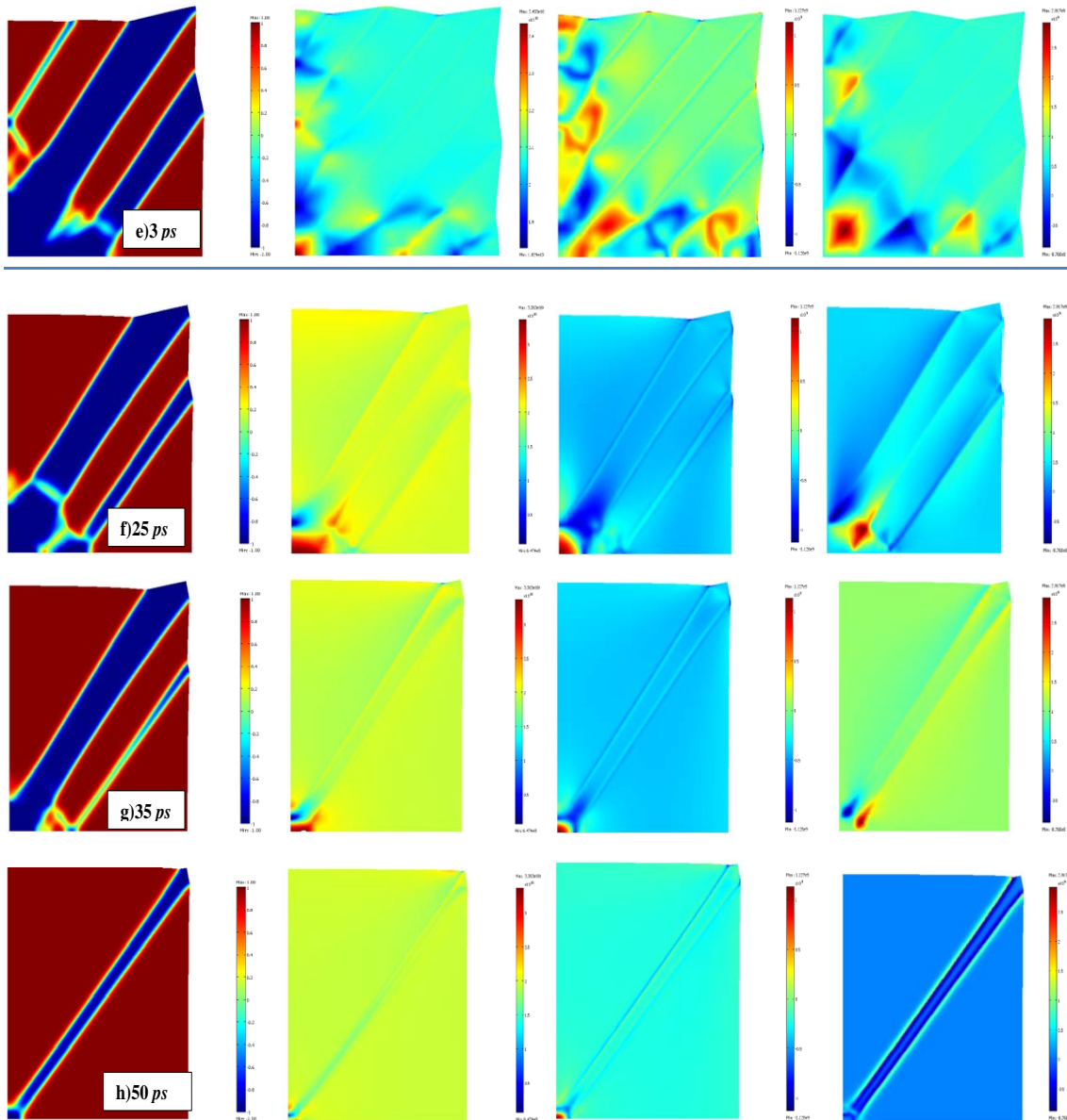
Figure 23: Evolution of martensitic variants due to homogenous loading in time (a-c) of an initial A sample. Left Column: $2r(\vartheta - 0.5)$; second and third columns: σ_x and $\sigma_x - \sigma_y$; right column:σ_{xy}. Here M_2 (red),M_1 (blue)and A(green) in time (e-h).

the sharp interface limit. A similar approach in terms of order parameters (r, ϑ_i) could be developed for electric and magnetic PTs and for other phenomena described by multiple order parameters.

References

[1] J. W. Christian and S. Mahajan, Prog. Mater. Sci. **39**, 1157 (1995).

[2] V. S. Boiko, R. I. Garber and A. M. Kosevich. *Reversible Crystal Plasticity* (New York: AIP, 1994).

[3] T. W. Heoa *et al.*, Phil. Mag. Lett. **91**, 110 (2011).

[4] L.Q. Chen, Annu. Rev. Mater. Res. **32**, 113 (2002).

[5] V.I. Levitas and D-W. Lee, Phys. Rev. Lett. **99**, 245701 (2007).

[6] A. Artemev, Y. Jin and A.G. Khachaturyan, Acta Mat. **49**, 1165 (2001).

[7] K.O. Rasmussen *et al.*, Phys. Rev. Lett. **87**, 055704 (2001).

[8] V.I. Levitas, V.A. Levin, K.M. Zingerman, E.I. Freiman, Phys. Rev. Lett. **103**, 025702 (2009).

[9] J.D. Clayton, J. Knap, Physica D. **240**, 841 (2011).

[10] J.D. Clayton, J. Knap, Model. Simul. Mater. Sci. Eng. **19**, 085005 (2011).

[11] V.I. Levitas and D.L. Preston, Phys. Rev. B **66**, 134206 (2002).

[12] V.I. Levitas and D.L. Preston, Phys. Rev. B **66**, 134207 (2002).

[13] V.I. Levitas, D.L. Preston and D.-W. Lee, Phys. Rev. B **68**, 134201 (2003).

[14] V.I. Levitas and D.L. Preston, Phys. Lett. A **343**, 32 (2005).

[15] V.I. Levitas and M. Javanbakht, Phys. Rev. Lett. **105**, 165701 (2010).

[16] Grinfeld, M.A. *Thermodynamic Methods in the Theory of Heterogeneous Systems* (Sussex, Longman, 1991).

[17] V.I. Levitas and M. Javanbakht, Int. J. Mat. Res. **102**, 652 (2011).

[18] V.I. Levitas, Int. J. Solids and Structures **35**, 889 (1998).

[19] K. Bhattacharya *et al.*, *Nature* **428**, 55 (2004).

[20] V.I. Levitas and M. Javanbakht, Phys. Rev. Lett. **105**, 165701 (2010).

[21] V.I. Levitas and M. Javanbakht, Int. J. Mat. Res. **102**, 652 (2011).

[22] V.I. Levitas, Phys. Rev. B (2013).

[23] Ph. Boullay, D. Schryvers, R.V. Kohn and J.M. Ball, J.de Physique IV, **11**, 23–30 (2001).

[24] Ph. Boullay, D. Schryvers and R.V. Kohn, Phys. Rev. B, **64**, 144105(2001).

[25] Ph. Boullaya, D. Schryvers, J.M. Ball, Acta Materialia **51**, 1421–1436 (2002).

[26] C. Denoual, A.M. Caucci, L. Soulard, Y.P. Pellegrini, Phys. Rev. Lett. **105**, 035703 (2010).

[27] K. Bhattacharya, *Microstructure of Martensite. Why it Forms and How It Gives Rise to the Shape-Memory Effect* (Oxford, Oxford University Press, 2003).

[28] See supplementary material at http://link.aps.org/supplemental.

[29] V.I. Levitas, D.-W. Lee and D.L. Preston, Int. J. Plast. **26**, 395 (2010).

CHAPTER 3. MULTIPHASE PHASE FIELD THEORY FOR TEMPERATURE- AND STRESS- INDUCED PHASE TRANSFORMATION

Modified from the paper published in Physical Review B

Valery I. Levitas[1] and Arunabha M. Roy[2]

[1]*Iowa State University, Departments of Aerospace Engineering, Mechanical Engineering, and Material Science and Engineering, Ames, Iowa 50011, U.S.A.*

[2]*Iowa State University, Department of Aerospace Engineering, Ames, Iowa 50011, U.S.A.*

Abstract

Thermodynamic Ginzburg-Landau potential for temperature- and stress-induced phase transformations (PTs) between n phases is developed. It describes each of the PTs with a single order parameter without an explicit constraint equation, which allows one to use an analytical solution to calibrate each interface energy, width, and mobility; reproduces the desired PT criteria via instability conditions; introduces interface stresses, and allows for a controlling presence of the third phase at the interface between the two other phases. A finite-element approach is developed and utilized to solve the problem of nanostructure formation for multivariant martensitic PTs. Results are in a quantitative agreement with the experiment. The developed approach is applicable to various PTs between multiple solid and liquid phases and grain evolution and can be extended for diffusive, electric, and magnetic PTs.

3.1 Introduction

One of the unresolved problems of the phase field approach (PFA) for PTs is a non-contradictory description of PTs between an arbitrary number of phases. One of the directions is related to the description of PTs between the austenite (A) and any of the n martensitic variants M_i and between martensitic variants [1]. It is described with the help of n independent order parameters η_i, each for every $A \leftrightarrow M_i$. This approach was significantly elaborated in [2, 3] by imposing additional physical requirements to the Landau potential. In particular, the desired PT

conditions for $A \leftrightarrow M_i$ and $M_j \leftrightarrow M_i$ PTs follow from the material instability conditions. Also, the thermodynamically equilibrium transformation strain tensor is stress- and temperature-independent, as in crystallographic theories. Each order parameter η_i encodes variation of atomic configuration along $A \leftrightarrow M_i$ transformation path; it is equal to 0 for A and 1 for M_i. In [2, 3] and here η_i is unambiguously related to transformation strain through some polynomial (see Eqs. (3) and (8)).

This theory was generalized for large strain and lattice rotations [4, 5] and interface stresses consistent with a sharp interface approach have been introduced for A-M_i interfaces [5–7]. However, the description of M_i-M_j is still not satisfactory. The $A \leftrightarrow M_i$ PT is described by a single order parameter η_i and analytic solutions for η_i for nonequilibrium interfaces [3, 5–7] allow one to calibrate interface energy, width, and mobility, as well as the temperature-dependence of the stress-strain curve. At the same time, at a M_i-M_j interface η_i and η_j vary independently along some transformation path in the $\eta_i - \eta_j$ plane connecting M_i ($\eta_i = 1$ and $\eta_j = 0$) and M_j ($\eta_i = 0$ and $\eta_j = 1$), see Fig. 1.

The interface energy, width, and mobility have an unrealistic dependence on temperature, stresses, and a number of material parameters, which cannot be determined analytically. Consequently, one cannot prescribe the desired M_i-M_j interface parameters, and also the expression for M_i-M_j interface stresses cannot be strictly derived [5, 6].

Other n-phase approaches are based on introducing $n + 1$ order parameters η_i obeying constraint $\sum \eta_i = 1$, similar to concentrations [8, 10, 11]. The idea is that each of the PTs should be described by a single order parameter; then interface parameters can be calibrated with the help of the analytical solution. However, a single constraint cannot ensure this and, in general, an undesired in this community third phase often appears at the interface between two phases. PT criteria in terms of instability conditions are not considered. In [10] special conditions are imposed for a three-phase system that guarantee that the third phase can never appear at the interface between two phases. This created some artifacts in the theory (e.g., the necessity of equal kinetic coefficients for all PTs). All homogeneous phases are stable or metastable independent of the driving force (temperature); i.e., thermodynamic instability, which is the source of the PT criteria, is impossible. On the other hand, for different materials and conditions, the third phase is observed in experiments [12] and conditions when it is present

or not are found within more advanced models [13]. Some drawbacks of imposing constraint with the help of Lagrangian multipliers are presented and overcame in [11]. However, again, instability conditions were not discussed in [11]. All of our attempts to formulate a theory with constraint to find polynomials (up to the tenth degree) in order to reproduce the proper PT criteria (which are known from two-phase treatment) from the thermodynamic instability conditions have been unsuccessful. This led us to the conclusion that utilizing constraint $\sum \eta_i = 1$ prevents a noncontradictory formulation of the PFA.

PFA in [3] is based on a potential in hyperspherical order parameters, in which one of the phases, O (e.g., A or melt), is at the center of the sphere, and all others, P_i (e.g., M_i or solid phases), are located at the sphere. Hyperspherical order parameters represent a radius Υ in the order-parameter space and the angles between radius vector $\boldsymbol{\Upsilon}$ and the axes η_i corresponding to P_i.

Due to some problems found in [14], the nonlinear constraint for the hyperspherical order parameters was substituted with the linear constraint of the type $\sum \eta_i = 1$, which, however, does not include A or melt [13, 14]. For three phases, when constraint is explicitly eliminated, the theory in [3, 13, 14] is completely consistent with the two-phase theory and produces proper PT criteria. However, due to the constraint, for more than three phases, these theories cannot produce correct PT criteria. Thus, noncontradictory PFA for more than three phases or two martensitic variants is currently lacking.

In the letter, we develop PFA, which with high and controllable accuracy satisfy all the desired conditions for arbitrary n phases. We utilize the same order parameters η_i like for martensitic PT and, instead of explicit constraints, include in the simplest potential the terms that penalize the deviation of the trajectory in the order parameter space from the straight lines connecting *each two phases*. These penalizing terms do not contribute to the instability conditions and the correct PT criteria strictly follow from the instability conditions for $O \leftrightarrow P_i$ PT only. However, when the magnitude of the penalizing term grows to infinity and imposes the strict constraint $\eta_i + \eta_j = 1$ and $\eta_k = 0$ for all $k \neq i, j$, correct PT conditions for $P_i \leftrightarrow P_j$ PTs do follow from the instability conditions. Because for a finite magnitude such a constraint is applied approximately only, there is some deviation from the ideal equilibrium phases and PT conditions. However, numerical simulations for the almost worst cases demonstrate that these

deviations are indeed negligible. This PFA allows for an analytical solution for the interfaces between each of the two phases, which can be used to calibrate interface width, energy, and mobility; it allows for the first time for a multiphase system to include a consistent expression for interface stresses for each interface; it includes or excludes the third phase within the interface between the two phases based on thermodynamic and kinetic consideration similar to those in [13].

We designate contractions of tensors $\boldsymbol{A} = \{A_{ij}\}$ and $\boldsymbol{B} = \{B_{ji}\}$ over one and two indices as $\boldsymbol{A} \cdot \boldsymbol{B} = \{A_{ij} B_{jk}\}$ and $\boldsymbol{A}{:}\boldsymbol{B} = A_{ij} B_{ji}$, respectively. The subscript s means symmetrization, the superscript T designates transposition, the sub- and superscripts e, th, and t mean elastic, thermal, and transformational strains, $\boldsymbol{I}$ is the unit tensor, and $\boldsymbol{\nabla}$ and $\boldsymbol{\nabla}_0$ are the gradient operators in the *deformed* and undefromed states.

3.2 General model

Model for n order parameters. For simplicity and compactness, the small strains will be considered but with some minimal geometric nonlinearities required to introduce interface stresses [5–7]. Generalization for large strain is straightforward [4, 5] (see Appendix) and the model problem will be solved in large strain formulation. The Helmholtz free energy ψ per unit undeformed volume has the following form:

$$= \frac{\rho_0}{\rho_t}\psi^e(\boldsymbol{\varepsilon}_e, \eta_i, \theta) + \frac{\rho_0}{\rho}\breve{\psi}^\theta + \tilde{\psi}^\theta + \frac{\rho_0}{\rho} \nabla + \psi_p; \tag{1}$$

$$\breve{\psi}^\theta = \sum A_i(\theta)\eta_i^2(1 - \eta_i)^2 + \sum \bar{A}_{ij}\eta_i^2\,\eta_j^2; \tag{2}$$

$$\tilde{\psi}^\theta = \sum \Delta G_i^\theta(\theta)q(\eta_i); \quad q(\eta_i) = \eta_i^2(3 - 2\eta_i); \tag{3}$$

$$\psi_p = \sum K_{ij}\,(\eta_i + \eta_j - 1)^2\,\eta_i^l\eta_j^l + \sum K_{ijk}\eta_i^2\eta_j^2\eta_k^2; \quad l \geq 2; \tag{4}$$

$$\psi^e = 0.5\boldsymbol{\varepsilon}_e{:}\boldsymbol{E}(\eta_i){:}\boldsymbol{\varepsilon}_e; \qquad \boldsymbol{E}(\eta_i) = \boldsymbol{E}_0 + \sum(\boldsymbol{E}_i - \boldsymbol{E}_0)q(\eta_i); \tag{5}$$

$$\nabla = \sum 0.5\beta_{ij}\boldsymbol{\nabla}\eta_i \cdot \boldsymbol{\nabla}\eta_j; \tag{6}$$

$$\boldsymbol{\varepsilon} = (\boldsymbol{\nabla}_0 \boldsymbol{u})_s = \boldsymbol{\varepsilon}_e + \boldsymbol{\varepsilon}_t + \boldsymbol{\varepsilon}_\theta; \quad \frac{\rho_0}{\rho} = 1 + \varepsilon_v; \quad \varepsilon_v = \boldsymbol{\varepsilon} \boldsymbol{:} \boldsymbol{I}; \quad \frac{\rho_0}{\rho_t} = 1 + (\boldsymbol{\varepsilon}_t + \boldsymbol{\varepsilon}_\theta) \boldsymbol{:} \boldsymbol{I}; \qquad (7)$$

$$\boldsymbol{\varepsilon}_t = \sum \boldsymbol{\varepsilon}_{ti} q(\eta_i); \quad \boldsymbol{\varepsilon}_\theta = \boldsymbol{\varepsilon}_{\theta 0} + \sum (\boldsymbol{\varepsilon}_{\theta i} - \boldsymbol{\varepsilon}_{\theta 0}) q(\eta_i). \qquad (8)$$

Here θ is the temperature, $\boldsymbol{u}$ is the displacements, $\boldsymbol{\varepsilon}$ is the strain tensor, ΔG_i^θ is the difference in the thermal energy between P_i and O, A_i and $\bar{A}_{ij}$ are the double-well barriers between P_i and O and between P_i and P_j, ρ, ρ_0, and ρ_t are the mass densities in the deformed, undeformed, and stress-free states, respectively; β_{ij} are the gradient energy coefficients, each coefficient, K_{ij}, $\bar{A}_{ij}$, and K_{ijk}, is equal to zero if two subscripts coincide. Despite small strain approximation, we keep some geometrically nonlinear terms (ρ_0/ρ_t, ρ_0/ρ, and gradient $\boldsymbol{\nabla}$ with respect to deformed state) in order to correctly reproduce interface and elastic stresses [5–7].

The application of the thermodynamic laws and linear kinetics (see, e.g. [5–7]) results in

$$\boldsymbol{\sigma} = \boldsymbol{\sigma}_e + \boldsymbol{\sigma}_{st}; \qquad \boldsymbol{\sigma}_e = \frac{\rho}{\rho_0} \frac{\partial \psi^e}{\partial \boldsymbol{\varepsilon}_e}; \qquad (9)$$

$$\boldsymbol{\sigma}_{st} = (\psi^\nabla + \breve{\psi}_\theta) \boldsymbol{I} - \sum \beta_{ij} \boldsymbol{\nabla} \eta_i \otimes \boldsymbol{\nabla} \eta_j. \qquad (10)$$

$$\dot{\eta}_i = \sum L_{ij} X_j = \sum L_{ij} \left(\boldsymbol{\sigma}_e \boldsymbol{:} \frac{\partial (\boldsymbol{\varepsilon}_t + \boldsymbol{\varepsilon}_\theta)}{\partial \eta_j} - \frac{\partial \psi}{\partial \eta_j} + \sum \beta_{jk} \boldsymbol{\nabla}^2 \eta_k \right); \quad L_{ij} = L_{ji}, \quad (11)$$

where X_i is the thermodynamic driving force to change η_i, L_{ij} are the kinetic coefficients, and $\boldsymbol{\sigma}$ is the true Cauchy stress tensor. We designate the set of the order parameters $\hat{\eta}_0 = (0, ..., 0)$ for O and $\hat{\eta}_i = (0, ..., \eta_i = 1, ..., 0)$ for P_i. It is easy to check that O and P_i are homogeneous solutions of the Ginzburg-Landau equations (11) for arbitrary stresses and temperature; consequently, the transformation strain and for any PT and elastic moduli are independent of stresses and temperature [2–4].

Without the term ψ_p, the local part of free energy is much simpler than in [2,3] and does not contain complex interaction between phases. The terms with K_{ijk} penalize the presence of the three phases at the same material point. By increasing K_{ijk} one can control and, in particular, completely exclude the third phase within the interface between the two other phases. For homogeneous states, this term always excludes the presence of the three phases at the same point, because it increases energy compared with a two-phase state. The terms with K_{ij} penalize deviations from hyperplanes $\eta_k = 0$ and $\eta_i + \eta_j = 1$ and exponent l determines

relative weight of these penalties. In combination with the penalization of more than two phases, this constraint penalizes deviation from the desirable transformation paths: along coordinate lines η_i along which $O \leftrightarrow P_i$ PTs occur, and lines $\eta_i + \eta_j = 1$, $\eta_k = 0 \; \forall k \neq i, j$, along which $P_i \leftrightarrow P_j$ PTs occur. In such a way, we do not need to impose the explicit constraint $\sum \eta_i = 1$ and will be able to (approximately) satisfy all desired conditions, including instability conditions. Note that there is no need for penalizing $\eta_i = 0$; however, for $l = 0$ the term with K_{ij} produces an undesired contribution to ψ for $\eta_i = 0$.

Thermodynamic instability conditions. For compactness, instability conditions will be presented for the case with the same elastic moduli of all phases and $\rho_0 \simeq \rho$. Since $\partial X_i(\hat{\eta}_k)/\partial \eta_j = 0$, instability conditions for thermodynamically equilibrium homogeneous phases result in the following PT criteria:

$$O \to P_i: \quad \partial X_i(\hat{\eta}_0)/\partial \eta_i \geq 0 \to \boldsymbol{\sigma}_e\boldsymbol{:}(\boldsymbol{\varepsilon}_{ti} + \boldsymbol{\varepsilon}_{\theta i} - \boldsymbol{\varepsilon}_{\theta 0}) - \Delta G_i^\theta \geq A_i(\theta)/3; \tag{12}$$

$$P_i \to O: \quad \partial X_i(\hat{\eta}_i)/\partial \eta_i \geq 0 \to \boldsymbol{\sigma}_e\boldsymbol{:}(\boldsymbol{\varepsilon}_{ti} + \boldsymbol{\varepsilon}_{\theta i} - \boldsymbol{\varepsilon}_{\theta 0}) - \Delta G_i^\theta \leq -A_i(\theta)/3; \tag{13}$$

$$P_j \to P_i: \quad \partial X_i(\hat{\eta}_j)/\partial \eta_i \geq 0 \to \boldsymbol{\sigma}_e\boldsymbol{:}(\boldsymbol{\varepsilon}_{ti} + \boldsymbol{\varepsilon}_{\theta i} - \boldsymbol{\varepsilon}_{\theta 0}) - \Delta G_i^\theta \geq (A_i(\theta) + \bar{A})/3 \; \Rightarrow \; \text{wrong.} \tag{14}$$

While conditions for $O \leftrightarrow P_i$ PTs are logical (work of stress on jump in transformation and thermal strains exceeds some threshold), condition for $P_j \to P_i$ does not contain information about phase P_j, which is contradictory even at zero stresses. Since first and second derivatives of ψ_p are zero for O and P_i, ψ_p does not change phase equilibrium and instability conditions for homogeneous phases. However, as we will see below, it plays a key role in the development of noncontradictory and flexible PFA.

$O \leftrightarrow P_i$ phase transformations. If $O \leftrightarrow P_i$ PT is considered only with all other $\eta_j = 0$, Eqs. (2)-(6) simplify:

$$\breve{\psi}^\theta = A_i(\theta)\eta_i^2(1 - \eta_i)^2; \quad \tilde{\psi}^\theta = \Delta G_i^\theta(\theta)q(\eta_i); \quad \psi_p = 0; \quad {}^\nabla = 0.5\beta_{ii}\boldsymbol{\nabla}\eta_i \cdot \boldsymbol{\nabla}\eta_i. \tag{15}$$

$$\boldsymbol{E}(\eta_i) = \boldsymbol{E}_0 + (\boldsymbol{E}_i - \boldsymbol{E}_0)q(\eta_i); \quad \boldsymbol{\varepsilon}_t = \boldsymbol{\varepsilon}_{ti}q(\eta_i); \quad \boldsymbol{\varepsilon}_\theta = \boldsymbol{\varepsilon}_{\theta 0} + (\boldsymbol{\varepsilon}_{\theta i} - \boldsymbol{\varepsilon}_{\theta 0})q(\eta_i). \tag{16}$$

$$\boldsymbol{\sigma}_{st} = (\psi^\nabla + \breve{\psi}_\theta)\boldsymbol{I} - \beta_{ii}\boldsymbol{\nabla}\eta_i \otimes \boldsymbol{\nabla}\eta_i. \tag{17}$$

$$\dot{\eta}_i = L_{ii}\left(\boldsymbol{\sigma}_e : (\boldsymbol{\varepsilon}_{ti} + \boldsymbol{\varepsilon}_{\theta i} - \boldsymbol{\varepsilon}_{\theta 0})\frac{dq}{d\eta_i} - \frac{\partial \psi}{\partial \eta_i} + \beta_{ii}\boldsymbol{\nabla}^2\eta_i\right). \tag{18}$$

These equations possess all desired properties [2–4] of two-phase models.

$P_j \leftrightarrow P_i$ *phase transformations.* Next, we consider how to make the description of $P_j \rightarrow P_i$ PTs completely similar to that of $O \leftrightarrow P_i$ PTs. Let us increase parameters K_{ij} and K_{ijk} to very high values so that they impose constraints $\eta_i + \eta_j = 1$ and $\eta_k = 0 \ \forall k \neq i, j$. Substituting these constraints in Eq. (1) and taking into account the following properties of function q, $q(1 - \eta_i) = 1 - q(\eta_i)$ (which is crucial for our PFA), we reduce all equations to the single order parameter:

$$\breve{\psi}^\theta = A_{ij}(\theta)\eta_i^2(1 - \eta_i)^2; \quad A_{ij} = A_i + A_j + \bar{A}_{ij}; \tag{19}$$

$$\tilde{\psi}^\theta = \Delta G_j^\theta + \Delta G_{ij}^\theta(\theta)q(\eta_i); \quad \Delta G_{ij}^\theta = \Delta G_i^\theta - \Delta G_j^\theta; \tag{20}$$

$$\boldsymbol{E} = \boldsymbol{E}_j + (\boldsymbol{E}_i - \boldsymbol{E}_j)q(\eta_i); \tag{21}$$

$$\nabla = 0.5b_{ij}\boldsymbol{\nabla}\eta_i \cdot \boldsymbol{\nabla}\eta_i; \quad b_{ij} = \beta_{ii} + \beta_{jj} - 2\beta_{ij}; \tag{22}$$

$$\boldsymbol{\varepsilon}_t = \boldsymbol{\varepsilon}_{tj} + (\boldsymbol{\varepsilon}_{ti} - \boldsymbol{\varepsilon}_{tj})q(\eta_i); \quad \boldsymbol{\varepsilon}_\theta = \boldsymbol{\varepsilon}_{\theta j} + (\boldsymbol{\varepsilon}_{\theta i} - \boldsymbol{\varepsilon}_{\theta j})q(\eta_i); \tag{23}$$

$$\boldsymbol{\sigma}_{st} = (\psi^\nabla + \breve{\psi}_\theta)\boldsymbol{I} - b_{ij}\boldsymbol{\nabla}\eta_i \otimes \boldsymbol{\nabla}\eta_i; \quad l_{ij} = (L_{ii}L_{jj} - L_{ij}^2)/(L_{jj} + L_{ij}); \tag{24}$$

$$\dot{\eta}_i = l_{ij}\left(\boldsymbol{\sigma}_e : (\boldsymbol{\varepsilon}_{ti} + \boldsymbol{\varepsilon}_{\theta i} - \boldsymbol{\varepsilon}_{tj} - \boldsymbol{\varepsilon}_{\theta j})\frac{dq}{d\eta_i} - \frac{\partial \psi}{\partial \eta_i} + b_{ij}\boldsymbol{\nabla}^2\eta_i\right). \tag{25}$$

$$P_j \rightarrow P_i: \quad \partial X_i(\hat{\eta}_j)/\partial \eta_i \geq 0 \rightarrow \boldsymbol{\sigma}_e : (\boldsymbol{\varepsilon}_{ti} + \boldsymbol{\varepsilon}_{\theta i} - \boldsymbol{\varepsilon}_{tj} - \boldsymbol{\varepsilon}_{\theta j}) - \Delta G_{ij}^\theta \geq A_{ij}(\theta)/3. \tag{26}$$

It is evident that Eqs.(19)-(26) for $P_j \rightarrow P_i$ PTs are non-contradictory (i.e., contain an expected combination of parameters of P_j and P_i) and coincide to within constants and designations with Eqs.(15)-(18) for $O \leftrightarrow P_i$ PTs, i.e., they are as good as the equations for $O \leftrightarrow P_i$ PTs. Thus, our goal is achieved.

Energy landscape and $P_j \leftrightarrow P_i$ instability conditions for finite K_{ij}. Note that instability condition (26) works in the limit $K_{ij} \rightarrow \infty$; for finite K_{ij} it is imposed approximately only.

To better understand the interaction between instability conditions (14) and (26), we consider some examples. We consider the case when PT conditions for $O \leftrightarrow P_i$ PTs (12), (13) and for $P_j \to P_i$ PT (26) are not met, but when the wrong condition (14) is fulfilled with quite large deviation from the stability region. Under such conditions, P_j loses its stability, but instead of transforming to P_i, the local energy minimum slightly shifts from $\eta_1 = 1$; $\eta_2 = 0$ to a close point $\eta_1 = 0.989$; $\eta_2 = 0.019$ (Fig. 1). There is an energy barrier (saddle point) between P_j and P_i and until it disappears (i.e., correct condition (26) for $P_j \to P_i$ PT is met), $P_j \to P_i$ PT is impossible. Thus, an approximate character of the imposed constraint through the penalty term exhibits itself in a slight shift of the local minimum from P_j to some very close point, which should essentially not affect the accuracy of the simulations. If PT conditions for
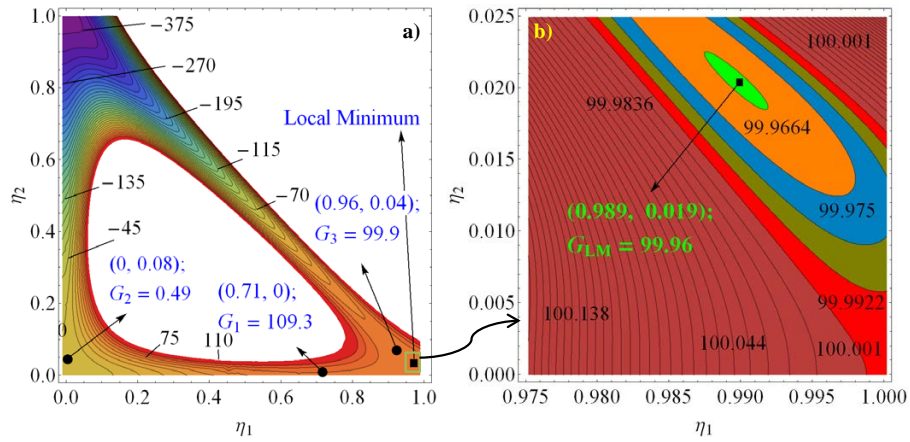
Figure 1: Energy level plot of the free energy at zero stresses for $A_1 + 3\Delta G_1^\theta = 1000$, $A_1 - 3\Delta G_1^\theta = 400$, $A_2 + 3\Delta G_2^\theta = 230$, $A_2 - 3\Delta G_2^\theta = 2570$, $\bar{A} + A_1(\theta) + 3\Delta G_1^\theta = -250$ and $A_{21}(\theta) - 3G_{21}^\theta = 150$, all in J/m^3. G_i are the points of the local minimaxes. (b) The zoomed part of the plot near P_1.

$O \leftrightarrow P_i$ **and** $\boldsymbol{P}_j \leftrightarrow \boldsymbol{P}_i$ PTs (13) and (14) are not fulfilled but the correct condition (26) for $P_j \to P_i$ PT is met, then these equations result in $\bar{A} < 0$. It is easy to show that in this case the wrong $P_j \to P_i$ PT condition (14) should be also fulfilled. Thus, if the correct $P_j \to P_i$ PT condition is met, this PT will occur.

3.3 Parameter identification

Due to equivalence of all equations for $O \leftrightarrow P_i$ and $P_j \to P_i$ PTs, the analytical solution for a propagating with velocity c interface is [8]:

$$\eta = 0.5 \tanh\left[3(x - ct)/\delta\right] + 0.5; \quad \delta = \sqrt{18\beta/A_i(\theta)}; \quad c = L\delta\Delta G^\theta(\theta); \quad \gamma = \beta/\delta, \qquad (27)$$

where δ and γ are the interface width and energy. In contrast to solutions for other interpolating functions q [5–7], interface width and energy are independent of $\Delta G^\theta(\theta)$. That is why $\breve{\psi}^\theta$ and interface stresses $\boldsymbol{\sigma}_{st}$ are also independent of $\Delta G^\theta(\theta)$. All material parameters for each bulk phase can be determined based on thermodynamic, experimental, and atomistic data as it was done, e.g., in [2, 3] for NiAl. Eqs.(27) allow calibration for each pair of phases the three interface-related parameters $A_i(\theta)$, β, and L when width, energy, and mobility of interfaces between each pair of phases are known.

The obtained system of equations has been solved with the help of the finite element code COMSOL for various problems. Here we solved exactly the same problem on the evolution of two-variant nanostructure in a NiAl alloy during martensitic PT including tip bending and splitting in martensitic variants as in [14]. Note that the theory in [14] for two variants satisfies all required conditions exactly but cannot be generalized for more than two variants. Some material parameters (like $\boldsymbol{E}, \boldsymbol{\varepsilon}_{ti}$, $\Delta G^\theta(\theta)$, θ_e, Δs) here have been chosen the same as in [14]; other ($A_{ij}(\theta)$, $\beta_{ij}(\theta)$, L_{ij}, θ_c) are chosen to get the temperature dependence of the energy, width, and mobility of all interfaces, and temperature for the loss of stability of P like in [14]. Note that all thermodynamic properties of martensitic variants M_1 and M_2 are the same; they differ by the transformation strain only.

We have the following definition of parameters: $\Delta G_1^\theta = \Delta G_2^\theta = -\Delta s(\theta - \theta_e)$, where $\Delta s = s_i - s_0$ is the jump in entropy between phases M_i and A, and θ_e is the thermodynamic equilibrium temperature for phases T_i and A. We express the coefficients $A_1(\theta) = A_2(\theta) = A_*(\theta - \theta_*)$. Here parameter A_* and the characteristic temperature θ_* are related to the critical temperatures for barrierless $A \to P_i$ (θ_c^{0i}) and $P_i \to A$ (θ_c^{i0}) PTs by the equations $\theta_c^{01} := (A_*\theta_* - 3\Delta s\theta_e)/(A_* - 3\Delta s)$ and $\theta_c^{10} := (A_*\theta_* + 3\Delta s\theta_e)/(A_* + 3\Delta s)$, which follow from the thermodynamic instability conditions.

$\theta_c^{01} = -183$ K, $\theta_c^{10} = -331.65$ K, $\theta_* = -245.75$ K, $A_* = 28 MPaK^{-1}$ $\beta_{01} = \beta_{02} = 5.31 \times 10^{-10}$ N, $\beta_{12} = 5.64 \times 10^{-10}$ N, $L_{0i} = L_{12} = 2596.5 m^2/Ns$. These parameters correspond to a twin interface energy $E_{P_1 P_2} = 0.543 J/m^2$ and width $\Delta_{P_1 P_2} = 0.645 nm$. Isotropic linear elasticity was utilized for simplicity; bulk modulus $K = 112.8\,GPa$ and shear modulus $\mu = 65.1\,GPa$. In the 2D plane stress problems, only P_1 and P_2 are considered. The components of the transformation strains were $\boldsymbol{U}_{t1} = (k_1, k_2, k_2)$ and $\boldsymbol{U}_{t2} = (k_2, k_1, k_2)$ with $k_1 = 1.15$ and $k_2 = 0.93$ corresponding to the NiAl alloy in [15]. In addition, $K_{ijk} = 0$ and two values of $K_{12} = 1.5 \times 10^{12}$ and $K_{12} = 7.25 \times 10^{13}$ J/m^3 have been used. All lengths, stresses, and times are given in units of nm, GPa, and ps, respectively. All external stresses are normal to the deformed surface.

3.4 Evolution of martensitic nanostructure

Numerical procedure. We used Lagrange quadratic triangular elements with 5-6 elements per interface width to achieve a mesh-independent solution, see [16]. This resulted in 165601 mesh points and 329760 elements with 1982883 degrees of freedom. Adaptive mesh generation was utilized. The time-dependent equations were solved using the segregated time-dependent solver and backward Euler integration technique [17] for $250\,ps$. Integration time steps were chosen automatically such that a relative tolerance of 0.001 and absolute tolerance of 0.0001 are held.

Nanostructure. Because numerous alternative solutions exist, one has to carefully choose the initial conditions. We did this using the following steps. An initial random distribution of the order parameters η_1 and η_2 in the range $[0.4; 0.8]$ were prescribed in a square sample sized 50×50 with the austenite lattice rotated by $\alpha = 45^o$. The roller support was used for one horizontal and one vertical surface, i.e., the normal displacements and shear stresses are zero. Homogeneous normal displacements at two other surfaces were prescribed and kept constant during simulations, which resulted in a biaxial normal strain of 0.01. Shear stresses were kept zero at external surfaces. A two-dimensional problem under plane stress condition and temperature $\theta = 100K$ was solved. The stationary solution for $\theta = 100K$ shown in Fig. 2a (which is practically the same as presented in [14]) was taken as an initial condition for the next stage of simulation with the following modifications: temperature was reduced to

$\theta = 0K$; parameter β_{12} was reduced to $\beta_{12} = 5.64 \times 10^{-11}\,N$, which led to twin interface energy $E_{P_1 P_2} = 0.371 J/m^2$ and width $\Delta_{P_1 P_2} = 0.363nm$. The final solution evolution of $\eta_1 - \eta_2$ is presented in Fig. 2b.

Results of the current simulations for both K_{12} practically coincide with those in [14] (Fig. 2c); they resemble the experimental nanostructure from [15] and quantitatively reproduce the bending angle (Fig. 2d). Thus, we proved that for two variants our theory does not work worse than the theory [14], which strictly satisfies all desired conditions for two variants. However, in contrast to [14], the current theory can be applied for an arbitrary number of variants. Since our theory splits the general $n-$phase case into a set of independent three-phase formulations, this means that it will work equally well for arbitrary n as well. An important point also is that such a complicated nanostructure was obtained from a completely different initial nanostructure (Fig. 2a). For example, the splitting and bending of the tips were also reproduced in [18] utilizing strain-based phase-field formulation. However, the initial conditions in [18] were very close to the final solution, because probably otherwise the solution converges to the primitive alternating twins. Note that the strain based order parameters are not as universal as η_i (e.g., they cannot be used for melting or grain evolution) and as was written in [2, 3], they do not allow one to satisfy the required conditions even for a single order parameter. Interface stresses also were not introduced for strain-based order parameters.

Stresses. Components of the stress fields, including interface stresses, are shown in Fig. 3. They are seldom presented in literature because of large artificial oscillations. Here, oscillations are absent, and stress concentration has a regular character, which underlines the advantages of the current simulations. Since twin boundaries represent invariant plane, it is generally assumed in a sharp interface approach that they are stress-free and do not generate elastic energy. Here, we unexpectedly observe large shear stress σ_{xy}, which changes the sign across the twin interface. Shear stress appears due to the accommodation of large alternating shears across a finite-width interface in a constraint sample.

3.5 Concluding remarks

To summarize, as a solution of a critical outstanding problem, we developed PFA for multiphase materials, which with high and controllable accuracy satisfy all the desired conditions for arbitrary n phases. Instead of explicit constraints, we included in the simplest potential

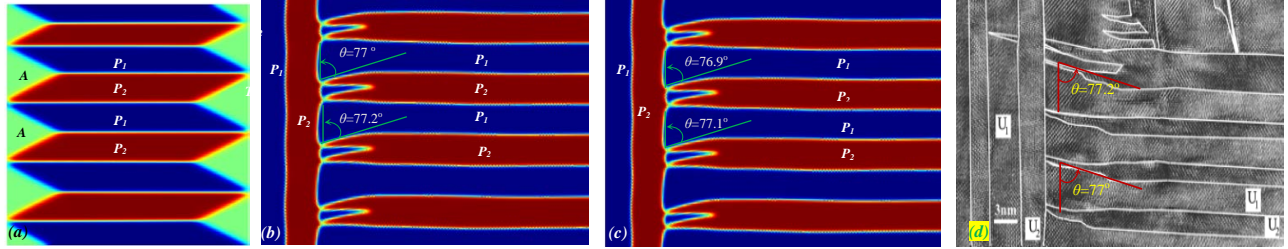Figure 2: Initial conditions (a) and stationary solution for two-variant martensitic nanostructure exhibiting bending and splitting martensitic tips based on the current theory (b) and theory in [14] (c); experimental nanostructure from [15] (d). Green color is for austenite, blue and red are for martensitic variants P_1 and P_2.
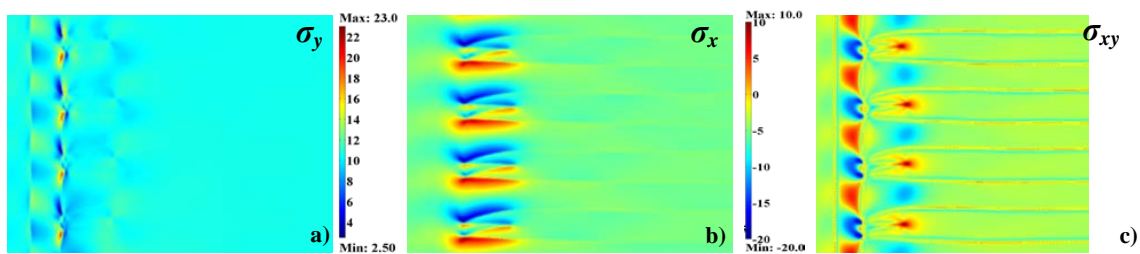

Figure 3: Stationary stress fields (in GPa) for $K_{12} = 1.5 \times 10^{12} \, J/m^3$.

the terms that penalize the deviation of the trajectory in the order parameter space from the straight lines connecting each of the two phases. It describes each of the PTs with the single order parameter, which allows us to use an analytical solution to calibrate each interface energy, width, and mobility. It reproduces the desired PT criteria via instability conditions; introduces interface stresses, and allows us to control the presence of the third phase at the interface between the two other phases. Finite-element simulations exhibit very good correspondence with results based on the exact three-phase model in [14] (which, however, cannot be generalized for $n > 3$) and with nontrivial experimental nanostructure. The developed approach unifies and integrates approaches developed in different communities (in particular, solidification and martensitic PTs) and is applicable to various PTs between multiple solid and liquid phases and grain evolution, and can be extended for diffusive, electric, and magnetic PTs.

References

[1] A. Artemev, Y. Jin, A. G. Khachaturyan, Acta Mat. **49**, 1165 (2001); Y. M. Jin, A. Artemev, A. G. Khachaturyan, Acta Mat. **49**, 2309 (2001); L. Q. Chen, Annu. Rev. Mater. Res. **32**, 113 (2002); Y. Wang, A. G. Khachaturyan, Mat. Sci. Engg. A **438**, 55 (2006); M. Mamivand, M. A. Zaeem, H. El Kadiri, Comp. Mat. Sci. **77**, 304 (2013).

[2] V. I. Levitas and D. L. Preston, Phys. Rev. B. **66**, 134206 (2002); 134207 (2002).

[3] V. I. Levitas, D. L. Preston and D-W. Lee, Phys. Rev. B. **68**, 134201 (2003).

[4] V. I. Levitas, V. A. Levin, K. M. Zingerman and E. I. Freiman, Phys. Rev. Lett. **103**, 025702 (2009); V.I. Levitas, Int. J. Plast. **49**, 85 (2013).

[5] V. I. Levitas, J. Mech. Phys. Solids **70**, 154 (2014).

[6] V. I. Levitas, Phys. Rev. B. **87**, 054112 (2013); Acta Mater. **61**, 4305 (2013).

[7] V.I. Levitas and M. Javanbakht, Phys. Rev. Lett. **105**, 165701 (2010); V.I. Levitas, Phys. Rev. B. **89**, 094107 (2014).

[8] I. Steinbach, F. Pezzolla, B. Nestler, M. Seelberg, R. Prieler, G.J. Schmitz and J. L. L. Rezende, Physica D **94**, 13547 (1996); I. Steinbach, Model. Simul. Mater. Sci. Eng. **17**, 073001 (2009).

[9] H. Garcke, B. Nestler and B. Stoth, Physica D **115**, 87 (1998); R. Kobayashi and J. Warren, Physica A **356**, 127132 (2005); G. I. Toth, J. R. Morris and L. Granasy, Phys. Rev. Lett. **106**, 045701 (2011); G. I. Toth, T. Pusztai, G. Tegze and L. Granasy, Phys. Rev. Lett. **107**, 175702 (2011); Y. Mishin, W. J. Boettinger, J. A. Warren and G. B. McFadden, Acta Mater. **57**, 3771 (2009).

[10] R. Folch and M. Plapp, Phys. Rev. E **68**, 010602 (2003); Phys. Rev. E **72**, 011602 (2005).

[11] P.C. Bollada, P. K. Jimack and A. M. Mullis, Physica D **241**, 816 (2012).

[12] V. I. Levitas, B. F. Henson, L. B. Smilowitz and B. W. Asay, Phys. Rev. Lett. **92**, 235702 (2004); V. I. Levitas, Z. Ren, Y. Zeng, Z. Zhang and G. Han, Phys. Rev. B **85**, 220104 (2012).

[13] V. I. Levitas and K. Momeni, Acta Mater. **65**, 125 (2014); K. Momeni and V.I. Levitas, Phys. Rev. B **89**, 184102 (2014); K. Momeni, V.I. Levitas, and J.A. Warren, Nano Letters, DOI: 10.1021/nl504380c (2015).

[14] V. I. Levitas, A. M. Roy and D. L. Preston, Phys. Rev. B. **88**, 054113 (2013).

[15] Ph. Boullay, D. Schryvers, R.V. Kohn and J.M. Ball, J. de Physique IV **11**, 23 (2001).

[16] V.I. Levitas and M. Javanbakht, Int. J. Mat. Res. **102**, 652 (2011).

[17] COMSOL, Inc., website: www.comsol.com.

[18] A. Finel, Y. Le Bouar, A. Gaubert and U. Salman, C. R. Phys. **11**, 245 (2010).

CHAPTER 4. MULTIPHASE PHASE FIELD THEORY FOR TEMPERATURE-INDDUCED PHASE TRANSFORMATION

Abstract

Main conditions for the the thermodynamic potential for two- and multiphase Ginzburg-Landau theory are formulated for temperature-induced phase transformations. Theory which satisfies all these conditions exactly for two-phase materials and approximately (but with controlled accuracy) for $n-$phase material is developed. to the Thermodynamic Ginzburg-Landau potential for temperature- and stress-induced phase transformations (PTs) between n phases is developed. It describes each of the PTs with a single order parameter without an explicit constraint equation, which allows one to use an analytical solution to calibrate each interface energy, width, and mobility; reproduces the desired PT criteria via instability conditions; introduces interface stresses, and allows for a controlling presence of the third phase at the interface between the two other phases. A finite-element approach is developed and utilized to solve the problem of nanostructure formation for multivariant martensitic PTs. Results are in a quantitative agreement with the experiment. The developed approach is applicable to various PTs between multiple solid and liquid phases and grain evolution and can be extended for diffusive, electric, and magnetic PTs.

4.1 Introduction

While in this section we focus on the temperature-induced multiphase PTs, we will mention some works which include stresses as well, because these theories reduce to the temperature-induced PTs at zero stresses. The main focus is on the description of the first-order PTs for the case when PT completes and there are no structural changes after completing PT, like for melting, martensitic PTs, and some reconstructive PTs. The main problem is to develop a consistent phase field approach (PFA) for PTs between an arbitrary number of phases. There are two very different approaches with different goals developed by two different communities. The first one is developed within community working on the description of PTs between the austenite (A) and any of the n martensitic variants M_i and between martensitic

variants $\mathsf{M}_j \leftrightarrow \mathsf{M}_i$ (which represents in most cases twinning) [1–8]. It utilizes n independent order parameters η_i, each of which describes $\mathsf{A} \leftrightarrow \mathsf{M}_i$ PTs between $n+1$ phases. In most papers, researches work within this approach at the actual spatial scales, rather than coarse-grained theories for microscale. Thus, typical actual interface width is on the order of nanometers and detail of distribution of all parameters within interface are of interest. That is why all simulations are limited to submicron samples.

The second multiphase approach is developed within community working on multiphase solidification (e.g., in eutectic and peritectic systems) and grain growth [9–18]. It operates with $n+1$ order parameters η_i satisfying constraint $\sum \eta_i = 1$, similar to phase concentrations. In most of these theories interface width artificially increased by several orders of magnitude (see, e.g., [10, 16, 17] or microscale theories [19, 20]), and detail of variation of material parameters and fields across an interface are unrealistic but this is not important for the chosen objectives. This is done in order to be able to treat much larger samples comparable to that relevant for studying solidification of actual materials.

Each of these approaches satisfies some important requirements formulated to achieve some specific goals and have their advantages and drawbacks. They will be analyzed in Section ??? and it will be shown that none of them meets all the desired requirements. Two of the requirements, which were imposed in the second approach and ignored in the first approach, are that each of the two-phase PTs should be described by a single order parameter and that interface between any of two phases should not contain the third phase [16–18]. The first of these conditions is required in order to have possibility to obtain analytical solution for an propagating interface, which can be used to calibrate parameters of the thermodynamic potential in terms of interface energy, width, and mobility that assumed to be known. In the coarse-grained approach computational interface width is usually used, which may be larger than the physical width by several orders of magnitude, but keeps the same (i.e., independent of the interface width) energy and mobility. If the order parameter corresponding to the third phase appears within an interface between two other phases, then (as it follows from the thin-interface consideration [16, 17, 21, 22]) results of solution depend on the interface width, which due to unphysical width leads to wrong results. Thus, PT between each two phases should occur along the straight line (or any line, which is independent on temperature, e.g., circle

[8, 23–25]) in the order parameter space. Since a single constraint $\sum \eta_i = 1$ does not lead to such a transformation paths, additional efforts are made to satisfy these two conditions [16–18]. These efforts, however, does not completely solve the problem either.

Different order parameters and nonlinear constraint were suggested in [8] for multivariant martensitic PTs. A thermodynamic potential in hyperspherical order parameters is developed, in which A is at the center of the sphere, and all martensitic variants M_i are located at the hypersphere.

Because of impossibility to satisfy some of requirements, namely to obtain consistent PT criteria from the thermodynamic instability conditions, the nonlinear constraint for the hyperspherical order parameters was substituted in [26] with the linear constraint of the type $\sum \eta_i = 1$, which, however, does not include A. Still, PT criteria could not be obtained in a consistent way for more than three phases. Only for three phases, when constraint is explicitly eliminated, the theory in [8, 23–26] is completely consistent with the two-phase theory and produces proper PT criteria. Note that requirements that PT criteria should follow from the thermodynamic instability conditions was never used for the second approach [9, 10, 16–18].

In the paper, we explicitly formulate all requirements which we want to satisfy, first for two-phase PFA, then for arbitrary number of phases. Then we develop theory which satisfies all these requirements. One of these requirements, that consistent PT criteria for all PTs should follow from the thermodynamic instability conditions, could be satisfied approximately only. Namely, instead of imposing constraints on the order parameter, we introduce simple terms penalizing deviation of the paths in the order parameter space from the straight lines connecting *each two phases*. By controlling these terms, we can either fully avoid third phase within an interface between two other phases or allow it in order to describe actual physical situation [23–25, 27, 28]. Comparison with previous requirements is performed. A number of model problems for three-phase PTs including problems on a solid-solid PT via intermediate melting in HMX energetic materials are solved and compared to solution based on different theory [23–25], in which all requirements are satisfied exactly but which cannot be generalized for more than three phases. Note that similar approach but with proper justification and with emphases on stress-induced PTs and twinning was presented in [29].

4.2 Two-phase model

4.2.A Ginzburg-Landau equation

The free energy ψ, dissipation rate D, and Ginzburg-Landau equation for a single order parameter η have the form

$$= \psi^\theta(\theta, \eta) + 0.5\beta|\boldsymbol{\nabla}\eta|^2; \qquad D = X\dot{\eta} \geq 0; \tag{1}$$

$$\dot{\eta} = LX = -L\frac{\delta\psi}{\delta\eta} = L\left(-\frac{\partial\psi^\theta}{\partial\eta} + \beta\boldsymbol{\nabla}^2\eta\right), \tag{2}$$

where ψ^θ is the local thermal (chemical) energy, $\beta > 0$ and $L > 0$ are the gradient energy and kinetic coefficients, X is the thermodynamic driving force conjugate to $\dot{\eta}$, and $\frac{\delta}{\delta}$ is the variational derivative. Our goal is to formulate requirements to $\psi^\theta(\theta, \eta)$ and some interpolation functions and find the simplest function that satisfies these requirements. Since all requirements are for homogeneous states, gradient-related term in X can be omitted.

4.2.B Conditions for free energy

1. We would like to enforce that $\eta = 0$ corresponds to the phase P_0 and $\eta = 1$ corresponds to the phase P_1. If any physically defined values of the order parameters are known, one can always arrive at these values by shifting and normalizing them. It is convenient to express any material property M (energy, entropy, specific heat, mass density, and when mechanics is included, also elastic moduli and thermal expansion) in the form

$$M(\eta, \theta) = M_0(\theta) + (M_1(\theta) - M_0(\theta))\varphi_m(\eta), \tag{3}$$

where M_0 and M_1 are values of the property M in phases P_0 and P_1, respectively, and $\varphi_m(\eta)$ is corresponding interpolation function, which satisfies evident conditions

$$\varphi_m(0) = 0, \qquad \varphi_m(1) = 1. \tag{4}$$

In application to free energy, we obtain

$$\psi^\theta(\theta, 0) = \psi_0^\theta(\theta), \qquad \psi^\theta(\theta, 1) = \psi_1^\theta(\theta), \tag{5}$$

where $\psi_0^\theta(\theta)$ and $\psi_1^\theta(\theta)$ are the free energies of the bulk phases P_0 and P_1. However, it is not sufficient to verbally impose that $\eta = 0$ corresponds to the phase P_0 and $\eta = 1$ corresponds to the phase P_1. This should directly follow from the thermodynamic equilibrium conditions, because bulk phases should be thermodynamically equilibrium solutions of the Ginzburg-Landau equations (2).

2. Values $\eta = 0$ and $\eta = 1$ should satisfy the thermodynamic equilibrium conditions

$$X = -\frac{\partial \psi^\theta(\theta, 0)}{\partial \eta} = -\frac{\partial \psi^\theta(\theta, 1)}{\partial \eta} = 0 \tag{6}$$

for *any temperature* θ. Otherwise, thermodynamically equilibrium values of the order parameters obtained from condition $X = 0$ will depend on temperature. Substituting them in Eq.(3) will introduce artificial temperature dependence of the property M and will not allow to obtain known properties M_0 and M_1 for bulk phases P_0 and P_1. It also follow from Eq.(6) that for any material property which participates in ψ^θ one has

$$\frac{d\varphi_p(0)}{d\eta} = \frac{d\varphi_p(0)}{d\eta} = 0. \tag{7}$$

3. The free energy should not possess unphysical minima for any temperature. Any minimum in the free energy that does not correspond to the desired minima for phase P_0 and P_1 represents spurious (unphysical) phase. It cannot be interpreted as a "discovery" of a new phase, because it is just consequence of chosen polynomial approximation rather than any physical knowledge. In particular, one can "discover" as many new phases as he/she wishes, if some periodic function of the order parameters is added to the potential.

The smallest degree potential potential that satisfies all these properties is the fourth degree. Thus, starting with the full fourth degree polynomial $\varphi = h + g\eta + a\eta^2 + b\eta^3 + c\eta^4$ and applying conditions 1-3, one obtains:

$$\varphi(a, \eta) := a\eta^2 + (4 - 2a)\eta^3 + (a - 3)\eta^4 = a\eta^2(1 - \eta)^2 + \eta^3(4 - 3\eta), \tag{8}$$

where a is a parameter. If properties vary monotonously between phase, i.e., the function $\varphi(a, \eta)$ does not have an extremum on the interval $0 \leq \eta \leq 1$, then one has to impose for

$0 \le a \le 6$. Similar, starting with $\psi^\theta = H + G\eta + A\eta^2 + B\eta^3 + C\eta^4$, and applying conditions 1-3, we derive

$$\psi^\theta(\theta, \eta) = \psi_0^\theta(\theta) + \Delta\psi^\theta(\theta)\eta^3(4 - 3\eta) + A\eta^2(1 - \eta)^2, \qquad \Delta\psi^\theta = \psi_1^\theta(\theta) - \psi_0^\theta(\theta), \qquad (9)$$

Here A is the material parameter, which depends or may depend on temperature (similar is true for a), $\Delta\psi^\theta$ is the negative thermal driving force for $\mathsf{P}_0 \to \mathsf{P}_1$ phase transformation. The first two terms in ψ^θ represent smooth interpolation between ψ_0^θ and ψ_1^θ, and the last one is a double-well barrier. Eq.(9) can make wrong impression that the function $\eta^3(4 - 3\eta)$ is the only interpolation function for $\Delta\psi^\theta$. However, A may include $\Delta\psi^\theta$ in some way as well. Eq.(9) was obtained by excluding parameters B and C while imposing our constrains. However, if we exclude A and B or A and C, we obtain two different expressions:

$$\psi^\theta(\theta, \eta) = \psi_0^\theta(\theta) + \Delta\psi^\theta(\theta)\eta^2(3 - 2\eta) + C\eta^2(1 - \eta)^2;$$
$$\psi^\theta(\theta, \eta) = \psi_0^\theta(\theta) + \Delta\psi^\theta(\theta)\eta^2(2 - \eta^2) - 0.5B\eta^2(1 - \eta)^2, \qquad (10)$$

satisfying the same conditions. To avoid this multiplicity of presentations, we define ψ^θ as the sum of double-barrier function (which is the same in all presentations) and the most general monotonous interpolation between ψ_0^θ and ψ_1^θ satisfying conditions 1-3:

$$\psi^\theta(\theta, \eta) = \psi_0^\theta(\theta) + \Delta\psi^\theta(\theta)\varphi(a, \eta) + A\eta^2(1 - \eta)^2. \qquad (11)$$

Now we can exclude dependence of A on $\Delta\psi^\theta$ without loss of generality. For different a we can obtain Eqs.(9)-(10).

4. Conditions for thermodynamic instability of equilibrium phases P_0 and P_1 should give specific instability temperatures, which are temperatures for barrierless PT or spinodal temperatures. Critical temperature should be below phase equilibrium temperature θ_e for high-temperature phase P_0 and above θ_e for low temperature phase P_1.

As we will see, this condition imposes some restrictions for the free energy (11), but it cannot be satisfied for some of popular fifth-degree potentials used in [16, 17, 30]. Thermodynamic instability conditions are

$$\mathsf{P}_0 \to \mathsf{P}_1: \quad \partial X(\theta, 0)/\partial\eta = -\partial^2\psi^\theta(\theta, 0)/\partial\eta^2 = -2(A + a\Delta\psi^\theta) \ge 0 \to -\Delta\psi^\theta \ge A(\theta)/a; \quad (12)$$

$$\mathsf{P}_1 \to \mathsf{P}_0: \quad \partial X(\theta, 1)/\partial\eta = -\partial^2\psi^\theta(\theta, 1)/\partial\eta^2 = -2(A + (a - 6)\Delta\psi^\theta) \ge 0 \to -\Delta\psi^\theta \le A(\theta)/(a - 6), (13)$$

where we took into account that $a < 6$. Thus, barrierless direct PT $\mathsf{P}_0 \to \mathsf{P}_1$ occurs when the driving force $-\Delta\psi^\theta$ exceeds some positive threshold and barrierless reverse PT $\mathsf{P}_1 \to \mathsf{P}_0$ occurs when the driving force $-\Delta\psi^\theta$ is smaller than some negative threshold; there is a hysteresis, which is logical and agrees with condition 4. Let us assume that A and $\Delta\psi^\theta$ are linear functions of temperature: $A(\theta) = A_*\theta - B_*$ and $\Delta\psi^\theta = -\Delta s(\theta - \theta_e)$, where A_* and B_* are parameters and $\Delta s = s_1 - s_0$ is the jump in entropy between phases P_1 and P_0. The linear temperature dependence of $\Delta\psi^\theta$ implies neglecting the difference between specific heats of phases. Then instability conditions (12)-(13) reduce to

$$\mathsf{P}_0 \to \mathsf{P}_1 : \quad \theta < \theta_c^0; \quad \theta_c^0 := (a\Delta s\,\theta_e - B_*)/(a\Delta s - A_*); \tag{14}$$

$$\mathsf{P}_1 \to \mathsf{P}_0 : \quad \theta > \theta_c^0; \quad \theta_c^1 := (a\Delta s\,\theta_e + B_*)/(a\Delta s + A_*), \tag{15}$$

where θ_c^0 and θ_c^1 are the critical temperatures for the loss of stability of phases P_0 and P_1. The required conditions $\theta_c^0 < \theta_e$ and $\theta_c^1 > \theta_e$ lead to

$$??? \tag{16}$$

For the case when $\theta_e = 0.5(\theta_c^0 + \theta_c^1)$ one has $A_* = 0$ and A is temperature independent.

5. Interpolating functions $\varphi(a, \eta)$ should satisfy the following antisymmetry condition:

$$\varphi(a, 1 - \eta) = 1 - \varphi(a, \eta). \tag{17}$$

This condition is not required for a single order parameter but will be required for consistent description for multiphase system and multiple order parameters. This condition is satisfied for $a = 3$ only. Thus, interpolating function reduces to

$$\phi(\eta) = \varphi(3, \eta) = \eta^2(3 - 2\eta) \tag{18}$$

and instability conditions to

$$\mathsf{P}_0 \to \mathsf{P}_1 : \quad -\Delta\psi^\theta \geq A(\theta)/3; \quad \mathsf{P}_1 \to \mathsf{P}_0 : \quad -\Delta\psi^\theta \leq -A(\theta)/3. \tag{19}$$

The critical temperatures are

$$\theta_c^0 := (3\Delta s\,\theta_e - B_*)/(3\Delta s - A_*); \qquad \theta_c^1 := (3\Delta s\,\theta_e + B_*)/(3\Delta s + A_*), \tag{20}$$

and for the case when $\theta_e = 0.5(\theta_c^0 + \theta_c^0)$ one has $A_* = 0$ and A is temperature independent..

Condition 5 means complete equivalence of phases P_1 and P_0 in the following sense. If we consider the order parameter $\bar{\eta} = 1 - \eta$, which is zero for P_1 and 1 for P_0, then

$$\phi(\bar{\eta}) = \phi(1 - \eta) = 1 - \phi(\eta) = 1 - \phi(1 - \bar{\eta}). \tag{21}$$

Plot of functions $\phi(\eta)$ and $\phi(\bar{\eta})$ is symmetric with respect to the vertical mirror at $\eta = \bar{\eta} = 0.5$. Substituting $\eta = 1 - \bar{\eta}$ in Eq.(4), we obtain

$$M(\eta, \theta) = M_0 + (M_1 - M_0)\phi(1 - \bar{\eta}) = M_0 + (M_1 - M_0)(1 - \phi(\bar{\eta})) = M_1 + (M_0 - M_1)\phi(\bar{\eta}). \tag{22}$$

Thus, all material properties, and consequently entire theory are invariant with respect to exchange $(\mathsf{P}_0, \eta) \leftrightarrow (\mathsf{P}_1, \bar{\eta})$. Eq.(11) simplifies to

$$\psi^\theta(\theta, \eta) = \psi_0^\theta(\theta) + \Delta\psi^\theta(\theta)\phi(\eta) + A\eta^2(1 - \eta)^2. \tag{23}$$

Condition 5 is definitely not a fundamental property and may not be true for various phase transformations. It is restrictive but this is a price that one must pay to be able to develop a multiphase PFA within given framework.

4.3 Model with n order parameters

4.3.A Ginzburg-Landau equations

We consider $n+1$ phases P_0 and P_i ($i = 1, 2, ..., n$) described by n order parameters η_i. Each PT $\mathsf{P}_0 \leftrightarrow \mathsf{P}_i$ is described by a single order parameter η_i. We designate the set of the arbitrary order parameters as $\tilde{\eta} = (\eta_1, ..., \eta_i, ..., \eta_n)$ with $\bar{\eta}_i = (0, ..., \eta_i, ..., 0)$ for one nonzero parameter only. The reference phase P_0 corresponds to $\hat{\eta}_0 := (0, ..., 0)$ and phase P_i is designated as $\hat{\eta}_i = (0, ..., \eta_i = 1, ..., 0)$. The generalization of Eqs.(1) and (2) for the free energy ψ, dissipation rate D, and Ginzburg-Landau equation is

$$= \psi^\theta(\theta, \eta_i) + \sum 0.5\beta_{ij}\boldsymbol{\nabla}\eta_i \cdot \boldsymbol{\nabla}\eta_j; \qquad \beta_{ij} = \beta_{ji}; \qquad D = \sum X_i\dot{\eta}_i \geq 0; \tag{24}$$

$$\dot{\eta}_i = L_{ij}X_j = L_{ij}\left(-\frac{\partial\psi}{\partial\eta_j} + \sum \beta_{jk}\boldsymbol{\nabla}^2\eta_k\right); \quad L_{ij} = L_{ji}, \tag{25}$$

where β_{ij} and L_{ij} are positively defined gradient energy and kinetic coefficients, X_i is the thermodynamic driving force conjugate to $\dot{\eta}_i$.

4.3.B Conditions for thermodynamic potential.

1n. Any material property M can be expressed in the form

$$M(\eta_i, \theta) = M_0(\theta) + \sum (M_i(\theta) - M_0(\theta))\phi(\eta_i); \quad \phi(\eta_i) = \eta_i^2(3 - 2\eta_i). \tag{26}$$

We used the simplest linear combination without interaction effects and with interpolation function which satisfies all requirements Eqs.(4), (7), and (21), i.e., $\phi(0) = 0$, $\phi(1) = 1$, $\frac{d\phi(0)}{d\eta} = \frac{d\phi(0)}{d\eta} = 0$, and $\phi(1 - \eta) = 1 - \phi(\eta)$. Thus, condition 5 is met.

2n. For the homogeneous states, the sets of constant order parameters for the phase P_0 $\tilde{\eta} = \hat{\eta}_0$ and for phase P_i $\tilde{\eta} = \hat{\eta}_i$ should satisfy the thermodynamic equilibrium conditions

$$X_i = -\frac{\partial \psi^\theta(\theta, \hat{\eta}_j)}{\partial \eta_i} = 0, \qquad i = 1, 2, ..., n; \qquad j = 0, 1, 2, ..., n \tag{27}$$

for any temperature θ.

3n. The free energy should not possess unphysical minima for any temperature.

This condition is not simple to prove for multiple order parameters, that is why one has to keep potential as simple as possible.

4n. Theory should be invariant with respect to the exchange of phases $\mathsf{P}_i \leftrightarrow \mathsf{P}_j$ for any i and j, including $i = 0$ and $j = 0$. Also, for some material parameters and temperature, which provide PT $\mathsf{P}_i \leftrightarrow \mathsf{P}_j$ without involvement any other phase P_k, description of this PT should be the same if we choose one of the phase as P_0.

It is clear that this condition does not have a counterpart for two-phase system. When we consider $\mathsf{P}_i \leftrightarrow \mathsf{P}_j$ PT alone, we can use theory for two phases described in the previous Section, in which one of the phases will be chosen as P_0. That means that we know all equations for this PT. Condition 4n requires that the same equations should be obtained for this PT within general n-phase theory for phases P_i and P_j for $i \neq 0$ and $j \neq 0$.

As we will see, each $\mathsf{P}_0 \leftrightarrow \mathsf{P}_j$ PT is described with the help of a single order parameter and does not differ essentially from the two-phase theory (provided that the third phase is not involved). However, $\mathsf{P}_i \leftrightarrow \mathsf{P}_j$ PT involves simultaneous change of two order parameters along some trajectory in $\eta_i - \eta_j$ plane, which depends on temperature. In order to make description of $\mathsf{P}_i \leftrightarrow \mathsf{P}_j$ PT equivalent to description of $\mathsf{P}_0 \leftrightarrow \mathsf{P}_j$ PT, this trajectory should be controlled.

5n. Conditions for thermodynamic instability of homogeneous equilibrium phases that lead to criteria of barrierless PTs between phases P_i and P_j in the general theory for n-phase system should coincide with those for two-phase system.

Thermodynamic equilibrium state $\hat{\eta}_j$ loses its stability when condition

$$\frac{\partial X_i(\theta, \hat{\eta}_j)}{\partial \eta_k} \dot{\eta}_i \, \dot{\eta}_k = -\frac{\partial^2 \psi^\theta(\theta, \hat{\eta}_j)}{\partial \eta_i \partial \eta_k} \dot{\eta}_i \, \dot{\eta}_k \geq 0 \tag{28}$$

is fulfilled for the first time for some $\dot{\eta}_i$. Thus, the instability occurs when $n \times n$ matrix $\partial X_i / \partial \eta_k$ first ceases to be negative definite or equivalently, $n \times n$ matrix $\frac{\partial^2 \psi^\theta(\theta, \hat{\eta}_j)}{\partial \eta_i \partial \eta_k}$ first ceases to be positive definite. According to Sylvester's criterion, the one of the following conditions should be fulfilled for instability of the phase $\hat{\eta}_j$:

$$B_{ik} := \frac{\partial^2 \psi^\theta(\boldsymbol{\sigma}, \hat{\eta}_j)}{\partial \eta_i \, \partial \eta_k}; \qquad B_{11} \leq 0; \qquad B_{11}B_{22} - B_{12}^2 \leq 0;$$
$$B_{11}(B_{22}B_{33} - B_{23}^2) - B_{12}(B_{21}B_{33} - B_{31}B_{23}) + B_{33}(B_{12}B_{32} - B_{22}B_{31}) \leq 0. \tag{29}$$

In general, it is quite difficult to design a potential for which such sophisticated conditions are reduced to simple conditions for each of $\mathsf{P}_0 \leftrightarrow \mathsf{P}_i$ or $\mathsf{P}_j \leftrightarrow \mathsf{P}_i$ transformations, when they are considered separately. Also, when we considered just two phases, when one of them loses its stability, transformation occurs to another one. In the general case, if, e.g., the third condition Eq.(29) is met, it is not clear to which phase it will transform. Thus, it would be difficult even to compare general results with results for a two-phase case. It is clear that additional simplifications are necessary.

It is natural to assume that if the instability condition Eq. (28) is met for one specific i only, the transformation from the phase $\hat{\eta}_j$ will occur toward this $\hat{\eta}_i$ phase. Our main point is that in thermodynamic approaches for a sharp interface, transformation conditions from the phase P_j to P_i are independent of any other phase P_k (including $\hat{\eta}_0$). It is reasonable to assume the same for our PFA. That is why we accept the following additional condition.

equilibrium phase $\hat{\eta}_j$:

$$\frac{\partial X_i(\theta, \hat{\eta}_j)}{\partial \eta_k} = \frac{\partial^2 \psi^\theta(\theta, \hat{\eta}_j)}{\partial \eta_i \partial \eta_k} = 0 \quad \forall k \neq i, \tag{30}$$

In this case, the instability conditions Eqs.(28) or (29) reduce to

$$-\frac{\partial X_i(\theta, \hat{\eta}_j)}{\partial \eta_i} = \frac{\partial^2 \psi^\theta(\theta, \hat{\eta}_j)}{\partial \eta_i^2} \leq 0. \tag{31}$$

Condition 6n significantly simplifies instability criteria and allows one to analyze them and apply to the choice of the specific expression for $\psi^\theta(\theta, \tilde{\eta}_j)$. Also, it leads to a much simpler expression for this function, for which one can determine all material parameters and have much more confidence that some artificial minima are absent. Thus, the transformation conditions between phases read as

$$\mathsf{P}_0 \to \mathsf{P}_i: \qquad -\frac{\partial X_i(\theta, \hat{\eta}_0)}{\partial \eta_i} = \frac{\partial^2 \psi^\theta(\theta, \hat{\eta}_0)}{\partial \eta_i^2} \leq 0;$$

$$\mathsf{P}_i \to \mathsf{P}_0: \qquad -\frac{\partial X_i(\theta, \hat{\eta}_i)}{\partial \eta_i} = \frac{\partial^2 \psi^\theta(\theta, \hat{\eta}_i)}{\partial \eta_i^2} \leq 0. \tag{32}$$

$$\mathsf{P}_j \to \mathsf{P}_i: \qquad -\frac{\partial X_i(\theta, \hat{\eta}_j)}{\partial \eta_i} = \frac{\partial^2 \psi^\theta(\theta, \hat{\eta}_j)}{\partial \eta_i^2} \leq 0;$$

$$\mathsf{P}_i \to \mathsf{P}_j: \qquad -\frac{\partial X_j(\theta, \hat{\eta}_i)}{\partial \eta_j} = \frac{\partial^2 \psi^\theta(\theta, \hat{\eta}_i)}{\partial \eta_j^2} \leq 0. \tag{33}$$

4.3.C Multiphase model.

The simplest expression for the local free energy ψ^θ that includes all what we derived for a single order-parameter theory and can satisfy all the desired conditions is accepted in the following form:

$$\psi^\theta = \breve{\psi}^\theta + \tilde{\psi}^\theta + \psi_p; \tag{34}$$

$$\breve{\psi}^\theta = \sum A_i(\theta)\eta_i^2(1 - \eta_i)^2 + \sum \bar{A}_{ij}\eta_i^2 \eta_j^2; \quad \bar{A}_{ii} = 0; \tag{35}$$

$$\tilde{\psi}^\theta = \psi_0^\theta(\theta) + \sum \Delta\psi_i^\theta(\theta)\phi(\eta_i); \quad \Delta\psi_i^\theta = \psi_i^\theta - \psi_0^\theta; \tag{36}$$

$$\psi_p = \sum K_{ij}(\eta_i + \eta_j - 1)^2\eta_i^l\eta_j^l + \sum K_{ijk}\eta_i^2\eta_j^2\eta_k^2; \quad l \geq 2; \quad K_{ii} = K_{iik} = K_{ikk} = K_{iji} = 0. \tag{37}$$

Here A_i is proportional to the magnitude of the double-well barriers between phases P_0 and P_i, $\bar{A}_{ij}$ contributes to the magnitude of the double-well barriers between phases P_i and P_j, and the term ψ_p containing coefficients $K_{ij} \geq 0$ and $K_{ijk} \geq 0$ penalizes deviation of the trajectory of the order parameters in n-dimensional space η_i from some lines and planes. Without ψ_p, the local part of free energy is much simpler than in $[1, 2, 8]$ and does not contain complex interaction between phases. The term with $\eta_i^2 \eta_j^2 \eta_k^2$ is nonnegative for any three nonzero order parameters, i.e., it penalizes the presence of the three phases at the same material point. This term gives additional means to control the presence of the third phase within the interface between the two other phases, especially, when it is desired to completely exclude it. It also contributes to the energy of triple junctions. For homogeneous states, this term always excludes the presence of the three phases at the same point, because it increases energy compared with a two-phase state. When one wants to study the third phase within the interface between the two other phases [23–25], one can set $K_{ijk} = 0$, which will simplify analysis. For homogeneous states, the positive terms in $\breve{\psi}^\theta$ and $\tilde{\psi}^\theta$ exclude appearance of two and three phases at the same point. The the first terms in ψ_p penalizes deviations from hyperplanes $\eta_i = 0$ orthogonal to the coordinate axes η_i in the order parameter space and hyperplanes $\eta_i + \eta_j = 1$ passing trough two phases P_i and P_j. The exponent l allows one to control relative contribution of these penalties. Since more than two phases, say P_i and P_j, are forbidden by other terms, the term $(\eta_i + \eta_j - 1)^2$ penalizes deviation from the straight lines $\eta_i + \eta_j = 1$, $\eta_k = 0 \; \forall k \neq i, j$, connecting phases P_i and P_j within plane $\eta_i - \eta_j$. The term with η_i penalizes deviation from the coordinate axes in η_j space, i.e., from straight lines connecting phases P_0 and P_i. Thus, evolution of η_i is (at least approximately) constrained to occur along the desired transformation paths. Note that we do not need to use additional constraints to impose evolution of η_i along the coordinate axes, because for the chosen potential even without them PTs between phases P_0 and P_i occur along straight line connecting these phases. However, without the multiplier $\eta_i^l \eta_j^l$, the first term in ψ_p will artificially penalize free energy along the coordinate axes in η_i space and spoil the thermodynamic potential.

For $\mathsf{P}_0 \leftrightarrow \mathsf{P}_i$ PTs described by a single order parameter η_i, ψ_p and the second term in $\breve{\psi}^\theta$ disappear and Eqs.(24)-(25) and (34)-(36) reduce to equations for two-phase system (1)-(2) and (23).

4.3.D Thermodynamic instability conditions.

Direct application of the instability conditions (32)-(33) to free energy (34)-(37) for thermodynamically equilibrium homogeneous phases produces the following PT criteria:

$$\mathsf{P}_0 \to \mathsf{P}_i : \qquad \frac{\partial^2 \psi^\theta (\theta, \hat{\eta}_0)}{\partial \eta_i^2} \leq 0 \to -\Delta\psi_i^\theta \geq A_i(\theta)/3;$$

$$\mathsf{P}_i \to \mathsf{P}_0 : \qquad \frac{\partial^2 \psi^\theta (\theta, \hat{\eta}_i)}{\partial \eta_i^2} \leq 0 \to -\Delta\psi_i^\theta \leq -A_i(\theta)/3; \qquad (38)$$

$$\mathsf{P}_j \to \mathsf{P}_i : \qquad \frac{\partial^2 \psi^\theta (\theta, \hat{\eta}_j)}{\partial \eta_i^2} \leq 0 \to -\Delta\psi_i^\theta \geq (A_i(\theta) + \bar{A})/3 \ \Rightarrow \ \text{wrong};$$

$$\mathsf{P}_i \to \mathsf{P}_j : \qquad \frac{\partial^2 \psi^\theta (\theta, \hat{\eta}_i)}{\partial \eta_j^2} \leq 0 \to -\Delta\psi_j^\theta \geq (A_j(\theta) + \bar{A})/3 \ \Rightarrow \ \text{wrong}. \qquad (39)$$

Criteria for $\mathsf{P}_0 \leftrightarrow \mathsf{P}_i$ PTs coincide with PT criteria (19) for the two-phase system, i.e. they satisfy condition 4n. In contrast, condition for $\mathsf{P}_i \leftrightarrow \mathsf{P}_j$ PTs are contradictory and do not meet condition 4n. Indeed, they do not depend on difference in energy between phases P_i and P_j, depend on the energy of phase P_0 (which does not participate in this PT) and contain the barrier A_i for one phase only. In addition, since the first and second derivatives of ψ_p vanish for all equilibrium phases P_i, the term ψ_p does not alter phase equilibrium conditions and PT criteria for homogeneous phases. Still, we will demonstrate below that this term is a key player in the development of consistent PFA for multiphase system, namely, in making the equations for $\mathsf{P}_i \leftrightarrow \mathsf{P}_j$ PTs fully equivalent to equations for $\mathsf{P}_0 \leftrightarrow \mathsf{P}_i$ PTs.

Constrained model for $\mathsf{P}_i \leftrightarrow \mathsf{P}_j$ transformations.

We increase parameters K_{ij} (and, if required, K_{ijk}) to very high values so that they impose constraints $\eta_i + \eta_j = 1$ and $\eta_k = 0 \ \forall k \neq i, j$ with any required accuracy. Implementing these constraints in Eqs.(24)-(25) and (34)-(36), we express them in terms of the single order parameter η_i:

$$\breve{\psi}^\theta = A_{ij}(\theta)\eta_i^2(1 - \eta_i)^2; \quad A_{ij} = A_i + A_j + \bar{A}_{ij} = A_{ji}; \qquad (40)$$

$$\tilde{\psi}^\theta = \Delta\psi_j^\theta + \Delta\psi_{ij}^\theta(\theta)\phi(\eta_i); \quad \Delta\psi_{ij}^\theta = \Delta\psi_i^\theta - \Delta\psi_j^\theta; \qquad (41)$$

$$\nabla = 0.5 b_{ij} |\boldsymbol{\nabla}\eta_i|^2; \quad b_{ij} = \beta_{ii} + \beta_{jj} - 2\beta_{ij} = b_{ji} > 0; \qquad (42)$$

$$\dot{\eta}_i = l_{ij}\left(-\frac{\partial\psi}{\partial\eta_i} + b_{ij}\boldsymbol{\nabla}^2\eta_i\right); \quad l_{ij} = (L_{ii}L_{jj} - L_{ij}^2)/(L_{jj} + L_{ij}) = l_{ij} > 0. \qquad (43)$$

Thermodynamic instability conditions look like

$$\mathsf{P}_j \to \mathsf{P}_i: \quad -\Delta\psi_i^\theta \geq A_{ij}(\theta)/3; \qquad \mathsf{P}_i \to \mathsf{P}_j: \quad -\Delta\psi_j^\theta \geq A_{ji}(\theta)/3 \ \to \ -\Delta\psi_i^\theta \leq -A_{ij}(\theta)/3. \quad (44)$$

It is clear that Eqs.(40)-(44) for $\mathsf{P}_j \to \mathsf{P}_i$ PTs coincide to within constants and designations with equations for two-phase system (1)-(2) and (23) and consequently for $\mathsf{P}_0 \to \mathsf{P}_i$ PTs, as it was required in condition 4n. Note that we explicitly took into account condition (21), without which Eqs.(40)-(43) will not look like for two-phase model.

Let $\Delta\psi_i^\theta = -\Delta s_i(\theta - \theta_e^i)$, where $\Delta s_i = s_i - s_0$ is the jump in entropy between phases P_i and P_0 and θ_e^i is the thermodynamic equilibrium melting temperature of phases P_i and P_0. The linear temperature dependence of $\Delta\psi_i^\theta$ implies neglecting the difference between specific heats of phases. Then by definition $\Delta\psi_{ji}^\theta = \Delta\psi_j^\theta - \Delta\psi_i^\theta = -\Delta s_j(\theta - \theta_e^j) + \Delta s_i(\theta - \theta_e^i) = -\Delta s_{ji}(\theta - \theta_e^{ji})$, where $\Delta s_{ji} = \Delta s_j - \Delta s_i$ and $\theta_e^{ji} = (\Delta s_j \theta_e^j - \Delta s_i \theta_e^i)/\Delta s_{ji}$.

We express coefficients $A_i(\theta) = A_*^i \theta - B_*$, where A_*^i is some characteristic value which will expressed in terms of the critical temperature at which phase P_0 loses its stability toward P_i and B_* is constant. A similar coefficient between phases P_j and P_i is accepted in a more general form $A_{ji}(\theta) = \bar{A}_{ji}^*(\theta) + A_*^{ji}\theta - B_*^{ji}$. For phases P_i with different thermal properties we can put $\bar{A}_{ji}^*(\theta) = 0$ without loss of generality, like for any P_0-P_i and P_j-P_i PT. Then, instability conditions Eqs.(38) and (44) transform to

$$\mathsf{P}_0 \to \mathsf{P}_i: \quad \theta < \theta_c^{i0}; \quad \theta_c^{i0} := (3\Delta s_i \theta_e^i - B_*)/(3\Delta s_i - A_*^i); \qquad (45)$$

$$\mathsf{P}_i \to \mathsf{P}_0: \quad \theta > \theta_c^{i0}; \quad \theta_c^{0i} := (3\Delta s_i \theta_e^i + B_*)/(3\Delta s_i + A_*^i), \qquad (46)$$

$$\mathsf{P}_i \to \mathsf{P}_j: \quad \theta < \theta_c^{ji}; \quad \theta_c^{ji} := (3\Delta s_{ji} \theta_e^{ji} - B_*^{ji})/(3\Delta s_{ji} - A_*^{ji}), \qquad (47)$$

$$\mathsf{P}_j \to \mathsf{P}_i: \quad \theta > \theta_c^{ji}; \quad \theta_c^{ij} := (3\Delta s_{ji} \theta_e^{ji} + B_*^{ji})/(3\Delta s_{ji} + A_*^{ji}), \qquad (48)$$

where θ_c^{i0} and θ_c^{0i} are the critical temperatures for barrierless $\mathsf{P}_0 \to \mathsf{P}_i$ and $\mathsf{P}_i \to \mathsf{P}_0$ PTs. Similarly, θ_c^{ji} and θ_c^{ij} are the critical temperatures for barrierless $\mathsf{P}_i \to \mathsf{P}_j$ and $\mathsf{P}_j \to \mathsf{P}_i$ PTs. For the case when $\theta_e^i = 0.5(\theta_c^{i0} + \theta_c^{0i})$ and $\theta_e^{ji} = 0.5(\theta_c^{ji} + \theta_c^{ij})$ one has $A_*^i = 0$, $A_*^{ji} = 0$ and A_i, A_{ji} are temperature independent. If we assume that the equilibrium temperature is the average

of critical temperatures, then we obtain $A^i = 3\Delta s_i(\theta_c^{i0} - \theta_e^i)$ and $A^{ji} = 3\Delta s_{ji}(\theta_c^{ji} - \theta_e^{ji})$. In the next subsection, it will be shown that this choice of parameters makes the interface energy and width to be temperature independent.

4.3.E Analytical Solution

In contrast to the other multiphase models [1-5], in the developed model each of the PTs can be described by a single order parameter without constraints. It allows us to utilize analytical solutions [9] for the interface between two phases propagating in the $x-$ direction, including its profile, energy γ, width δ, and velocity c. Due to equivalence of all equations for $P_0 \leftrightarrow P_i$ and $P_j \to P_i$ PTs, the analytical solution for a propagating with velocity c interface [9] for the $P_i P_j$ interface solutions are:

$$\eta_{ji} = 0.5\tanh\left[3(x - c_{ji}t)/\delta_{ji}\right] + 0.5; \quad \delta_{ji} = \sqrt{18\beta_{ji}/A_{ji}(\theta)}; \quad c_{ji} = L_{ji}\delta_{ji}\Delta\psi_{ji}^\theta(\theta); \quad \gamma_{ji} = \beta_{ji}/\delta_{ji}, \tag{49}$$

and for $P_0 P_i$ they are presented below

$$\eta_{i0} = 0.5\tanh\left[3(x - c_{i0}t)/\delta_{i0}\right] + 0.5; \quad \delta_{i0} = \sqrt{18\beta_{i0}/A_{i0}(\theta)}; \quad c_{i0} = L_{i0}\delta_{i0}\Delta\psi_{i0}^\theta(\theta); \quad \gamma_{i0} = \beta_{i0}/\delta_{i0}, \tag{50}$$

Energy of the nonequilibrium interfaces is defined as an excess energy, with respect to bulk phases, assuming that the Gibbs dividing surface is located where the corresponding order parameter is equal to 0.5 (see justification in [57]). Thus,

$$E^{21} = \int_{-\infty}^{x_{\vartheta=0.5}} (\psi - \psi_1)dx + \int_{x_{\vartheta=0.5}}^{\infty} (\psi - \psi_2)dx; \quad E^{s0} = \int_{-\infty}^{x_{\Upsilon=0.5}} (\psi - \psi_0)dx + \int_{x_{\Upsilon=0.5}}^{\infty} (\psi - \psi_s)dx \tag{51}$$

Here, $x_{\vartheta=0.5}$ and $x_{\Upsilon=0.5}$ define the locations where $\vartheta = 0.5$ and $\Upsilon = 0.5$, respectively. For the particular case $A_c^{ij} = -3\Delta s_{ij}$, the interface energies and width became temperature-independent:

$$\gamma_{ji} = \sqrt{\beta_{ji}\left[\Delta s_{ji}(\theta_c^{ji} - \theta_e^{ji})\right]/6}; \quad \delta_{ji} = \sqrt{6\beta_{ji}/\left\{\left[\Delta s_{ji}(\theta_c^{ji} - \theta_e^{ji})\right]\right\}}; \tag{52}$$

$$\gamma_{i0} = \sqrt{\beta_{i0}\left[\Delta s_{i0}(\theta_c^{i0} - \theta_e^{i0})\right]/6}; \quad \delta_{i0} = \sqrt{6\beta_{i0}/\left\{\left[\Delta s_{i0}(\theta_c^{i0} - \theta_e^{i0})\right]\right\}}. \tag{53}$$

Equations (49)-(50) and (52)-(53) allow us to calibrate material parameters β_{ji}, β_{i0}, A_{ji}, A_{i0}, θ_c^{ji}, θ_c^{i0}, L_{ji}, and L_{i0} when the temperature dependence of the interface energy, width, and velocity are known, along with the thermodynamic parameters Δs_{ij} and θ_e^{ij}. The ratios of $P_i P_j$ to $P_i P_0$ interface energies and widths, k_E^{ji} and k_δ^{ji}, play the key role in determining the

material response. Using the equations (52) and (53), k_E and k_δ are:

$$k_E^{ji} = \frac{\gamma_{ji}}{\gamma^{io}} = \sqrt{\frac{\beta_{ji}}{\beta_{i0}} \frac{\Delta s_{ji}(\theta_c^{ji} - \theta_e^{ji})}{\Delta s_{i0}(\theta_c^{i0} - \theta_e^{i0})}}; \tag{54}$$

$$k_\delta^{ji} = \frac{\delta_{ji}}{\delta_{i0}} = \sqrt{\frac{\beta_{ji}}{\beta^{i0}} \frac{\Delta s_{s0}(\theta_c^{i0} - \theta_e^{i0})}{\Delta s_{ji}(\theta_c^{ji} - \theta_e^{ji})}}. \tag{55}$$

which are temperature independent.

4.4 Effect of finite K_{ij}.

It is necessary to stress that the PT criteria (44) are valid in the limit $K_{ij} \to \infty$. For finite K_{ij}, wrong PT criteria (39) hold and one need to analyze how this affects the position of thermodynamically equilibrium phases P_j and P_i and transformation path between them. Let us consider typical examples.

1. In the first one, we analyze the case when none of PT criteria (38), 39) and (44) is met. **show me such example.**

2. The second example is for more critical but rare situation when instability conditions for $P_0 \to P_i$ (38) and correct criteria for $P_j \to P_i$ PT (44) are not fulfilled, but the wrong (unconstrained) $P_j \to P_i$ PT criterion (39) is meet with significant deviation from the stability region. Thus, accepting positive $A_1 + 3\Delta G_1^\theta = 1000$, $A_1 - 3\Delta G_1^\theta = -400$; $A_2 + 3\Delta G_2^\theta = 230$, $A_2 - 3\Delta G_2^\theta = 2570$ (all energies are in J/m^3), we are making barrierless PTs $P_0 \to P_i$ impossible. Also accepting positive $A_{21}(\theta) - 3G_{21}^\theta = 150$, we do not meet the correct instability criterion for $P_j \to P_i$ PT. Finally, setting negative $\bar{A} + A_1(\theta) + 3\Delta G_1^\theta = -250$ we fulfill wrong $P_j \to P_i$ PT condition. In this case while phase P_j loses its stability, but it does not transform to the phase P_i. Instead, the local free energy minimum slightly shifts from $\eta_1 = 1$; $\eta_2 = 0$ to a close point $\eta_1 = 0.989$; $\eta_2 = 0.019$ (Fig. 5). The energy barrier between phases P_j and P_i does not allow further transformation toward P_i. When the correct PT criterion (44) $P_j \to P_i$ PT is satisfied, this energy barrier disappears and $P_j \to P_i$ PT will occur. Consequently, inaccuracy for finite K_{ij} insignificant even for such an extreme case.

3. Let us consider the opposite case, when correct PT criterion (44) for $P_j \to P_i$ PT is fulfilled, but wrong criterion (39) for $P_j \to P_i$ PT is not met. If criteria (38) for $P_0 \leftrightarrow P_i$ PTs are not fulfilled then these equations result in $\bar{A} < 0$ **(show)**. It is easy to show **show detail** that in this case the wrong $P_j \to P_i$ PT condition (39) should be also fulfilled. Thus, there is
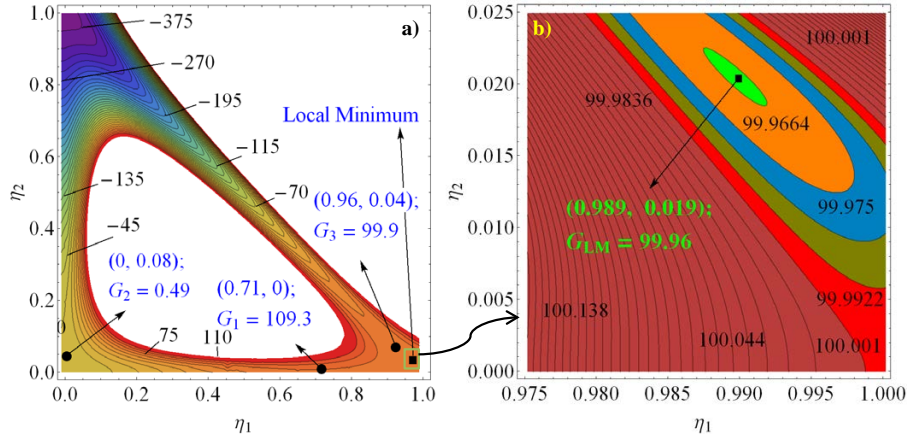
Figure 1: Free energy landscape for example 2. G_i are the points of the local minimaxes.

no contradiction between correct and wrong $\mathsf{P}_j \to \mathsf{P}_i$ PT conditions: if the correct $\mathsf{P}_j \to \mathsf{P}_i$ PT criterion (44) is fulfilled, this PT will occur.

4.5 Comparison with existing potentials

4.5.A Single order parameter

For a single order parameter, the formal theory for the Landau potential of practically arbitrary degree based on group theoretical (symmetry) consideration is presented in [31, 32]. Analysis, including phase diagrams, was performed in terms of coefficients of Landau potentials. Such potentials exhibit multiple minima corresponding to multiple phases. When PTs between two phases are considered, especially polymorphic PTs in solids, thermodynamic potentials $\psi^\theta = \bar{a}\eta^2 + \bar{b}\eta^3 + \bar{c}\eta^4$ or $\psi^\theta = \bar{a}\eta^2 + \bar{b}\eta^4 + \bar{c}\eta^6$ were used without any general requirements, except that they should have two minima separated by an energy barrier [3–7, 31–37]. In most works $\bar{a} = \bar{a}_0(\theta - \theta_c)$ was assumed, which defines θ_c as the critical temperature when thermodynamic instability occurs, i.e., energy minimum at $\eta = 0$ disappears. Thermodynamically equilibrium value of the order parameter at the second minimum was dependent on the temperature, similar to the continuous second-order PTs. This means that PT does not have the end point and structural changes occur continuously. Order parameter is assumed to be small, like in Landau theory of the second-order PTs [38], which justifies Taylor expansion for the energy with limited number of terms. There are no specifically introduced interpolation functions

and variation of material properties, like in Eq.(3). Variation of all material properties follows directly from the chosen potential and in many cases they correspond to experiments [33] for the second order and close to the second order PTs.

For the description of the first-order PTs, which have end point and further structural changes do not occur after completing of PT (like melting and martensitic phase transformations in steels and shape memory alloys), the order parameter should not change after PT. Then the order parameters for bulk phases can be taken as 0 and 1. It cannot be considered as a small number and higher degrees of η make similar contributions as the lower degrees. This condition as well as thermodynamic consistency, which are very similar to conditions 1 and 2, were formulated and satisfied in [30, 39, 40] for melting. Since interaction between communities working on melting and martensitic PTs, twinning, and dislocations was very limited, such conditions were not used and satisfied in these fields for a long time, even now (see, e.g., [3–7] for martensitic PT, including twinning, and [41–44] for dislocations). Also, for twinning and dislocations these conditions are related to transformation strain and Burgers vector rather than to change in free energy, which is zero. Conditions 1-4 were formulated and satisfied in [1, 2, 8, 45, 46] for martensitic PTs and twinning, and in [8, 47] for dislocations, where they were motivated by correctness of the stress-strain curve, which also lead to conditions for the free energy and interpolating functions for all parameters. For melting thermodynamic stability condition was imposed (i.e., the pre-factor of a double-well barrier must be positive) [16, 17, 30, 39, 40] instead of condition 4. We believe that the main reason for this is the following. To increase interface width by a factor of k without changing interface energy and velocity (see Eq.(64)), one has to increase β by a factor of k and reduce A and L by a factor of k. Thus, the magnitude of the double well barrier significantly reduces (k may be as large as 1000) and correct description of thermodynamic instability and barrierless nucleation is impossible. For such a small double well barrier, thermodynamic instability may occur quite close to the thermodynamic equilibrium temperature, which will lead to artificial barrierless nucleation of a (meta)stable phase within unstable one. To avoid this, one has to insure satisfaction of stability condition for any temperature, i.e., instability criterion should not be affected by the thermodynamic driving force. This was done by choosing interpolating

function

$$\bar{\varphi}(\eta) = \eta^3(10 - 15\eta + 6\eta^2), \tag{56}$$

which satisfies all desired conditions ($\bar{\varphi}(0) = \bar{\varphi}'(0) = \bar{\varphi}'(1) = 0$, and $\bar{\varphi}(1) = 1$, and $\bar{\varphi}(1 - \eta) = 1 - \bar{\varphi}(\eta)$). It also satisfies conditions $\bar{\varphi}''(0) = \bar{\varphi}''(1) = 0$, which eliminates participation of any material parameter or function multiplied by $\bar{\varphi}(\eta)$ from the instability condition. Thus, for the energy

$$\bar{\psi}^\theta(\theta, \eta) = \psi_0^\theta(\theta) + \Delta\psi^\theta(\theta)\bar{\varphi}(\eta) + A\eta^2(1 - \eta)^2 \tag{57}$$

accepted in [16, 17, 30] instability conditions (12) and (13) reduce to

$$\mathsf{P}_0 \to \mathsf{P}_1 : \quad \partial^2\bar{\psi}^\theta(\theta, 0)/\partial\eta^2 = 2A \le 0;$$

$$\mathsf{P}_1 \to \mathsf{P}_0 : \quad \partial^2\bar{\psi}^\theta(\theta, 1)/\partial\eta^2 = 2A \le 0. \tag{58}$$

Such instability conditions are contradictory because both phases simultaneously loose their stability. That is why interpolation function (57) is not suitable for our purposes. However, if stability conditions were imposed instead of instability [16, 17, 30], function (57) is very convenient because the system is stable for $A > 0$ independent of the driving force (temperature).

In contrast, the thermodynamic instability was included in consideration in [1, 2, 8], which resulted in PT criteria. This allows one to consider problems on the actual physical space scale where thermodynamic instability is important, e.g., for very fast heating much above the melting and even solid instability temperatures [48, 49], as well as for barrierless surface-induced melting, especially for nanoparticles [50, 51], and for melting within interface between two solids [23–25, 27, 28], which all may occur significantly below melting and melt instability temperatures. The interpolation function (18) that satisfies all conditions have been used for various applications for a long time [1, 2, 30, 39, 40, 45, 46].

Within even six-degree potential (2-4-6 potential), we obtained [8] that the interpolating function

$$\varphi_6(\eta) = 0.5a\eta^2 + (3 - a)\eta^4 + 0.5(-4 + a)\eta^6 \tag{59}$$

satisfies conditions 1-4. However, it does not satisfy condition $\varphi_6(1 - \eta) = 1 - \varphi_6(\eta)$. That means that it cannot be used not only in our multiphase system but also for a two-phase

system when both phases are equivalent. The same is true for the function (8) for $a \neq 3$. In particular, it cannot be used for twinning, while cases $a \neq 3$ were studied exploratory for twinning in [52].

Note that for larger-scale theories one can waive the requirement of differentiability of thermodynamic (and consequently, interpolation) functions. Thus, it was accepted in [19, 20]

$$\psi^\theta(\theta, \eta) = \psi_0^\theta(\theta) + \Delta\psi^\theta(\theta)\eta + A\eta(1 - \eta), \tag{60}$$

where $0 \leq \eta \leq 1$ was interpreted as the concentration of phase 1. Similar barrier term was used in the double obstacle potential [10] but with different smooth interpolating function for $\Delta\psi^\theta$.

4.5.B Multiple order parameter

Theories without a constraint. They are mostly devoted to the description of multivariant martensitic PTs [3–7]. They are based of the fourth or six degrees polynomials in terms of order parameters η_i that describe PTs austenite A - martensitic variants M_i and satisfy the required symmetry conditions. Since all martensitic variants are symmetry-related and have the same thermal (chemical) free energy, these theories represent particular case of the general theory for multiphase system. None of the above requirements to the free energy is imposed and met in [3–7], i.e., thermodynamically equilibrium order parameter for each M_i $\eta_i \neq 1$ and depends on temperature (and stresses), thermodynamic instability conditions are not considered, and PTs $M_j \leftrightarrow M_i$ occur along some temperature dependent path within $\eta_i - \eta_j$ plane. No specific interpolating function have been introduced, i.e., they directly follow from the chose polynomial. This is similar to the description of the second-order and close to the second order continuous PTs in [33] but was applied to the strongly first-order PTs. Also, matrixes L_{ij} and β_{ij} are reduced to the unit matrix multiplied by a scalar. Since theories [3–7] possess minima corresponding to A and all martensitic variants M_i, they reproduce evolution of complex multivariant microstructure. However, it could not quantitatively correspond to a chosen specific material because material properties were not properly interpolated between their values in the bulk phases and thermodynamically equilibrium order parameters were not constant but depended on temperature (and stress tensor). Conditions close to 1-4 and 1n-6n have been formulated and satisfied in [1, 2, 8], but without condition 5, i.e., still PTs

$M_j \leftrightarrow M_i$ were not properly described and parameters of $M_j - M_i$ interfaces could not be properly calibrated and controlled. Matrix form of β_{ij}, i.e., additional material parameters, have been introduced in [53, 54], which in particular allowed us to introduce and study the effect of the energy of $M_j \leftrightarrow M_i$ interface independent of the energy of A-M_i interfaces.

Theories with hyperspherical order parameters. In order to describe $M_j \leftrightarrow M_i$ PTs in the same way as $A \leftrightarrow M_i$ Pts, a thermodynamic potential in hyperspherical order parameters is developed [8], in which A is at the center of the sphere, and all martensitic variants M_i are located at the hypersphere. Belonging to the hypersphere represents a nonlinear constraint, which was substituted in [26] with the linear constraint of the type $\sum \eta_i = 1$, which, however, does not include A. Still, PT criteria could not be obtained in a consistent way for more than three phases. For three phases the constraint is linear for both models [8] and [26] and in polar order parameters this theory is completely consistent with the two-phase theory and produces proper PT criteria. It was generalized for three arbitrary phases in [23–25]. Thus, theory in [23–25] is currently the only theory that satisfies exactly all requirements for three-phase material. Due to polar order parameters, it does not need to satisfy condition 5, that is why it can utilize interpolation function Eq.(8) with arbitrary $0 \leq a \leq 6$ for each pair of phases. However, we fail to generalize it for more than three phases. In this case, constraint should be used which does not allow to derive consistent PT criteria from thermodynamic instability conditions.

Theories with a constraint. Traditional multiphase theories [9–18] include constraint $\sum \eta_i = 0$ applied to all phases. It can be explicitly excluded for two phases only, in contrast the case with three phases for polar order parameters [8, 23–25]. This means that the problem to derive consistent PT criteria from thermodynamic instability conditions exists even for three phases. The first theory [9] does not make special efforts that the PT between any two phases occurs along the fixed line in the order parameter space. That is why the third phase may appear at the interface between two phases. This does not allow one to use analytical solution to calibrate material parameters in terms of interface energy, mobility, as well as width (if kept physical rather than computational). Also, potential in [9] does not include products of more than two order parameters, which however, is easy to correct. If a computational interface width is much larger than the actual one, presence of the third phase contributes to the width-dependence

of the solution, which is desirably to avoid. That is why in [16, 17] equations are derived in a way enforcing that PTs always occur along the straight line connecting two phases. With the choice of interpolating function generalizing (56) for multiple phases, all bulk phases are stable or metastable independent of the driving force or temperature. It is not clear how to generalize theory for more than three phases. Also, kinetic coefficients must be scalar and equal for all PTs. While in [9] constraint was imposed by excluding one of the order parameters, in [11, 16, 17] method of Lagrangian multipliers was used. When a Lagrangian multiplier was used, the Ginzburg-Landau equations for n phases take the form

$$\dot{\eta}_i = L(X_i - \Lambda) = L\left(-\frac{\delta\psi}{\delta\eta_i} - \Lambda\right). \tag{61}$$

Adding all equations and using constrain, we obtain $\Lambda = \sum X_j/n$ and substituting it in Eq.(61) it transforms to

$$\dot{\eta}_i = L(X_i - \sum X_j/n) = L_{ij}X_j; \quad L_{ij} = L_{ji} = \delta_{ij} - U_{ij}/n, \tag{62}$$

where δ_{ij} is the Kronecker delta and all components of the matrix U_{ij} are equal to one. With such a matrix L_{ij}, constraint $\sum \dot{\eta}_i = 0$ is fulfilled automatically. It was, however, stated in [18] that the use of Lagrangian multiplier method gives results different from direct exclusion of one of the order parameter, even for two phases. Let us analyze this statement for two order parameters obeying constraint $\eta_1 + \eta_2 = 1$. The dissipation rate is $D_1 = X_1\dot{\eta}_1 + X_2\dot{\eta}_2 = (X_1 - X_2)\dot{\eta}_1$ when η_2 is directly excluded and $D_2 = X_1\dot{\eta}_1 + X_2\dot{\eta}_2 - \Lambda(\dot{\eta}_1 + \dot{\eta}_2) = (X_1 - \Lambda)\dot{\eta}_1 + (X_2 - \Lambda)\dot{\eta}_2$ when Lagrangian multiplier is used. Then, using the same kinetic coefficient, the linear relationship between thermodynamic force and rates for both cases are:

$$\dot{\eta}_1 = L(X_1 - X_2); \quad \dot{\eta}_1 = L(X_1 - \Lambda) = L(X_1 - X_2)/2, \tag{63}$$

which lead to conclusion that "the Lagrange multiplier approach does not reduce to the single phase formulation," see [18]. The main reason for this discrepancy is that the thermodynamic forces and rates in different representations should not be connected by the same kinetic coefficient. If, e.g., in Eq.(63)$_2$ we would chose the kinetic coefficient L_2 different from L in Eq.(63)$_1$, we would not have problem, and from equivalence of both kinetic equations we can conclude that $L = L_2/2$. This is getting more clear if we substitute expression for $\Lambda = (X_1+X_2)/2$ in D_2: $D_2 = 0.5(X_1-X_2)\dot{\eta}_1 - 0.5(X_1-X_2)\dot{\eta}_2$. It is evident that using constraint we

obtain $D_1 = D_2$. However, thermodynamic force $0.5(X_1 - X_2)$ cannot be connected to $\dot{\eta}_1$ by the same kinetic coefficient as $(X_1 - X_2)$. For multiple order parameters, even if force obtained by direct exclusion of one of the order parameters can be connected to the conjugate rate using a single scalar, one may need matrix connection between all forces and rates for the Lagrangian multiplier method to obtain equivalent result. Primary expressions for the thermodynamic forces and rate should be taken from the expression for the dissipation rate expressed in terms of independent rates, i.e., after direct exclusion of one of the order parameters.

It is claimed in [18] that the relationships $\dot{\eta}_i = L_{ij}X_j$ that ensure that PTs between each pair of phases without the presence of the third phase for arbitrary n can be achieved by a special choice of the matrix L_{ij}, which is quite sophisticated nonlinear function of the order parameters. This matrix is ill-defined in the vicinity of each single phase and is substituted with other matrixes. Here, we achieved similar goal by using a simple penalizing term, which allows us to control (if it is observed in experiment [27, 28]) and, if necessary, avoid appearance of the third phase.

4.6 Parameter Identification

Let us consider such material parameters and temperature ranges, for which interfaces between any two phases do not contain the third one. For different pairs of phases, temperature intervals may be different. Then for any of these pairs, one can apply system of equation for two phases (1)-(2) and (23). The analytical solution for a propagating with velocity c interface is [10]:

$$\eta = 0.5(\tanh[3(x - ct)/\delta] + 1); \quad \delta = \sqrt{18\beta/A}; \quad c = L\delta\Delta G^\theta(\theta); \quad \gamma = \sqrt{\beta A/18} = \beta/\delta, \text{ (64)}$$

where δ and γ are the width and energy of the nonequilibrium interface. Note that in [10] the equilibrium interface energy was given; here we derived an expression for the energy of the propagating interface, which requires definition of the Gibbsian dividing surface [55]. This can be done using methods developed in [56, 57]. However, due to complete equivalence of both phases in our theory, dividing surface is located at the point corresponding to $\eta = 0.5$. Then we found that the energy (and width) of the nonequilibrium interface are independent of

$\Delta G^\theta(\theta)$ and coincide with those for the equilibrium interface. This is in contrast to solutions for other interpolating functions [56–59]. All material parameters for each bulk phase can be determined based on thermodynamic, experimental, and atomistic data as it was done, e.g., in [1, 2, 8] for NiAl. Eqs.(64) allow calibration for each pair of phases the three interface-related parameters $A_i(\theta)$, β, and L when width, energy, and mobility of interfaces between each pair of phases are known.

The obtained system of equations has been solved with the help of the finite element code COMSOL for various problems. Here we solved exactly the same problem on the evolution of two-variant nanostructure in a NiAl alloy during martensitic PT including tip bending and splitting in martensitic variants as in [26]. Note that the theory in [26] for two variants satisfies all required conditions exactly but cannot be generalized for more than two variants. Some material parameters (like $\boldsymbol{E}$, $\boldsymbol{\varepsilon}_{ti}$, $\Delta G^\theta(\theta)$, θ_e, Δs) here have been chosen the same as in [26]; other ($A_{ij}(\theta)$, $\beta_{ij}(\theta)$, L_{ij}, θ_c) are chosen to get the temperature dependence of the energy, width, and mobility of all interfaces, and temperature for the loss of stability of P like in [26]. Note that all thermodynamic properties of martensitic variants M_1 and M_2 are the same; they differ by the transformation strain only.

Since temperature dependence of the interface width and energy are unknown, we assume $\theta_e = 0.5(\theta_c^0 + \theta_c^0)$ and consequently $B_* = 0$, which makes them temperature independent.

We have the following definition of parameters: $\Delta G_1^\theta = \Delta G_2^\theta = -\Delta s(\theta - \theta_e)$, where $\Delta s = s_i - s_0$ is the jump in entropy between phases M_i and A, and θ_e is the thermodynamic equilibrium temperature for phases T_i and A. We express the coefficients $A_1(\theta) = A_2(\theta) = A_*(\theta - \theta_*)$. Here parameter A_* and the characteristic temperature θ_* are related to the critical temperatures for barrierless $A \to P_i$ (θ_c^{0i}) and $P_i \to A$ (θ_c^{i0}) PTs by the equations $\theta_c^{01} := (A_*\theta_* - 3\Delta s\theta_e)/(A_* - 3\Delta s)$ and $\theta_c^{10} := (A_*\theta_* + 3\Delta s\theta_e)/(A_* + 3\Delta s)$, which follow from the thermodynamic instability conditions.

In the current simulation we used the following values: $\Delta s = -1.467 MPaK^{-1}$, $\theta_e = 215$ K, $\theta_c^{01} = -183$ K, $\theta_c^{10} = -331.65$ K, $\theta_* = -245.75$ K, $A_* = 28 MPaK^{-1}$ $\beta_{01} = \beta_{02} = 5.31 \times 10^{-10}$ N, $\beta_{12} = 5.64 \times 10^{-10}$ N, $L_{0i} = L_{12} = 2596.5 m^2/Ns$. These parameters correspond to a twin interface energy $E_{P_1P_2} = 0.543 J/m^2$ and width $\Delta_{P_1P_2} = 0.645 nm$. In addition, $K_{ijk} = 0$ and two values of $K_{12} = 1.5 \times 10^{12}$ and $K_{12} = 7.25 \times 10^{13} J/m^3$ have been used.

4.7 Results and Discussion

The SM interface is considered to be coherent with vanishing shear modulus for melt, $\mu_0 = 0$. For simplicity, all transformation strains are pure volumetric. Properties of melt, δ phase (S_1) and β phase (S_2) of energetic material HMX ($C_4H_8N_8O_8$) will be used (when available), for which IM was considered. It is assumed that all $a = 3$; all phases have $K = 15 GPa$, solid phases posses $\mu = 7 GPa$ and $\beta^{s0}(\vartheta) = const$; $L_\Upsilon = 2\,L_\vartheta = 2596.5 m^2/(Ns)$, $\Delta s_{10} = -793.79 kJ/m^3 K$, $\Delta s_{20} = -935.45 kJ/m^3 K$, melting temperatures $\theta_e^{10} = 550K$ and $\theta_e^{20} = 532.14K$; $\theta_e^{21} = 432K$, $\varepsilon_{0t}^{10} = -0.067$, $\varepsilon_{0t}^{20} = -0.147$ (i.e., $\varepsilon_{0t}^{21} = -0.08$); $\tilde{A}_c^{21} = 0$, $A_c^{ij} = -3\Delta s_{ij}$ (such a choice corresponds to the temperature-independent interface energies and widths $E^{21} = 1 J/m^2$ and $\delta^{21} = 1 nm$. A $24 \times 8\,nm^2$ rectangular sample with a roller boundary condition on the left side and fixed lower left point is modeled. Two initial conditions are considered: (a) equilibrium SS interface and (b) equilibrium S_1M and MS_2 interfaces with quite a broad melt region between two solids.

Stress-free IM — First, we will consider the case without mechanics. In Fig. [2], minimum value of ($\eta_1 + eta_2$) is plotted for $\theta = \theta_e^{21} = 432K$ (i.e., 100 K below θ_e^m), and different k_E, k_δ, K_{12} and initial conditions. Note that the effect of temperature is similar to the effect of k_δ. For small k_δ, there is only a single stationary solution independent of the initial conditions, corresponding to barrierless premelting and melting within SS interface. Degree of melting (disordering) continuously increases with increasing k_E and temperature. There is not any hysteresis while increasing/decreasing temperature. While for $k_E \geq 2.7$ increase in k_δ promotes IM (reduces Υ_{min}), for $k_E \leq 2.5$, dependence $\Upsilon_{min}(k_\delta)$ is surprisingly *nonmonotonous*, with disappearance of IM above critical k_δ. In contrast, for larger k_δ, different initial conditions result in *two different stationary nanostructures*. For SS initial condition, premelting does not start up to some quite large critical value k_E (e.g., $k_E = 3.39$ for $k_\delta = 1$), above which jump-like (i.e., first-order) premelting or complete melting occurs. For SMS initial conditions, almost complete melt is stabilized at $k_E = 1.94$ (for $k_\delta = 1$), i.e., even below the critical value $k_E = 2$ for pre-melting at θ_e^m. While for $k_E \geq 2.7$, increase in k_δ promotes IM (similar to SS initial state), for $k_E \leq 2.5$, dependence $\Upsilon_{min}(k_\delta)$ is very nontrivial, with IM *gap*

(i.e., lack of IM) in some range of k_δ, which increases with decreasing k_E. Outside the IM gap, with increasing/decreasing temperature, discontinuous first-order phase transformations to and from melt occur at different temperatures, exhibiting significant hysteresis. Increase in k_δ increases value of k_E for melting from SS state and reduces critical k_E for keeping melt from SMS state. Thus, at $k_\delta = 1.2$, almost complete melt can be kept within SS interface for $k_E = 1.58$. Increasing k_δ increases the width of the hysteresis loop and also shifts melting to higher temperatures.
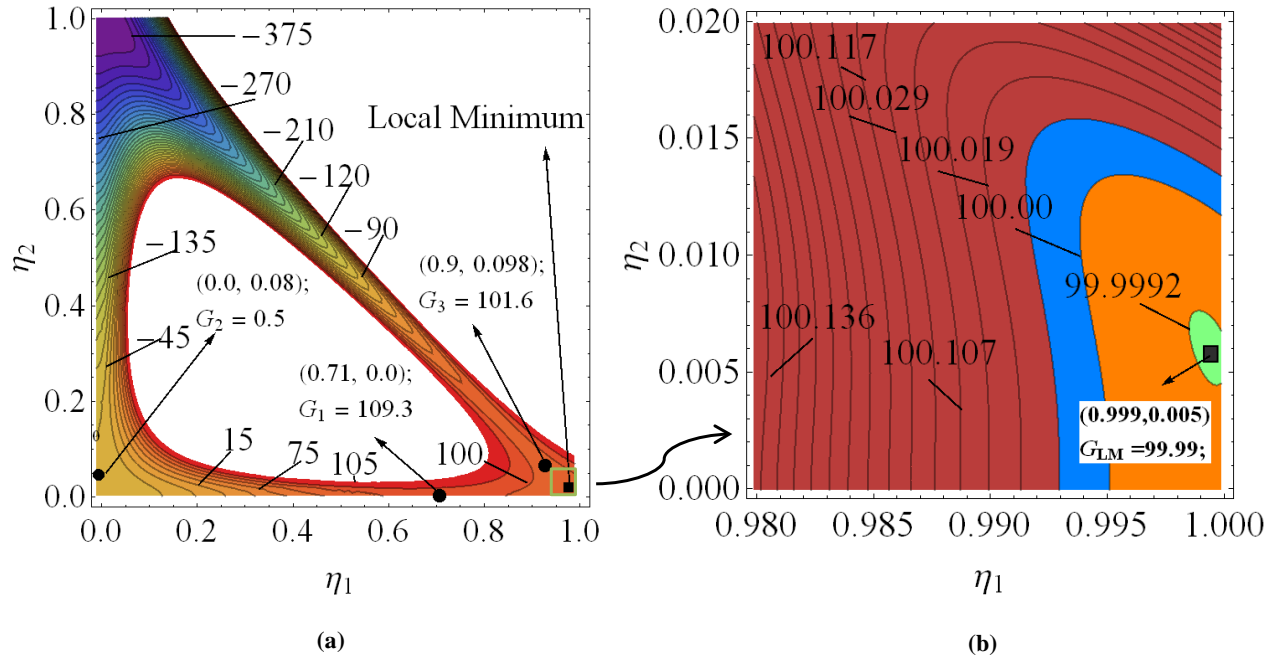

Figure 2: (a) Minimum stationary value of $\eta_1 + \eta_2$. for both SMS and SS initial interface for different K_{12} values,; (b) distribution of η_1; (c) distribution of η_2 for some specific case of K_{12} values.

Presence of two stable stationary nanostructures indicates that there is one more unstable nanostructure between them, which represents a critical nucleus. If the difference between energy of the critical nucleus and SS (or SMS) interfaces is smaller than $(40 - 80)k_B\theta$, where k_B is the Boltzmann constant, then melting (or solidification) within SS interface will occur due to thermal fluctuations. Finding critical nucleus and kinetic studies will be performed elsewhere.
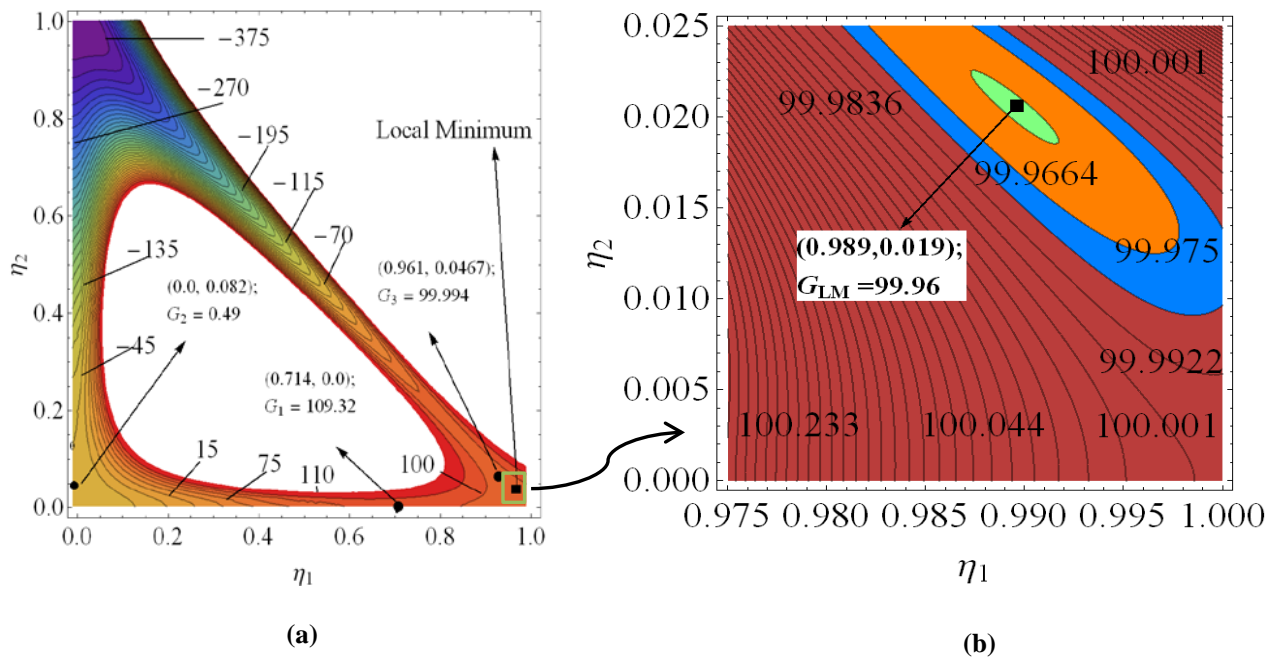
Figure 3: (a,d,g)Total energy distribution; (b,e,h)local Energy distribution; (c,f,i) gradient energy distribution for both SMS and SS initial interface for different K_{12} values,
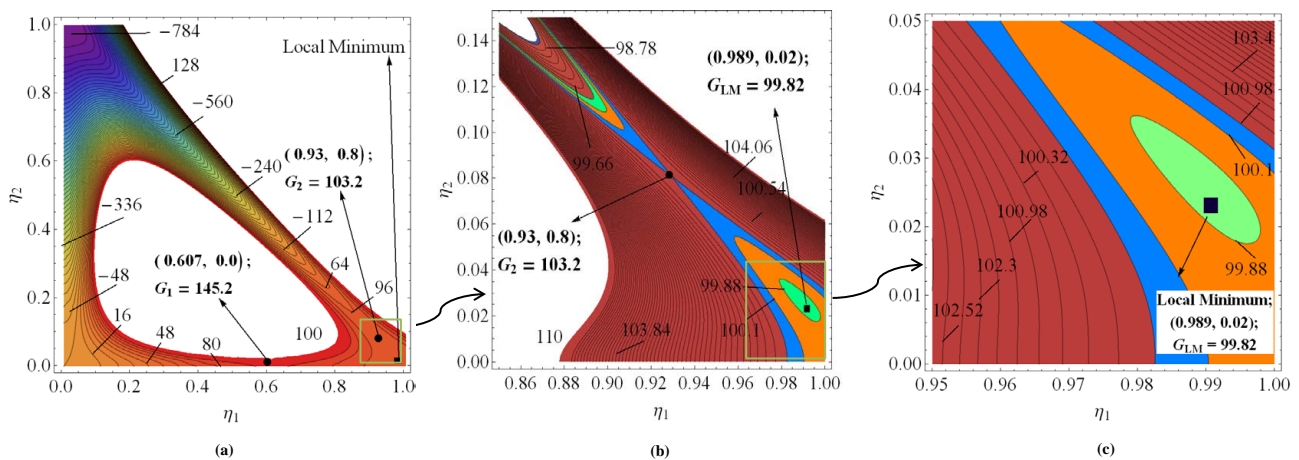

Figure 4: Distribution of minimum of $(\eta_1 + \eta_2)$ vs k_δ for both SMS and SS initial interface for different K_{12} values.
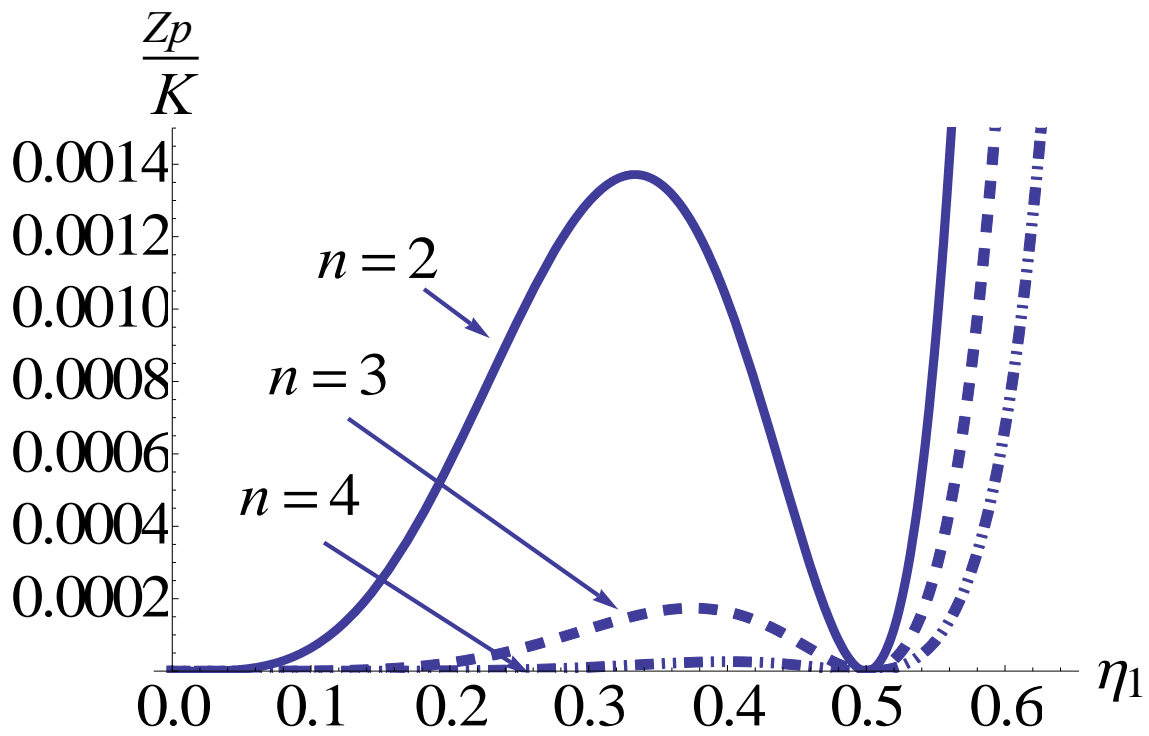
Figure 5: Distribution of minimum of $(\eta_1 + \eta_2)$ vs k_E for both SMS and SS initial interface for different K_{12} values.

interface energy, interface width, and velocity were studied for $k_E = 4$ and $k_\delta = 1$ (Fig. **??**). The width of IM, δ^*, is defined as the difference between locations of two SM interfaces where $\Upsilon = 0.5$. Note that almost complete melt of the width exceeding $1nm$ exists at $0.65\theta_e^{21}$, i.e., $240K$ below the melting temperature. For any a_0, increasing temperature promotes melting, i.e., reduces Υ_{min} and the SMS interface energy, and increases δ^* and interface velocity (for $\theta/\theta_e^{21} > 1$). When temperature approaches the melting temperature of β phase, $\Upsilon_{min} \simeq 0$ and the width of IM is determined by $\partial E^*/\partial \delta^* = 0$, which results in $\delta^* = \sqrt{0.5\beta^{21}a_0/(G^0 - G^s)}$; δ^* diverges when $\theta \to \theta_e^m$ and $G^0 \to G^s$. The energy of IM tends to the energy of two SM interfaces, which is $0.5E^{21}$ for our case. Velocity of SMS interface is below the velocity of SS interface (even for $L_\Upsilon = 500L_\vartheta$), is zero at θ_e^{21}, and varies linearly with deviation from θ_e^{21} with some acceleration close to the melting temperature. At very small a_0, interface velocity tends to zero. Since for very small a_0, SS interface width within melt tends to zero, a very large number of finite elements is required to obtain mesh-independent results.

4.8 Results and Discussion

To summarize, as a solution of a critical outstanding problem, we developed PFA for multiphase materials, which with high and controllable accuracy satisfy all the desired conditions for arbitrary n phases. Instead of explicit constraints, we included in the simplest potential the terms that penalize the deviation of the trajectory in the order parameter space from the straight lines connecting each of the two phases. It describes each of the PTs with the single order parameter, which allows us to use an analytical solution to calibrate each interface energy, width, and mobility. It reproduces the desired PT criteria via instability conditions; introduces interface stresses, and allows us to control the presence of the third phase at the interface between the two other phases. Finite-element simulations exhibit very good correspondence with results based on the exact three-phase model in [26] (which, however, cannot be generalized for $n > 3$) and with nontrivial experimental nanostructure. The developed approach unifies and integrates approaches developed in different communities (in particular, solidification and martensitic PTs) and is applicable to various PTs between multiple solid and liquid phases and grain evolution, and can be extended for diffusive, electric, and magnetic PTs.

References

[1] Levitas VI, Preston DL. Phys Rev B 2002a;66:134206.

[2] Levitas VI, Preston DL. Phys Rev B 2002b;66:134207.

[3] Artemev A, Jin Y, Khachaturyan AG. Acta Mat 2001;49:1165-1177.

[4] Jin YM, Artemev A, Khachaturyan AG. Acta Mat 2001;49:2309-2320.

[5] Chen LQ. Annu Rev Mater Res 2002;32:113-140.

[6] Wang Y, Khachaturyan AG. Mat Sci Engg A 2006;438:55-63.

[7] Mamivand M, Zaeem MA, El Kadiri H, Comp Mat Sci 2013;77:304.

[8] Levitas VI, Preston DL, Lee D-W. Phys Rev B 2003;68:134201.

[9] Steinbach I, Pezzolla F, Nestler B, Seelberg M, Prieler R, Schmitz GJ, Rezende JLL. Physica D 1996;94:13547.

[10] Steinbach I. Model Simul Mater Sci Eng 2009;17:073001.

[11] Garcke H, Nestler B, Stoth B, Physica D 1998;115:87.

[12] Kobayashi R, Warren J. Physica A 2005:356:127132.

[13] Toth GI, Morris JR, Granasy L. Phys Rev Lett 2011;106:045701.

[14] Toth GI, Pusztai T, Tegze G, Granasy L. Phys Rev Lett 2011;107: 175702.

[15] Mishin Y, Boettinger WJ, Warren JA, McFadden GB. Acta Mater 2009;57:3771.

[16] Folch R, Plapp M. Phys Rev E 2003;68:010602.

[17] Folch R, Plapp M. Phys Rev E 2005;72:011602.

[18] Bollada PC, Jimack PK, Mullis AM. Physica D 2012;241:816.

[19] Levitas VI, Idesman AV, Preston DL. Phys Rev Let 2004;93:105701.

[20] Idesman AV, Levitas VI, Preston DL, and Cho J-Y. J Mech Phys Solids 2005;53:495-523. Karma-Rappel,Karma-Rappel-1

[21] Karma A, Rappel W-J, Phys Rev E 1996;53:R3017.

118

[22] Karma A, Rappel W-J, Phys Rev E 1998;57:4323.

[23] Levitas VI, Momeni K. Acta Mater 2014;65:125.

[24] Momeni K, Levitas VI. Phys Rev B 2014;89:184102.

[25] Momeni K, Levitas VI, Warren JA. Nano Letters 2015;15:2298-2303.

[26] Levitas VI, Roy AM, Preston DL. Phys Rev B 2013;88:054113.

[27] Levitas VI, Henson BF, Smilowitz LB, Asay BW. Phys Rev Lett 2004;92:235702.

[28] Levitas VI, Ren Z, Zeng Y, Zhang Z, Han G. Phys Rev B 2012;85:220104.

[29] Levitas VI, Roy AM. Phys Rev B 2015 (in press).

[30] Wang S-L, Sekerka RF, Wheeler AA, Murray BT, Coriell SR, Rraun RJ, McFadden GB. Physica D 1993;69:189200.

[31] Toledano P, Dmitriev V. Reconstructive Phase Transitions. World Scientific, New Jersey;1996.

[32] Toledano JC, Toledano P. The Landau Theory of Phase Transitions. World Scientific;1988.

[33] Salje EKH. Phase Transitions in Ferroelastic and Co-Elastic Crystals. Cambridge University Press, New York;1990.

[34] Umantsev A. Field Theoretic Method in Phase Transformations. Lecture Notes in Physics Vol. 840, Springer, New York;2012.

[35] Ichitsubo T, Tanaka K, Koiwa M, Yamazaki Yo. Phys Rev B 2000;62:5435-5441.

[36] Lindgård PA, Mouritsen OG. Phys Rev Let 1986;57:2458-2461.

[37] Boulbitch AA, Toledano P. Phy Rev Let 1998;81:838.

[38] Landau LD, Lifshitz EM. Statistical Physics. Vol. 5 (3rd ed.). Butterworth-Heinemann, Oxford;1980.

[39] Umantsev A. J Chemical Physics 1992;96:605-617.

[40] Umantsev A, Roitburd AL. Soviet Physics Solid State 1988;30:651.

[41] Wang YU, Jin YM, Cuitino AM, Khachaturyan AG. Acta Mater 2001;49:1847-1857.

[42] Hu SY, Chen LQ. Acta Mater 2001;49:463-472.

[43] Wang YU, Li J. Acta Mater 2010;58:1212-1235.

[44] Hunter A, Beyerlein IJ, Germann TC, Koslowski M. Phys Rev B 2011;84:144108.

[45] Levitas VI, Levin VA, Zingerman KM, Freiman EI. Phys Rev Lett 2009;103:025702.

[46] Levitas VI. Int J Plast 2013;49:85.

[47] Levitas VI, Javanbakht M. Phys Rev B 2012;86:140101.

[48] Hwang YS, Levitas VI. App Phys Let 2013;103:263107.

[49] Hwang YS, Levitas VI. App Phys Let 2014;104:263106.

[50] Levitas VI, Samani K. Phys Rev B 2011;84:140103.

[51] Levitas VI, Samani K. Phys Rev B 2014;89:075427.

[52] Clayton JD, Knap J. Physica D 2011;240:841.

[53] Levitas VI, Javanbakht M. Phys Rev Let 2010;105:165701.

[54] Levitas VI, Javanbakht M. Int J Mat Res 2011;102:652.

[55] Gibbs JW, The Collected Works of J. Willard Gibbs, Yale University Press;1948.

[56] Levitas VI. J Mech Phys Solids 2014;70:154.

[57] Levitas VI. Phys Rev B 2014;89:094107.

[58] Levitas VI. Phys Rev B 2013;87:054112.

[59] Levitas VI. Acta Mater 2013;61:4305.

[60] Boullay Ph, Schryvers D, Kohn RV, Ball JM. Journal de Physique IV 2001;11:23.

[61] COMSOL, Inc., website: www.comsol.com.

[62] Finel A, Le Bouar Y, Gaubert A, Salman U. C R Phys 2010;11:245.

[63] L.D. Landau, *Zh. Eksp. Teor. Fiziki* **7**, 19, (1937); **7**, 627, (1937). Transl. in *Collected Papers of L.D. Landau*, ed. D. Ter Haar (Pergamon Press, Oxford, 1965) p. 193, 216.

[64] Kundin J, Emmerich H, Zimmer J. Philos Mag 2011;91:97-121.

CHAPTER 5. DETAILED PHASE FIELD THEORY FOR MULTIPHASE PHASE FIELD THEORY FOR TEMPERATURE- AND STRESS-INDUCED PHASE TRANSFORMATION: GENERAL MODEL, STABILITY CONDITIONS AND SIMULATIONS

Abstract

Thermodynamic Ginzburg-Landau potential for temperature and stress-induced phase transformations (PTs) between n phases is developed. It describes each of the PTs with a single order parameter without explicit constraint equation, which allows one to use analytical solution to calibrate each interface energy, width, and mobility; reproduces the desired PT criteria via instability conditions; introduces interface stresses, and allows to control presence of the third phase at the interface between two other phases. A finite-element approach is developed and utilized to solve problem on microstructure formation for multivariant martensitic PTs. Results are in quantitative agreement with experiment. The developed approach is applicable to various PTs between multiple, solid, and liquid phases and grain evolution and can be extended for diffusive, electric, and magnetic PTs.

5.1 Introduction

One of the unresolved problems of the phase field approach (PFA) to PTs is non-contradictory description of PTs between arbitrary number of phases. One of the directions is related to the description of PTs between the austenite (A) and any of the n martensitic variants P_i and between martensitic variants [1]. It is described with the help of n independent order parameters η_i, each for every $\mathsf{A}\leftrightarrow\mathsf{P}_i$. This approach was significantly elaborated in [2, 3] by imposing additional physical requirements to the Landau potential. In particular, the desired PT conditions for $\mathsf{A}\leftrightarrow\mathsf{P}_i$ and $\mathsf{P}_j\leftrightarrow\mathsf{P}_i$ PTs follow from the material instability conditions. Also, the thermodynamically equilibrium transformation strain tensor is stress- and temperature-independent, like in crystallographic theories. This theory was generalized for large strain and lattice rotations [4, 9] and interface stresses consistent with sharp interface approach have been introduced for A-P_i interfaces [6, 8, 9]. However, description of P_i-P_j is still not satisfactory. The $\mathsf{A}\leftrightarrow\mathsf{P}_i$ PT is described by a single order parameter η_i and analytic solutions for η_i for nonequilibrium

interfaces [3, 6, 8, 9] allows one to calibrate interface energy, width, and mobility, as well as the temperature-dependence of the stress-strain curve. At the same time, at a P_i-P_j interface η_i and η_j vary independently along some transformation path in the $\eta_i - \eta_j$ plane; the interface energy, width, and mobility have an unrealistic dependence on temperature, stresses, and a number of material parameters, which cannot be determined analytically. Consequently, one cannot prescribe the desired P_i-P_j interface parameters. Due to the same reasons, expression for P_i-P_j interface stresses cannot be strictly derived [6, 9]. Approach to multivariant martensitic PTs with total strain-related order parameters is also quite popular [10, 11]. In addition to the critique of this approach in [2], it also cannot describe P_i-P_j interface with the single order parameter and is not applicable to multiphase system for which strain is not a relevant parameter.

5.2 Drawback to other multiphase approaches

Other multiphase approaches are based on introducing $n + 1$ order parameters η_i obeying constraint $\sum \eta_i = 1$, similar to concentrations [12–15]. The idea is that each of PTs should be described by a single order parameter; then interface parameters can be calibrated with the help of the analytical solution. However, in general, undesired third phase often appears at the interface between two phases. PT criteria in terms of instability conditions are not considered. In [14] special conditions are imposed for three-phase system that guarantee that the third phase can never appear at the interface between two phases. This casused some artifacts in the theory (e.g., necessity of equal kinetic coefficients for all PTs). All homogeneous phases are stable independent of the driving force (temperature). Also, in many cases, third phase is observed in experiments [16] and conditions when it is present or not are found within more advanced model [17]. Some drawbacks of imposing constraint with the help of Lagrangian multipliers are presented in [15]. They are claimed to be overcome in [15]. Again, instability conditions were not discussed in [15]. All our attempts for a theory with constraint to find polynomials (up to tenth degree) to reproduce proper PT criteria (which are known from two-phase treatment) from the thermodynamic instability conditions have been unsuccessful. This led us to conclusion that utilizing constraint $\sum \eta_i = 1$ prevents noncontradictory formulation of the PFA. Also, these approaches do not include mechanics.

5.2.A Drawback in Folch Paper

In [14],a free-energy functional was introduced in the following form

$$F = \int_v f \, dv, \tag{1}$$

where, the volume integral of free- energy density defined as:

$$f(\vec{p}, \vec{\nabla}\vec{p}, c, T) = K f_{grad}(\vec{\nabla}\vec{p}) + H f_p(\vec{p}) + X f_c(\vec{p}, c, T), \tag{2}$$

Where, p_i is the volume fraction. H and X are constants with dimensions of energy per unit volume. f_{grad} is the gradient energy, f_p contains the analoge of the double well potential of single-phase solidification, f_c couples the phase fields to concentration. Additionally, a fifth order antisymmetric polynomial function is introduced as (g_i). For two phases(i, j) polynomial reduced to using the constraint $(p_i + p_j = 1)$as following:

$$g_i = p_i^3(10 - 15p_i + 6p_i^2), \tag{3}$$

The function f_p, called as triple-well (f_{TW}) potential as a sum of equal double-well potentials $f_{DW}(p)$ for all the phases as following:

$$f_p = f_{TW} = \sum_i f_{DW}(p_i), \tag{4}$$

For two phases, f_p can be written explicitly :

$$f_p = (1 - p_i)^2 p_i^2 + (1 - p_j)^2 p_j, \tag{5}$$

If we ignore the contribution from concentration part, we can write f_c as following:

$$f_c = X(g_i B_i + g_j B_j), \tag{6}$$

Further, ignoring gradient term, only considering bulk phase field enegy (F) :

$$F = H f_p + X(g_i B_i + g_j B_j) \tag{7}$$

Normalize the above equation with respect to X :

$$f = \frac{F}{X} = \frac{H}{X} f_p + (g_i B_i + g_j B_j) \tag{8}$$

Now, we evaluate $\partial^2 f / \partial p_i^2$ to find the transformation conditions:

$$\frac{\partial^2 f}{\partial p_i^2} = 4 \frac{H}{X} (1 - 6p_i + 6p_i^2) + 15 (B_i - B_j) p_i (1 - 3p_i + 2p_i^2). \tag{9}$$

$$p_j \rightarrow p_i : \qquad \frac{\partial^2 f(\theta, p_i = 0)}{\partial p_i^2} \leq 0 \rightarrow 4 \frac{H}{X} \leq 0; \tag{10}$$

$$p_i \rightarrow p_j : \qquad \frac{\partial^2 f(\theta, p_i = 1)}{\partial p_i^2} \leq 0 \rightarrow 4 \frac{H}{X} \leq 0; \tag{11}$$

Eq.(10) to Eq.(11) are phase transformation conditions for $p_i \leftrightarrow p_j$ respectively. Here we see the instability conditions are independent on driving force, which is not good. Now , we substitute $p_j = 1 - p_i$ in Eq.(8) and use following parameter value:$H, X = 1$. Now we consider following three cases:

CASE I:

Here, we consider $B_i = 10$ and $B_j = 11$, i.e phase i should loose its stability. We plot Eq.(8) with respect p_i in Fig.(1a). But local barrier at point (B) corresponding $p_i = 0.112$ in Fig.(1b) is noticed. So we have small barrier in $p_i \rightarrow p_j$ transformation , even though criteria of loss of stability of p_i is already satisfied, which is not a desired condition.

CASE II:

Here, we consider $B_i = 15$ and $B_j = 10$, i.e phase j should loose its stability. We plot Eq.(8) with respect p_i in Fig.(2a). Here also we noticed a local barrier at point (B) corresponding $p_i = 0.972$ in Fig. (2b). So we also have undesired barrier in $p_j \rightarrow p_i$ transformation, even though criteria of loss of stability of p_j is already satisfied.

CASE III:

To confirm the drawback, we consider $B_i = 10$ and $B_j = 100$, i.e phase i should definitely loose its stability.But surprisingly we again noticed a local barrier at point (B) corresponding $p_i = 0.0015$ in Fig.(3b). So we have small barrier in $p_j \rightarrow p_i$ transformation which is not satisfactory.
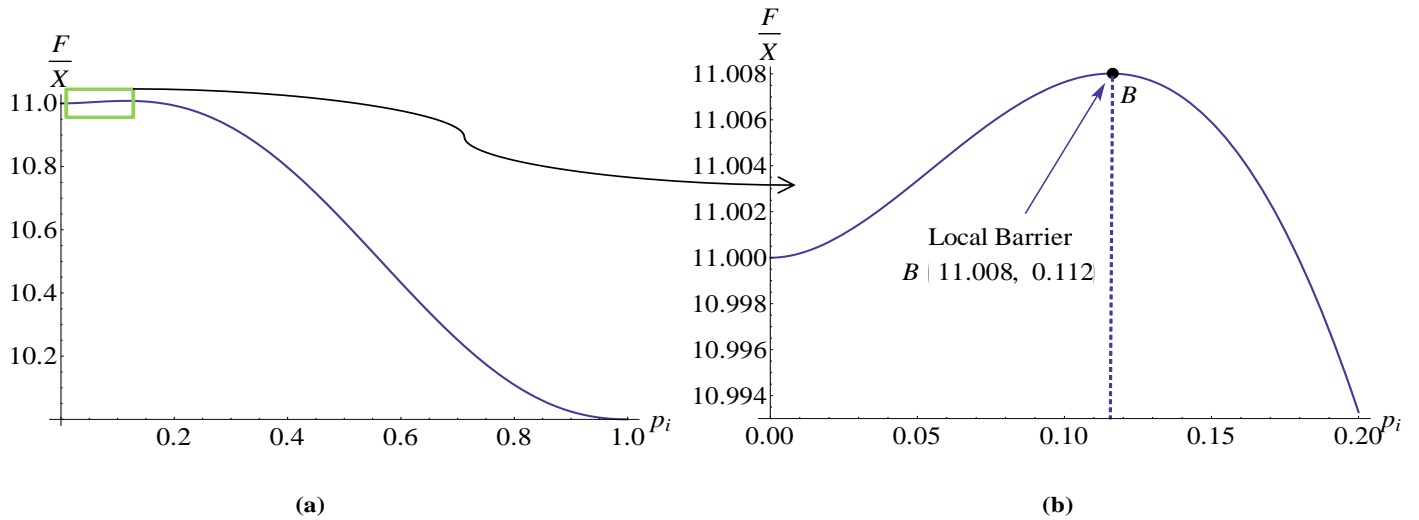
Figure 1: Plot of function F/X vs p_i for $B_i = 10$, $B_j = 11$; (b) is the zoomed plot of F/X vicinity of local barrier (B).
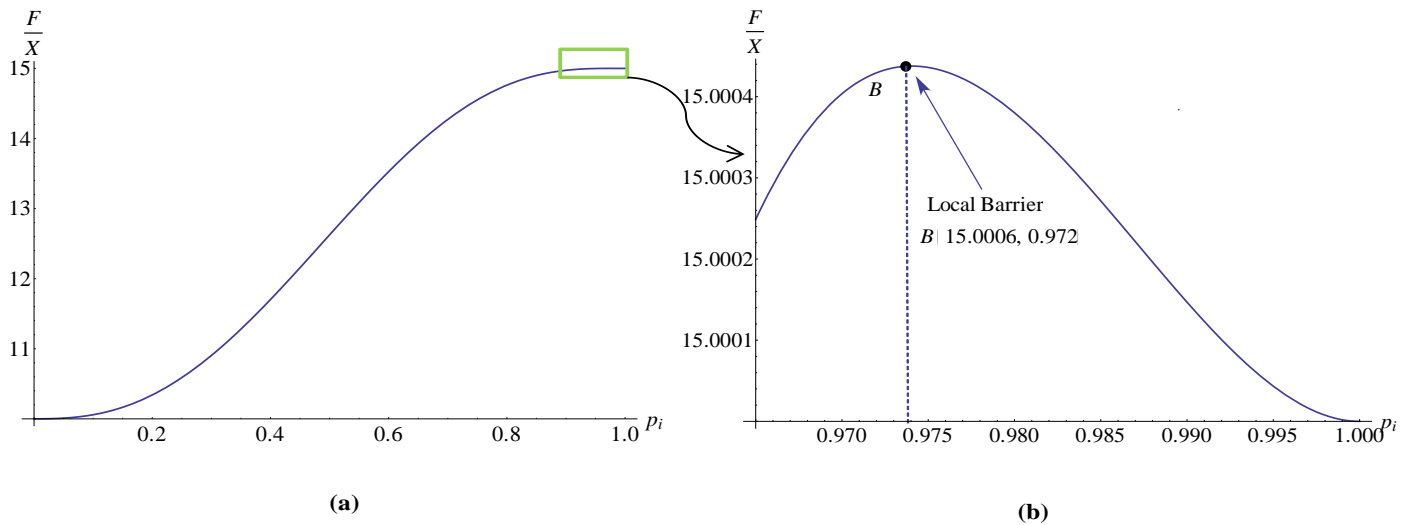

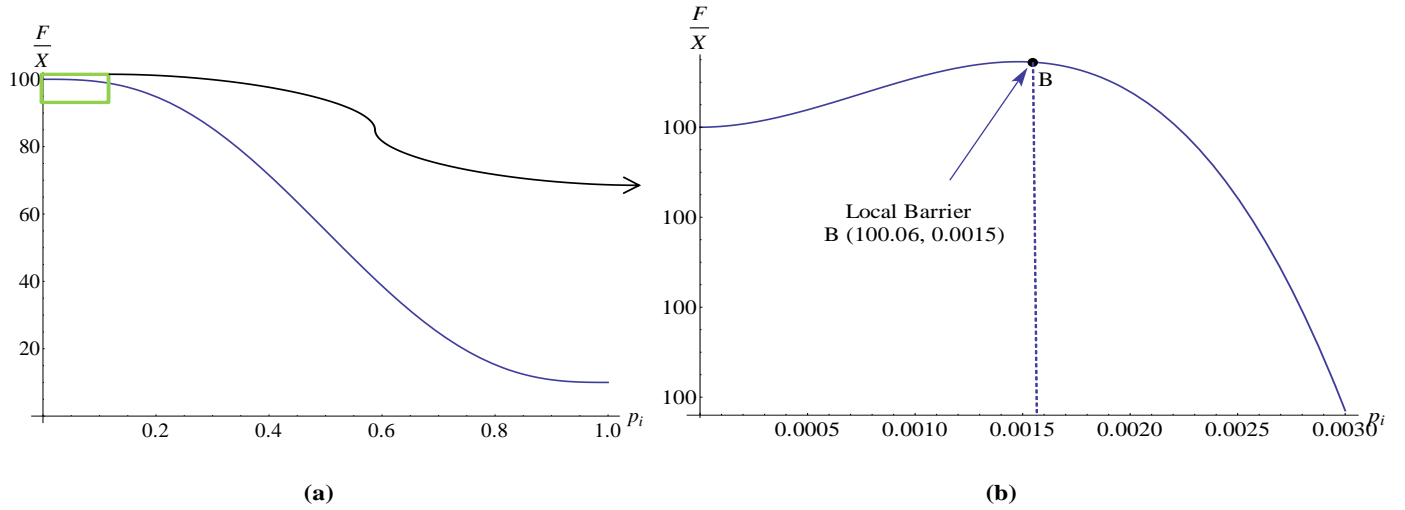Figure 2: Plot of function F/X vs p_i for $B_i = 15$, $B_j = 10$; (b) is the zoomed plot of F/X vicinity of local barrier (B).

Figure 3: Plot of function F/X vs p_i for $B_i = 10$, $B_j = 100$; (b) is the zoomed plot of F/X vicinity of local barrier (B).

5.2.B Drawback in Hyperspherical Order Parameter

PFA in [3] are based on a potential in hyperspherical order parameters, in which one of the phases, O, at the center of the sphere, and all other, P_i, are located at the sphere. Thus, A (or it can be melt) is located at the center and M_i (or solid phases) are located at the sphere. Correct PT criteria have been derived. However, it was done in terms of cartesian order parameters η_i, with assumption that they then are true for any order parameters. This is unfortunately not the case for the hyperspherical order parameters, because the Jacobian of transformation from one set of order parameters to another is singular at some points and the first derivatives of energy tends to infinity at these points. Due to this, nonlinear constraint for the hyperspherical order parameters was substituted with the linear constraint of the type $\sum \eta_i = 1$, which, however, does not include A or melt [7, 17]. For three phases, when strain is explicitly eliminated, the theory in [7, 17] is completely consistent with two-phase theory and produces proper PT criteria. However, for more than three phases, due to constraint, these theories cannot produce correct PT criteria. Thus, noncontradictory PFA for more than three phases or two martensitic variants is currently lacking.

5.2.C Advantage of current theory

In this theory, a critical outstanding problem on developing of phase field approach for temperature- and stress-induced phase transformations between arbitrary n phases is solved. This theory has the following advantages:

1. It describes each of the phase transformations with a single order parameter, in contrast to all known theories for multivariant martensitic transformations and multiple twinning. This allows one to use analytical solution to calibrate each interface energy, width, and mobility.

2. In contrast to all theories for multiphase materials, this is achieved without explicit constraint equation. As it was demonstrated, imposing explicit constraint produces significant problems in the theory, in particular, does not allow introducing the desired transformation criteria via thermodynamic instability conditions.

3. The problem is resolved by combining our previous theory for multivariant martensitic transformations with the terms that penalize deviation of the trajectory in the order parameter space from the desired straight lines connecting each two phases. It is demonstrated that this approximately (but with controlled accuracy) reproduces all the desired constraints.

4. The developed theory satisfies all the desired conditions. It introduces the desired phase transformation criteria via thermodynamic instability conditions.

5. It allows for the first time for a multiphase system to include consistent expression for interface stresses for each interface.

6. It allows controlling presence of the third phase at the interface between two other phases.

The developed approach is applicable to various phase transformations between multiple solid and liquid phases and grain evolution and can be extended for diffusive, electric, and magnetic transformations. Till recently, several communities, which develop and apply phase field modeling to various fields, practically did not interact and had quite different priorities, requirements, and degree of strictness. Main point was to reproduce the desired microstructure with the simplest models containing minimum physics. Currently, such interaction started (in particular, at the International Symposium on Phase-field Method, State College, PA, 2014) and there are definite needs for much more physically advanced and unified theories, which are imbedded in the framework of nonlinear continuum mechanics and satisfy extra physical requirements. Current work gives a general framework for the phase field approach for various communities.

5.3 Specification of the Gibbs energy for two order parameters

5.3.A Two stress-free martensitic phases

First, let us present the expression for Gibbs potential for two different martensitic phases, neglecting stress:

$$G(\theta, \eta_1, \eta_2) = f_1(\theta, \eta_1) + f_2(\theta, \eta_2) + \bar{A}\eta_1^2\eta_2^2 + Z_p(\eta_1, \eta_2) + \frac{1}{2}\sum \beta_i |\nabla \eta_i|^2. \qquad (12)$$

where, f_1 and f_2 corresponds to the parts of thermal (chemical) energy related to thermal driving force for phase transformation and the double-well barrier between $P_1 \leftrightarrow A$ and $P_2 \leftrightarrow A$, respectively. In more general form:

$$f_i(\theta, \eta_i) = A_i(\theta)\, q(\eta_i) + \Delta G_i^\theta\, g(\eta_i). \qquad (13)$$

where,

$$q(\eta_i) = \eta_i^2 (1 - \eta_i)^2; \qquad (14)$$

$$g(\eta_i) = \eta_i^2 (3 - 2\eta_i). \qquad (15)$$

Here, the terms $\Delta G_i^\theta \eta_i^2(3 - 2\eta_i)$ and $A(\theta)\eta_i^2(1 - \eta_i)^2$ are parts of the thermal (chemical) energy, related to the thermal driving force for phase transformation and double-well barrier,

respectively. ΔG_i^θ is the difference between the thermal parts of the Gibbs energies of P_i and A. A_i are the double-well energy coefficients between P_i and A. Again, here fourth degree term $\bar{A}\,\eta_1^2\,\eta_2^2$ is the barrier between two phases. The sixth degree polynomial $Z_p(\eta_1,\,\eta_2)$ is the penalty term which gives the correct transformation condition between $P_1 \leftrightarrow P_2$ along the diagonal. The function $Z_p(\eta_1,\,\eta_2)$ have the following form:

$$Z_p(\eta_1,\,\eta_2) = K\,\eta_1^2\,\eta_2^2\,(1 - \eta_1 - \eta_2)^2\,. \tag{16}$$

The goal of this function is to penalize deviations of the order parameters from three desirable transformation lines in $\eta_1\eta_2$ plane: $\eta_1 = 0$; $\eta_2 = 0$, and diagonal $\eta_1 + \eta_2 = 1$. In this way, we do not need to impose explicit constraint $\eta_1 + \eta_2 = 1$ and have chance to satisfy all desired conditions, including instability conditions. Here instead of using $\eta_1^2\,\eta_2^2$; $(n = 2)$, we can use higher order polynomial like $\eta_1^3\,\eta_2^3$; $(n = 3)$, $\eta_1^4\,\eta_2^4$; $(n = 4)$. For higher degree, it reduces the barrier inside the $P_1 \leftrightarrow P_2$ path, which facilitate to from triple junction, higher order polynomial less restrained to existence of all phases. In Figure 1. we consider $\eta_1 = \eta_2$, and we notice as polynomial degree increases the barrier reduces. Its easy to check that if we substitute $\eta_2 = 1 - \eta_1$ in Eq.(16), it vanishes along the diagonal, which is the proper transformation path between $P_1 \leftrightarrow P_2$. Additionally, this term does not contribute the stability conditions for different phases. Here, thermal part of energy developed such a way that it only affects along the transformation path between $P_1 \leftrightarrow A$ and $P_2 \leftrightarrow A$ and interfaces between two phases remain unaffected. This require $g_i(\eta_i) = \eta_i^2\,(3 - 2\,\eta_i)$ to be anti-symmetric with respect to the saddle point of double well barrier $A(\theta)\,\eta_i^2\,(1 - \eta_i)^2$ at $\eta_i = \frac{1}{2}$,

$$g_i\,(1 - \eta_i) = 1 - g_i\,(\eta_i)\,. \tag{17}$$

This requirement is necessary to avoid undesirable thin-interface correction in the matching to the free-boundary problems and to adjust surface tension independently of the phase diagram and is hence important. We formulate G such a way, it gives the free energies of P_1 and P_2 at $\eta_1 = 1$ and $\eta_2 = 0$, respectively, the followings :

$$f_1(1,0) = \Delta G_1^\theta\,, \qquad f_2(1,0) = 0\,, \qquad Z_p(1,0) = 0\,. \tag{18}$$

Similarly, at $\eta_1 = 0$ and $\eta_2 = 1$, it produce the following :

$$f_1(0,1) = 0\,, \qquad f_2(0,1) = \Delta G_2^\theta\,, \qquad Z_p(0,1) = 0\,. \tag{19}$$
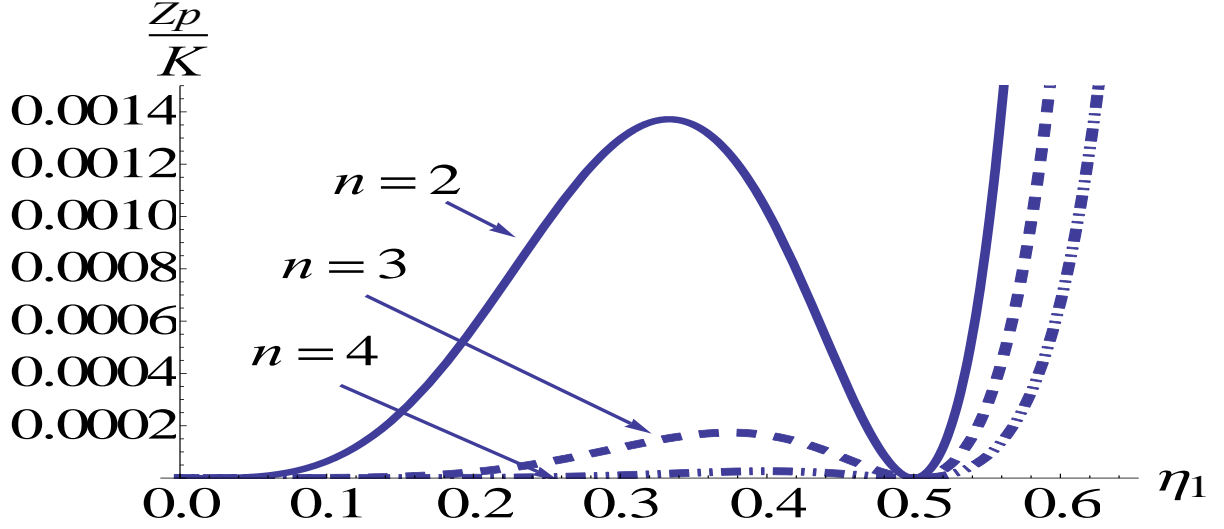
Figure 4: Plot of function $Z_p(\eta_1)/K$ vs η considering different degree of polynomial,i.e $\eta_1^n \eta_1^n f(\eta_1); n = 2, 3, 4$, where $f(\eta_1) = (1 - 2\eta_1)^2$

To satisfy proper stability conditions, we require the derivative of $G(\eta_1, \eta_2)$ to vanish at the origin, $\mathsf{A}(\eta_1 = 0, \eta_2 = 0)$, $\mathsf{P}_1(\eta_1 = 1, \eta_2 = 0)$ and at $\mathsf{P}_2(\eta_1 = 0, \eta_2 = 1)$. Our potential satisfies all the required conditions, which are the followings :

$$\frac{\partial G(0,0)}{\partial \eta_{1,2}} = 0 \;\Rightarrow\; \frac{\partial f_{1,2}(0,0)}{\partial \eta_{1,2}} = \frac{\partial Z_p(0,0)}{\partial \eta_{1,2}} = 0; \tag{20}$$

$$\frac{\partial G(1,0)}{\partial \eta_{1,2}} = 0 \;\Rightarrow\; \frac{\partial f_{1,2}(1,0)}{\partial \eta_{1,2}} = \frac{\partial Z_p(1,0)}{\partial \eta_{1,2}} = 0; \tag{21}$$

$$\frac{\partial G(0,1)}{\partial \eta_{1,2}} = 0 \;\Rightarrow\; \frac{\partial f_{1,2}(0,1)}{\partial \eta_{1,2}} = \frac{\partial Z_p(0,1)}{\partial \eta_{1,2}} = 0. \tag{22}$$

5.3.B Thermodynamic equilibrium and its stability conditions for two phases without using constraint

Explicit expressions for the first derivatives of the thermodynamic potential, which will be used in GL equations, for homogeneous states are:

$$\frac{\partial G(\eta_1, \eta_2)}{\partial \eta_1} = 6\,\Delta G_1^\theta\,\eta_1\,(1-\eta_1) + 2A_1\left(\eta_1 - 3\eta_1^2 + 2\eta_1^3\right) + 2\,\bar{A}\,\eta_1\,\eta_2^2$$
$$-2K\,\eta_1\,\eta_2\,(1-\eta_1-\eta_2)\left[\eta_1\eta2 - \eta_2(1-\eta_1-\eta_2)\right]; \tag{23}$$

$$\frac{\partial G(\eta_1, \eta_2)}{\partial \eta_2} = 6\,\Delta G_2^\theta\,\eta_2\,(1-\eta_2) + 2A_2\left(\eta_2 - 3\eta_2^2 + 2\eta_2^3\right) + 2\,\bar{A}\,\eta_1^2\,\eta_2$$
$$-2K\,\eta_1\,\eta_2\,(1-\eta_1-\eta_2)\left[\eta_1\eta2 - \eta_1(1-\eta_1-\eta_2)\right]. \tag{24}$$

It is clear that both derivatives are zero at any temperature (θ) for each of the phases for $\mathsf{A}\,(\eta_1 = 0,\, \eta_2 = 0)$, $\mathsf{P}_1\,(\eta_1 = 1,\, \eta_2 = 0)$ and at $\mathsf{P}_2\,(\eta_1 = 0,\, \eta_2 = 1)$. To determine the stability conditions, we require second and mixed derivatives, which are given in the explicit form :

$$\frac{\partial^2 G(\eta_1, \eta_2)}{\partial \eta_1^2} = 6\,\Delta G_1^\theta\,(1-2\eta_1) + 2A_1\left(\eta_1 - 6\eta_1 + 6\eta_1^2\right) + 2\,\bar{A}\,\eta_2^2 + 2K\,\eta_1^2\,\eta_2^2$$
$$-8K\eta_1\,\eta_2^2\,(1-\eta_1-\eta_2) + 2K\eta_2^2\,(1-\eta_1-\eta_2)^2; \tag{25}$$

$$\frac{\partial^2 G(\eta_1, \eta_2)}{\partial \eta_2^2} = 6\,\Delta G_2^\theta\,(1-2\eta_2) + 2A_2\left(\eta_2 - 6\eta_2 + 6\eta_2^2\right) + 2\,\bar{A}\,\eta_1^2 + 2K\,\eta_1^2\,\eta_2^2$$
$$-8K\eta_1^2\,\eta_2\,(1-\eta_1-\eta_2) + 2K\eta_1^2\,(1-\eta_1-\eta_2)^2; \tag{26}$$

$$\frac{\partial^2 G(\eta_1, \eta_2)}{\partial \eta_1 \partial \eta_2} = 2K\eta_1^2\eta_2^2 - 4K\,\eta_1^2\,\eta_2\,(1-\eta_1-\eta_2) - 4K\,\eta_1\,\eta_2^2\,(1-\eta_1-\eta_2)$$
$$+4K\,\eta_1\,\eta_2\,(1-\eta_1-\eta_2)^2 + 4\,\bar{A}\,\eta_1\,\eta_2. \tag{27}$$

In this case, the conditions for the loss of stability of each phase or phase transformation criteria, simplify to:

$$A \to P_1: \qquad \frac{\partial^2 G(\theta, \eta_1 = 0, \eta_2 = 0)}{\partial \eta_1^2} \le 0 \;\to\; A_1(\theta) + 3\Delta G_1^\theta \le 0; \tag{28}$$

$$P_1 \to A: \qquad \frac{\partial^2 G(\theta, \eta_1 = 1, \eta_2 = 0)}{\partial \eta_1^2} \le 0 \;\to\; A_1(\theta) - 3\Delta G_1^\theta \le 0; \tag{29}$$

$$A \to P_2: \qquad \frac{\partial^2 G(\theta, \eta_1 = 0, \eta_2 = 0)}{\partial \eta_2^2} \le 0 \;\to\; A_2(\theta) + 3\Delta G_2^\theta \le 0; \tag{30}$$

$$P_2 \to A: \qquad \frac{\partial^2 G(\theta, \eta_1 = 0, \eta_2 = 1)}{\partial \eta_2^2} \le 0 \;\to\; A_2(\theta) - 3\Delta G_2^\theta \le 0; \tag{31}$$

$$P_1 \rightarrow P_2 : \quad \frac{\partial^2 G(\theta, \eta_1 = 1, \eta_2 = 0)}{\partial \eta_2^2} \leq 0 \rightarrow \bar{A} + A_2(\theta) + 3\Delta G_2^\theta \leq 0; \tag{32}$$

$$P_2 \rightarrow P_1 : \quad \frac{\partial^2 G(\theta, \eta_1 = 0, \eta_2 = 1)}{\partial \eta_1^2} \leq 0 \rightarrow \bar{A} + A_1(\theta) + 3\Delta G_1^\theta \leq 0; \tag{33}$$

Eq.(28) to Eq.(31) are desired phase transformation conditions for $A \leftrightarrow P_1$ and $A \leftrightarrow P_2$ respectively. Other two conditions, Eq.(32) and Eq.(33) for $P_1 \leftrightarrow P_2$ PT just follow from the potential and are non-contradictory. But they does not represent proper PT criteria. At this moment, we designate them as 'Unconstrained PT condition' (UC) as following:

$$[P_1 \rightarrow P_2]^{UC} \Rightarrow \bar{A} + A_1(\theta) + 3\Delta G_1^\theta \leq 0; \tag{34}$$

$$[P_2 \rightarrow P_1]^{UC} \Rightarrow \bar{A} + A_2(\theta) + 3\Delta G_2^\theta \leq 0. \tag{35}$$

5.3.C Thermodynamic equilibrium and its stability conditions for two phases using constraint

If we assume that the $P_1 \leftrightarrow P_2$ PT occurs along the straight path between the points $P_1(\eta_1 = 1, \eta_2 = 0)$ and $P_2(\eta_1 = 0, \eta_2 = 1)$, i.e along the constrain $\eta_2 = 1 - \eta_1$, we can get desired criterion for $P_1 \leftrightarrow P_2$ PT. We substitute $\eta_2 = 1 - \eta_1$ into Eq.(12) to get Gibbs potential as function of single order parameter η_1 as follows :

$$\begin{aligned} G(\theta, \eta_1) = \; & A_1(\theta) \left(\eta_1^2 - 2\eta_1^3 + \eta_1^4 \right) + \Delta G_1^\theta \left(3\eta_1^2 - 2\eta_1^3 \right) + \bar{A} \eta_1^2 (1 - \eta_1)^2 \\ & + A_2(\theta) \left[(1 - \eta_1)^2 - 2(1 - \eta_1)^3 + (1 - \eta_1)^4 \right] \\ & + \Delta G_2^\theta \left[3(1 - \eta_1)^2 - 2(1 - \eta_1)^3 \right]. \end{aligned} \tag{36}$$

Eq.(36) can be written in the following compact form:

$$G(\theta, \eta_1) = A_{12}(\theta) \, q(\eta_1) + \Delta G_2^\theta + \Delta G_{12}^\theta g(\eta_1). \tag{37}$$

where

$$A_{12}(\theta) = A_1(\theta) + A_2(\theta) + \bar{A}; \tag{38}$$

$$\Delta G_{12}^\theta = \Delta G_1^\theta - \Delta G_2^\theta. \tag{39}$$

Explicit form of first and second derivatives:

$$\frac{\partial\, G(\theta,\eta_1)}{\partial\, \eta_1} = \eta_1\,(1-\eta_1)\,\big[\,A_{12}(\theta)\,(1-2\eta_1)+3\,\Delta\,G_{12}^{\theta}\,\big]\,; \tag{40}$$

$$\frac{\partial^2\, G(\theta,\eta_1)}{\partial\, \eta_1^2} = 2(A_{12}+3\,\Delta\,G_{12}^{\theta}-6A_{12}\eta_1-6\,\Delta\,G_{12}^{\theta}\eta_1+6A_{12}\eta_1^2). \tag{41}$$

In this case, the conditions for the loss of stability of all phases–i.e., phase transformation of criteria, simplify to:

$$P_1 \to P_2: \qquad \frac{\partial^2\, G(\theta,\vartheta_1=1)}{\partial\vartheta_1^2} \le 0 \;\to\; A_{12}(\theta)-3G_{12}^{\theta} \;\le 0$$
$$\to\; A_1(\theta)+A_2(\theta)+\bar{A}-3\Delta G_1^{\theta}+3\Delta G_2^{\theta} \;\le 0; \tag{42}$$

$$P_2 \to P_1: \qquad \frac{\partial^2\, G(\theta,\vartheta_1=0)}{\partial\vartheta_1^2} \le 0 \;\to\; A_{12}(\theta)+3G_{12}^{\theta} \;\le 0$$
$$\to\; A_1(\theta)+A_2(\theta)+\bar{A}-3\Delta G_2^{\theta}+3\Delta G_1^{\theta} \;\le 0; \tag{43}$$

Eq.(42) to Eq.(43) are desired phase transformation conditions for $P_1 \leftrightarrow P_2$ respectively. We designate them as 'constrained PT condition':

$$P_1 \to P_2 \;\Rightarrow\; A_{12}(\theta)-3\Delta G_{12}^{\theta} \;\le 0; \tag{44}$$

$$P_2 \to P_1 \;\Rightarrow\; A_{12}(\theta)+3\Delta G_{12}^{\theta} \;\le 0. \tag{45}$$

Let $\Delta G_i^{\theta}=-\Delta s_i(\theta-\theta_e^i)$, where $\Delta s_i = s_i - s_0$ is the jump in entropy between phases P_i and A and θ_i is the thermodynamic equilibrium melting temperature of phases P_i and A. The linear temperature dependence of ΔG_{12}^{θ} implies neglecting the difference between specific heats of phases. Then by definition $\Delta G_{12}^{\theta}=\Delta G_1^{\theta}-\Delta G_2^{\theta}=-\Delta s_1(\theta-\theta_e^1)+\Delta s_2(\theta-\theta_e^2)=-\Delta s_{12}(\theta-\theta_e^{12})$, where $\Delta s_{12}=\Delta s_1-\Delta s_2$ and $\theta_e^{12}=(\Delta s_1\theta_e^1-\Delta s_2\theta_e^2)/\Delta s_{12}$.

We express coefficients $A_i(\theta)=A_*^i(\theta-\theta_*^i)$, where θ_*^i is some characteristic temperature which will expressed in terms of the critical temperature at which phase A_i loses its stability toward P_i. A similar coefficient between phases P_i is accepted in a more general form $A_{12}(\theta)=\bar{A}_{12}^*(\theta)+A_{12}^*(\theta-\theta_{12}^*)$ with the temperature θ_{12}^* related below to the critical temperature of the loss of stability of the phase P_1 towards P_2. This equation together with definition of $\bar{A}(\theta)$ (Eqs.(??)) defines temperature dependence of $\bar{A}(\theta)$. For phases P_i with different thermal

properties we can put $\bar{A}^*_{12}(\theta) = 0$ without loss of generality, like for A-P$_i$ PT. If critical temperature does not exist and instability can be caused by stresses only, e.g., for two martensitic variants, which possess the same thermal properties, one has to skip the term with θ^*_{12} and accept $A_{12}(\theta) = \bar{A}^*_{12}(\theta)$. Then, instability conditions Eqs.(28)-(29) transform to

$$A \to P_1: \quad 0 < (A^1_* - 3\Delta s_1)\theta \le A^1_*\theta^1_* - 3\Delta s_1\theta^1_e \ \to \ \theta \le \theta^{01}_c := \frac{A^1_*\theta^1_* - 3\Delta s_1\theta^1_e}{A^1_* - 3\Delta s_1}; \quad (46)$$

$$P_1 \to A: \quad 0 > (A^1_* + 3\Delta s_1)\theta \le A^1_*\theta^1_* + 3\Delta s_1\theta^1_e \ \to \ \theta \ge \theta^{10}_c := \frac{A^1_*\theta^1_* + 3\Delta s_1\theta^1_e}{A^1_* + 3\Delta s_1}, \quad (47)$$

where θ^{01}_c and θ^{10}_c are the critical temperatures for barrierless $A \to P_1$ and $P_1 \to A$ PTs. Inequalities $A^1_* - 3\Delta s_1 > 0$ and $A^1_* + 3\Delta s_1 < 0$ are accepted from the conditions that $A \to P_1$ PT occurs at cooling and $P_1 \to A$ PT occurs at heating. In a similar way we obtain

$$A \to P_2: \quad 0 < (A^2_* - 3\Delta s_2)\theta \le A^2_*\theta^2_* - 3\Delta s_2\theta^2_e \ \to \ \theta \le \theta^{02}_c := \frac{A^2_*\theta^2_* - 3\Delta s_2\theta^2_e}{A^2_* - 3\Delta s_2}; \quad (48)$$

$$P_2 \to A: \quad 0 > (A^2_* + 3\Delta s_2)\theta \le A^2_*\theta^2_* + 3\Delta s_2\theta^2_e \ \to \ \theta \ge \theta^{20}_c := \frac{A^2_*\theta^2_* + 3\Delta s_2\theta^2_e}{A^2_* + 3\Delta s_2}. \quad (49)$$

For phases P$_i$ with different thermal properties ($\bar{A}^c_{12}(\theta) = 0$), Eqs.(42)-(43) transform to

$$P_1 \to P_2: \quad 0 < (A^{12}_* - 3\Delta s_{12})\theta \le A^{12}_*\theta^{12}_* - 3\Delta s_{12}\theta^{12}_e \ \to \ \theta \le \theta^{12}_c := \frac{A^{12}_*\theta^{12}_* - 3\Delta s_{12}\theta^{12}_e}{A^{12}_* - 3\Delta s_{12}}; \quad (50)$$

$$P_2 \to P_1: \quad 0 > (A^{12}_* + 3\Delta s_{12})\theta \le A^{12}_*\theta^{12}_* + 3\Delta s_{12}\theta^{12}_e \ \to \ \theta \ge \theta^{12}_c := \frac{A^{12}_*\theta^{12}_* + 3\Delta s_{12}\theta^{12}_e}{A^{12}_* + 3\Delta s_{12}}, \quad (51)$$

where the accepted inequalities $A^{12}_* - 3\Delta s_{12} > 0$ and $A^{12}_* + 3\Delta s_{12} < 0$ assume that $P_1 \to P_2$ PT occurs at cooling and $P_2 \to P_1$ PT takes place at heating. If phases P_1 and P_2 have the same thermal properties, than instability cannot be caused by changing temperature. Note that each of the characteristic temperatures, θ^1_*, θ^2_*, and θ^{12}_*, can be determined from Eqs.(46), (48), and (50) in terms of each critical temperatures θ^{01}_c, θ^{02}_c, and θ^{12}_c.

5.3.D Interface energy for 2 phases

For isotropic interface energies for two phases one has following explicit form:

$$\nabla = \left(\frac{\beta_{10}}{2}|\nabla\eta_1|^2 + \frac{\beta_{20}}{2}|\nabla\eta_2|^2 + b\,\nabla\eta_1\,\nabla\eta_2\right). \quad (52)$$

where, β_{10}, β_{20}, β_{12} are the mobility coefficients of $A - P_1$, $A - P_2$ and $P_1 - P_2$ interfaces respectively. Now, from the constrain equation $\eta_2 = 1 - \eta_1$, we get:

$$\nabla \eta_2 = -\nabla \eta_1. \tag{53}$$

Substitute Eq.(53) into Eq.(52), gives:

$$\nabla = \frac{1}{2} (\beta_{10} + \beta_{20} - 2\,b) \, |\nabla \eta_1|^2 = \frac{1}{2} \beta_{12} \, |\nabla \eta_1|^2. \tag{54}$$

where, β_{12} is the effective mobility coefficient of $P_1 - P_2$ interface. Is to be noted $\beta_{12} \geq 0$. So constraint on b is following :

$$b \;\leq\; \frac{\beta_{10} + \beta_{20}}{2}. \tag{55}$$

5.3.E Kinetic equations

As in customary in irreversible thermodynamics, one has to assume a general, nonlinear kinetic equation $\dot{\eta}_i = f(X_j)$, connecting the i th flux with j th force-i.e., including cross effects. In the linear approximation $\dot{\eta}_i = L_{ij} \, f(X_j)$, where L_{ij} are positive definite kinetic coefficients, for which $L_{ij} = L_{ji}$ according to Onsager reciprocal relationship. The kinetic equation for P_1 and P_2 are :

$$\dot{\eta}_1 = L_{11} X_1 + L_{12} X_2; \tag{56}$$

$$\dot{\eta}_2 = L_{12} X_1 + L_{22} X_2; \tag{57}$$

from Onsager reciprocal relationship, $L_{12} = L_{12}$. Now, from the constrain equation $\eta_2 = 1 - \eta_1$, we get:

$$\dot{\eta}_2 = -\dot{\eta}_1. \tag{58}$$

Substitute Eq.(58) into Eq.(57), we get:

$$X_2 = -\frac{\dot{\eta}_1 + L_{12} X_1}{L_{22}}; \tag{59}$$

Substitute Eq.(59) into Eq.(56), we get :

$$\dot{\eta_1} = \left(\frac{L_{11} L_{22} - L_{12}^2}{L_{22} + L_{12}} \right) X_1; \tag{60}$$

For $P_1 \leftrightarrow P_2$ PT, we can write kinetic equation in the following form:

$$\dot{\eta_1} = l_{12} X_1; \tag{61}$$

Where,

$$l_{12} = \left(\frac{L_{11} L_{22} - L_{12}^2}{L_{22} + L_{12}} \right); \tag{62}$$

5.3.F Numerical Analysis of stability condition

As we have mentioned earlier, we received different PT criterion for $P_1 \leftrightarrow P_2$ for considering without constraint and with constraint. In the following discussion we analyze which conditions hold good. For this analysis, we always make $A_1(\theta) - 3\Delta G_2^\theta \geq 0$, so that PT can only occure between P_1 and P_2. We have following cases to analyze :

Case :I When $\bar{A} + A_1(\theta) + 3\Delta G_1^\theta < 0$; $A_{12}(\theta) - 3G_{12}^\theta > 0$:

First we consider, $A_2(\theta) + 3\Delta G_2^\theta = 230$, $\bar{A} + A_1(\theta) + 3\Delta G_1^\theta = -50$ and $A_{12}(\theta) - 3G_{12}^\theta = 350$, we get one minima at the vicinity of P_1 from numerical solution, which is $(\eta_1, \eta_2) = (0.999, 0.005)$. It indicates that there is a local minima exist, which is metastable [Fig .2]. In this case transformation from $P_1 \rightarrow P_2$ initiate, but stuck on metastable point and transformation is not complete.

Then we consider $A_2(\theta) + 3\Delta G_2^\theta = 230$, $\bar{A} + A_1(\theta) + 3\Delta G_1^\theta = -250$ and $A_{12}(\theta) - 3G_{12}^\theta = 150$, again we found minima at $(\eta_1, \eta_2) = (0.989, 0.019)$, vicinity of P_1[Fig .3]. If we further decrease $\bar{A} + A_1(\theta) + 3\Delta G_1^\theta$ to -500 and keep $A_{12}(\theta) - 3G_{12}^\theta = 500$, again we found local minima at $(\eta_1, \eta_2) = (0.989, 0.02)$[Fig .4]. So we conclude that though PT condition for $P_1 \rightarrow P_2$ satisfy for unconstrained case, the transformation is not possible, because we have local metastable phase exist which produce local energy barrier between $P_1 \rightarrow P_2$ PT. The position of this local minima does not change significantly with driving force. Here it is also noted that we did not satisfy PT condition for constrained case.
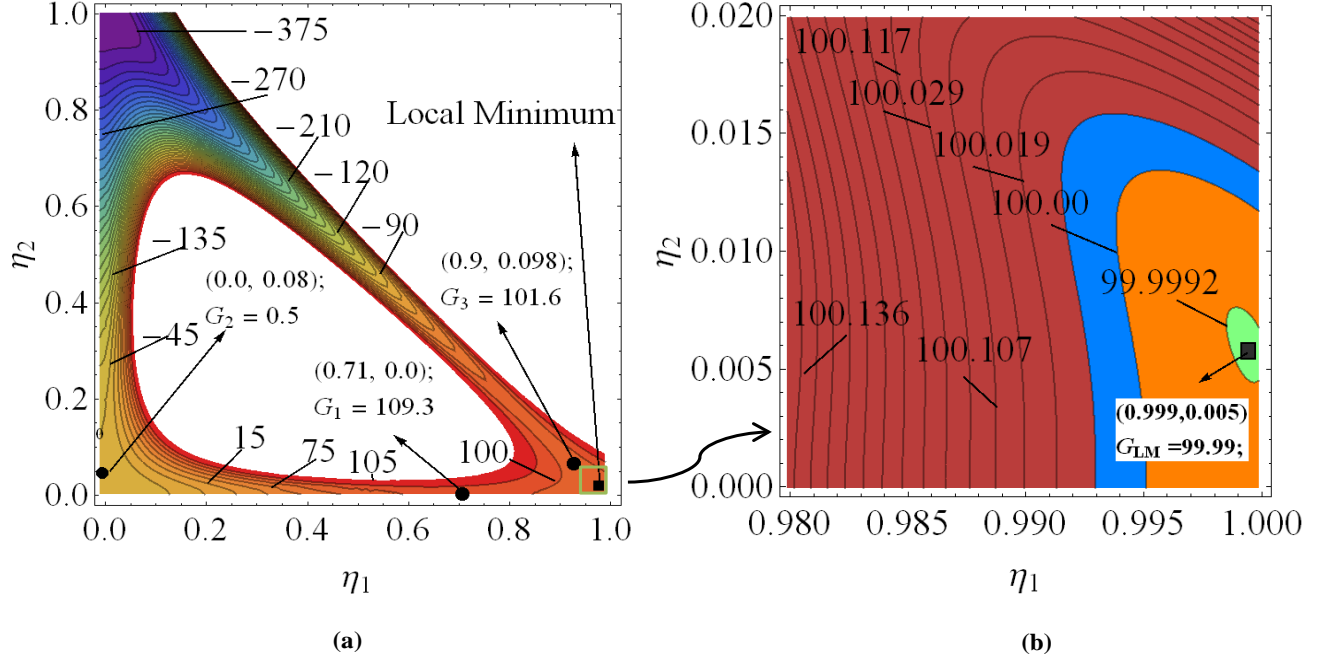
Figure 5: Counter plot of Gibbs energy for $\bar{A}+A_1(\theta)+3\Delta G_1^\theta = -50$ and $A_{12}(\theta)-3G_{12}^\theta = 350$; (b) is the enlarged plot of energy vicinity of P_1

Case :II   When $\bar{A} + A_1(\theta) + 3\Delta G_1^\theta < 0;\ A_{12}(\theta) - 3G_{12}^\theta < 0$ **:**

Here we satisfy PT criterion of $\mathsf{P}_1 \to \mathsf{P}_2$ for both without constraint and with constraint. For example, we set $\bar{A} + A_1(\theta) + 3\Delta G_1^\theta = -805$ and $A_{12}(\theta) - 3G_{12}^\theta = -5$. We observe no local minima vicinity of P_1 and transformation occurs along the diagonal line (Fig. 1 (a)-(c)). So we can conclude that Eq.(44) is the proper transformation criterion for $\mathsf{P}_1 \to \mathsf{P}_2$ PT. Similarly, we can show that Eq.(45) is the correct condition for reverse phase transformation.

5.3.G Solution to the Ginzburg-Landau equation for a propagating interface

Traveling wave solution for the double well potential

Here we consider phase transformation of A to P_1 describe by single order parameter η_1. Here the phase-field equation is presented in one dimensional form and the corresponding functional. The temperature will be treated as constant. Total Gibbs functional over the domain Ω.

$$G_\Omega = \int_\Omega \left[A_1(\theta)\, \eta_1^2 \left(1 - \eta_1 \right)^2 + \Delta\, G_1^\theta \left(3\eta_1^2 - 2\eta_1^3 \right) + \frac{1}{2}\, \beta |\nabla\, \eta_1|^2 \right] dx, \tag{63}$$

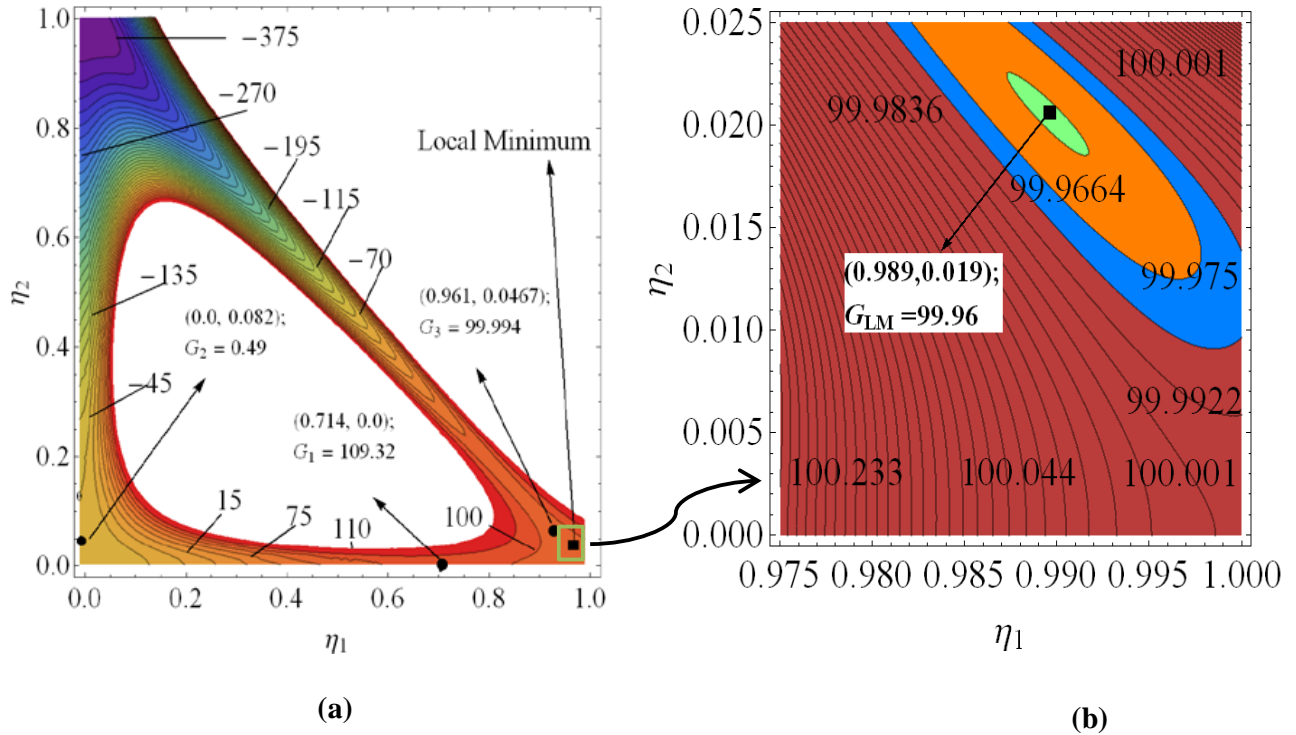Figure 6: Counter plot of Gibbs energy for $\bar{A}+A_1(\theta)+3\Delta G_1^\theta = -250$ and $A_{12}(\theta)-3G_{12}^\theta = 150$; (b) is the enlarged plot of energy vicinity of P_1
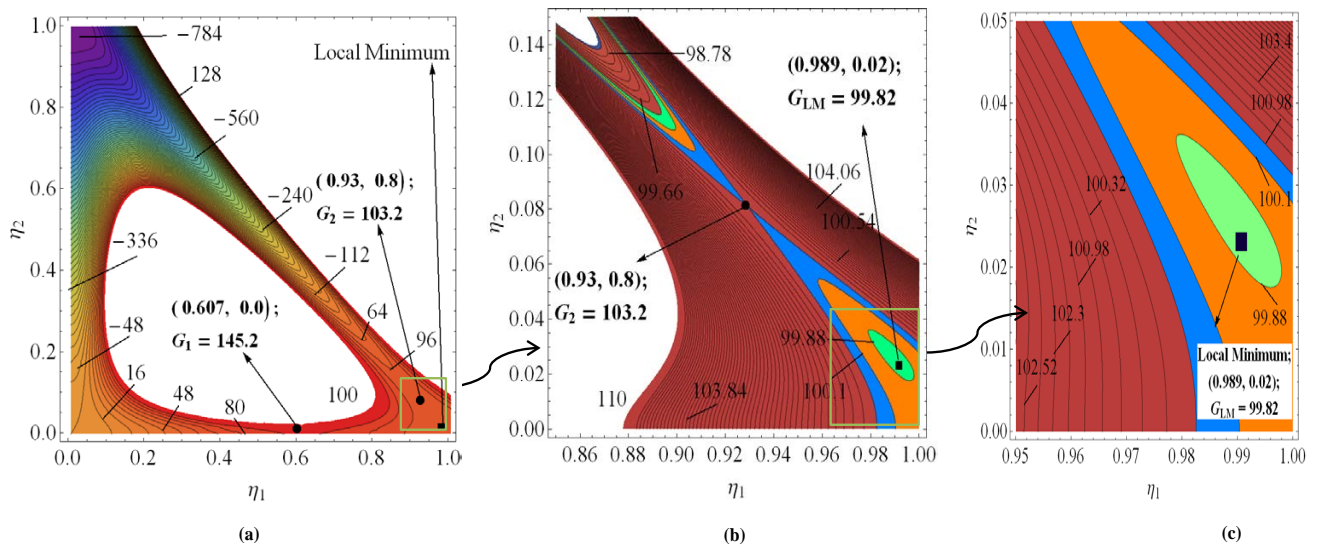

Figure 7: Counter plot of Gibbs energy for $\bar{A}+A_1(\theta)+3\Delta G_1^\theta = -500$ and $A_{12}(\theta)-3G_{12}^\theta = 500$; (b)and (c) are the enlarged plots of energies vicinity of P_1

The thermodynamic driving force $\Delta G_1^\theta (3\eta_1^2 - 2\eta_1^3)$ is directly related to the Gibbs free energy difference $\Delta G_1^\theta = G(\eta_1 = 1) - G(\eta_1 = 0)$ between the bulk phases. Then from From Eq.(63), the simplest Ginzburge-Landau equation reads:

$$L\dot{\eta}_1 = \left[A_1(\theta)\, \eta_1(1 - \eta_1)(1 - 2\eta_1) + \Delta G_1^\theta\, \eta_1\, (1 - \eta_1) + \beta\, \nabla \cdot \nabla\, \eta_1 \right] \tag{64}$$

The steady state solution of Eq.(64) has the form of a hyperbolic tangent profile of width δ marking the transition zone between 5% and 95% traveling with constant speed c

$$\eta_1(x,t) = \frac{1}{2} \tanh\left[\frac{3(x - ct)}{\delta} \right] + \frac{1}{2} \tag{65}$$

Lets calculate the derivatives

$$\frac{\partial \eta_1}{\partial x} = \frac{6}{\delta}\, \eta_1\, (1 - \eta_1) \tag{66}$$

$$\frac{\partial^2 \eta_1}{\partial x^2} = \frac{72}{\delta^2}\, \eta_1\, (1 - \eta_1) \left(\frac{1}{2} - \eta_1 \right) \tag{67}$$

Inserting Eq.(66) and Eq.(67) into Eq.(64)we have:

$$L\dot{\eta}_1 = L\, c\, \frac{\partial \eta_1}{\partial x} = c\, \frac{6L}{\delta}\, \eta_1\, (1 - \eta_1) = \left(\beta \frac{72}{\delta^2} - 4A_1 \right) \eta_1(1 - \eta_1) \left(\eta_1 - \frac{1}{2} \right)$$
$$+ 6\, \Delta G_1^\theta\, \eta_1(1 - \eta_1) \tag{68}$$

Eq.(68) becomes independent of η_1 if the term $(\beta \frac{72}{\delta^2} - 4A_1)$ vanishes and we have:

$$c = \frac{\delta}{L}\, \Delta G_1^\theta \tag{69}$$

From the condition $\beta \frac{72}{\delta^2} - 4A_1 = 0$ we have :

$$\delta = \sqrt{\frac{18\, \beta}{A_1}} \tag{70}$$

With the interface mobility μ as the proportionality constant between velocity and driving force ΔG_1^θ the time scale became $L = \delta/\mu$. The fixation of the length scale δ follows form the definition of interfacial energy. At equilibrium $\Delta G_1^\theta = 0$ the only energy contribution in the system is the interfacial energy per unit area γ :

$$\gamma = \int_{-\infty}^{\infty} \left[A_1(\theta)\, \eta_1^2\, (1 - \eta_1)^2 + \frac{1}{2}\, \beta |\nabla\, \eta_1| \right] \mathrm{d}x$$

$$= \int_{-1}^{1} \left[\left(\frac{\beta}{\delta^2} + \frac{72\beta}{\delta^2} \right) \eta_1^2 \left(1 - \eta_1 \right)^2 \frac{dx}{d\eta} \right] \mathrm{d}\eta_1$$

$$= \int_{-1}^{1} \left[\frac{6\beta}{\delta} \eta_1 \left(1 - \eta_1 \right) \mathrm{d}\eta_1 \right] = \frac{\beta}{\delta} = \frac{\bar{A}\,\delta}{4} \tag{71}$$

It is to be noted that both gradient term proportional to β and the term proportional to $\bar{A}$ contribute to equal parts to the interfacial energy. This is the equivalent of law of equal partitioning of kinetic and potential energy in stationary mechanical system. Summarizing, we find the relations between the model parameters and the physical parameters that are valid close to steady state solutions

$$\beta = \gamma\,\delta, \quad \bar{A} = 4\,\frac{\gamma}{\delta}, \quad L = \frac{\delta}{\mu}. \tag{72}$$

5.3.H Energy of a propagating interface

For the neglected strains and stresses, propagation of the nonequilibrium plane interface moving in an infinite space along axes x is described by closed-form solution to Eq.(65):

$$\eta_1(x, t) = \frac{1}{2} \tanh \left[\frac{3(x - ct)}{\delta} \right] + \frac{1}{2} \tag{73}$$

Here, $c = \frac{\delta}{L}\,\Delta\,G_1^\theta/k$ is the interface velocity, defines the interface width, δ. Now we get explicit equation of gradient energy (ψ^∇) for propagating interface:

$$\nabla = \frac{\beta}{2} |\boldsymbol{\nabla}\eta_{in}|^2 = \frac{\beta}{2} \left(\frac{d\eta_{in}}{dx} \right)^2 = \frac{18\beta}{\delta^2} \eta_{in}^2 (1 - \eta_{in})^2. \tag{74}$$

By the definition of the interface energy under the non equilibrium condition, it is equal to the excess energy with respect to austenite in the austenitic region $x \leq x_i$ and with respect to martensite in the martensitic region $x > x_i$:

$$\gamma := \int_{-\infty}^{x_i} \rho_0 \left(\psi - \psi_A \right) dx + \int_{x_i}^{\infty} \rho_0 \left(\psi - \psi_{P_1} \right) dx, \tag{75}$$

where x_i is the interface position, at which we assume $\eta_1 = 0.5$. We have: $\psi_A = 0$, $\psi_{P_1} = \Delta G_1^\theta$, and it follows from the condition $\eta_1 = 0.5$. Let us first evaluate the gradient energy contribution to γ:

$$\Psi^\nabla := \int_{-\infty}^{\infty} \rho_0 \psi^\nabla dx = \frac{\rho_0\,\beta}{2} \int_{-\infty}^{\infty} \left(\frac{d\eta_{in}}{dx} \right)^2 dx$$

$$= \frac{3\rho_0\,\beta}{\delta} \int_0^1 \eta_{in}(1 - \eta_{in})d\eta \;=\; \frac{\rho_0\,\beta}{2\delta}. \tag{76}$$

From Eq.(75) we can see that total interface energy has two parts:

Interface energy w.r.t austenite (γ_A):

$$\gamma_A := \int_{-\infty}^{x_i} \rho_0\,(\psi - \psi_A)dx = \int_{-\infty}^{x_i} \rho_0\,\psi\,dx \tag{77}$$

$$\gamma_A := \frac{\delta\rho_0}{6} \int_0^{0.5} \left[\Delta G_1^\theta\, g(\eta_{in}) + A_1\, q(\eta_{in}) + \frac{\beta}{2}\left(\frac{d\eta_{in}}{dx}\right)^2 \right] \frac{1}{\eta_{in}(1 - \eta_{in})}d\eta$$

$$= \quad \frac{\rho_0}{4}\left(\frac{\beta}{\delta} + \frac{A_1\,\delta}{18} + \frac{2\Delta G_1^\theta\delta}{7}\right) \tag{78}$$

Interface energy w.r.t martensite phase (γ_{P_1}):

$$\gamma_{P_1} := \int_{x_i}^{-\infty} \rho_0\,(\psi - \psi_{P_1})dx = \int_{x_i}^{-\infty} \rho_0\,(\psi - \Delta G_1^\theta)dx \tag{79}$$

$$\gamma_{P_1} := \frac{\delta\rho_0}{6} \int_{0.5}^1 \left[(\Delta G_1^\theta - 1)\, g(\eta_{in}) + A_1\, q(\eta_{in}) + \frac{\beta}{2}\left(\frac{d\eta_{in}}{dx}\right)^2 \right] \frac{1}{\eta_{in}(1 - \eta_{in})}d\eta$$

$$= \quad \frac{\rho_0}{4}\left(\frac{\beta}{\delta} + \frac{A_1\,\delta}{18} - \frac{2\Delta G_1^\theta\delta}{7}\right) \tag{80}$$

Hence,

$$\gamma = \frac{\rho_0\,\beta}{2\delta} + \frac{\rho_0\,A_1\,\delta}{36} = 2\Psi^\nabla. \tag{81}$$

From Eq.(76):

$$\gamma = \frac{\rho_0\,\beta}{\delta} = 2\Psi^\nabla. \tag{82}$$

Thus, an important result is that for the non-equilibrium interface the total energy is twice the gradient energy.

5.3.I Final expression for free energy

To obtain biaxial interface tension for the propagating interface, one has to define for the general case (i.e., for arbitrary distribution of η)

$$\breve{\psi}^\theta := A_1(\theta)\eta_1^2(1 - \eta_1)^2. \tag{83}$$

For the non equilibrium interface $\breve{\psi}^\theta = \psi^\nabla = \frac{\beta_{10}}{2\rho_0}|\boldsymbol{\nabla}\eta_{in}|^2$. It is clear that for the propagating interface, the function $\breve{\psi}^\theta$ is localized at the diffuse interface, as required. Substituting this in the general expression for the interface tension, we obtain for the propagating interface

$$\boldsymbol{\sigma}_{st} = \beta_{10}|\boldsymbol{\nabla}\eta_1|^2\left(\boldsymbol{I} - \boldsymbol{n}\otimes\boldsymbol{n}\right) = 2\rho_0\breve{\psi}^\theta\left(\boldsymbol{I} - \boldsymbol{n}\otimes\boldsymbol{n}\right) = \sigma_{st}\left(\boldsymbol{I} - \boldsymbol{n}\otimes\boldsymbol{n}\right), \tag{84}$$

where σ_{st} is the magnitude of the biaxial interface stresses. Since $\psi^\nabla > 0$, interface stress $\sigma_{st} > 0$, i.e., it is always tensile. Then for the solution for the propagating interface, the magnitude of the force per unit interface length is equal to

$$\int_{-\infty}^{\infty} \beta_{10}|\boldsymbol{\nabla}\eta_{in}|^2\,dx = 2\int_{-\infty}^{\infty}\rho_0\breve{\psi}dx = 2\Psi^\nabla = \gamma, \tag{85}$$

5.4 Two stress-induced martensitic phases

If we substitute ΔG_i^θ with $\Delta G_i^\theta - \boldsymbol{\sigma}:\boldsymbol{\varepsilon}_{ti}$, we can reproduce the potential for stress induced two martensitic phase correctly. We can rewrite Eq.(13) for stress induced case:

$$f_i\left(\theta,\eta_i\right) = A_i(\theta)\,q(\eta_i) + \left(\Delta G_i^\theta - \boldsymbol{\sigma}:\boldsymbol{\varepsilon}_{ti}\right)\,g(\eta_i), \tag{86}$$

where $\boldsymbol{\varepsilon}_{ti}$ is the transformation strain for P_i.

5.4.A Thermodynamic equilibrium and its stability conditions without using constraint for stress-induced case

In this case, the conditions for the loss of stability of each phase-i.e., phase transformation criteria, simplify to:

$$A \to P_1: \quad \frac{\partial^2 G(\theta, \eta_1 = 0, \eta_2 = 0)}{\partial\eta_1^2} \leq 0 \to \boldsymbol{\sigma}:\boldsymbol{\varepsilon}_{t1} \geq \frac{A_1(\theta) + 3\Delta G_1^\theta}{3}; \tag{87}$$

$$P_1 \to A: \quad \frac{\partial^2 G(\theta, \eta_1 = 1, \eta_2 = 0)}{\partial\eta_1^2} \leq 0 \to \boldsymbol{\sigma}:\boldsymbol{\varepsilon}_{t1} \geq \frac{A_1(\theta) - 3\Delta G_1^\theta}{3}; \tag{88}$$

$$A \to P_2: \quad \frac{\partial^2 G(\theta, \eta_1 = 0, \eta_2 = 0)}{\partial\eta_2^2} \leq 0 \to \boldsymbol{\sigma}:\boldsymbol{\varepsilon}_{t2} \geq \frac{A_2(\theta) + 3\Delta G_2^\theta}{3}; \tag{89}$$

$$P_2 \to A: \quad \frac{\partial^2 G(\theta, \eta_1 = 0, \eta_2 = 1)}{\partial \eta_2^2} \leq 0 \to \boldsymbol{\sigma} : \boldsymbol{\varepsilon}_{t2} \geq \frac{A_2(\theta) - 3\Delta G_2^\theta}{3} ; \tag{90}$$

$$P_1 \to P_2: \quad \frac{\partial^2 G(\theta, \eta_1 = 1, \eta_2 = 0)}{\partial \eta_2^2} \leq 0 \to \boldsymbol{\sigma} : (\boldsymbol{\varepsilon}_{t2} - \boldsymbol{\varepsilon}_{t1}) \geq \frac{\bar{A} + A_2(\theta) + 3\Delta G_2^\theta}{3} ; \tag{91}$$

$$P_2 \to P_1: \quad \frac{\partial^2 G(\theta, \eta_1 = 0, \eta_2 = 1)}{\partial \eta_1^2} \leq 0 \to \boldsymbol{\sigma} : (\boldsymbol{\varepsilon}_{t1} - \boldsymbol{\varepsilon}_{t2}) \geq \frac{\bar{A} + A_1(\theta) + 3\Delta G_1^\theta}{3} ; \tag{92}$$

Eq.(87) to Eq.(90) are desired phase transformation conditions for $A \leftrightarrow P_1$ and $A \leftrightarrow P_2$ respectively. Other two conditions, Eq.(91) and Eq.(92) for $P_1 \leftrightarrow P_2$ PT just follow from the potential and are non-contradictory. But they does not represent proper PT criteria. At this moment, we designate them as 'Unconstrained PT condition' (UC) as following:

$$[P_1 \to P_2]^{UC} \quad \Rightarrow \quad \boldsymbol{\sigma} : (\boldsymbol{\varepsilon}_{t2} - \boldsymbol{\varepsilon}_{t1}) \geq \frac{\bar{A} + A_2(\theta) + 3\Delta G_2^\theta}{3} ; \tag{93}$$

$$[P_2 \to P_1]^{UC} \quad \Rightarrow \quad \boldsymbol{\sigma} : (\boldsymbol{\varepsilon}_{t1} - \boldsymbol{\varepsilon}_{t2}) \geq \frac{\bar{A} + A_1(\theta) + 3\Delta G_1^\theta}{3} ; ; \tag{94}$$

5.4.B Thermodynamic equilibrium and its stability conditions using constraint

If we assume that the $P_1 \leftrightarrow P_2$ PT occurs along the straight path between the points $P_1(\eta_1 = 1, \eta_2 = 0)$ and $P_2(\eta_1 = 0, \eta_2 = 1)$, i.e along the constrain $\eta_2 = 1 - \eta_1$, we can get desired criterion for $P_1 \leftrightarrow P_2$ PT. We substitute $\eta_2 = 1 - \eta_1$ into Eq.(12) to get Gibbs potential as function of a single order parameter η_1 in the following compact form :

$$G(\theta, \eta_1) = A_{12}(\theta)\, q(\eta_1) + \Delta G_2^\theta - \boldsymbol{\sigma} : \boldsymbol{\varepsilon}_{t2} + \Delta G_{12}^\theta g(\eta_1) \tag{95}$$

where

$$A_{12}(\theta) = A_1(\theta) + A_2(\theta) + \bar{A}; \tag{96}$$

and

$$\Delta G_{12}^\theta = \Delta G_1^\theta - \Delta G_2^\theta - \boldsymbol{\sigma} : (\boldsymbol{\varepsilon}_{t1} - \boldsymbol{\varepsilon}_{t2}) \tag{97}$$

In this case, the conditions for the loss of stability of all phases -i.e., phase transformation of criteria, simplify to:

$$P_1 \rightarrow P_2 : \qquad \frac{\partial^2 G(\theta, \vartheta_1 = 1)}{\partial \vartheta_1^2} \leq 0 \rightarrow \boldsymbol{\sigma} : (\boldsymbol{\varepsilon}_{t2} - \boldsymbol{\varepsilon}_{t1}) \geq \frac{A_{12}(\theta) - 3G_{12}^\theta}{3}; \tag{98}$$

$$P_2 \rightarrow P_1 : \qquad \frac{\partial^2 G(\theta, \vartheta_1 = 0)}{\partial \vartheta_1^2} \leq 0 \rightarrow \boldsymbol{\sigma} : (\boldsymbol{\varepsilon}_{t2} - \boldsymbol{\varepsilon}_{t1}) \geq \frac{A_{12}(\theta) + 3G_{12}^\theta}{3}; \tag{99}$$

Eq.(98) to Eq.(99) are desired phase transformation conditions for $P_1 \leftrightarrow P_2$ respectively. At this moment, we designate them as 'Constrained PT condition' as following:

$$P_1 \rightarrow P_2 \quad \Rightarrow \quad \boldsymbol{\sigma} : (\boldsymbol{\varepsilon}_{t2} - \boldsymbol{\varepsilon}_{t1}) \geq \frac{A_{12}(\theta) - 3G_{12}^\theta}{3}; \tag{100}$$

$$P_2 \rightarrow P_1 \quad \Rightarrow \quad \boldsymbol{\sigma} : (\boldsymbol{\varepsilon}_{t2} - \boldsymbol{\varepsilon}_{t1}) \geq \frac{A_{12}(\theta) + 3G_{12}^\theta}{3}; \tag{101}$$

5.5 Three stress-free martensitic phases

For three stress free phases, we can generalized our potential Eq.(12) as

$$G(\theta, \eta_1, \eta_2, \eta_3) = \sum_{i=1}^{n=3} f_i(\theta, \eta_i) + \sum_{i,j=1; i \neq j}^{n=3} \bar{A}_{ij} \, \eta_i^2 \eta_j^2 + \frac{1}{2} \sum_{i=1}^{n=3} \beta_i \, |\nabla \eta_i|^2 + Z_p(\eta_1, \eta_2, \eta_3)$$
$$+ \bar{Z}_p(\eta_1, \eta_2, \eta_3), \quad (102)$$

where,

$$Z_p(\eta_1, \eta_2, \eta_3) = \sum_{i,j=1; i \neq j}^{n=3} K_{ij} \, \eta_i^2 \eta_j^2 \, (1 - \eta_i - \eta_j)^2, \tag{103}$$

and

$$\bar{Z}_p(\eta_1, \eta_2, \eta_3) = \bar{K}_{123} \, \eta_1^2 \eta_2^2 \eta_3^2, \tag{104}$$

Here, $\bar{Z}_p(\eta_1, \eta_2, \eta_3)$ is the term introduced for $n > 2$, which will restrict any spurious growth of additional phases at binary phases. Consequently, at a triple point, where three phases meet,

the dynamics of the system would be governed by the three, two-phase interfaces stretching out from the triple point. It means formation of 2 phases are independent of third phase interface energy. It is also noted that this new term does not affect any stability conditions and transformation conditions. It eliminates problems in all other earlier formulations. Here we consider $\eta_1 = \eta_2 = \eta_3$ and plot Z_p/K for different degree of polynomial of η_1 (Fig.5). Here, n corresponds to $\eta_i^n \eta_j^n$ term. If we increase the n, the barrier between A, P_1, P_2 and P_3 get reduced, which gives more flexibility to $P_i \leftrightarrow A \leftrightarrow P_j$ PT.
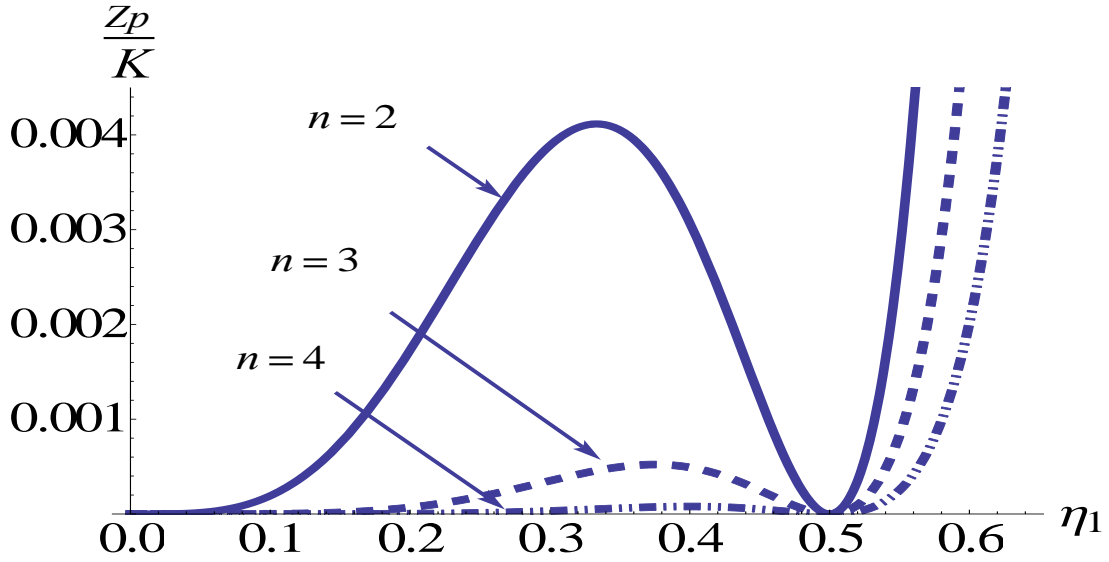
Figure 8: Plot of function $Z_p(\eta_1)/K$ vs η considering different degree of polynomial,i.e $\eta_1^n \eta_1^n f(\eta_1); n = 2, 3, 4$, where $f(\eta_1) = 3(1 - 2\eta_1)^2$

5.5.A Thermodynamic equilibrium and its stability conditions for three phases without using constraint

In this case, the conditions for the loss of stability of each phase-i.e., phase transformation criteria, simplify to:

$$A \to P_1: \qquad \frac{\partial^2 G(\theta, \eta_1 = 0, \eta_2 = 0, \eta_3 = 0)}{\partial \eta_1^2} \leq 0 \to A_1(\theta) + 3\Delta G_1^\theta \leq 0; \qquad (105)$$

$$P_1 \to A: \qquad \frac{\partial^2 G(\theta, \eta_1 = 1, \eta_2 = 0, \eta_3 = 0)}{\partial \eta_1^2} \leq 0 \to A_1(\theta) - 3\Delta G_1^\theta \leq 0; \qquad (106)$$

$$A \to P_2: \qquad \frac{\partial^2 G(\theta, \eta_1 = 0, \eta_2 = 0, \eta_3 = 0)}{\partial \eta_2^2} \leq 0 \to A_2(\theta) + 3\Delta G_2^\theta \leq 0; \qquad (107)$$

$$P_2 \to A: \qquad \frac{\partial^2 G(\theta, \eta_1 = 0, \eta_2 = 1, \eta_3 = 0)}{\partial \eta_2^2} \leq 0 \to A_2(\theta) - 3\Delta G_2^\theta \leq 0; \qquad (108)$$

$$A \to P_3: \qquad \frac{\partial^2 G(\theta, \eta_1 = 0, \eta_2 = 0, \eta_3 = 0)}{\partial \eta_3^2} \leq 0 \to A_3(\theta) + 3\Delta G_3^\theta \leq 0; \qquad (109)$$

$$P_3 \to A: \qquad \frac{\partial^2 G(\theta, \eta_1 = 0, \eta_2 = 0, \eta_3 = 1)}{\partial \eta_2^2} \leq 0 \to A_3(\theta) - 3\Delta G_3^\theta \leq 0; \qquad (110)$$

$$P_1 \to P_2: \quad \frac{\partial^2 G(\theta, \eta_1 = 1, \eta_2 = 0, \eta_3 = 0)}{\partial \eta_2^2} \leq 0 \to \bar{A}_{12} + A_2(\theta) + 3\Delta G_2^\theta \leq 0; \qquad (111)$$

$$P_2 \to P_1: \quad \frac{\partial^2 G(\theta, \eta_1 = 0, \eta_2 = 1, \eta_3 = 0)}{\partial \eta_1^2} \leq 0 \to \bar{A}_{12} + A_1(\theta) + 3\Delta G_1^\theta \leq 0; \qquad (112)$$

$$P_2 \to P_3: \quad \frac{\partial^2 G(\theta, \eta_1 = 0, \eta_2 = 1, \eta_3 = 0)}{\partial \eta_3^2} \leq 0 \to \bar{A}_{23} + A_3(\theta) + 3\Delta G_3^\theta \leq 0; \qquad (113)$$

$$P_3 \to P_2: \quad \frac{\partial^2 G(\theta, \eta_1 = 0, \eta_2 = 0, \eta_3 = 1)}{\partial \eta_2^2} \leq 0 \to \bar{A}_{23} + A_2(\theta) + 3\Delta G_2^\theta \leq 0; \qquad (114)$$

$$P_1 \to P_3: \quad \frac{\partial^2 G(\theta, \eta_1 = 1, \eta_2 = 0, \eta_3 = 0)}{\partial \eta_3^2} \leq 0 \to \bar{A}_{13} + A_3(\theta) + 3\Delta G_3^\theta \leq 0; \qquad (115)$$

$$P_3 \to P_1: \quad \frac{\partial^2 G(\theta, \eta_1 = 0, \eta_2 = 0, \eta_3 = 1)}{\partial \eta_1^2} \leq 0 \to \bar{A}_{13} + A_1(\theta) + 3\Delta G_1^\theta \leq 0; \qquad (116)$$

Eq.(105) to Eq.(110) are desired phase transformation conditions for $\mathsf{A} \leftrightarrow \mathsf{P}_1$ and $\mathsf{A} \leftrightarrow \mathsf{P}_2$ respectively. Other conditions, Eq.(111) to Eq.(116) for $\mathsf{P}_1 \leftrightarrow \mathsf{P}_2$, $\mathsf{P}_2 \leftrightarrow \mathsf{P}_3$ and $\mathsf{P}_1 \leftrightarrow \mathsf{P}_3$ PT just follow from the potential and are non-contradictory. But they does not represent proper PT criteria.

5.5.B Thermodynamic equilibrium and its stability conditions for three phases using constraint

If we assume that the $P_i \leftrightarrow P_j$ PT occurs along the straight path between the points P_i and P_j, i.e along the constrain $\eta_j = 1 - \eta_i$, while $\eta_k = 0$, we can get desired criterion for $P_i \leftrightarrow P_j$ PT. For $P_i \leftrightarrow P_j$ PT, we substitute $\eta_j = 1 - \eta_i$ and $\eta_k = 0$ into Eq.(102) to get following generalized conditions for the loss of stability :

$$P_i \to P_j : \qquad \frac{\partial^2 G(\theta, \eta_i = 1)}{\partial \eta_i^2} \leq 0 \to A_{ji}(\theta) - 3\Delta G_{ji}^\theta \leq 0; \qquad (117)$$

$$P_j \to P_i : \qquad \frac{\partial^2 G(\theta, \eta_i = 0)}{\partial \eta_1^2} \leq 0 \to A_{ji}(\theta) + 3\Delta G_{ji}^\theta \leq 0; \qquad (118)$$

where

$$A_{ji}(\theta) = A_i(\theta) + A_j(\theta) + \sum_{i,j=1; i \neq j}^{n=3} \bar{A}_{ij} \qquad (119)$$

and

$$\Delta G_{ji}^\theta = \Delta G_i^\theta - \Delta G_j^\theta \qquad (120)$$

In explicit form

$$P_1 \to P_2 : \qquad \frac{\partial^2 G(\theta, \eta_1 = 1)}{\partial \eta_1^2} \leq 0 \to A_{12}(\theta) - 3\Delta G_{12}^\theta \leq 0$$
$$\to A_1(\theta) + A_2(\theta) + \bar{A}_{12} + \bar{A}_{13} + \bar{A}_{23} - 3\Delta G_1^\theta + 3\Delta G_2^\theta \leq 0; \qquad (121)$$

$$P_2 \to P_1 : \qquad \frac{\partial^2 G(\theta, \eta_1 = 0)}{\partial \eta_1^2} \leq 0 \to A_{12}(\theta) + 3\Delta G_{12}^\theta \leq 0$$
$$\to A_1(\theta) + A_2(\theta) + \bar{A}_{12} + \bar{A}_{13} + \bar{A}_{23} - 3\Delta G_2^\theta + 3\Delta G_1^\theta \leq 0; \qquad (122)$$

$$P_2 \to P_3 : \qquad \frac{\partial^2 G(\theta, \eta_2 = 0)}{\partial \eta_2^2} \leq 0 \to A_{32}(\theta) - 3\Delta G_{32}^\theta \leq 0$$
$$\to A_2(\theta) + A_3(\theta) + \bar{A}_{12} + \bar{A}_{13} + \bar{A}_{23} - 3\Delta G_3^\theta + 3\Delta G_2^\theta \leq 0; \qquad (123)$$

$$P_3 \to P_2 : \qquad \frac{\partial^2 G(\theta, \eta_2 = 1)}{\partial \eta_2^2} \leq 0 \to A_{32}(\theta) + 3\Delta G_{32}^\theta \leq 0$$
$$\to A_2(\theta) + A_3(\theta) + \bar{A}_{12} + \bar{A}_{13} + \bar{A}_{23} - 3\Delta G_2^\theta + 3\Delta G_3^\theta \leq 0; \qquad (124)$$

$$P_1 \to P_3: \qquad \frac{\partial^2 G(\theta, \eta_1 = 1)}{\partial \eta_1^2} \leq 0 \to A_{31}(\theta) - 3\Delta G_{31}^\theta \leq 0$$
$$\to A_1(\theta) + A_3(\theta) + \bar{A}_{12} + \bar{A}_{13} + \bar{A}_{23} - 3\Delta G_1^\theta + 3\Delta G_3^\theta \leq 0; \tag{125}$$

$$P_3 \to P_1: \qquad \frac{\partial^2 G(\theta, \eta_1 = 0)}{\partial \eta_1^2} \leq 0 \to A_{31}(\theta) + 3\Delta G_{31}^\theta \leq 0$$
$$\to A_1(\theta) + A_3(\theta) + \bar{A}_{12} + \bar{A}_{13} + \bar{A}_{23} - 3\Delta G_3^\theta + 3\Delta G_1^\theta \leq 0; \tag{126}$$

Eq.(121) to Eq.(122) are desired phase transformation conditions for all $\mathsf{P}_i \leftrightarrow \mathsf{P}_j$ respectively. At this moment, we designate them as 'Constrained PT condition' as following:

$$P_i \to P_j \quad \Rightarrow \quad A_{ji}(\theta) - 3G_{ji}^\theta \leq 0; \tag{127}$$

$$P_j \to P_i \quad \Rightarrow \quad A_{ji}(\theta) + 3G_{ji}^\theta \leq 0; \tag{128}$$

5.6 n-stress induced martensitic phases

We can immediately generalized our theory for n-th martensitic phases as following:

$$G = \sum_{i=1}^{n} f_i(\theta, \eta_i) + \sum_{i,j=1; i \neq j}^{n} \bar{A}_{ij} \eta_i^2 \eta_j^2 + \sum_{i,j=1; i \neq j}^{n=3} K_{ij} \eta_i^2 \eta_j^2 (1 - \eta_i - \eta_j)^2$$
$$+ \bar{K}_{12...n} \eta_1^2 \eta_2^2 ... \eta_n^2 + \frac{1}{2} \sum_{i=1}^{n} \beta_i |\nabla \eta_i|^2, \tag{129}$$

where

$$f_i(\theta, \eta_i) = A_i(\theta) q(\eta_i) + \left(\Delta G_i^\theta - \boldsymbol{\sigma} : \boldsymbol{\varepsilon}_{ti} \right) g(\eta_i), \tag{130}$$

and the generalized PT condition :

$$A \to P_i: \qquad \frac{\partial^2 G}{\partial \eta_i^2} \leq 0 \to \boldsymbol{\sigma} : \boldsymbol{\varepsilon}_{ti} \geq \frac{A_i(\theta) + 3\Delta G_i^\theta}{3}; \tag{131}$$

$$P_i \to A: \qquad \frac{\partial^2 G}{\partial \eta_i^2} \leq 0 \to \boldsymbol{\sigma} : \boldsymbol{\varepsilon}_{ti} \geq \frac{A_i(\theta) - 3\Delta G_i^\theta}{3}; \tag{132}$$

$$P_i \to P_j: \qquad \frac{\partial^2 G}{\partial \eta_i^2} \leq 0 \; \to \; \boldsymbol{\sigma} : (\boldsymbol{\varepsilon}_{tj} - \boldsymbol{\varepsilon}_{ti}) \geq \frac{A_{ji}(\theta) - 3\Delta G_{ji}^\theta}{3}; \tag{133}$$

$$P_j \to P_i: \qquad \frac{\partial^2 G}{\partial \eta_i^2} \leq 0 \; \to \; \boldsymbol{\sigma} : (\boldsymbol{\varepsilon}_{tj} - \boldsymbol{\varepsilon}_{ti}) \geq \frac{A_{ji}(\theta) + 3\Delta G_{ji}^\theta}{3}; \tag{134}$$

5.7 Specification of the Helmholtz energy of a single order parameter

First, let us present the expression for the Helmholtz free energy for one phase potential Eq.(12) in terms of η_1, which neglects the interface tension:

$$\bar{\psi}_0(\boldsymbol{\varepsilon}, \eta_1, \theta, \boldsymbol{\nabla}\eta_1) = \psi^e(\boldsymbol{\varepsilon} - \boldsymbol{\varepsilon}_t(\eta_1) - \boldsymbol{\varepsilon}_\theta(\theta, \eta_1), \eta_1, \theta) + f_1(\theta, \eta_1) + {}^\nabla; \tag{135}$$

$$f_1(\theta, \eta_1) = \Delta G_1^\theta \eta_1^2(3 - 2\eta_1) + A_1(\theta)\eta_1^2(1 - \eta_1)^2; \qquad \nabla = \frac{\beta_{10}}{2\rho_0}|\boldsymbol{\nabla}_0\eta_1|^2. \tag{136}$$

Here, ψ^e is the elastic energy and ψ^∇ is the simplest gradient energy; the terms $\Delta G_1^\theta \eta_1^2(3 - 2\eta_1)$ and $A_1(\theta)\eta_1^2(1 - \eta_1)^2$ are parts of the thermal (chemical) energy $f_1(\theta, \eta_1)$ related to the thermal driving force for phase transformation and double-well barrier, respectively, ΔG_1^θ is the difference between the thermal parts of the Gibbs energies of P_1 and A; A_1 and β_{10} are the double-well energy and gradient energy coefficients. To introduce interface tension, we accept the free energy in the following form:

$$\bar{\psi}(\boldsymbol{\varepsilon}, \eta_1, \theta, \boldsymbol{\nabla}\eta_1) = \psi^e(\boldsymbol{\varepsilon} - \boldsymbol{\varepsilon}_t(\eta_1) - \boldsymbol{\varepsilon}_\theta(\theta, \eta_1), \eta_1, \theta) + \frac{\rho_0}{\rho}\breve{\psi}^\theta + \tilde{\psi}^\theta + \frac{\rho_0}{\rho}{}^\nabla; \tag{137}$$

$$\tilde{\psi}^\theta + \breve{\psi}^\theta = f_1(\theta, \eta_1); \quad \frac{\rho_0}{\rho} = 1 + \varepsilon_0; \qquad \nabla = \frac{\beta_{10}}{2\rho_0}|\boldsymbol{\nabla}\eta_1|^2, \tag{138}$$

where the proper division of $f_1(\theta, \eta_1)$ into two functions, $\tilde{\psi}^\theta$ and $\breve{\psi}^\theta$, is to be determined and ε_0 is the volumetric strain. Note that the material constants and functions in terms without ρ_0/ρ are defined per unit mass or (since $\rho_0 = const$) per unit undeformed volume. The terms with ρ_0/ρ are multiplied by $dm\rho_0/\rho = \rho_0 dV$; then the material constants and functions (β_{10} and A_1) are defined per unit deformed volume dV. The reason why the two terms, $\breve{\psi}^\theta$ and ψ^∇,

are multiplied by ρ_0/ρ to reproduce surface stress correctly. While usually in the small strain approximation it is assumed $\rho_0/\rho \simeq 1$, since ρ_0/ρ is a linear function of volumetric strain ε_0, keeping ρ_0/ρ results in additional contribution to stress even at infinitesimal strains. Indeed, since

$$\rho_0/\rho = 1 + \varepsilon_0 = 1 + \boldsymbol{I}{:}\boldsymbol{\varepsilon}, \quad \text{then} \quad d(\rho_0/\rho)/d\boldsymbol{\varepsilon} = \boldsymbol{I}. \tag{139}$$

$$\text{Also,} \quad \frac{\partial \bar{\psi}}{\partial \boldsymbol{\varepsilon}} = \frac{\partial \bar{\psi}}{\partial \boldsymbol{\varepsilon}_e}{:}\frac{\partial \boldsymbol{\varepsilon}_e}{\partial \boldsymbol{\varepsilon}} = \frac{\partial \bar{\psi}}{\partial \boldsymbol{\varepsilon}_e}. \tag{140}$$

Now, constitutive equations for the stress tensor and an evolution equation for η_i from :

$$\boldsymbol{\sigma} = \rho\frac{\partial\bar{\psi}}{\partial\boldsymbol{\varepsilon}} - \rho\left(\boldsymbol{\nabla}\eta_i \otimes \frac{\partial\bar{\psi}}{\partial\boldsymbol{\nabla}\eta_i}\right)_s + \boldsymbol{\sigma}_d; \qquad X_i = -\rho\frac{\partial\bar{\psi}}{\partial\eta_i} + \boldsymbol{\nabla}\cdot\left(\rho\frac{\partial\bar{\psi}}{\partial\boldsymbol{\nabla}\eta_i}\right), \tag{141}$$

Then it follows from Eqs.(137), (138), and (141)

$$\boldsymbol{\sigma} = \rho_0\frac{\partial\bar{\psi}}{\partial\boldsymbol{\varepsilon}} - \rho\frac{\partial\bar{\psi}}{\partial\boldsymbol{\nabla}\eta_1} \otimes \boldsymbol{\nabla}\eta_1 + \boldsymbol{\sigma}_d = \rho_0\frac{\partial\psi^e}{\partial\boldsymbol{\varepsilon}_e} + \rho_0(\breve{\psi}^\theta + {}^{\nabla})\boldsymbol{I} - \beta_{10}\boldsymbol{\nabla}\eta_1 \otimes \boldsymbol{\nabla}\eta_1 + \boldsymbol{\sigma}_d. \tag{142}$$

In the first term, we used the simplification $\rho \simeq \rho_0$. Let us introduce $\boldsymbol{n}_1 = \boldsymbol{\nabla}\eta_1/|\boldsymbol{\nabla}\eta_1|$, which for the solution representing diffuse interface defines the unit normal to the diffuse interface. Substituting Eq.(138) for ψ^∇ in Eq.(142), we further specify

$$\boldsymbol{\sigma} = \boldsymbol{\sigma}_e + \boldsymbol{\sigma}_{st} + \boldsymbol{\sigma}_d; \qquad \boldsymbol{\sigma}_e = \rho_0\frac{\partial\psi^e}{\partial\boldsymbol{\varepsilon}_e}; \tag{143}$$

$$\boldsymbol{\sigma}_{st} = (\rho_0\breve{\psi}^\theta + \frac{\beta_{10}}{2}|\boldsymbol{\nabla}\eta_1|^2)\boldsymbol{I} - \beta_{10}\boldsymbol{\nabla}\eta_1 \otimes \boldsymbol{\nabla}\eta_1 = \beta_{10}|\boldsymbol{\nabla}\eta_1|^2\,(\boldsymbol{I} - \boldsymbol{n}_1 \otimes \boldsymbol{n}_1)$$
$$+(\rho_0\breve{\psi}^\theta - \frac{\beta_{10}}{2}|\boldsymbol{\nabla}\eta_1|^2)\boldsymbol{I}, \tag{144}$$

Thus, we obtained decomposition of the stress tensor into an elastic part, $\boldsymbol{\sigma}_e$ (which looks exactly the same as without surface tension), dissipative part, and a surface tension contribution, which should be localized at the diffuse interface and equal to zero in the bulk, i.e., for $\eta_1 = 0$ and $\eta_1 = 1$. This implies the requirement that the function $\breve{\psi}^\theta$ should be localized at the diffuse interface. To obtain desired biaxial surface tension, the last term must be identically zero for the solution representing propagating interface.

1. Kinematics

1.1. Decomposition of the strain tensor $\boldsymbol{\varepsilon}$; volumetric strain ε_0

$$\boldsymbol{\varepsilon} = (\overset{\circ}{\boldsymbol{\nabla}}\, \boldsymbol{u})_s; \quad \boldsymbol{\varepsilon} = \boldsymbol{\varepsilon}_e + \boldsymbol{\varepsilon}_t(\eta_1) + \boldsymbol{\varepsilon}_\theta(\theta, \eta_1); \quad \frac{\rho_0}{\rho} = 1 + \varepsilon_0; \quad \varepsilon_0 = \boldsymbol{\varepsilon}{:}\boldsymbol{I}. \tag{145}$$

1.2. Transformation $\boldsymbol{\varepsilon}_t$ and thermal $\boldsymbol{\varepsilon}_\theta$ strains

$$\boldsymbol{\varepsilon}_t = \bar{\boldsymbol{\varepsilon}}_t\, g(\eta_1); \qquad \boldsymbol{\varepsilon}_\theta = \boldsymbol{\varepsilon}_{\theta A} + (\boldsymbol{\varepsilon}_{\theta P_1} - \boldsymbol{\varepsilon}_{\theta A})\, g(\eta_1);$$

$$g(\eta_1) = \eta_1^2(3 - 2\eta_1). \tag{146}$$

2. Helmholtz free energy per unit mass and its contributions

$$\bar{\psi}(\boldsymbol{\varepsilon}, \eta_1, \theta, \boldsymbol{\nabla}\eta_1) = \psi^e(\boldsymbol{\varepsilon} - \boldsymbol{\varepsilon}_t(\eta_1) - \boldsymbol{\varepsilon}_\theta(\theta, \eta_1), \eta_1, \theta) + \frac{\rho_0}{\rho}\breve{\psi}^\theta + \tilde{\psi}^\theta + \frac{\rho_0}{\rho}\,{}^\nabla; \tag{147}$$

$$\breve{\psi}^\theta = A_1(\theta)\eta_1^2(1 - \eta_1)^2; \quad \tilde{\psi}^\theta = \Delta\, G_1^\theta \eta_1^2(3 - 2\eta_1);$$

$$\psi^e = \frac{1}{2\rho_0}\boldsymbol{\varepsilon}_e{:}\boldsymbol{E}(\eta_1){:}\boldsymbol{\varepsilon}_e; \qquad \boldsymbol{E}(\eta_1) = \boldsymbol{E}_A + (\boldsymbol{E}_{P1} - \boldsymbol{E}_A)\varphi(a_E, \eta_1); \qquad {}^\nabla = \frac{\beta_{10}}{2\rho_0}|\boldsymbol{\nabla}\eta_1|^2 \tag{148}$$

3. Stress tensor

$$\boldsymbol{\sigma} = \boldsymbol{\sigma}_e + \boldsymbol{\sigma}_{st} + \boldsymbol{\sigma}_d; \tag{149}$$

$$\boldsymbol{\sigma}_e = \rho_0\frac{\partial\,\psi^e}{\partial\,\boldsymbol{\varepsilon}_e} = \boldsymbol{E}(\eta_1){:}\boldsymbol{\varepsilon}_e; \quad \boldsymbol{\sigma}_{st} = (\rho_0\breve{\psi}^\theta + \frac{\beta_{10}}{2}|\boldsymbol{\nabla}\eta_1|^2)\boldsymbol{I} - \beta_{10}\boldsymbol{\nabla}\eta_1 \otimes \boldsymbol{\nabla}\eta_1; \quad \boldsymbol{\sigma}_d = \boldsymbol{B}{:}\dot{\boldsymbol{\varepsilon}}. \tag{150}$$

4. Ginzburg–Landau equation

$$\dot{\eta}_1 = LX = L\left(\frac{\rho}{\rho_0}\boldsymbol{\sigma}_e{:}\frac{\partial\boldsymbol{\varepsilon}_t}{\partial\eta_1} + \frac{\rho}{\rho_0}\boldsymbol{\sigma}_e{:}\frac{\partial\boldsymbol{\varepsilon}_\theta}{\partial\eta_1} - \rho\frac{\partial\psi^e}{\partial\eta_1}\Big|_{\boldsymbol{\varepsilon}_e} - \rho_0\frac{\partial\breve{\psi}^\theta}{\partial\eta_1} - \rho\frac{\partial\tilde{\psi}^\theta}{\partial\eta_1} + \beta_{10}\boldsymbol{\nabla}^2\eta_1\right). \tag{151}$$

5. Momentum balance equation

$$\nabla{\cdot}\boldsymbol{\sigma} + \rho\boldsymbol{f} = \rho\dot{\boldsymbol{v}}. \tag{152}$$

6. Boundary conditions for the order parameter

$$\boldsymbol{n}_1 \cdot \frac{\partial\psi}{\partial\boldsymbol{\nabla}\eta_1} = H. \tag{153}$$

While the above equations are derived for an arbitrary nonlinear elasticity rule and relationship

for dissipative stresses $\boldsymbol{\sigma}_d$, we specified them for linear anisotropic constitutive with $\boldsymbol{E}$ and $\boldsymbol{B}$

for fourth rank elastic moduli and viscosity tensors. Expressions for $\boldsymbol{\varepsilon}_t(\eta)$, $\boldsymbol{\varepsilon}_\theta(\theta, \eta)$, and $\boldsymbol{E}(\eta)$ are derived in [2], where a, a_θ, and a_E are the material parameters and subscript A and P designate austenite and martensite.

5.7.A Specification of the Helmholtz energy for two order parameters

Here, we present the expression for the Helmholtz free energy for two phase potential Eq.(12) in terms of η_1, η_2 which neglects the interface tension:

$$\bar{\psi}_0(\boldsymbol{\varepsilon}, \eta_1, \eta_2, \theta, \boldsymbol{\nabla}\eta_1, \boldsymbol{\nabla}\eta_2) = \psi^e(\boldsymbol{\varepsilon}_0, e, \eta_i, \theta) + f_1(\theta, \eta_1) + f_2(\theta, \eta_2) + \bar{A}\eta_1^2\eta_2^2$$
$$+ Z_p(\eta_1, \eta_2) + \psi^\nabla; \tag{154}$$

$$f_1(\theta, \eta_1) = \Delta G_1^\theta \eta_1^2(3 - 2\eta_1) + A_1(\theta)\eta_1^2(1 - \eta_1)^2;$$
$$f_2(\theta, \eta_2) = \Delta G_2^\theta \eta_2^2(3 - 2\eta_2) + A_2(\theta)\eta_2^2(1 - \eta_2)^2;$$
$$\nabla = \frac{\beta_{10}}{2\rho_0}|\boldsymbol{\nabla}_0\eta_1|^2 + \frac{\beta_{20}}{2\rho_0}|\boldsymbol{\nabla}_0\eta_2|^2 + b\boldsymbol{\nabla}_0\eta_1\boldsymbol{\nabla}_0\eta_2. \tag{155}$$

To introduce interface tension, we accept the free energy in the following form:

$$\bar{\psi}(\boldsymbol{\varepsilon}, \eta_1, \eta_2, \theta, \boldsymbol{\nabla}\eta_1, \boldsymbol{\nabla}\eta_2) = \psi^e(\boldsymbol{\varepsilon}_0, e, \eta_i, \theta) + \frac{\rho_0}{\rho}\breve{\psi}^\theta + \tilde{\psi}^\theta + \frac{\rho_0}{\rho} \nabla; \tag{156}$$

$$\tilde{\psi}^\theta + \breve{\psi}^\theta = f_1(\theta, \eta_1) + f_2(\theta, \eta_2) + \bar{A}\eta_1^2\eta_2^2 + Z_p(\eta_1, \eta_2);$$
$$\frac{\rho_0}{\rho} = 1 + \varepsilon_0; \qquad \nabla = \frac{\beta_{10}}{2\rho_0}|\boldsymbol{\nabla}_0\eta_1|^2 + \frac{\beta_{20}}{2\rho_0}|\boldsymbol{\nabla}_0\eta_2|^2 + b\boldsymbol{\nabla}_0\eta_1\boldsymbol{\nabla}_0\eta_2., \tag{157}$$

More explicitly :

$$\breve{\psi}^\theta = A_1(\theta)\eta_1^2(1 - \eta_1)^2 + A_2(\theta)\eta_2^2(1 - \eta_2)^2 + \bar{A}\eta_1^2\eta_2^2; \tag{158}$$

$$\tilde{\psi}^\theta = \Delta G_1^\theta \eta_1^2(3 - 2\eta_1) + \Delta G_2^\theta \eta_2^2(3 - 2\eta_2) + Z_p; \tag{159}$$

$$\rho_0/\rho = 1 + \varepsilon_0 = 1 + \boldsymbol{I}{:}\boldsymbol{\varepsilon}, \quad \text{then} \quad d(\rho_0/\rho)/d\boldsymbol{\varepsilon} = \boldsymbol{I}. \tag{160}$$

$$\text{Also,} \quad \frac{\partial\bar{\psi}}{\partial\boldsymbol{\varepsilon}} = \frac{\partial\bar{\psi}}{\partial\boldsymbol{\varepsilon}_e}{:}\frac{\partial\boldsymbol{\varepsilon}_e}{\partial\boldsymbol{\varepsilon}} = \frac{\partial\bar{\psi}}{\partial\boldsymbol{\varepsilon}_e}. \tag{161}$$

Now, constitutive equations for the stress tensor and an evolution equation for η_i from :

$$\boldsymbol{\sigma} = \rho\frac{\partial\bar{\psi}}{\partial\boldsymbol{\varepsilon}} - \sum\rho\left(\boldsymbol{\nabla}\eta_i \otimes \frac{\partial\bar{\psi}}{\partial\boldsymbol{\nabla}\eta_i}\right)_s + \boldsymbol{\sigma}_d; \qquad X_i = -\rho\frac{\partial\bar{\psi}}{\partial\eta_i} + \sum\boldsymbol{\nabla}\cdot\left(\rho\frac{\partial\bar{\psi}}{\partial\boldsymbol{\nabla}\eta_i}\right), \tag{162}$$

Then it follows from Eqs.(156), (157), and (162)

$$\boldsymbol{\sigma} = \rho_0 \frac{\partial \bar{\psi}}{\partial \boldsymbol{\varepsilon}} - \sum \rho \frac{\partial \bar{\psi}}{\partial \boldsymbol{\nabla} \eta_i} \otimes \boldsymbol{\nabla} \eta_i + \boldsymbol{\sigma}_d = \rho_0 \frac{\partial \psi^e}{\partial \boldsymbol{\varepsilon}_e} + \rho_0 (\breve{\psi}^\theta + \quad^\nabla) \boldsymbol{I}$$
$$- \beta_{10} \boldsymbol{\nabla} \eta_1 \otimes \boldsymbol{\nabla} \eta_1 - \beta_{20} \boldsymbol{\nabla} \eta_2 \otimes \boldsymbol{\nabla} \eta_2 - 2b \boldsymbol{\nabla} \eta_1 \otimes \boldsymbol{\nabla} \eta_2 + \boldsymbol{\sigma}_d. \qquad (163)$$

In the first term, we used the simplification $\rho \simeq \rho_0$. Let us introduce $\boldsymbol{n}_1 = \boldsymbol{\nabla} \eta_1 / |\boldsymbol{\nabla} \eta_1|$, which for the solution representing diffuse interface defines the unit normal to the diffuse interface. Substituting Eq.(155) for ψ^∇ in Eq.(163), we further specify

$$\boldsymbol{\sigma} = \boldsymbol{\sigma}_e + \boldsymbol{\sigma}_{st} + \boldsymbol{\sigma}_d; \qquad \boldsymbol{\sigma}_e = \rho_0 \frac{\partial \psi^e}{\partial \boldsymbol{\varepsilon}_e}; \qquad (164)$$

$$\boldsymbol{\sigma}_{st} = (\rho_0 \breve{\psi}^\theta + \frac{\beta_{10}}{2} |\boldsymbol{\nabla} \eta_1|^2 + \frac{\beta_{20}}{2} |\boldsymbol{\nabla} \eta_2|^2 + b \boldsymbol{\nabla} \eta_1 \boldsymbol{\nabla} \eta_2) \boldsymbol{I} - \beta_{10} \boldsymbol{\nabla} \eta_1 \otimes \boldsymbol{\nabla} \eta_1$$
$$- \beta_{20} \boldsymbol{\nabla} \eta_2 \otimes \boldsymbol{\nabla} \eta_2 - 2b \boldsymbol{\nabla} \eta_1 \otimes \boldsymbol{\nabla} \eta_2; \qquad (165)$$

Lets consider P_1 -P_2 interface and using the condition $\boldsymbol{\nabla} \eta_1 = -\boldsymbol{\nabla} \eta_2$, we can rewrite Eq.(165):

$$\boldsymbol{\sigma}_{st} = \left(\rho_0 \breve{\psi}^\theta + \frac{1}{2} (\beta_{10} + \beta_{20} - 2b) |\boldsymbol{\nabla} \eta_1|^2 \right) \boldsymbol{I} - (\beta_{10} + \beta_{20} - 2b) \boldsymbol{\nabla} \eta_1 \otimes \boldsymbol{\nabla} \eta_1; \qquad (166)$$

Earlier, we have $\beta_{12} = \beta_{10} + \beta_{20} - 2b$, substituting in Eq.(166)we get:

$$\boldsymbol{\sigma}_{st} = \left(\rho_0 \breve{\psi}^\theta + \frac{1}{2} \beta_{12} |\boldsymbol{\nabla} \eta_1|^2 \right) \boldsymbol{I} - \beta_{12} \boldsymbol{\nabla} \eta_1 \otimes \boldsymbol{\nabla} \eta_1; \qquad (167)$$

which similar to A -P interface stress.

Thus, we obtained decomposition of the stress tensor into an elastic part, $\boldsymbol{\sigma}_e$ (which looks exactly the same as without surface tension), dissipative part, and a surface tension contribution, which should be localized at the diffuse interface and equal to zero in the bulk, i.e., for $\eta_1 = 0$ and $\eta_1 = 1$. This implies the requirement that the function $\breve{\psi}^\theta$ should be localized at the diffuse interface. To obtain desired biaxial surface tension, the last term must be identically zero for the solution representing propagating interface.

5.8 Complete system of equations for two order parameters

Below we collect the final complete system of equations for two order parameters.

1. Kinematics 1.1. Decomposition of the strain tensor $\boldsymbol{\varepsilon}$; volumetric strain ε_0

$$\boldsymbol{\varepsilon} = (\overset{\circ}{\boldsymbol{\nabla}} \boldsymbol{u})_s; \quad \boldsymbol{\varepsilon} = \boldsymbol{\varepsilon}_e + \sum \boldsymbol{\varepsilon}_t(\eta_i) + \sum \boldsymbol{\varepsilon}_\theta(\theta, \eta_i); \quad \frac{\rho_0}{\rho} = 1 + \varepsilon_0; \quad \varepsilon_0 = \boldsymbol{\varepsilon}{:}\boldsymbol{I}. \tag{168}$$

1.2. Transformation $\boldsymbol{\varepsilon}_t$ and thermal $\boldsymbol{\varepsilon}_\theta$ strains

$$\boldsymbol{\varepsilon}_t = \sum \bar{\boldsymbol{\varepsilon}}_{ti}\, g(\eta_i); \qquad \boldsymbol{\varepsilon}_\theta = \boldsymbol{\varepsilon}_{\theta A} + \sum (\boldsymbol{\varepsilon}_{\theta P_i} - \boldsymbol{\varepsilon}_{\theta A})\, g(\eta_i);$$

$$g(\eta_i) = \eta_i^2(3 - 2\eta_i). \tag{169}$$

2. Helmholtz free energy per unit mass and its contributions

$$\bar{\psi}(\boldsymbol{\varepsilon}, \eta_1, \eta_2, \theta, \boldsymbol{\nabla}\eta_1, \boldsymbol{\nabla}\eta_2) = \psi^e(\varepsilon_0, e, \eta_i, \theta) + \frac{\rho_0}{\rho}\breve{\psi}^\theta + \tilde{\psi}^\theta + \frac{\rho_0}{\rho}\,{}^\nabla; \tag{170}$$

$$\breve{\psi}^\theta = \sum A_i(\theta)\eta_i^2(1 - \eta_i)^2 + \bar{A}\eta_1^2\eta_2^2; \quad \tilde{\psi}^\theta = \sum \Delta G_i^\theta \eta_i^2(3 - 2\eta_i) + Z_p;$$

$$\psi^e = \frac{1}{2\rho_0} \sum \boldsymbol{\varepsilon}_e{:}\boldsymbol{E}(\eta_1){:}\boldsymbol{\varepsilon}_e; \qquad \boldsymbol{E}(\eta_i) = \boldsymbol{E}_A + (\boldsymbol{E}_{Pi} - \boldsymbol{E}_A)\varphi(a_E, \eta_i); \quad . \tag{171}$$

$$^\nabla = \frac{\beta_{10}}{2\rho_0}|\boldsymbol{\nabla}\eta_1|^2 + \frac{\beta_{20}}{2\rho_0}|\boldsymbol{\nabla}\eta_2|^2 + \frac{b}{\rho_0}\boldsymbol{\nabla}\eta_1\boldsymbol{\nabla}\eta_2; \tag{172}$$

3. Stress tensor

$$\boldsymbol{\sigma} = \boldsymbol{\sigma}_e + \boldsymbol{\sigma}_{st} + \boldsymbol{\sigma}_d; \tag{173}$$

$$\boldsymbol{\sigma}_e = \rho_0 \frac{\partial\ ^e}{\partial\boldsymbol{\varepsilon}_e} = \boldsymbol{E}(\eta_i){:}\boldsymbol{\varepsilon}_e; \quad \boldsymbol{\sigma}_d = \boldsymbol{B}{:}\dot{\boldsymbol{\varepsilon}}. \tag{174}$$

$$\boldsymbol{\sigma}_{st} = (\rho_0\breve{\psi}^\theta + \frac{\beta_{10}}{2}|\boldsymbol{\nabla}\eta_1|^2 + \frac{\beta_{20}}{2}|\boldsymbol{\nabla}\eta_2|^2 + b\boldsymbol{\nabla}\eta_1\boldsymbol{\nabla}\eta_2)\boldsymbol{I} - \beta_{10}\boldsymbol{\nabla}\eta_1 \otimes \boldsymbol{\nabla}\eta_1$$

$$- \beta_{20}\boldsymbol{\nabla}\eta_2 \otimes \boldsymbol{\nabla}\eta_2 - 2b\boldsymbol{\nabla}\eta_1 \otimes \boldsymbol{\nabla}\eta_2; \tag{175}$$

4. Ginzburg–Landau equation

$$\dot{\eta}_i = LX = L\left(\frac{\rho}{\rho_0}\boldsymbol{\sigma}_e{:}\frac{\partial\boldsymbol{\varepsilon}_t}{\partial\eta_i} + \frac{\rho}{\rho_0}\boldsymbol{\sigma}_e{:}\frac{\partial\boldsymbol{\varepsilon}_\theta}{\partial\eta_i} - \rho\frac{\partial\psi^e}{\partial\eta_i}\Big|_{\boldsymbol{\varepsilon}_e} - \rho_0\frac{\partial\breve{\psi}^\theta}{\partial\eta_i} - \rho\frac{\partial\tilde{\psi}^\theta}{\partial\eta_i} + \sum \beta_{i0}\boldsymbol{\nabla}^2\eta_i\right). \tag{176}$$

5. Momentum balance equation

$$\nabla\cdot\boldsymbol{\sigma} + \rho\boldsymbol{f} = \rho\dot{\boldsymbol{v}}.\tag{177}$$

6. Boundary conditions for the order parameter

$$\boldsymbol{n}_i \cdot \frac{\partial\psi}{\partial\boldsymbol{\nabla}\eta_i} = H.\tag{178}$$

While the above equations are derived for an arbitrary nonlinear elasticity rule and relationship for dissipative stresses $\boldsymbol{\sigma}_d$, we specified them for linear anisotropic constitutive Eqs with $\boldsymbol{E}$ and $\boldsymbol{B}$ for fourth rank elastic moduli and viscosity tensors. Expressions for $\boldsymbol{\varepsilon}_t(\eta)$, $\boldsymbol{\varepsilon}_\theta(\theta,\eta)$, and $\boldsymbol{E}(\eta)$ are derived in [2], where a, a_θ, and a_E are the material parameters and subscript A and M designate austenite and martensite.

5.8.A Explicit Ginzburg-Landau equation for $P_1 - P_2$ PT

For stress induced case, We can rewrite Eq.(86) for stress induced case:

$$\begin{aligned}G(\theta,\eta_1) = A_{12}(\theta)\,q(\eta_1) &+ (\Delta G_2^\theta - \boldsymbol{\sigma}:\boldsymbol{\varepsilon}_{t2}) + \Delta G_{12}^\theta g(\eta_1)\\ &-(\boldsymbol{\sigma}:\boldsymbol{\varepsilon}_{t1} - \boldsymbol{\sigma}:\boldsymbol{\varepsilon}_{t2})g(\eta_1) + \frac{1}{2}\beta_{12}|\nabla\eta_1|^2\end{aligned}\tag{179}$$

where,

$$\begin{aligned}\Delta G_{12}^\theta &= \Delta G_1^\theta - \Delta G_2^\theta\\ A_{12}(\theta) &= A_1(\theta) + A_2(\theta) + \bar{A}\\ \beta_{12} &= (\beta_{10} + \beta_{20} - 2b)\end{aligned}\tag{180}$$

$$\begin{aligned}g(\eta_1) &= \eta_1^2(3 - 2\eta_1)\\ q(\eta_1) &= \eta_1^2(1 - \eta_1)^2\end{aligned}$$

$$\tag{181}$$

For two variants:

$$\dot{\eta}_1 = LX = L\left(\frac{\rho}{\rho_0}\boldsymbol{\sigma}_e:\frac{\partial\boldsymbol{\varepsilon}_t}{\partial\eta_1} - \rho_0\frac{\partial\breve{\psi}^\theta}{\partial\eta_1} - \rho\frac{\partial\tilde{\psi}^\theta}{\partial\eta_1} + \beta_{12}\boldsymbol{\nabla}^2\eta_1\right).\tag{182}$$

Here 1st term ,

$$\frac{\rho}{\rho_0}\boldsymbol{\sigma}_e\mathbf{:}\frac{\partial\boldsymbol{\varepsilon}_t}{\partial\eta_1} = 6\frac{\rho}{\rho_0}\left(\boldsymbol{\sigma}_e\mathbf{:}\boldsymbol{\varepsilon}_{t1} - \boldsymbol{\sigma}_e\mathbf{:}\boldsymbol{\varepsilon}_{t2}\right)\eta_1\left(1-\eta_1\right). \tag{183}$$

2nd term ,

$$\rho_0\frac{\partial\breve{\psi}^\theta}{\partial\eta_1} = 2\rho_0 A_{12}\eta_1\left(1-3\eta_1+2\eta_1^2\right). \tag{184}$$

3rd term ,

$$\rho\frac{\partial\tilde{\psi}^\theta}{\partial\eta_1} = 6\rho\left(\Delta G_1^\theta - \Delta G_2^\theta\right)\eta_1\left(1-\eta_1\right). \tag{185}$$

Complete G-L equation :

$$\frac{\dot{\eta}_1}{L} = 6\frac{\rho}{\rho_0}\left(\boldsymbol{\sigma}_e\mathbf{:}\boldsymbol{\varepsilon}_{t1} - \boldsymbol{\sigma}_e\mathbf{:}\boldsymbol{\varepsilon}_{t2}\right)\eta_1\left(1-\eta_1\right) - 2\rho_0 A_{12}\eta_1\left(1-3\eta_1+2\eta_1^2\right)$$
$$-6\rho\left(\Delta G_1^\theta - \Delta G_2^\theta\right)\eta_1\left(1-\eta_1\right) + \beta_{12}\boldsymbol{\nabla}^2\eta_1. \tag{186}$$

5.8.B Explicit Ginzburge-Lindau equation for $\mathsf{A}_1 - \mathsf{P}_1$ and $\mathsf{A}_1 - \mathsf{P}_2$ PT

For stress induced case We can rewrite Eq.(12) for stress induced case:

$$G(\boldsymbol{\sigma},\ \theta,\ \eta_1,\ \eta_2) = \left(\Delta\ G_1^\theta - \boldsymbol{\sigma}\mathbf{:}\boldsymbol{\varepsilon}_{t1}\right)g(\eta_1)\ +\left(\Delta\ G_2^\theta - \boldsymbol{\sigma}\mathbf{:}\boldsymbol{\varepsilon}_{t2}\right)g(\eta_2)$$
$$+A_1(\theta)\,q(\eta_1) + A_2(\theta)\,q(\eta_2) + \bar{A}\eta_1^2\,\eta_2^2 + K_{12}\,\eta_1^2\,\eta_2^2\left(1-\eta_1-\eta_2\right)^2$$
$$+\frac{1}{2}\left(\beta_{10}\left|\nabla\eta_1\right|^2 + \beta_{20}\left|\nabla\eta_2\right|^2 + 2b\,\nabla\eta_1.\nabla\eta_2\right); \tag{187}$$

Where

$$g(\eta) = \eta^2\left(3-2\,\eta\right)$$
$$q(\eta) = \eta^2\left(1-\eta\right)^2$$

$$\tag{188}$$

Complete system of equations for $\mathsf{A}_1 - \mathsf{P}_i$ PT

Below we collect the final complete system of equations for a $\mathsf{A}_1 - \mathsf{P}_i$ PT.

1. Kinematics

1.1. Decomposition of the strain tensor $\ \boldsymbol{\varepsilon}$; volumetric strain ε_0

$$\boldsymbol{\varepsilon} = (\overset{\circ}{\boldsymbol{\nabla}}\boldsymbol{u})_s;\quad \boldsymbol{\varepsilon} = \boldsymbol{\varepsilon}_e + \boldsymbol{\varepsilon}_t(\eta_1,\eta_2);\quad \frac{\rho_0}{\rho} = 1 + \varepsilon_0;\quad \varepsilon_0 = \boldsymbol{\varepsilon}\mathbf{:}\boldsymbol{I}. \tag{189}$$

1.2. Transformation strain $\boldsymbol{\varepsilon}_t$

$$\boldsymbol{\varepsilon}_t = \boldsymbol{\varepsilon}_{t1}\,\eta_1^2(3 - 2\eta_1) + \boldsymbol{\varepsilon}_{t2}\,\eta_2^2(3 - 2\eta_2). \tag{190}$$

2. Helmholtz free energy per unit mass and its contributions

$$\bar{\psi}(\boldsymbol{\varepsilon}, \eta_1, \eta_2, \theta, \boldsymbol{\nabla}\eta_1, \boldsymbol{\nabla}\eta_2) = \psi^e(\boldsymbol{\varepsilon}_0, e, \eta_1, \eta_2, \theta) + \frac{\rho_0}{\rho}\breve{\psi}^\theta + \tilde{\psi}^\theta + \tilde{\psi}^p + \frac{\rho_0}{\rho}\,^\nabla; \tag{191}$$

Barrier between phases:

$$\breve{\psi}^\theta = A_1\,\eta_1^2\,(1 - \eta_1)^2 + A_2\,\eta_2^2\,(1 - \eta_2)^2 + \bar{A}\,\eta_1^2\,\eta_2^2; \tag{192}$$

Driving force for phase transformation:

$$\tilde{\psi}^\theta = \Delta\,G_1^\theta\,\eta_1^2(3 - 2\eta_1) + \Delta\,G_2^\theta\,\eta_2^2(3 - 2\eta_2); \tag{193}$$

Penalty contribution:

$$\tilde{\psi}^p = K_{12}\,\eta_1^2\,\eta_2^2\,(1 - \eta_1 - \eta_2)^2; \tag{194}$$

Gradient energy:

$$^\nabla = \frac{1}{2}\,\left(\beta_{10}\,|\nabla\eta_1|^2 + \beta_{20}\,|\nabla\eta_2|^2 + 2b\,\nabla\eta_1\,.\nabla\eta_2\right); \tag{195}$$

3. Stress tensor

$$\boldsymbol{\sigma} = \boldsymbol{\sigma}_e + \boldsymbol{\sigma}_{st}; \tag{196}$$

$$\boldsymbol{\sigma}_e = \frac{\partial\,\psi^e}{\partial\,\boldsymbol{\varepsilon}_e} = \boldsymbol{E}{:}\boldsymbol{\varepsilon}_e. \tag{197}$$

Surface tension:

$$\begin{aligned}
\boldsymbol{\sigma}_{st} \quad &= (\breve{\psi}^\theta + \,^\nabla)\boldsymbol{I} - \beta_{10}\,\boldsymbol{\nabla}\eta_1 \otimes \boldsymbol{\nabla}\eta_1 - \beta_{20}\,\boldsymbol{\nabla}\eta_2 \otimes \boldsymbol{\nabla}\eta_2 - 2b\,\boldsymbol{\nabla}\eta_1 \otimes \boldsymbol{\nabla}\eta_2 \\
&= [A_1\,\eta_1^2\,(1 - \eta_1)^2 + A_2\,\eta_2^2\,(1 - \eta_2)^2 + \bar{A}\,\eta_1^2\,\eta_2^2 + \frac{1}{2}\,\beta_{10}\,|\nabla\eta_1|^2 \\
&\quad + \frac{1}{2}\,\beta_{20}\,|\nabla\eta_2|^2 + 2b\,\nabla\eta_1\,.\nabla\eta_2]\,\boldsymbol{I} - (\beta_{10}\,\boldsymbol{\nabla}\eta_1 \otimes \boldsymbol{\nabla}\eta_1 \\
&\quad\quad + \beta_{20}\,\boldsymbol{\nabla}\eta_2 \otimes \boldsymbol{\nabla}\eta_2 + 2b\,\boldsymbol{\nabla}\eta_1 \otimes \boldsymbol{\nabla}\eta_2); \tag{198}
\end{aligned}$$

4. Ginzburg–Landau equation

For two variants:

$\mathsf{A} - \mathsf{P}_1$ PT:

$$\dot{\eta}_1 = L_1 X_1 = L_1 \left(\frac{\rho}{\rho_0} \boldsymbol{\sigma}_e \colon \frac{\partial \boldsymbol{\varepsilon}_t}{\partial \eta_1} - \rho_0 \frac{\partial \breve{\psi}^\theta}{\partial \eta_1} - \rho \frac{\partial \tilde{\psi}^\theta}{\partial \eta_1} - \rho \frac{\partial \tilde{\psi}^p}{\partial \eta_1} + \beta_{10} \boldsymbol{\nabla}^2 \eta_1 + 2b \boldsymbol{\nabla}^2 \eta_2 \right). \qquad (199)$$

Here 1st term ,

$$\frac{\rho}{\rho_0} \boldsymbol{\sigma}_e \colon \frac{\partial \boldsymbol{\varepsilon}_t}{\partial \eta_1} = 6 \frac{\rho}{\rho_0} \left(\boldsymbol{\sigma}_e \colon \boldsymbol{\varepsilon}_{t1} \right) \eta_1 \left(1 - \eta_1 \right). \qquad (200)$$

2nd term ,

$$\rho_0 \frac{\partial \breve{\psi}^\theta}{\partial \eta_1} = 2 \rho_0 \left(A_1 \eta_1 \left(1 - 3\eta_1 + 2\eta_1^2 \right) + \bar{A} \eta_1 \eta_2^2 \right). \qquad (201)$$

3rd term ,

$$\rho \frac{\partial \tilde{\psi}^\theta}{\partial \eta_1} = 6 \rho \left(\Delta G_1^\theta \right) \eta_1 \left(1 - \eta_1 \right). \qquad (202)$$

.

4th term ,

$$\rho \frac{\partial \tilde{\psi}^p}{\partial \eta_1} = 2 \rho \, K_{12} \, \eta_1 \eta_2 \left(1 - \eta_1 - \eta_2 \right) \left[\eta_2 (1 - \eta_1 - \eta_2) - \eta_1 \eta_2 \right] \qquad (203)$$

Complete G-L equation $\mathsf{A}_1 - \mathsf{P}_1$ PT:

$$\frac{\dot{\eta}_1}{L_1} = 6 \frac{\rho}{\rho_0} \left(\boldsymbol{\sigma}_e \colon \boldsymbol{\varepsilon}_{t1} \right) \eta_1 \left(1 - \eta_1 \right) - 2 \rho_0 \left(A_1 \eta_1 \left(1 - 3\eta_1 + 2\eta_1^2 \right) + \bar{A} \eta_1 \eta_2^2 \right)$$
$$- 6 \rho \left(\Delta G_1^\theta \right) \eta_1 \left(1 - \eta_1 \right) - 2 \rho \, K_{12} \, \eta_1 \eta_2 \left(1 - \eta_1 - \eta_2 \right) \left[\eta_2 (1 - \eta_1 - \eta_2) - \eta_1 \eta_2 \right]$$
$$+ \beta_{10} \boldsymbol{\nabla}^2 \eta_1 + 2b \boldsymbol{\nabla}^2 \eta_2 \qquad (204)$$

$\mathsf{A} - \mathsf{P}_2$ PT:

$$\dot{\eta}_2 = L_2 X_2 = L_2 \left(\frac{\rho}{\rho_0} \boldsymbol{\sigma}_e \colon \frac{\partial \boldsymbol{\varepsilon}_t}{\partial \eta_2} - \rho_0 \frac{\partial \breve{\psi}^\theta}{\partial \eta_2} - \rho \frac{\partial \tilde{\psi}^\theta}{\partial \eta_2} - \rho \frac{\partial \tilde{\psi}^p}{\partial \eta_2} + \beta_{20} \boldsymbol{\nabla}^2 \eta_2 + 2b \boldsymbol{\nabla}^2 \eta_1 \right). \qquad (205)$$

Here 1st term ,

$$\frac{\rho}{\rho_0} \boldsymbol{\sigma}_e \colon \frac{\partial \boldsymbol{\varepsilon}_t}{\partial \eta_2} = 6 \frac{\rho}{\rho_0} \left(\boldsymbol{\sigma}_e \colon \boldsymbol{\varepsilon}_{t2} \right) \eta_2 \left(1 - \eta_2 \right). \qquad (206)$$

2nd term ,

$$\rho_0 \frac{\partial \breve{\psi}^\theta}{\partial \eta_2} = 2 \rho_0 \left(A_2 \eta_2 \left(1 - 3\eta_2 + 2\eta_2^2 \right) + \bar{A} \eta_2 \eta_1^2 \right). \qquad (207)$$

3rd term ,

$$\rho \frac{\partial \tilde{\psi}^\theta}{\partial \eta_2} = 6\rho \, (\Delta G_2^\theta) \, \eta_2 \, (1 - \eta_2). \tag{208}$$

. 4th term ,

$$\rho \frac{\partial \tilde{\psi}^p}{\partial \eta_2} = 2\rho \, K_{12}\eta_1\eta_2(1 - \eta_1 - \eta_2) \left[\eta_1(1 - \eta_1 - \eta_2) - \eta_1\eta_2\right] \tag{209}$$

Complete G-L equation $\mathsf{A} - \mathsf{P}_2$ PT:

$$\frac{\dot{\eta}_1}{L} = 6\frac{\rho}{\rho_0} \, (\boldsymbol{\sigma}_e{:}\boldsymbol{\varepsilon}_{t2}) \, \eta_2 \, (1 - \eta_2) - 2\rho_0 \left(A_2\eta_2 \, (1 - 3\eta_2 + 2\eta_2^2) + \bar{A}\eta_2\eta_1^2\right)$$
$$-6\rho \, (\Delta G_2^\theta) \, \eta_2 \, (1 - \eta_2) - 2\rho \, K_{12}\eta_1\eta_2(1 - \eta_1 - \eta_2) \left[\eta_1(1 - \eta_1 - \eta_2) - \eta_1\eta_2\right]$$
$$+\beta_{20}\boldsymbol{\nabla}^2\eta_2 + 2b\boldsymbol{\nabla}^2\eta_1 \tag{210}$$

5. Momentum balance equation

$$\nabla\cdot\boldsymbol{\sigma} + \rho\boldsymbol{f} = \rho\dot{\boldsymbol{v}}. \tag{211}$$

6. Boundary conditions for the order parameter

$$\boldsymbol{n}_i \cdot \frac{\partial \psi}{\partial \boldsymbol{\nabla}\eta_i} = H. \tag{212}$$

5.9 Generalized theory for multivarient transformation

We will use the following expression for the isotropic gradient energy [5]:

$$\rho_0\psi^\nabla = \sum_{i=1}^n \frac{\beta_{i0}}{2}|\boldsymbol{\nabla}\eta_i|^2 + b\sum_{i=1}^n \sum_{j=1,i\neq j}^n \boldsymbol{\nabla}\eta_i \cdot \boldsymbol{\nabla}\eta_j. \tag{213}$$

the expression for stress tensor:

$$\boldsymbol{\sigma} = \rho_0\frac{\partial \bar{\psi}}{\partial \boldsymbol{\varepsilon}} - \sum_{i=1}^n (\beta_{i0} \, \boldsymbol{\nabla}\eta_i \otimes \boldsymbol{\nabla}\eta_i + b\boldsymbol{\nabla}\eta_i \otimes \sum_{j=1,i\neq j}^n \boldsymbol{\nabla}\eta_j) + \boldsymbol{\sigma}_d. \tag{214}$$

driving force for change in η_i, and then in the simplest Ginzburg-Landau equation $\dot{\eta}_j = L_{ji}X_i$, leads to

$$\dot{\eta}_j = L_{ji}\left(-\rho\frac{\partial \bar{\psi}}{\partial \eta_i} + (\beta_{i0}\boldsymbol{\nabla}^2\eta_i + b\sum_{k=1,k\neq i}^n \boldsymbol{\nabla}^2\eta_k)\right), \quad L_{ji} = L_{ij}; \quad j = 1,...,n. \tag{215}$$

Thus, the kinetic equations for the order parameters for $b \neq 0$ are coupled through Laplacians in addition to traditional coupling through the local energy terms and transformation strain. The expression for the Helmholtz free energy in the form :

$$\bar{\psi}(\boldsymbol{\varepsilon}, \eta_i, \theta, \boldsymbol{\nabla}\eta_i) = \psi^e(\boldsymbol{\varepsilon} - \boldsymbol{\varepsilon}_t(\eta_i) - \boldsymbol{\varepsilon}_\theta(\theta, \eta_i), \eta_i, \theta) + \frac{\rho_0}{\rho}\breve{\psi}^\theta + \tilde{\psi}^\theta + \frac{\rho_0}{\rho} \ \nabla. \tag{216}$$

where,

$$\breve{\psi}^\theta = \sum_{i=1}^{n} A_i(\theta)\eta_i^2(1-\eta_i)^2 + \sum_{i=1}^{n-1}\sum_{j=i+1}^{n} \bar{A}_{ij}\eta_i^2\,\eta_j^2. \tag{217}$$

$$\tilde{\psi}^\theta = \sum_{i=1}^{n} \Delta G_i^\theta(\theta)\eta_i^2(3-2\eta_i)) + \sum_{i=1}^{n-1}\sum_{j=i+1}^{n} Z_{ij}. \tag{218}$$

$$Z_{ij} = K_{ij}\left(\eta_i + \eta_j - 1\right)^2 \eta_i^2\eta_j^2. \tag{219}$$

Similarly, we obtain for the stress tensor and its elastic and interface tension components:

$$\boldsymbol{\sigma} = \boldsymbol{\sigma}_e + \boldsymbol{\sigma}_{st} + \boldsymbol{\sigma}_d; \qquad \boldsymbol{\sigma}_e = \rho_0\frac{\partial \psi^e}{\partial \boldsymbol{\varepsilon}_e}. \tag{220}$$

$$\boldsymbol{\sigma}_{st} = \rho_0(\psi^\nabla + \breve{\psi}_\theta)\boldsymbol{I} - \sum_{i=1}^{n}(\beta_{i0}\boldsymbol{\nabla}\eta_i \otimes \boldsymbol{\nabla}\eta_i + b\boldsymbol{\nabla}\eta_i \otimes \sum_{j=1,i\neq j}^{n} \boldsymbol{\nabla}\eta_j). \tag{221}$$

At the $\mathsf{P}_i - \mathsf{P}_j$ diffuse interface, all $\eta_k = 0$ for $k \neq i$ and $k \neq j$. Also, $\boldsymbol{n}_i = \dfrac{\boldsymbol{\nabla}\eta_i}{|\boldsymbol{\nabla}\eta_i|} = -\boldsymbol{n}_j = -\dfrac{\boldsymbol{\nabla}\eta_j}{|\boldsymbol{\nabla}\eta_j|}$. Consequently, at the $\mathsf{P}_i - \mathsf{P}_j$ diffuse interface one has

$$\rho_0\psi^\nabla = \frac{\beta_{i0}}{2}|\boldsymbol{\nabla}\eta_i|^2 + \frac{\beta_{j0}}{2}|\boldsymbol{\nabla}\eta_j|^2 + b\boldsymbol{\nabla}\eta_i \cdot \boldsymbol{\nabla}\eta_j = \frac{(\beta_{i0} + \beta_{j0} - 2b)}{2}|\boldsymbol{\nabla}\eta_i|^2 = \frac{\beta_{ji}}{2}|\boldsymbol{\nabla}\eta_i|^2. \tag{222}$$

$$\boldsymbol{\sigma}_{st} = \rho_0(\psi^\nabla + \breve{\psi}_\theta)\boldsymbol{I} - (\beta_{i0}\,\boldsymbol{\nabla}\eta_i \otimes \boldsymbol{\nabla}\eta_i + \beta_{j0}\,\boldsymbol{\nabla}\eta_j \otimes \boldsymbol{\nabla}\eta_j + 2b\boldsymbol{\nabla}\eta_i \otimes \boldsymbol{\nabla}\eta_j) \tag{223}$$

Thus, at the structure of the expression for surface tension for the $\mathsf{P}_i - \mathsf{P}_j$ diffuse interface is completely similar to that for the $\mathsf{A} - \mathsf{P}$ interface .

After substitution of all contributions in the Ginzburg-Landau equation, one obtains

$$\dot{\eta}_j = L_{ji}\left(\frac{\rho}{\rho_0}\boldsymbol{\sigma}_e{:}\frac{\partial\boldsymbol{\varepsilon}_t}{\partial\eta_i} + \frac{\rho}{\rho_0}\boldsymbol{\sigma}_e{:}\frac{\partial\boldsymbol{\varepsilon}_\theta}{\partial\eta_i} - \rho\frac{\partial\psi^e}{\partial\eta_i}\Big|_{\boldsymbol{\varepsilon}_e} - \rho_0\frac{\partial\breve{\psi}^\theta}{\partial\eta_i} - \rho\frac{\partial\tilde{\psi}^\theta}{\partial\eta_i} + (\beta_{i0}\boldsymbol{\nabla}^2\eta_i + b\sum_{k=1,k\neq i}^{n}\boldsymbol{\nabla}^2\eta_k)\right) \tag{224}$$

Similar to the single-variant case.

In this section, we develop PFA, which with high and controllable accuracy satisfy all the desired conditions for arbitrary n phases. We utilize the same order parameters η_i like

for martensitic PT and, instead of explicit constraints, include in the simplest potential the terms that penalize deviation of the trajectory in the order parameter space from the straight lines connecting each two phases. These penalizing terms do not contribute to the instability conditions and strictly speaking correct PT criteria follow from the instability conditions for $O \leftrightarrow P_i$ PT only. However, when the magnitude of the penalizing term grows to infinity and impose strict constraint $\eta_i + \eta_j = 1$ and $\eta_k = 0$ for all $k \neq i, j$, correct PT conditions for $P_i \leftrightarrow P_j$ PTs do follow from the instability conditions. Since for a finite magnitude such a constraint is applied approximately only, there is some deviation from the ideal equilibrium phases and PT conditions. However, numerical simulations for the almost worst cases demonstrate that these deviations are indeed small. This PFA allows analytical solution for interfaces between each two phases, which can be used to calibrate interface, width, energy, and mobility; it allows for the first time for a multiphase system to include consistent expression for interface stresses for each interface; it includes or excludes the third phase within interface between two phases phased thermodynamic and kinetic consideration.

We designate contractions of tensors $\boldsymbol{A} = \{A_{ij}\}$ and $\boldsymbol{B} = \{B_{ji}\}$ over one and two indices as $\boldsymbol{A \cdot B} = \{A_{ij} B_{jk}\}$ and $\boldsymbol{A:B} = A_{ij} B_{ji}$, respectively. The subscript s mean symmetrization, the superscript T designates transposition, the sub- and superscripts e, th, and t mean elastic, thermal, and transformational strains, and $\boldsymbol{\nabla}$ and $\boldsymbol{\nabla}_0$ are the gradient operators in the *deformed* and undefromed states.

For simplicity and compactness, the small strains will be considered but with some minimal geometric nonlinearities required to introduce interface stresses [6, 8, 9]. Generalization for large strain is straightforward [4, 9] and the model problem will be solved in large strain formulation. The Helmholtz free energy per unit undeformed volume has the following form:

$$= \frac{\rho_0}{\rho_t} \psi^e(\boldsymbol{\varepsilon}_e, \eta_i, \theta) + \frac{\rho_0}{\rho} \breve{\psi}^\theta + \tilde{\psi}^\theta + \frac{\rho_0}{\rho} \nabla + {}_p. \tag{225}$$

$$\breve{\psi}^\theta = \sum A_i(\theta) \eta_i^2 (1 - \eta_i)^2 + \sum \bar{A}_{ij} \eta_i^2 \eta_j^2; \tag{226}$$

$$\tilde{\psi}^\theta = \sum \Delta G_i^\theta(\theta) q(\eta_i); \quad q(\eta_i) = \eta_i^2(3 - 2\eta_i); \tag{227}$$

$$\psi_p = \sum K_{ij} (\eta_i + \eta_j - 1)^2 \eta_i^l \eta_j^l + \sum K_{ijk} \eta_i^2 \eta_j^2 \eta_k^2; \quad l \geq 2. \tag{228}$$

$$\psi^e = \boldsymbol{\varepsilon}_e : \boldsymbol{E}(\eta_i) : \boldsymbol{\varepsilon}_e; \qquad \boldsymbol{E}(\eta_i) = \boldsymbol{E}_0 + \sum (\boldsymbol{E}_i - \boldsymbol{E}_0) q(\eta_i); \tag{229}$$

$$\triangledown = \sum 0.5\beta_{ij}\boldsymbol{\nabla}\eta_i \cdot \boldsymbol{\nabla}\eta_j. \tag{230}$$

$$\boldsymbol{\varepsilon} = (\boldsymbol{\nabla}_0\boldsymbol{u})_s = \boldsymbol{\varepsilon}_e + \boldsymbol{\varepsilon}_t(\eta_i) + \boldsymbol{\varepsilon}_\theta(\theta,\eta_i); \quad \frac{\rho_0}{\rho} = 1 + \varepsilon_0; \quad \varepsilon_0 = \boldsymbol{\varepsilon}\!:\!\boldsymbol{I}; \quad \frac{\rho_0}{\rho_t} = 1 + (\boldsymbol{\varepsilon}_t + \boldsymbol{\varepsilon}_\theta)\!:\!\boldsymbol{I} \tag{231}$$

$$\boldsymbol{\varepsilon}_t = \sum \boldsymbol{\varepsilon}_{ti}q(\eta_i); \quad \boldsymbol{\varepsilon}_\theta = \boldsymbol{\varepsilon}_{\theta 0} + \sum (\boldsymbol{\varepsilon}_{\theta i} - \boldsymbol{\varepsilon}_{\theta 0})\,q(\eta_i). \tag{232}$$

Here θ is the temperature, $\boldsymbol{u}$ is the displacements, ΔG_i^θ is the difference in the thermal energy between P_i and O, A_i and $\bar{A}_{ij}$ are the double-well barriers between P_i and O and between P_i and P_j, $\boldsymbol{\varepsilon}_{ti}$ and $\boldsymbol{\varepsilon}_{\theta i}$ are the transformation and thermal strains of P_i, $\boldsymbol{\varepsilon}_{\theta 0}$ is the thermal strains of O; ρ, ρ_0, and ρ_t are the mass densities in the deformed, undeformed, and stress-free states, β_{ij} are the gradient energy coefficients, respectively, and ψ^e is the elastic energy; each coefficient, $\bar{A}_{ij}$, $\bar{A}_{ij}$, and K_{ijk}, is equal to zero if two subscripts coincide. Despite small strain approximation, we keep some geometrically nonlinear terms (ρ_0/ρ_t, ρ_0/ρ, and gradient $\boldsymbol{\nabla}$ with respect to deformed state) in order to correctly reproduce interface and elastic stresses.

Application of the thermodynamic laws and linear kinetics (see, e.g. [6, 8, 9]) results in

$$\boldsymbol{\sigma} = \boldsymbol{\sigma}_e + \boldsymbol{\sigma}_{st}; \qquad \boldsymbol{\sigma}_e = \frac{\rho}{\rho_0}\frac{\partial\psi^{\mathrm{e}}}{\partial\boldsymbol{\varepsilon}_e}. \tag{233}$$

$$\boldsymbol{\sigma}_{st} = (\psi^\nabla + \breve{\psi}_\theta)\boldsymbol{I} - \sum \beta_{ij}\boldsymbol{\nabla}\eta_i \otimes \boldsymbol{\nabla}\eta_j; \tag{234}$$

$$\dot{\eta}_i = L_{ij}X_j = L_{ij}\left(\boldsymbol{\sigma}_e\!:\!\frac{\partial(\boldsymbol{\varepsilon}_t + \boldsymbol{\varepsilon}_\theta)}{\partial\eta_j} - \frac{\partial\psi}{\partial\eta_j} + \sum \beta_{ij}\boldsymbol{\nabla}^2\eta_j\right); \quad L_{ij} = L_{ji}, \tag{235}$$

where X_i is the thermodynamic driving force to change η_i, L_{ij} are the kinetic coefficients, and $\boldsymbol{\sigma}$ is the true Cauchy stress tensor. We designate the set of the arbitrary order parameters as $\tilde{\eta} = (\eta_1, ..., \eta_i, ..., \eta_n)$, with $\hat{\eta}_0 = (0, ..., 0)$ for O and $\hat{\eta}_i = (0, ..., \eta_i = 1, ..., 0)$ for P_i, and with $\bar{\eta}_i = (0, ..., \eta_i, ..., 0)$ for one nonzero parameter only. It is easy to check that O and P_i are homogeneous solutions of the Ginzburg-Landau equations (235) for arbitrary stresses and temperature; consequently, the transformation strain for any PT is independent of stresses and temperature.

Without the term ψ_p, the local part of free energy is much simpler than in [2, 3] and does not contain interaction between phases. The terms with K_{ijk} penalize presence of three phases at the same material point. By increasing K_{ijk} one can control and, in particular, completely exclude the third phase within interface between two other phases. For homogeneous states, this term always excludes presence of three phases at the same point, because it increases energy in comparison with two-phase state. The terms with K_{ij} penalize deviations from hyperplanes

$\eta_i = 0$ and $\eta_i + \eta_j = 1$ and exponent l determines relative weight of these penalties. In combination with penalization of more than two phases, this constraint penalizes deviation from the desirable transformation paths: along coordinate lines $\bar{\eta}_i$ along which $O \leftrightarrow P_i$ PTs occur, and lines $\eta_i + \eta_j = 1$, $\eta_k = 0\ \forall k \neq i, j$, along which $P_i \leftrightarrow P_j$ PTs occur. In such a way, we do not need to impose explicit constraint $\sum \eta_i = 1$ and will be able to (approximately) satisfy all desired conditions, including instability conditions. Note that there is no need for penalizing $\eta_i = 0$; however, for $l = 0$ the term with K_{ij} produces undesired contribution to ψ for $\eta_i = 0$.

For compactness, instability conditions will be presented for the case with the same elastic moduli of all phases and $\rho_0 \simeq \rho$. Since $\partial X_i / \partial \eta_j(\hat{\eta}_k) = 0$, instability conditions for thermodynamically equilibrium homogeneous phases result in the following PT criteria:

$$O \to P_i: \quad \partial X_i(\hat{\eta}_0)/\partial \eta_i \geq 0 \to \boldsymbol{\sigma}_e{:}(\boldsymbol{\varepsilon}_{ti} + \boldsymbol{\varepsilon}_{\theta i} - \boldsymbol{\varepsilon}_{\theta 0}) - \Delta G_i^\theta \geq A_i(\theta)/3; \quad (236)$$

$$P_i \to O: \quad \partial X_i(\hat{\eta}_i)/\partial \eta_i \geq 0 \to \boldsymbol{\sigma}_e{:}(\boldsymbol{\varepsilon}_{ti} + \boldsymbol{\varepsilon}_{\theta i} - \boldsymbol{\varepsilon}_{\theta 0}) - \Delta G_i^\theta \leq -A_i(\theta)/3; \quad (237)$$

$$P_j \to P_i: \quad \partial X_i(\hat{\eta}_j)/\partial \eta_i \geq 0 \to \boldsymbol{\sigma}_e{:}(\boldsymbol{\varepsilon}_{ti} + \boldsymbol{\varepsilon}_{\theta i} - \boldsymbol{\varepsilon}_{\theta 0}) - \Delta G_i^\theta \geq (A_i(\theta) + \bar{A})/3 \Rightarrow \text{ wrong.} (238)$$

While conditions for $O \leftrightarrow P_i$ PTs are logical (work of stress on jump in transformation and thermal strains exceeds some threshold), condition for $P_j \to P_i$ does not contain information about phase P_j, which is contradictory. Since first and second derivatives of ψ_p are zero for O and P_i, these terms do not change phase equilibrium and instability conditions for homogeneous phases. However, as we will see below, these terms play key role in the development of noncontradictory and flexible PFA.

If $O \leftrightarrow P_i$ PT is considered only with all other $\eta_j = 0$, Eqs. (226)-(230) simplify:

$$\breve{\psi}^\theta = A_i(\theta)\eta_i^2(1 - \eta_i)^2; \quad \tilde{\psi}^\theta = \Delta G_i^\theta(\theta)q(\eta_i); \quad \psi_p = 0; \quad {}^\nabla = 0.5\beta_{ii}\boldsymbol{\nabla}\eta_i \cdot \boldsymbol{\nabla}\eta_i. \quad (239)$$

$$\boldsymbol{E}(\eta_i) = \boldsymbol{E}_0 + (\boldsymbol{E}_i - \boldsymbol{E}_0)q(\eta_i); \quad \boldsymbol{\varepsilon}_t = \boldsymbol{\varepsilon}_{ti}q(\eta_i); \quad \boldsymbol{\varepsilon}_\theta = \boldsymbol{\varepsilon}_{\theta 0} + (\boldsymbol{\varepsilon}_{\theta i} - \boldsymbol{\varepsilon}_{\theta 0})q(\eta_i). \quad (240)$$

$$\boldsymbol{\sigma}_{st} = (\psi^\nabla + \breve{\psi}_\theta)\boldsymbol{I} - \beta_{ii}\boldsymbol{\nabla}\eta_i \otimes \boldsymbol{\nabla}\eta_i; \quad (241)$$

$$\dot{\eta}_i = L_{ii}\left(\boldsymbol{\sigma}_e{:}(\boldsymbol{\varepsilon}_{ti} + \boldsymbol{\varepsilon}_{\theta i} - \boldsymbol{\varepsilon}_{\theta 0})\frac{dq}{d\eta_i} - \frac{\partial \psi}{\partial \eta_i} + \sum \beta_{ii}\boldsymbol{\nabla}^2\eta_i\right). \quad (242)$$

These equations possess all desired properties [2–4] of two-phase models.

Next, we consider how to make description of $P_j \rightarrow P_i$ PTs completely similar to that of $O \leftrightarrow P_i$ PTs. Let us increase parameters K_{ij} and K_{ijk} to very high value so that they impose constraints $\eta_i + \eta_j = 1$ and $\eta_k = 0 \; \forall k \neq i, j$. Substituting these constraints in Eq. (225) and taking into account the following properties of function q, $q(1 - \eta_i) = 1 - q(\eta_i)$ (we could not find any other low-degree polynomial that satisfies this condition, which is crucial for our PFA), we reduce all equations to the single order parameter:

$$\breve{\psi}^\theta = A_{ij}(\theta)\eta_i^2(1 - \eta_i)^2; \quad A_{ij} = A_i + A_j + \bar{A}_{ij}; \tag{243}$$

$$\tilde{\psi}^\theta = \Delta G_j^\theta + \Delta G_{ij}^\theta(\theta)q(\eta_i); \quad \Delta G_{ij}^\theta = \Delta G_i^\theta - \Delta G_j^\theta; \tag{244}$$

$$\boldsymbol{E}(\eta_i) = \boldsymbol{E}_j + (\boldsymbol{E}_i - \boldsymbol{E}_j)q(\eta_i); \tag{245}$$

$$^\nabla = 0.5b_{ij}\boldsymbol{\nabla}\eta_i \cdot \boldsymbol{\nabla}\eta_i; \quad b_{ij} = \beta_{ii} + \beta_{jj} - \beta_{ij}. \tag{246}$$

$$\boldsymbol{\varepsilon}_t = \boldsymbol{\varepsilon}_{tj} + (\boldsymbol{\varepsilon}_{ti} - \boldsymbol{\varepsilon}_{tj})q(\eta_i); \quad \boldsymbol{\varepsilon}_\theta = \boldsymbol{\varepsilon}_{\theta j} + (\boldsymbol{\varepsilon}_{\theta i} - \boldsymbol{\varepsilon}_{\theta j})q(\eta_i). \tag{247}$$

$$\boldsymbol{\sigma}_{st} = (\psi^\nabla + \breve{\psi}_\theta)\boldsymbol{I} - \beta_{ij}\boldsymbol{\nabla}\eta_i \otimes \boldsymbol{\nabla}\eta_i; \quad l_{ij} = (L_{ii}L_{jj} - L_{ij}^2)/(L_{jj} + L_{ij}); \tag{248}$$

$$\dot{\eta}_i = l_{ij}\left(\boldsymbol{\sigma}_e{:}(\boldsymbol{\varepsilon}_{ti} + \boldsymbol{\varepsilon}_{\theta i} - \boldsymbol{\varepsilon}_{tj} - \boldsymbol{\varepsilon}_{\theta j})\frac{dq}{d\eta_i} - \frac{\partial\psi}{\partial\eta_i} + \sum\beta_{ii}\boldsymbol{\nabla}^2\eta_i\right). \tag{249}$$

$$P_j \rightarrow P_i: \quad \partial X_i(\hat{\eta}_j)/\partial\eta_i \geq 0 \rightarrow \boldsymbol{\sigma}_e{:}(\boldsymbol{\varepsilon}_{ti} + \boldsymbol{\varepsilon}_{\theta i} - \boldsymbol{\varepsilon}_{tj} - \boldsymbol{\varepsilon}_{\theta j}) - \Delta G_{ij}^\theta \geq A_{ij}(\theta)/3. \tag{250}$$

It is evident that Eqs.(243)-(250) for $P_j \rightarrow P_i$ PTs are non-contradictory (i.e., contain an expected combination of parameters of P_j and P_i) and coincide to within constants and designations with Eqs.(239)-(242) for $O \leftrightarrow P_i$ PTs, i.e., they are as good as equations for $O \leftrightarrow P_i$ PTs. Thus, our goal is achieved.

Note that instability condition (250) works in the limit $K_{ij} \rightarrow \infty$; for finite K_{ij} it is imposed approximately only. To better understand interaction between instability conditions (238) and (250), we consider some examples. We consider the case when PT conditions for $O \leftrightarrow P_i$ PTs (238), (238) and (250) for $P_j \rightarrow P_i$ PT are not met, but when wrong condition (238) is fulfilled with quite large deviation from stability region. Under such conditions, P_j loses its stability, but instead of transforming to P_j, the local energy minimum slightly shifts from $\eta_1 = 1; \eta_2 = 0$ to close point $\eta_1 = 0.989; \eta_2 = 0.019$ (Fig. 9). There is an energy barrier (saddle point) between P_j and P_i and until it disappears (i.e., correct condition (250) for $P_j \rightarrow P_i$ PT is met), $P_j \rightarrow P_i$ PT is impossible. Thus, approximate character of the imposed constraint

through the penalty term exhibits itself in slight shift of the local minimum from P_j to some very close point, which should essentially not affect accuracy of simulations. If PT conditions
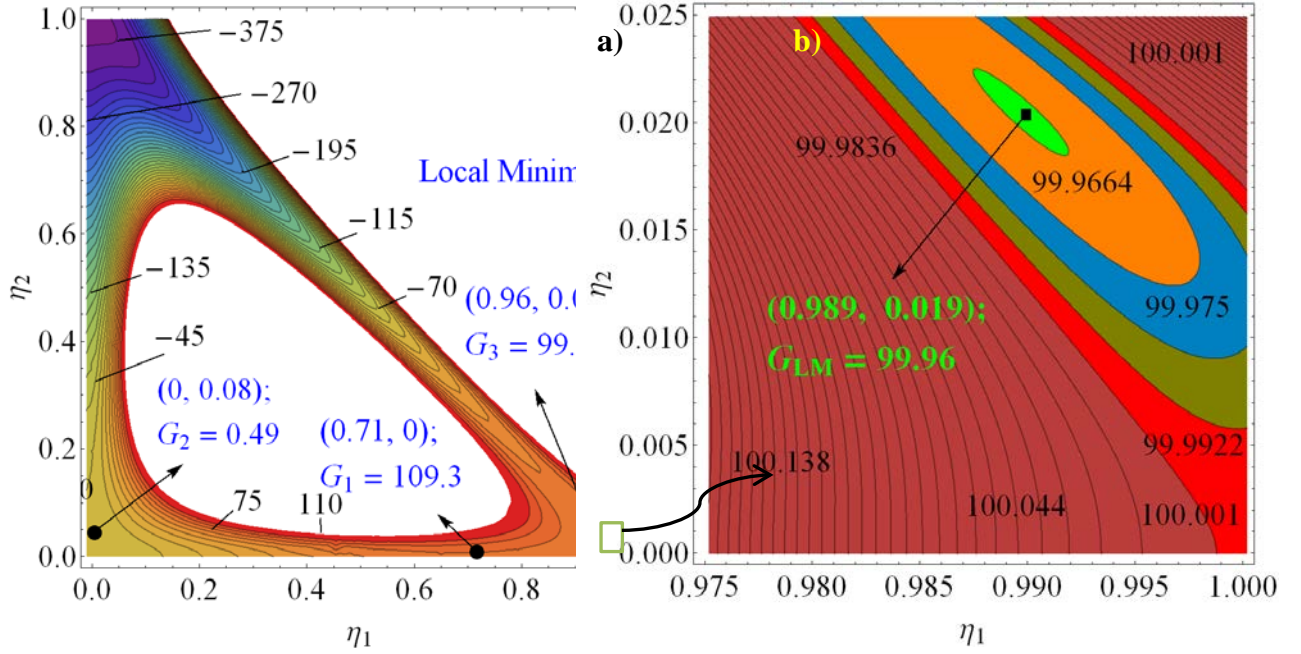

Figure 9: Energy level plot of the free energy at zero stresses for $A_1 + 3\Delta G_1^\theta = 1000$, $A_1 - 3\Delta G_1^\theta = 400$, $A_2 + 3\Delta G_2^\theta = 230$, $A_2 - 3\Delta G_2^\theta = 2570$, $\bar{A} + A_1(\theta) + 3\Delta G_1^\theta = -250$ and $A_{21}(\theta) - 3G_{21}^\theta = 150$, all in J/m^3 ; (b) the zoomed part of the plot near P_1 .

for $O \leftrightarrow P_i$ PTs (238) and (238) are not fulfilled but correct condition (250) for $P_j \rightarrow P_i$ PT is met, then these equations results in $\bar{A} < 0$. It is easy to show that in this case the wrong $P_j \rightarrow P_i$ PT condition (238) should be also fulfilled. Thus, if correct $P_j \rightarrow P_i$ PT condition is met, this PT will occur.

Due to equivalence of all equations for $O \leftrightarrow P_i$ and $P_j \rightarrow P_i$ PTs, analytical solution for any propagating with velocity c interface is [12]:

$$\eta = 0.5 \tanh\left[3(x - ct)/\delta\right] + 0.5; \quad \delta = \sqrt{18\beta/A_i(\theta)}; \quad c = \delta\Delta G^\theta(\theta)/L; \quad \gamma = \beta/\delta, \quad (251)$$

where δ and γ are the interface width and energy. In contrast to solutions for other interpolating functions q [6, 8, 9], interface width and energy are independent of $\Delta G^\theta(\theta)$. That is why $\check{\psi}^\theta$ and interface stresses $\boldsymbol{\sigma}_{st}$ are also independent of $\Delta G^\theta(\theta)$. Eq.(251) allow to calibrate for each phase $A_i(\theta)$, β, and L when width, energy, and mobility of interfaces between each pair of phases are known.

5.10 Simulation Results

Obtained system of equations have been solved with the help of finite element code COM-SOL for various problems. We solved exactly the same problem on evolution of two-variant microstructure in NiAl alloy during martensitic PT including tip bending and splitting in martensitic variants as in [7]. Note that the theory in [7] for two variants satisfies all required conditions exactly but cannot be generalized for more than two variant. Some material parameters (like $\boldsymbol{E}$, $\boldsymbol{\varepsilon}_{ti}$, $\Delta G^{\theta}(\theta)$, θ_e, Δs) here have been chosen the same as in [7]; other ($A_{ij}(\theta)$, $\beta_{ij}(\theta)$, L_{ij}, θ_c) are chosen in way to get the temperature dependence of the energy, width, and mobility of all interfaces, and temperature for the loss of stability of P like in [7]. In our example simulations, we use the material parameters for the cubic to tetragonal PT in NiAl found in [2]: $\Delta s_0 = 1.46 MPaK^{-1}$, $\theta_e = 125$ K, unless other stated. These parameters correspond to a twin interface energy $E_{12} = 0.978 J/m^2$ and width $\Delta_{12} = 0.927$ nm. Isotropic linear elasticity is used for simplicity; Young's modulus $E = 177.034 GPa$ and Poisson's ratio $\nu = 0.238$. The equilibrium equation $\boldsymbol{\nabla} \cdot \boldsymbol{\sigma} = 0$ is utilized. In the plane stress 2D problems, only P_1 and P_2 are considered; the corresponding transformation strains in the cubic axes are $\boldsymbol{\varepsilon}_{t1} = (0.125, -0.078, -0.078)$ and $\boldsymbol{\varepsilon}_{t2} = (-0.078, 0.125, -0.078)$. The FEM approach was developed and incorporated in the COMSOL code. All lengths, stresses, and times are given in units of nm, GPa, and ps. All external stresses are normal to the deformed surface

Example 1

$P_1 \leftrightarrow P_1$ Interface Problem

Here, we consider $P_1 \leftrightarrow P_1$ interface problem and investigate the effect of K_{12} on order parameter distribution (Figs.6, 7). Ideally, $1 - \eta_1 - \eta_2$ should be equal to zero. But we observed as we increase the value of K_{12}, the quantity $1 - \eta_1 - \eta_2$ goes to zero. That's validate the correctness of the formulation.
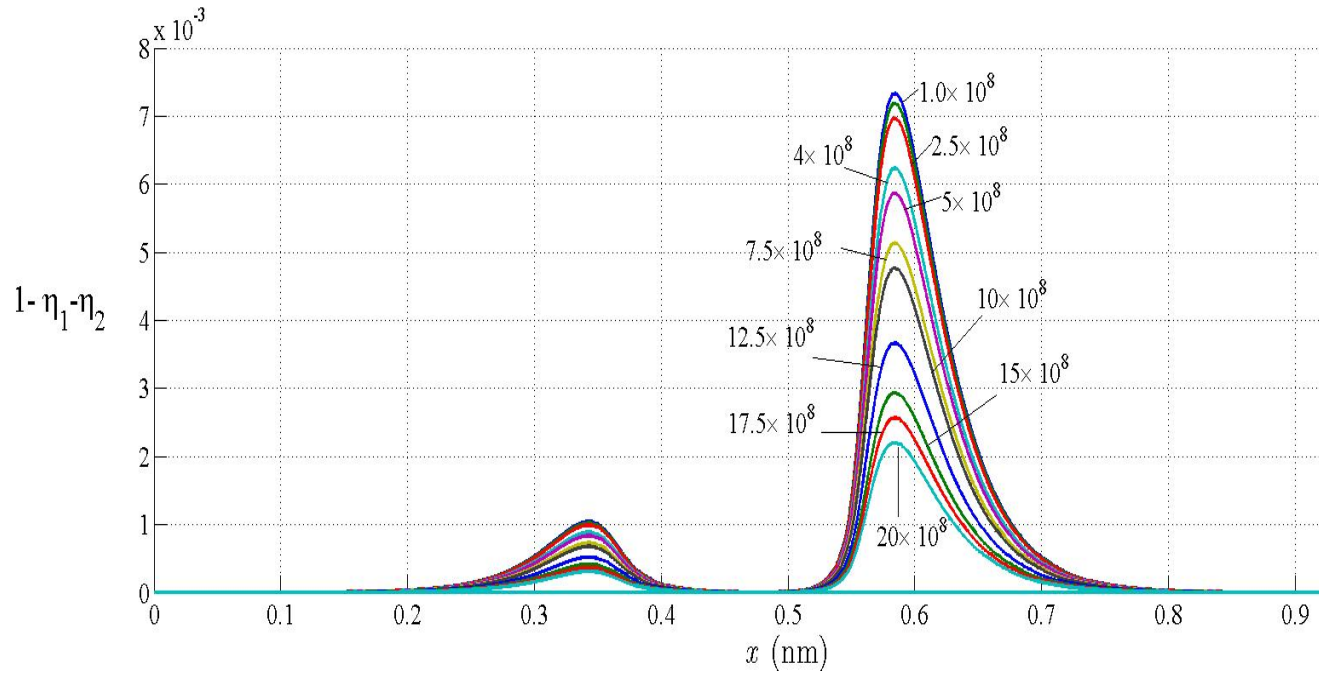
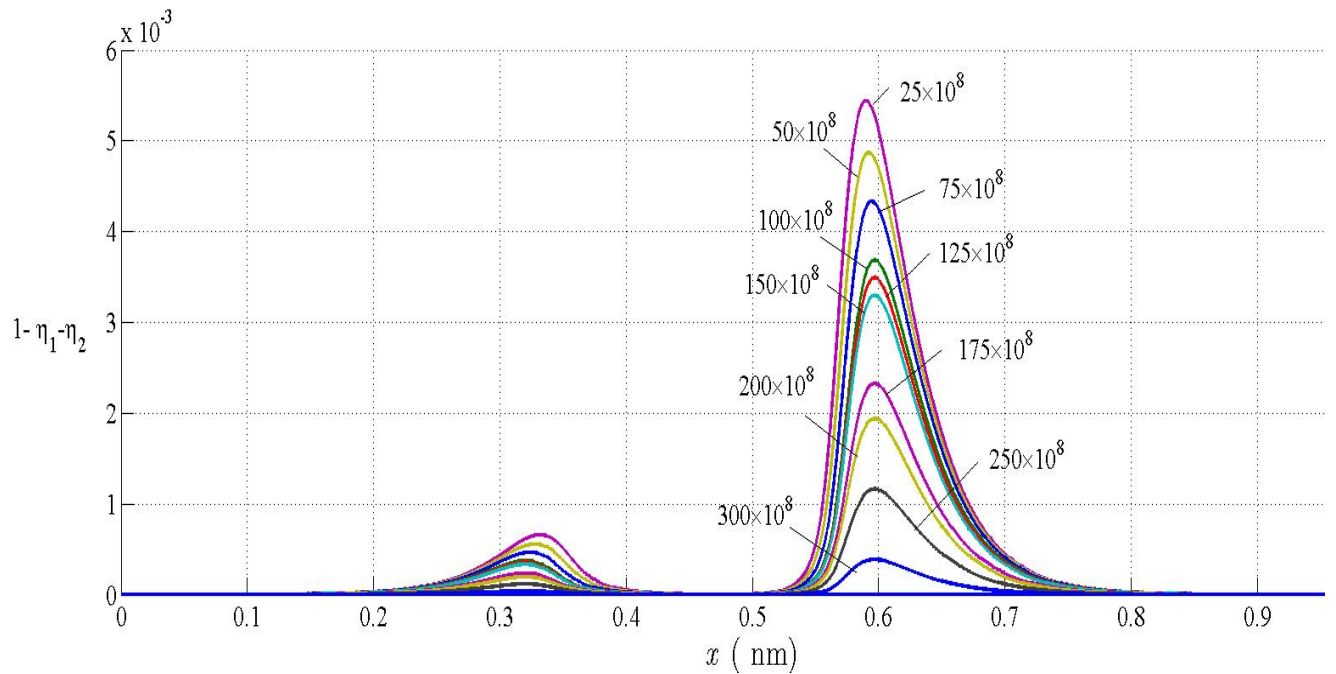Levitasetal-PRB-twin-13

Figure 10: Distribution of $1-\eta_1-\eta_2$ along the mid section of sample for $\mathsf{P}_1 \leftrightarrow \mathsf{P}_1$ transformation. K_{12} varies from 1.0×10^8 to 20.0×10^8

Figure 11: Distribution of $1-\eta_1-\eta_2$ along the mid section of sample for $\mathsf{P}_1 \leftrightarrow \mathsf{P}_1$ transformation. K_{12} varies from 20.0×10^8 to 300.0×10^8

The solution to a benchmark problem is described in [7] and main results are presented here. We consider a square 50×50 sample with the austenite lattice rotated by $\alpha = 45^o$ at $\theta = 50K$. On one horizontal and one vertical surface, a roller support (zero normal displacements and zero shear stresses) was used. Homogeneous normal displacements at the other two surfaces were prescribed and held constant during the simulations, resulting in a biaxial normal strain of 0.01. Shear stresses were kept at zero on the external surfaces. The stationary solution from Fig.3 [7] was taken as an initial condition for the problem with the following modifications: temperature was reduced to $\theta = 0K$; the parameter β_{12} was reduced to $\beta_{12} = 5.18 \times 10^{-11} \, N$, which led to a twin interface energy $E_{12} = 0.303 J/m^2$ and width $\Delta_{12} = 0.263 nm$; the components of the transformation strain have been changed to the values $\boldsymbol{U}_{t1} = (1.15, 0.93, 0.93)$ and $\boldsymbol{U}_{t2} = (0.93, 1.15, 0.93)$ corresponding to NiAl alloy in [18]; . Due to the reduction in the interface energy, the number of twins increased by splitting of the initial twins (Figs. 14, 15). Without austenite, the rigid vertical boundaries led to a high elastic energy. That is why restructuring produced vertical twins near each of the vertical sides in proportion, reducing the energy of elastic stresses due to the prescribed horizontal strain. When the microstructure transformed to fully formed twins separated by diffuse interfaces, narrowing and bending of the tips of the horizontal P_2 plates was observed (Figs. 8c and 9c), as in experiments [?] and strain-based simulations [11]. Since the invariant plane interface between P_1 and P_2 requires mutual rotation of these variants by the angle $\omega = 12.1^o$ ($\cos \omega = 2k_1 k_2/(k_1^2 + k_2^2) = 0.9778$) [18], the angle between the horizontal and vertical P_2 variants is $1.5\,\omega = 18.15^o$, which is in good agreement with our simulations. Measured angles between the tangent to the bent tip and the horizontal line in the experiment [18] and calculations (Fig. 14c,15c) are in good quantitative agreement.Here we consider two cases corresponding $K_{12} = 1.5 \times 10^{12}$ (Fig. 14) and $K_{12} = 7.25 \times 10^{13}$ (Fig. 15), where we get same evolution of micro-structure.Since, we always get same evolution, so its independent of K_{12}. This is very important conclusion . Additionally, large value of K_{12} helps to reach final micro-structure faster and its induced less stress (Figs. 14,15).In addition, $K_{ijk} = 0$ and two values of $K_{12} = 1.5 \times 10^{12}$ and $K_{12} = 7.25 \times 10^{13} \, J/m^3$ have been used. Results of the current simulations for both K_{12} practically coincide with those in [7]; they resemble experimental microstructure from [18, 19] and reproduce quantitatively the bending angle (Fig. 12). Corresponding stress fields, including interface stresses is presented
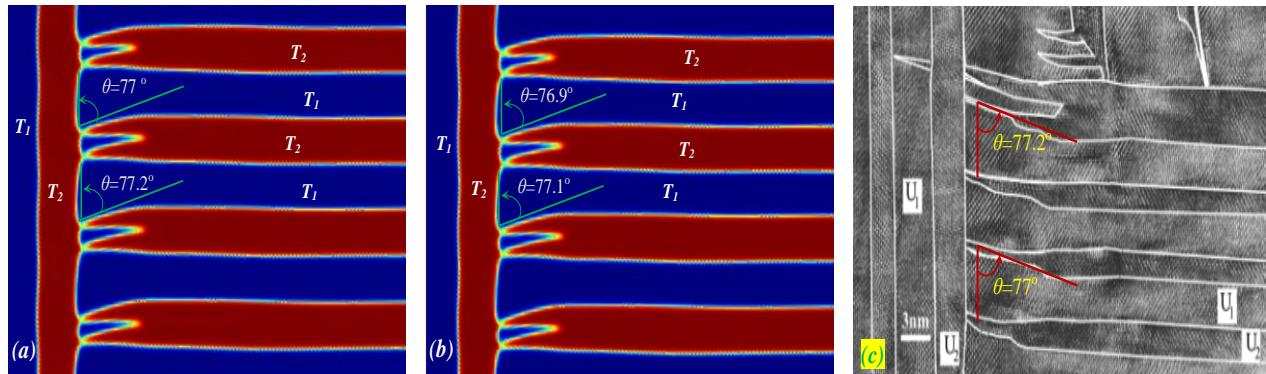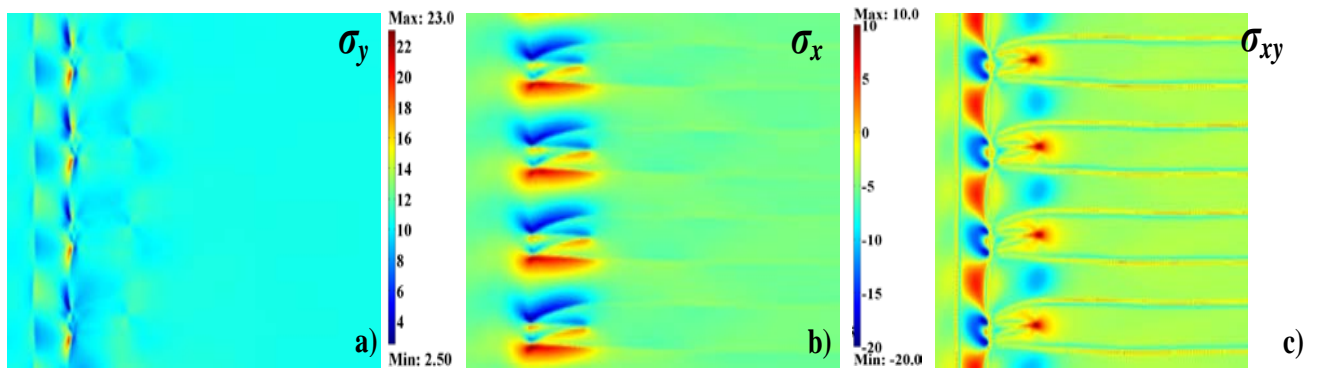
in Fig. 13.

Figure 12: Stationary solution for two-variant martensitic microstructure exhibiting bending and splitting martensitic tips based on the current theory (a) and theory in [7] (b); experimental microstructure from [18, 19] (c).
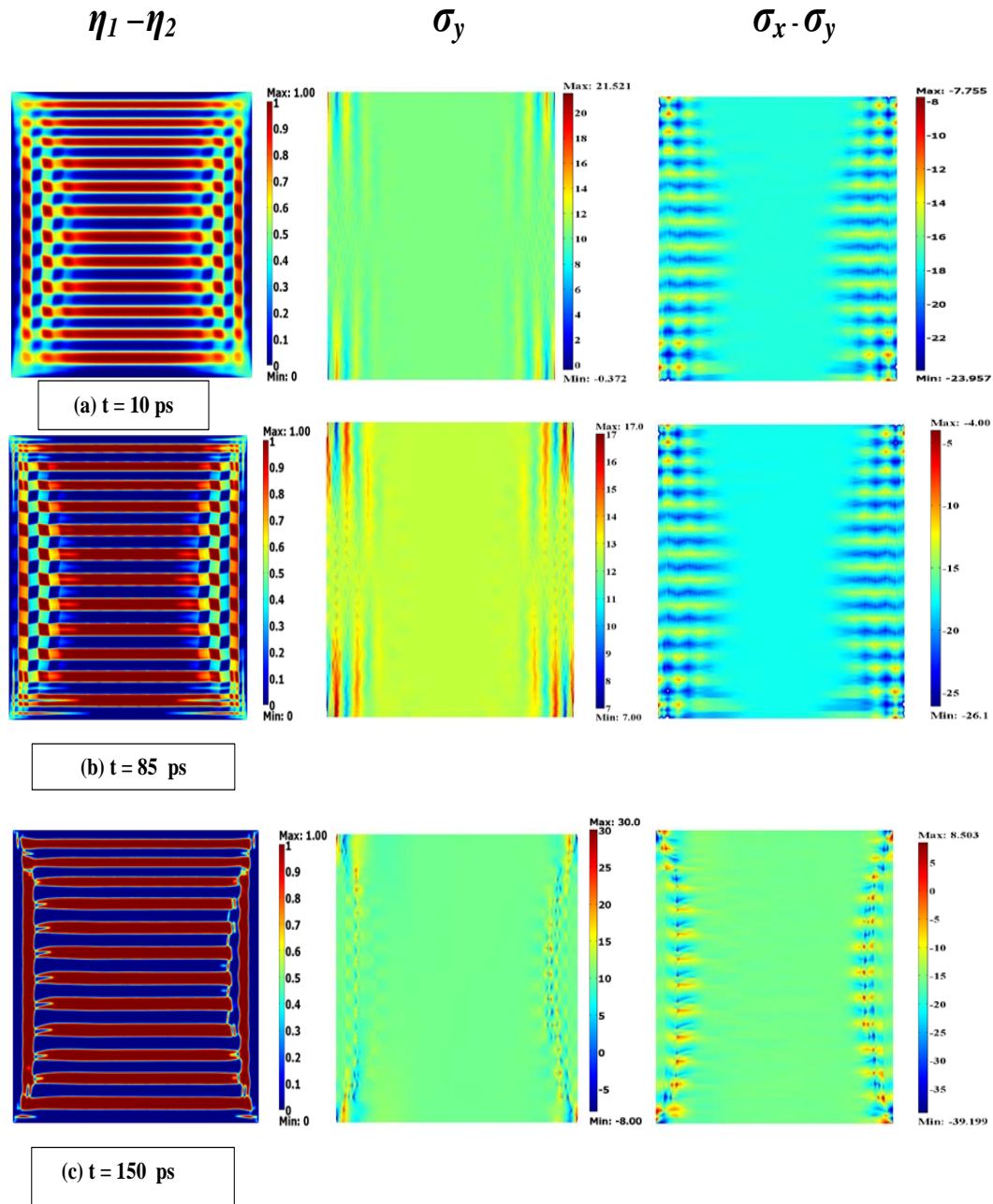
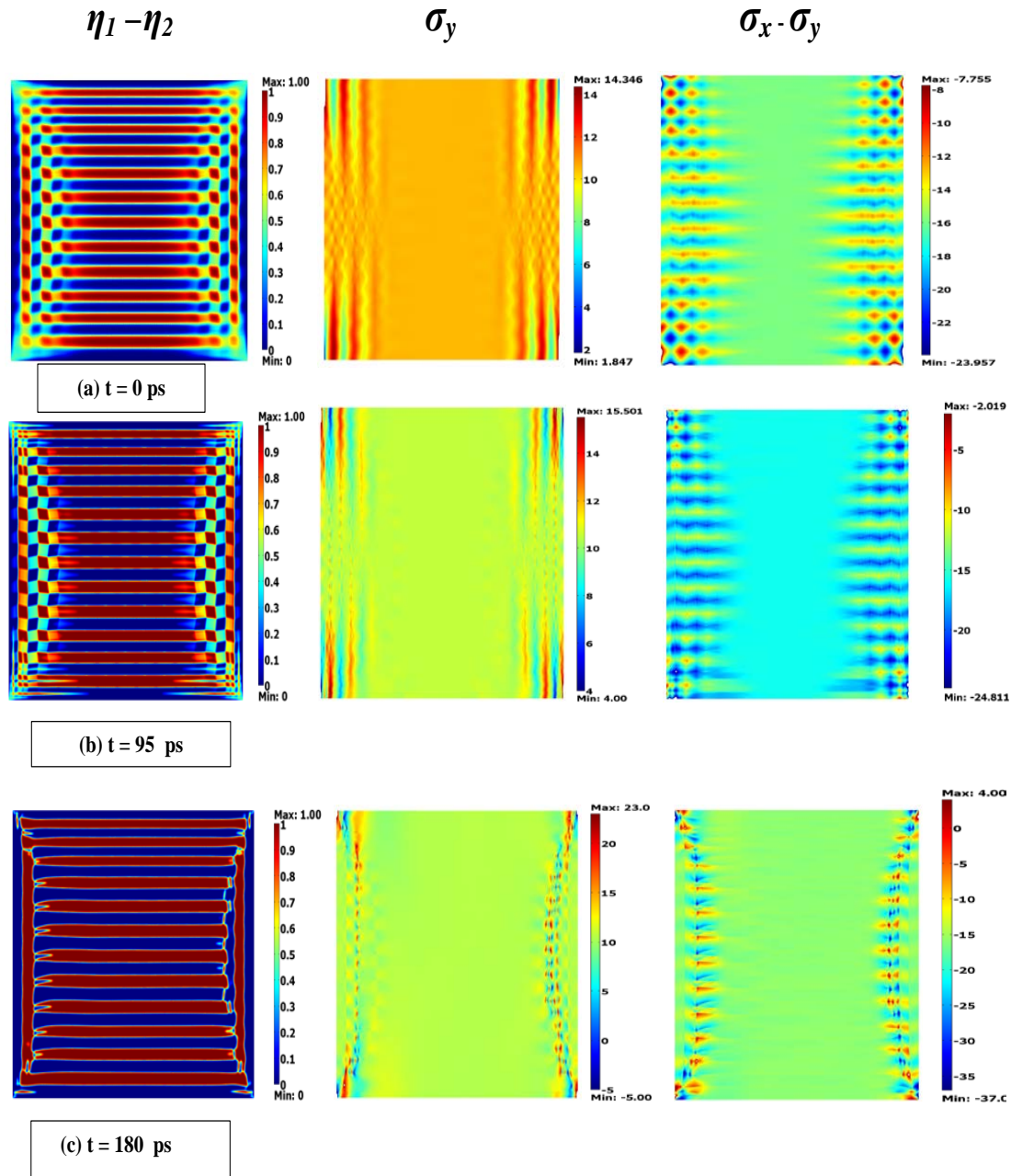$\eta_1-\eta_2$ σ_y σ_x - σ_y

Figure 14: Evolution of bending and splitting microsture in time (a-c) for initial randomly distributed order parameter η_1, η_2 and $K_{12} = 1.5 \times 10^{12}$ of an A sample. Left Column: $\eta_1 - \eta_2$; second and third columns: σ_x and $\sigma_x - \sigma_y$; right column:σ_{xy}. Here P$_2$ (red),P$_1$ (blue)and A(green) in time (a-c).

Figure 15: Evolution of bending and splitting microsture in time (a-c) for initial randomly distributed order parameter η_1, η_2 and $K_{12} = 7.25 \times 10^{13}$ of an A sample. Left Column: $\eta_1 - \eta_2$; second and third columns: σ_x and $\sigma_x - \sigma_y$; right column:σ_{xy}. Here P_2 (red),P_1 (blue)and A(green) in time (a-c).

Nanoindentation-induced twinning $P_2 \to P_1$ was studied in a P_2 sample with a pre-existing P_1 embryo of radius 2 under the indentor (Fig. 16-17). The sample was obtained from a square A sample of size 50×50 by transforming it homogeneously to P_2. The cubic axes and transformation strain were rotated by $\alpha = 31^o$ with respect to the coordinate axes. The value $K_{12} = 5 \times 10^{11}$ was used. Initial conditions were: $\eta_1 = 0$ everywhere; $\eta_2 = 0.9$ inside the embryo and $\eta_1 = 0.999$ in the rest of the sample. A uniform pressure between the indentor of width 4 and the sample was increased linearly from 2 to 3 GPa over $110ps$. The bottom sample surface was constrained by a roller support (zero normal displacements and zero shear stresses) and point F was fixed; all other surfaces are stress-free. With increasing load, a twin P_1 appears under the indenter and grows in a wedge shape with a sharp tip (Fig. 16a, b). Since the bottom of the sample was constrained by the roller support, the twin P_1 could not propagate through the entire sample. In the same problem but with a stress-free section of length 20 at the bottom (Fig.17d-e), the twin propagated completely through the sample and widened with increasing load. The load was then reduced to zero: the width of the twin then decreased to zero without a change in length (Fig.17f-g). These results are in qualitative agreement with experiments [21] and previous simulations [**?**]. Since dislocation plasticity and interface friction [20, 22] are neglected, there is no residual twin.

To summarize, we developed PFA for multiphase materials, which with high and controllable accuracy satisfy all the desired conditions for arbitrary n phases. Instead of explicit constraints, we included in the simplest potential the terms that penalize deviation of the trajectory in the order parameter space from the straight lines connecting each two phases. It describes each of the PTs with the single order parameter, which allows us to use analytical solution to calibrate each interface energy, width, and mobility. It reproduces the desired PT criteria via instability conditions; introduces interface stresses, and allows to control presence of the third phase at the interface between two other phases.

A finite-element simulations exhibit very good correspondence with results based on exact three-phase model in [7] (which, however, cannot be generalized for $n > 3$) and with nontrivial experimental microstructure. Developed approach is applicable to various PTs between multiple, solid and liquid phases and grain evolution and can be extended for diffusive, electric, and magnetic PTs.
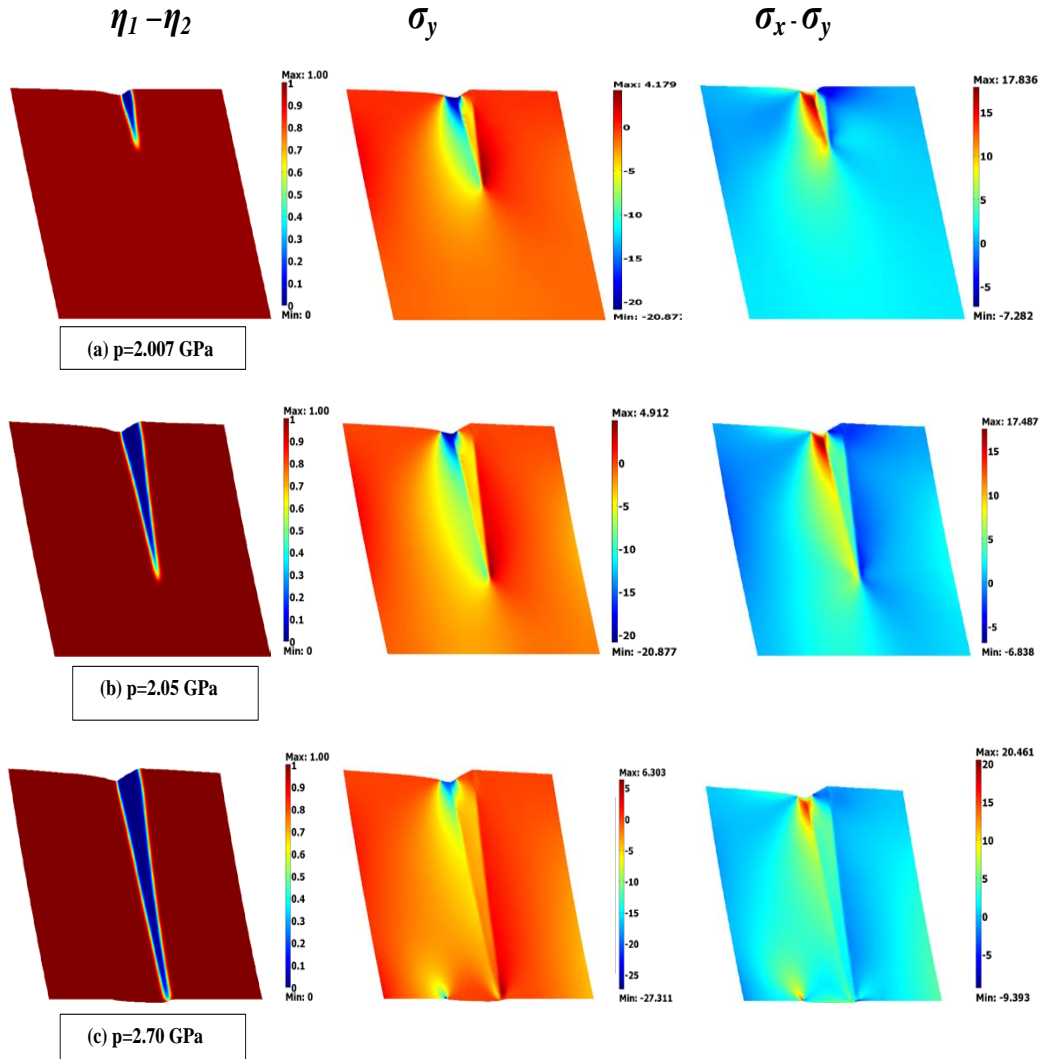
Figure 16: Evolution of twin microsture under dynamic pressure and $K_{12} = 5 \times 10^{11}$ in an intial P_2 sample.Left Column: $\eta_1 - \eta_2$; second and third columns: σ_y and $\sigma_x - \sigma_y$; right column:σ_{xy}. Twinning P_2 (red) $\rightarrow P_1$ (blue) under indentation with the rigid support (a)-(b), support with the hole (c).
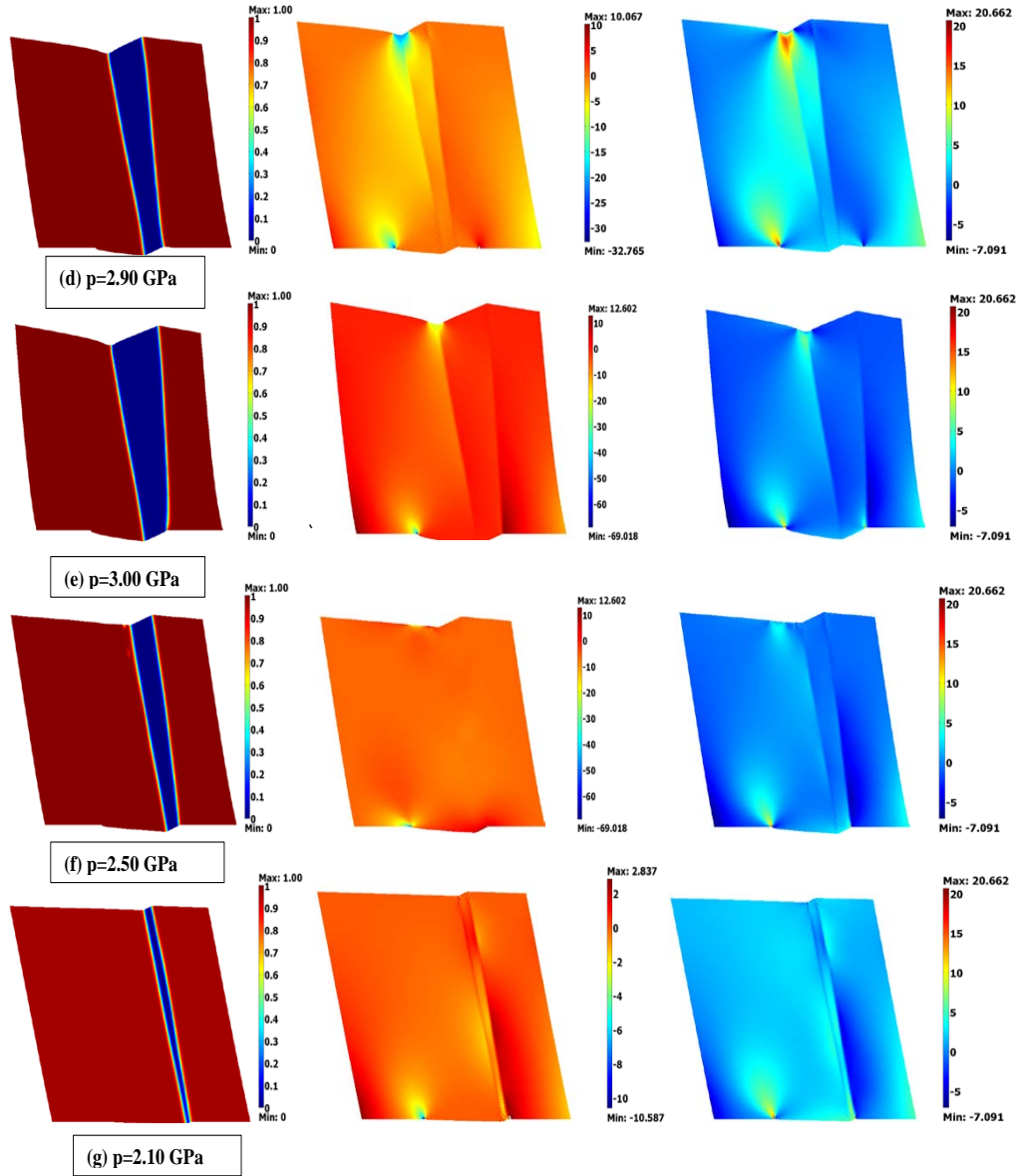
Figure 17: (continue) Evolution of twin microsture under dynamic pressure and $K_{12} = 5 \times 10^{11}$ in an intial P_2 sample.Left Column: $\eta_1 - \eta_2$; second and third columns: σ_y and $\sigma_x - \sigma_y$; right column:σ_{xy}. Twinning P_2 (red) $\rightarrow \mathsf{P}_1$ (blue) under indentation when support with the hole (d)-(e) and during unloading (f)-(g).

References

[1] A. Artemev, Y. Jin, A. G. Khachaturyan, Acta Mat. **49**, 1165 (2001); Y. M. Jin, A. Artemev, A. G. Khachaturyan, Acta Mat. **49**, 2309 (2001); L. Q. Chen Annu. Rev. Mater Res. **32**, 113 (2002).

[2] V. I. Levitas and D. L. Preston, Phys. Rev. B. **66**, 134206 (2002); 134207 (2002).

[3] V. I. Levitas, D. L. Preston and D-W. Lee, Phys. Rev. B. **68**, 134201 (2003).

[4] V. I. Levitas *et al.*, Phys. Rev. Lett. **103**, 025702 (2009); V.I. Levitas, Int. J. Plast. **49** (2013), 10.1016/j.ijplas.2013.03.002.

[5] V. I. Levitas and M. Javanbakht, Phys. Rev. Lett. **105**, 165701 (2010); Int. J. Mater. Res. **102**, 652 (2011).

[6] V. I. Levitas, Phys. Rev. B. **87**, 054112 (2013); Acta Mater. **61**, 4305 (2013).

[7] V. I. Levitas, A. M. Roy and D. L. Preston, Phys. Rev. B. **88**, 054113 (2013).

[8] V.I. Levitas, Phys. Rev. B. **89**, 094107 (2014).

[9] V. I. Levitas, J. Mech. Phys. Solids **70**, 154 (2014)

[10] G. R. Barsch, J. A.Krumhansl, Phys. Rev. Lett. **53**, 1069 (1984).

[11] A. Finel, Y. Le Bouar, A. Gaubert and U. Salman, C. R. Phys. **11**, 245 (2010).

[12] I. Steinbach *et al.*, Physica D **94**, 13547 (1996); I. Steinbach, Model. Simul. Mater. Sci. Eng. **17**, 073001 (2009).

[13] A. A. Wheeler, G. B. McFadden and W. J. Boettinger, Proc. Royal Soc. London A, **452**, 495 (1996).

[14] R. Folch and M. Plapp, Phys. Rev. E **68**, 010602 (2003); Phys. Rev. E **72**, 011602 (2005).

[15] P.C. Bollada *et al.*, Physica D **241**, 816 (2012).

[16] V. I. Levitas *et al.*, Phys. Rev. Lett. **92**, 235702 (2004); V. I. Levitas *et al.*, Phys. Rev. B **85**, 220104 (2012).

[17] V. I. Levitas and K. Momeni, Acta Mater. **65**, 125 (2014); K. Momeni and V.I. Levitas, Phys. Rev. B **89**, 184102 (2014).

[18] Ph. Boullay, D. Schryvers, R.V. Kohn and J.M. Ball, J. de Physique IV **11**, 23 (2001); Ph. Boullay, D. Schryvers and R.V. Kohn, Phys. Rev. B **64**, 144105 (2001).

[19] Ph. Boullaya, D. Schryvers, J.M. Ball, Acta Mater. **51**, 1421 (2002).

[20] V.I. Levitas and D-W. Lee, Phys. Rev. Lett. **99**, 245701 (2007).

[21] J. W. Christian and S. Mahajan, Prog. Mater. Sci. **39**, 1157 (1995); V. S. Boiko, R. I. Garber and A. M. Kosevich, *Reversible Crystal Plasticity* (New York: AIP, 1994).

[22] V.I. Levitas, D.-W. Lee and D.L. Preston, Int. J. Plast. **26**, 395 (2010).

[23] J.D. Clayton, J. Knap, Physica D. **240**, 841 (2011);

[24] COMSOL, Inc., website: www.comsol.com.